



UNIVERSITY OF
BIRMINGHAM

**Studies of Cyclisation Reactions of
Highly Substituted Diketopiperazines:
New Access to Prenylated Indole
Alkaloids**

by

Ilias Pavlakos

A thesis submitted to
The University of Birmingham
For the degree of
DOCTOR OF PHILOSOPHY

School of Chemistry
The University of Birmingham

UNIVERSITY OF
BIRMINGHAM

University of Birmingham Research Archive

e-theses repository

This unpublished thesis/dissertation is copyright of the author and/or third parties. The intellectual property rights of the author or third parties in respect of this work are as defined by The Copyright Designs and Patents Act 1988 or as modified by any successor legislation.

Any use made of information contained in this thesis/dissertation must be in accordance with that legislation and must be properly acknowledged. Further distribution or reproduction in any format is prohibited without the permission of the copyright holder.

Abstract

The size of the prenylated indole alkaloid family sharing the unique bicyclo[2.2.2]diazaoctane core ring system has grown steadily over the last decades. Due to the complex structures, and in some cases the potent biological activity, these molecules have been adopted as challenging targets for several synthetic groups. Chapter One gives an introduction to these alkaloids, their origin, biological activity and biosynthetic studies.

Our strategies to deliver 5,6- and 6,6-fused diketopiperazines (DKPs) and monoketopiperazines (MKPs) are discussed in Chapter Two. Radical cyclisation of a phenylselenenyl DKP **108** (Scheme 2.10) and a bromo MKP **140** (Scheme 2.22) gave mixtures of *exo* and *endo* products. An alternative thio-mediated radical approach allowed access to *exo* products (Table 2.2 and Scheme 2.28)

Previous experiments on the established cationic cyclisation showed that the pyran ring present in the stephacidins is particularly sensitive to the presence of acid. These results prompted us to explore alternative approaches in which the formation of the pyran ring occurs after the key-step (Scheme 3.19 and 3.20). Our progress towards stephacidin A and previous syntheses are discussed in Chapter Three.

Synthesis of a sulfide DKP **218** (Scheme 4.22) allowed access to indoline products via radical approach (Scheme 4.27). An oxidative radical approach as well as a cationic approach is also discussed in Chapter Four. In comparison with our new strategy there is also a review of all previously described approaches to assemble the bicyclo[2.2.2]diazaoctane framework.

Among the different approaches to access the core structure of these natural products the radical cyclisation approach appeared to be the most efficient. Based on this strategy, synthesis of indolines **348/349** which is structural related to avrainvillamide is discussed in Chapter Five (Scheme 5.10). Our rapid radical methodology allows synthesis of these indolines in 6 steps and 28% overall yield.

Declaration

I declare that the thesis is the result of my own work except where due reference is made to other authors, and has not, whether in the same or different form, been submitted for any other degree at this or any other university.

Ilias Pavlakos

Acknowledgments

First and foremost, I would like to thank my supervisor Professor Nigel S. Simpkins for giving me the opportunity to be a member of his research team and also for his continued support and guidance. I am also grateful to him for his endless encouragement and enthusiasm which were really helpful especially when the chemistry did not go our way

I would also like to thank the analytical facility for their assistance, Dr Neil Spencer for NMR, Pete Ashton and Nick May for mass spectrometry. A special thanks to Dr Louise Male for her important assistance with X-Ray crystallography.

I am grateful to the EPSRC for funding this research and to the University of Birmingham for providing the necessary laboratory and facilities.

Big thanks to all past and present members of the Simpkins' group for making a very enjoyable and noisy environment to work in. It was a real pleasure to work and socialise with Fred, Valérie, Mike, Cynthia, Sammy, Mark, Jen, Damian, Séb, Jim and off course the breakfast team, Pete and Bick. I am also grateful for the lovely time I spend with Vicky, Bene, Bhaven, Marilena, Vaggelis, Lazaros, Alex, Dimitrios, Sissy and Marilenaki.

Finally, special thanks must go to my parents, Lenaki and all the rest of the members of my big-family for their support and love.

Table of Contents

ABSTRACT	II
DECLARATION	III
ACKNOWLEDGMENTS	IV
LIST OF FIGURES	VIII
LIST OF TABLES	X
LIST OF APPENDIXES	XI
GLOSSARY OF ABBREVIATIONS	XIII
CHAPTER 1	1
INTRODUCTION	1
1.1 DIKETOPIPERAZINES	1
1.2 PRENYLATED INDOLE ALKALOID FAMILY	2
1.3 ORIGIN OF THE BICYCLO[2.2.2]DIAZAOCTANE FRAMEWORK	8
1.4 STEPHACIDINS – THE BIOSYNTHETIC STUDIES	13
1.5 AVRINVILLAMIDE, STEPHACIDIN B – THE DIMERIZATION STEP	16
1.6 AVRINVILLAMIDE, STEPHACIDIN B – BIOLOGICAL ACTIVITY	19
CHAPTER 2	23
SYNTHESIS OF FUSED DKP AND MKP	23
2.1 MARCFORTINES, PARAHERQUAMIDES AND ASPERPARALINES	23
2.2 SYNTHESIS OF THE PIPECOLATE MOIETY	24
2.3 SYNTHESIS OF <i>B</i> -METHYLPROLINE MOIETY	27
2.4 RETROSYNTHETIC PLAN	29
2.5 RADICAL CYCLISATION OF DKP AND MKP SUBSTRATES	30
2.6 RADICAL CYCLISATION –THE THIOPHENOL MEDIATED APPROACH.....	39

CHAPTER 3	45
TOWARDS STEPHACIDIN A.....	45
3.1 PREVIOUS SYNTHESSES.....	45
3.2 PREVIOUS WORK BY SIMPKINS' GROUP - STUDIES TOWARDS COMPLEX BRIDGED ALKALOIDS	57
3.3 INVESTIGATING THE NEW STRATEGY.....	60
3.4 SYNTHESIS OF 6-BENZYLOXY-HYDROXY-DKP PRECURSOR	62
3.5 CATIONIC CYCLISATION OF 6-BENZYLOXY-HYDROXY-DKP	64
3.6 SYNTHESIS OF DKP PRECURSOR OF 6-BROMOINDOLE-HYDROXY-DKP	67
3.7 CATIONIC CYCLISATION OF 6-BROMOINDOLE-HYDROXY-DKP.....	68
3.8 PROGRESS TOWARD STEPHACIDIN A.....	71
CHAPTER 4	75
STUDIES OF CYCLISATION REACTION	75
OF PRENYLATED DKP	75
4.1 SYNTHETIC APPROACHES TO THE BICYCLO[2.2.2]DIAZAOCTANE RING SYSTEM.....	75
4.2 BIOMIMETIC DIELS-ALDER APPROACH	75
4.3 INTRAMOLECULAR S _N 2' CYCLISATION APPROACH	79
4.4 RADICAL CYCLISATION APPROACH.....	81
4.5 INVESTIGATION OF A NEW STRATEGY TOWARDS STEPHACIDINS	85
4.6 SYNTHESIS OF THE DKP PRECURSOR – THE SULFENYLATION REACTION	85
4.7 A NEW STEREOSPECIFIC ALKYLATION – SULFENYLATION REACTION.....	90
4.8 THE CATIONIC CYCLISATION	90
4.9 THE RADICAL CASCADE CYCLISATION	91
4.10 THE OXIDATIVE RADICAL CYCLISATION REACTION	97
4.11 AN INTER/INTRA-MOLECULAR RADICAL ATTEMPT.....	100

CHAPTER 5	104
SYNTHESIS OF INDOLINES VIA RADICAL CYCLISATION APPROACH.....	104
5.1 STEPHACIDINS, AVRAINVILLAMIDE AND ASPERGAMIDE A	104
5.2 PREVIOUS SYNTHESIS OF STEPHACIDIN B AND AVRAINVILLAMIDE.....	105
5.3 SYNTHESIS OF THE RADICAL PRECURSOR.....	110
5.4 THE RADICAL CYCLISATION STEP	112
5.5 SUMMARY AND FUTURE WORK	118
CHAPTER 6	123
EXPERIMENTAL	123
6.1 GENERAL PROCEDURES.....	123
6.2 EXPERIMENTAL	124
CRYSTALLOGRAPHIC INFORMATION.....	181
APPENDIX	196
LIST OF REFERENCES	233

List of Figures

Figure 1.1 Structure of DKP regioisomers

Figure 1.2 Distribution of the DKPs, reported from marine-derived microorganism

Figure 1.3 General structure of the bicyclo[2.2.2]diazaoctane ring system

Figure 1.4 Structure of the brevianamides

Figure 1.5 Structures of the marcfortines

Figure 1.6 Structures of the stephacidins, aspergamides and avrainvillamide

Figure 1.7 Structures of the malbrancheamides

Figure 1.8 Proposed Diels-Alder reaction

Figure 1.9 Structures of synthetic analogues of avrainvillamide

Figure 1.10 Structures of synthetic analogues of avrainvillamide

Figure 1.11 Structures of synthetic analogues of avrainvillamide

Figure 2.1 Structures of the paraherquamides, marcfortines and asperparalines

Figure 2.2 Radical cyclisation of enantiopure DKP and MKP substrates

Figure 2.3 Frontier orbital interaction of an electrophilic and nucleophilic radical with alkene

Figure 3.1 Structures of the stephacidins and avrainvillamide

Figure 3.2 Key disconnections of stephacidin A (35)

Figure 3.3 Possible scenarios for bond formation

Figure 3.4 Metal chelation

Figure 3.5 CD measurements of natural and synthetic stephacidins A

Figure 3.6 Key disconnections of bridged lactim ether

Figure 3.7 Key disconnections of stephacidin A (35)

Figure 3.8 Structure of Pd-ligands

Figure 4.1 Transition states of enolate **298**

Figure 4.2 Crystal structure of sulfide **218**

Figure 4.3 ^1H -NMR spectrum of indoline **316**

Figure 4.4 nOe spectrum of **316**. nOE correlations of H15 with H14/H4 and H27 with H4

Figure 4.5 Crystal structure of indoline **318**

Figure 5.1 Oxidation state of stephacidins, aspergamide A and avrainvillamide

Figure 5.2 Key disconnections of avrainvillamide (**36**)

Figure 5.3 Key disconnections of stephacidin A (**35**)

Figure 5.4 Key disconnections of stephacidin A (**35**)

Figure 5.5 Crystal structure of indoline **352**

Figure 5.6 Crystal structure of indoline **353**

Figure 5.7 ^1H -NMR spectrum of indoline **354**

Figure 5.8 nOe spectrum of indoline **354**. nOe correlations of H15 with H14 and NH with H4

Figure 5.9 Structures of the marcfortines, paraherquamides, notoamides, versicolamide B

List of Tables

Table 1.1 Structures of the paraherquamides

Table 1.2 Structures of the notoamides

Table 1.3 Structures of the asperparalines

Table 1.4 *In Vitro* Cytotoxicity of (+)-stephacidin A (**35**) and (-)-stephacidin B (**39**), IC₅₀ in μ M

Table 1.5 Measured IC₅₀ Values for (\pm)-stephacidin B (**39**) and (\pm)-avrainvillamide (**36**)

Table 2.1 Comparison of thiophenol-mediated with tin-initiated approach

Table 2.2 Thiophenol-mediated cyclisation reaction of **166**

Table 4.1 Intramolecular S_N2' cyclisation of **298**

Table 4.2 nOe correlations of indolines **316** and *epi*-**316**

Table 4.3 Radical cyclisation of **326**

List of Appendixes

- Appendix 1.** ^1H -NMR spectrum of (**116**) (500 MHz, CDCl_3)
- Appendix 2.** ^{13}C -NMR spectrum of (**116**) (126 MHz, CDCl_3)
- Appendix 3.** ^1H -NMR spectrum of (**117**) (500 MHz, CDCl_3)
- Appendix 4.** ^{13}C -NMR spectrum of (**117**) (126 MHz, CDCl_3)
- Appendix 5.** ^1H -NMR spectrum of (**155**) (500 MHz, CDCl_3)
- Appendix 6.** ^{13}C -NMR spectrum of (**155**) (126 MHz, CDCl_3)
- Appendix 7.** ^1H -NMR spectrum of (**170**) (400 MHz, CDCl_3)
- Appendix 8.** ^{13}C -NMR spectrum of (**170**) (101 MHz, CDCl_3)
- Appendix 9.** ^1H -NMR spectrum of (**181**) (500 MHz, CDCl_3)
- Appendix 10.** ^{13}C -NMR spectrum of (**181**) (126 MHz, CDCl_3)
- Appendix 11.** ^1H -NMR spectrum of (**240**) (400 MHz, CDCl_3)
- Appendix 12.** ^{13}C -NMR spectrum of (**240**) (101 MHz, CDCl_3)
- Appendix 13.** ^1H -NMR spectrum of (**230**) (500 MHz, CDCl_3)
- Appendix 14.** ^{13}C -NMR spectrum of (**230**) (126 MHz, CDCl_3)
- Appendix 15.** ^1H -NMR spectrum of (*epi*-**230**) (300 MHz, CDCl_3)
- Appendix 16.** ^{13}C -NMR spectrum of (*epi*-**230**) (75 MHz, CDCl_3)
- Appendix 17.** ^1H -NMR spectrum of (**S3**) (300 MHz, CDCl_3)
- Appendix 18.** ^{13}C -NMR spectrum of (**S3**) (101 MHz, CDCl_3)
- Appendix 19.** ^1H -NMR spectrum of (**274**) (300 MHz, CDCl_3)
- Appendix 20.** ^1H -NMR spectrum of (**316**) (400 MHz, CDCl_3)
- Appendix 21.** ^{13}C -NMR spectrum of (**316**) (101 MHz, CDCl_3)
- Appendix 22.** ^1H -NMR spectrum of (*epi*-**316**) (400 MHz, CDCl_3)

Appendix 23. ^{13}C -NMR spectrum of (*epi*-**316**) (101 MHz, CDCl_3)

Appendix 24. ^1H -NMR spectrum of (**318**) (400 MHz, CDCl_3)

Appendix 25. ^{13}C -NMR spectrum of (**318**) (101 MHz, CDCl_3)

Appendix 26. ^1H -NMR spectrum of (**350**) (400 MHz, CDCl_3)

Appendix 27. ^{13}C -NMR spectrum of (**350**) (101 MHz, CDCl_3)

Appendix 28. ^1H -NMR spectrum of (**352**) (400 MHz, CDCl_3)

Appendix 29. ^{13}C -NMR spectrum of (**352**) (101 MHz, CDCl_3)

Appendix 30. ^1H -NMR spectrum of (**353**) (300 MHz, CDCl_3)

Appendix 31. ^{13}C -NMR spectrum of (**353**) (101 MHz, CDCl_3)

Appendix 32. ^1H -NMR spectrum of (**354**) (400 MHz, CDCl_3)

Appendix 33. ^{13}C -NMR spectrum of (**354**) (101 MHz, CDCl_3)

Appendix 33. Published work

Glossary of Abbreviations

1D	one dimensional
1,2-DCE	1,2-dichloroethane
2D	two dimensional
4-DMAP	<i>N,N</i> -dimethyl-4-aminopyridine
Ac	acetyl
ACCN	1,1'-Azobis(cyanocyclohexane)
acac	acetylacetonate
AIBN	azobisisobutyronitrile
BINAP	2,2'-bis(diphenylphosphino)-1,1'-binaphthyl
Bn	benzyl
Boc	<i>tert</i> -butoxycarbonyl
Bop	bis(2-oxo-3-oxazolidinyl)phosphonic
Burgess reagent	methyl <i>N</i> -(triethylammoniosulfonyl)carbamate
Bz	benzoyl
CAN	ceric ammonium nitrate
Cbz	carbobenzyloxy
CD	circular dichroism
COSY	correlation spectroscopy
CHex	cyclohexane
DABCO	1,4-diazabicyclo[2.2.2]octane
dba	dibenzylideneacetone
DBU	1,8-diazabicyclo[5.4.0]undec-7-ene

DCC	1,3-dicyclohexylcarbodiimide
DCM	dichloromethane
DDQ	2,3-dicyano-5,6-dichloro-parabenzoquinone
DEAD	diethyl azodicarboxylate
DIBAL-H	dibutylaluminium hydride
DIC	<i>N,N'</i> -diisopropylcarbodiimide
DIPA	diisopropylamine
DIPEA	diisopropylethylamine
DKP	diketopiperazine
DMF	<i>N,N</i> -dimethylformamide
DMP	Dess-Martin periodinane
DMS	dimethyl sulfide
DMSO	dimethyl sulfoxide
EDC	<i>N</i> -(3-dimethylaminopropyl)- <i>N'</i> -ethylcarbodiimide
ESI	electron spray ionisation
eq	equivalent
FAB	fast atom bombardment
GIX	concentration of inhibitor required for X% growth inhibition
h	hours
HAT	hydrogen abstraction translocation
HATU	2-(7-aza-1 <i>H</i> -benzotriazole-1-yl)-1,1,3,3-tetramethyluronium hexafluorophosphate
HBTU	2-(1 <i>H</i> -benzotriazole-1-yl)-1,1,3,3-tetramethyluronium hexafluorophosphate

HMDS	hexamethyldisilazane
HMPA	hexamethylphosphoric triamide
HOBt	1-hydroxybenzotriazole
HOMO	highest occupied molecular orbital
HRMS	high resolution mass spectrometry
IMDA	intramolecular Diels-Alder
KHMDS	potassium bis(trimethylsilyl)amide
LiHMDS	lithium bis(trimethylsilyl)amide
LDA	lithium di- <i>iso</i> -propylamide
LUMO	lowest unoccupied molecular orbital
<i>m</i>-CPBA	<i>meta</i> -chloroperbenzoic acid
MDR	multi-drug resistant
MEM	methoxy(ethoxy)methyl
MeS	mesitylene
MIC	minimum inhibitory concentration
min	minutes
MKP	monoketopiperazine
MOM	methoxymethyl
Ms	methanesulfonyl
MS	mass spectroscopy
MW	microwaves
NMM	<i>N</i> -methylmorpholine
NMR	nuclear magnetic resonance spectrometry

nOe	nuclear Overhauser effect
NOESY	nuclear Overhauser effect spectroscopy
PG	protective group
Ph	phenyl
PHQ	parahequamide
Piv	pivaloyl
PMB	<i>para</i> -methoxybenzyl
PP	pyrophosphate
ppm	parts per million
Prep	preparative
Pro	Proline
PSI	pounds per square inch
PTSA	<i>para</i> -toluenesulfonic acid
Py	pyridine
PyBOP(R)	(benzotriazol-1-yloxy)tripyrrolidinophosphonium hexafluorophosphate
quant	quantitative
rt	room temperature
R_f	retardation factor
SEM	2-(trimethylsilyl)ethoxymethyl
sm	starting material
SOMO	singly occupied molecular orbital
TBAF	tetra- <i>n</i> -butylammonium fluoride
TBAI	tetra- <i>n</i> -butylammonium iodide

TBAT	tetra- <i>n</i> -butylammonium triphenyldifluorosilicate
TBDMS	<i>tert</i> -butyldimethylsilyl
TBDPS	<i>tert</i> -butyldiphenylsilyl
TEA	triethylamine
Tf	trifluoromethanesulfonyl
TFA	trifluoroacetic acid
TFAA	trifluoroacetic anhydride
THF	tetrahydrofuran
TLC	thin layer chromatography
TMEDA	<i>N,N,N',N'</i> -tetramethylethylenediamine
TMM	triethylenemethane
tol	toluene
TMS	trimethylsilyl
Trp	tryptophan
Ts	tosyl
TS	transition state

Chapter 1

Introduction

1.1 Diketopiperazines

Diketopiperazines (DKPs) are cyclic dipeptides, commonly biosynthesised from amino acids by different organisms including mammals, marine microorganisms, sponges, sea stars, tunicates and red algae. They are considered as secondary functional metabolites or undesired by-products and in some cases degradation products in the synthesis of oligopeptides. Similarly to peptides, DKPs display favourable pharmacodynamic and pharmacokinetic properties due to reduced susceptibility to metabolic amide bond reactions and the conformational mobility. The above characteristics confer drug-like properties whereas the presence of mimicking peptidic pharmacophoric groups enhances favourable interactions with macromolecules. The potent biological activities of DKPs have increased the interest in the synthesis of these compounds.¹ Inhibitors of plasminogen activator inhibitor-1 (PAI-1)², alteration of the cardiovascular and blood-clotting functions are some examples of the important biological activities showed by the DKPs.³ They also display activities such as antitumour,⁴ antiviral,⁵ antifungal,⁶ antibacterial,⁷ and antihyperglycaemic activity,⁸ and have been shown to display affinities for calcium channels and opioid,⁹ GABAergic,¹⁰ serotonergic 5-HT_{1A},¹¹ and oxytocin¹² receptors.

There are three DKP regioisomers **1-3** sharing this particular heterocyclic core system (Figure 1.1). Our synthetic investigations have been focused exclusively on the 2,5-diketopiperazine systems (**2**).

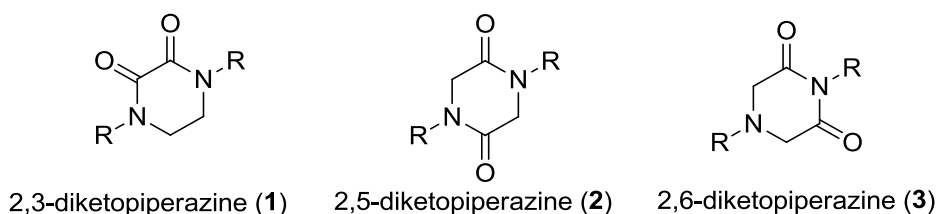


Figure 1.1 Structure of DKP regioisomers

2,5-DKPs, head-to-tail dipeptides, represent a common naturally occurring structural unit.¹³ According to recent literature reviews, there have been reported more than 124 DKPs from bacteria, fungi and several marine organisms.¹⁴ Figure 1.2 shows the distribution of the DKP sources, reported from marine-derived microorganism. It is interesting that, even though the number of isolated DKPs has significantly increased during the last decades, the biosynthesis of many of these natural products still remains largely unexplored.

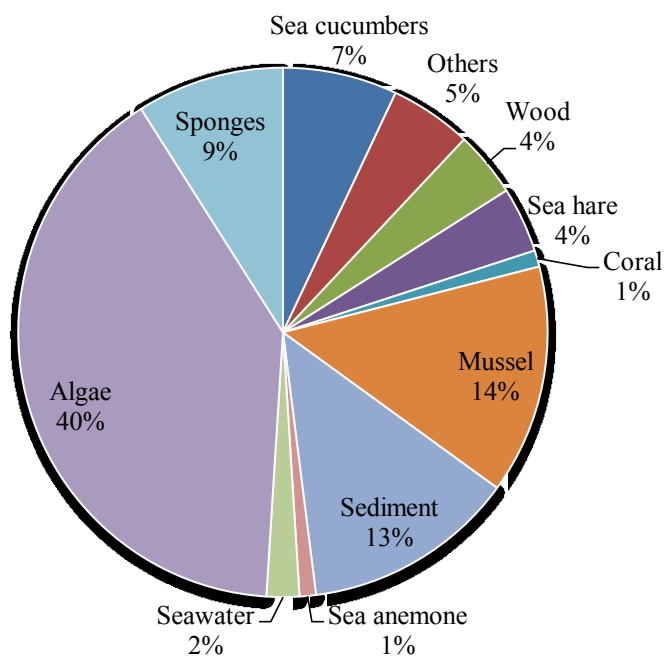


Figure 1.2 Distribution of the DKPs, reported from marine-derived microorganism¹⁴

1.2 Prenylated indole alkaloid family

The size of the prenylated indole alkaloids family has grown steadily over the last decades. Nowadays more than 69 alkaloids have been isolated from a wide selection of fungi of the genera *Aspergillus* and

Penicillium. The unique bicyclo[2.2.2]diazaoctane framework of these alkaloids is present in the form of a DKP or a partially reduced derivative incorporating different structural features (Figure 1.3). The DKP core of these alkaloids is often linked with five- or six-membered rings and additionally with indole, *spiro*-oxindole or *spiro*-indoxyl motifs. Pyrrolidine and piperidine derivatives are also common in many natural products of this family. Two distinct stereochemistries have been observed with respect to the relative configuration at the C4 stereogenic centre.¹⁵ The *anti*-configuration or a *syn*-configuration refers to the relative relationship between the C4–C3 bond and the C6–N bond of the cyclic amino acid residue (pyrrolidine, piperidine). To date within the family of prenylated indole alkaloids only brevianamides¹⁶ and versicolamide B^{15a} possess the *anti*-configuration.

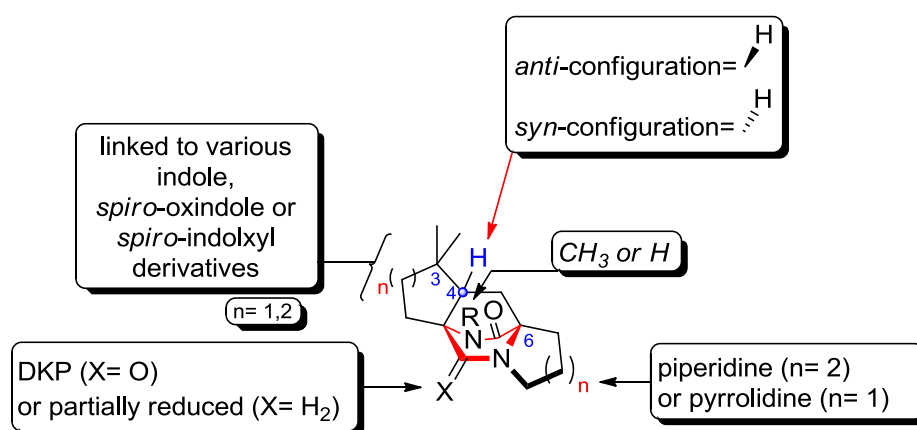


Figure 1.3 General structure of the bicyclo[2.2.2]diazaoctane ring system

Members of the brevianamide family were the first isolated alkaloids within this interesting family of alkaloids sharing the bicyclo[2.2.2]diazaoctane core. Brevianamide A (**4**) was isolated as a major fluorescent metabolite from *Penicillium brevicompactum* in 1969 (Figure 1.4).¹⁶ The absolute stereochemistry was determined by X-ray crystallography of a semisynthetic derivative.¹⁷ It was also reisolated from the culture extracts of *Penicillium viridicatum* and *Penicillium ochraceum*¹⁸ while the rest members of this family were isolated¹⁹ from the same fungus afterwards. It was reported that brevianamide C (**6**) and D (**7**) were photochemically delivered artifacts during the isolation process.^{15c} This was proved by growing a culture of *P. brevicompactum* in the absence of light where neither brevianamide C (**6**) or D (**7**) were not detected after the analysis of the crude extraction. Brevianamide

A (**4**) and B (**5**) share a bicyclo[2.2.2]diazaoctane framework which is equipped with a proline residue and a *spiro*-indoxyl unit. The most important structural characteristic of the brevianamide family is the *anti*-configuration at C4.

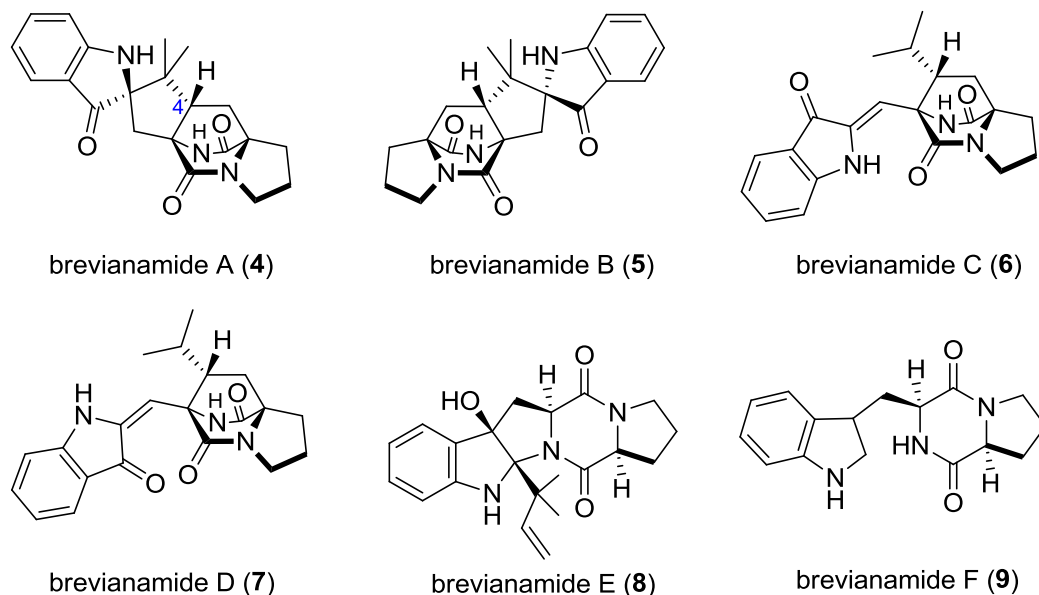
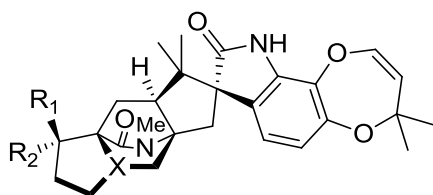


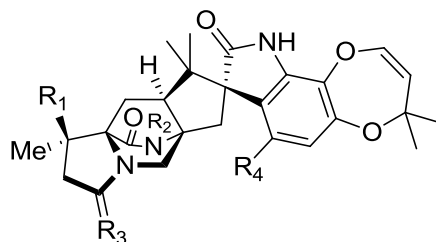
Figure 1.4 Structure of the brevianamides

Another important subclass of the prenylated indole alkaloid family includes paraherquamides. Paraherquamide A (**10**) was isolated from cultures of *Penicillium paraherquei* in 1980 and displays the highest biological activity among the group of paraherquamides (Table 1.1).²⁰ Since then, the family of paraherquamides has grown steadily with the most of the recent members paraherquamide B–G (**11–14**, **19–21**),²¹ VM55595 (**22**), VM55596 (**15**) and VM55597 (**16**),²² SB203105 (**17**) and SB200437 (**18**),²³ and sclerotiamide (**23**),²⁴ being isolated from various *Penicillium Aspergillus* species. Moya and co-workers isolated paraherquamide H (**19**) and I (**24**) along with other structurally related alkaloids from cultures of *Penicillium cluoniae*. Structurally similar but more complex than the brevianamides is the paraherquamide family which shares tryptophan and variously substituted proline motifs (Table 1.1). Unlike the brevianamides, they possess a partially reduced DKP core which is linked with a *spiro*-oxindole rather than the *spiro*-indoxyl ring system. Finally, they further characterised by either a dioxygenated 7-membered ring or pyran ring on the tryptophan unit.

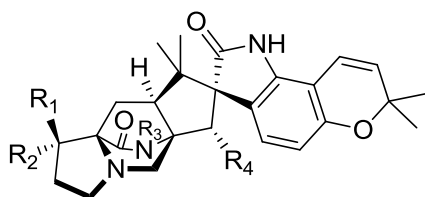
Paraherquamides as well as the majority of alkaloids in the prenylated indolic family possess the *syn*-configuration.



	R₁	R₂	X
paraherquamide A (10)	OH	Me	N
paraherquamide B (11)	H	H	N
paraherquamide C (12)	=CH ₂	=CH ₂	N
paraherquamide D (13)	-OCH ₂ -		N
paraherquamide E (VM54159) (14)	H	Me	N
VM55596 (15)	OH	Me	N ⁺ -O ⁻



	R₁	R₂	R₃	R₄
VM55597 (16)	OH	Me	O	H
SB203105 (17)	H	Me	2H	OH
SB200437 (18)	H	H	2H	H
paraherquamide H (19)	H	Me	O	H



	R₁	R₂	R₃	R₄
paraherquamide F (VM55594) (20)	H	Me	Me	H ₂
paraherquamide G (VM54158) (21)	OH	Me	Me	H ₂
VM55595 (22)	H	Me	H	H ₂
sclerotiamide (23)	H	H	H	OH

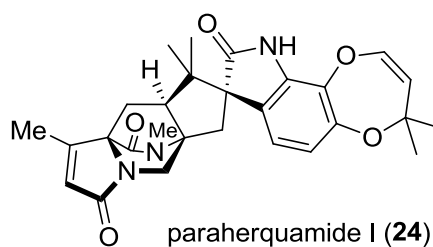


Table 1.1 Structures of the paraherquamides

Marcfortines A–C (**25–27**), isolated from *Penicillium roqueforti*, are compounds closely related to paraherquamides but they are equipped with a piperidine unit in the place of pyrrolidine moiety (Figure 1.5).²⁵ Unlike with marcfortines A–B (**25–26**), marcfortine C (**27**) possesses a pyran ring in the place of the dioxepin ring.

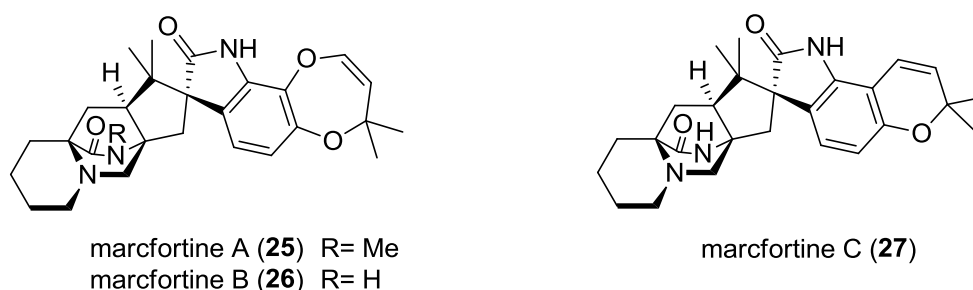
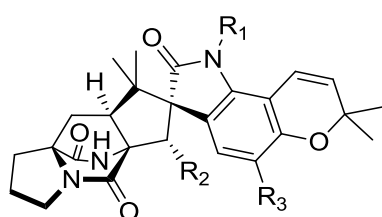


Figure 1.5 Structures of the marcfortines

Notoamide A (**28**), B (**29**) and N (**31**) are also important members of prenylated alkaloid family. In 2002, notoamides A–D were isolated from *Aspergillus* sp. by the Qian-Cutrone's group (Table 1.2).²⁶ More recently, notoamide F–K were also detected from *Aspergillus* sp.²⁷



	R₁	R₂	R₃
notoamide A (28)	OH	H	H
notoamide B (29)	OH	H	H
notoamide H (30)	OH	OH	H
notoamide N (31)	H	H	Cl

Table 1.2 Structures of the notoamides

Asperparalines are a reduced bicyclo[2.2.2]diazaoctane DKP derivatives (monoketopiperazines - MKPs), sharing a *spiro*-succinimide unit in place of the *spiro*-oxindole or indole (Table 1.3). Asperparaline A (**32**) was isolated^{23,28} in 1997 from the fungus *Aspergillus japonicus* JV-23 and later on in the same group of fungi were also detected asperparaline B (**33**) and C (**34**).²⁹

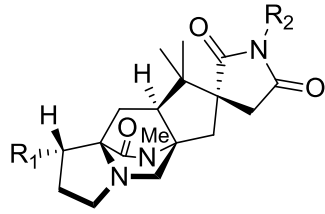
	R ₁	R ₂
	Me	Me
asperparaline A, aspergillimide, (32) (VM55598)	Me	H
asperparaline B (33)	H	OMe
asperparaline C (34)		

Table 1.3 Structures of the asperparalines

Avrainvillamide (**36**) and the stephacidins are a recently isolated group of natural products which attracted the attention of the synthetic chemical community due to their complex architectures as well as their potent biological activity (Figure 1.6). Avrainvillamide (**36**) was first isolated from the marine-delivered fungus *Aspergillus* sp. by Fenical and co-workers³⁰ and a year after from *Aspergillus ochraceus* by Sugie *et al.* who described it as CJ-17,665.^{7c} In 2001, Qian-Cutrone and co-workers reported isolation of stephacidin A (**35**) and B (**39**) from the fungal species *Aspergillus ochraceus* WC76466.³¹⁻³⁴ Isolation of the antipodal stephacidin A (**35**) by Williams *et al.* sparked further interest into biogenesis pathways of these compounds.³² It was originally suggested that these compounds were closely related natural products to the aspergamides A (**38**) and B (**37**) (isolated from *Aspergillus ochraceus* by Fuchser and co-workers)³³ in a different oxidation state. The dimer of avrainvillamide (**36**), stephacidin B (**39**), possessing 15 rings and 9 stereogenic centres represents one of the most complex alkaloids in Nature. Another fascinating architectural feature of avrainvillamide (**36**) and aspergamide A (**38**) is the unsaturated nitronium function, which plays an important role in the dimerization process and the observed potent activity.

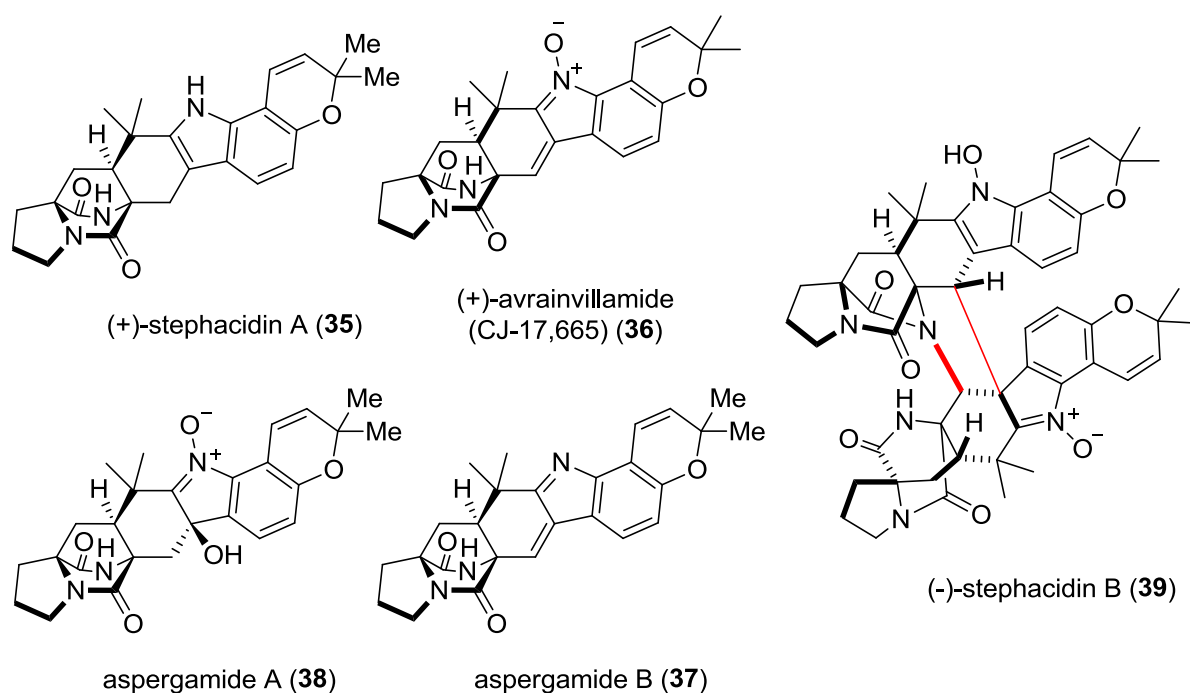


Figure 1.6 Structures of the stephacidins, aspergamides and avrainvillamide

Mata and co-workers increased the number of reported prenylated indole alkaloids by isolating malbrancheamides from *Malbranchea aurantiaca* fungus (Figure 1.7).³⁴ Unique features of malbrancheamide (40) and malbrancheamide B (41) are the chlorinated indole ring and the lack of a tertiary amide in the bicyclo[2.2.2]diazaoctane core ring system.

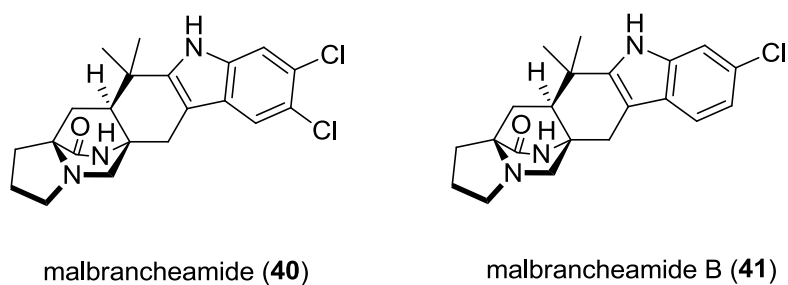


Figure 1.7 Structures of the malbrancheamides

1.3 Origin of the bicyclo[2.2.2]diazaoctane framework

A year after the original isolation of brevianamide A (4) by Birch and Wright,¹⁶ Sammes and Porter proposed that the bicyclo[2.2.2]diazaoctane core arises through a hetero-Diels-Alder reaction (Figure 1.8).³⁵

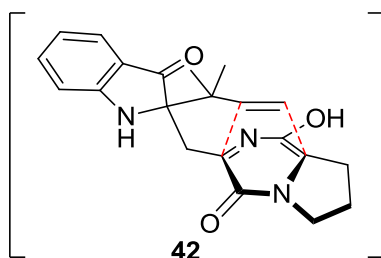
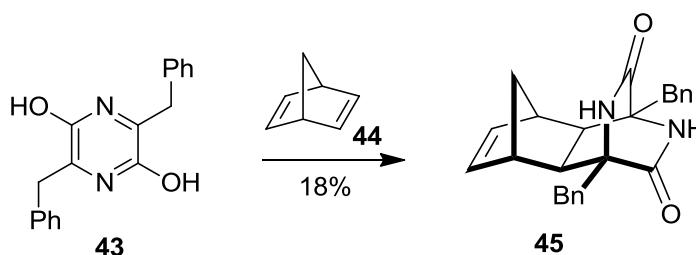


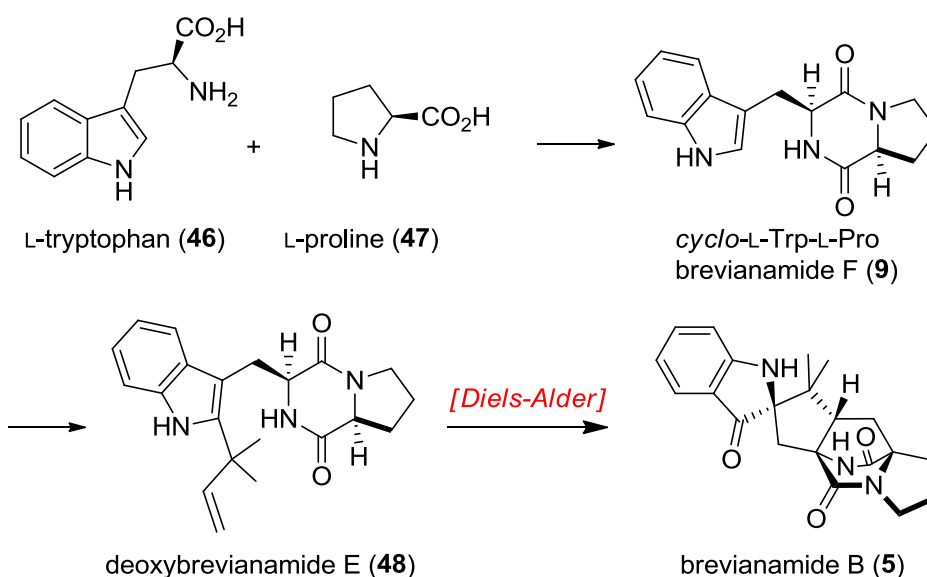
Figure 1.8 Proposed Diels-Alder reaction

In order to support the possibility of this scenario Sammes and Porter tested pyrazine derivative **43** with a selection of dienophiles to effect a Diels-Alder reaction (Scheme 1.1). One of the most relevant examples was cycloaddition reaction of pyrazine **43** with an unactivated dienophile to give **45** in 18% yield.^{35a}



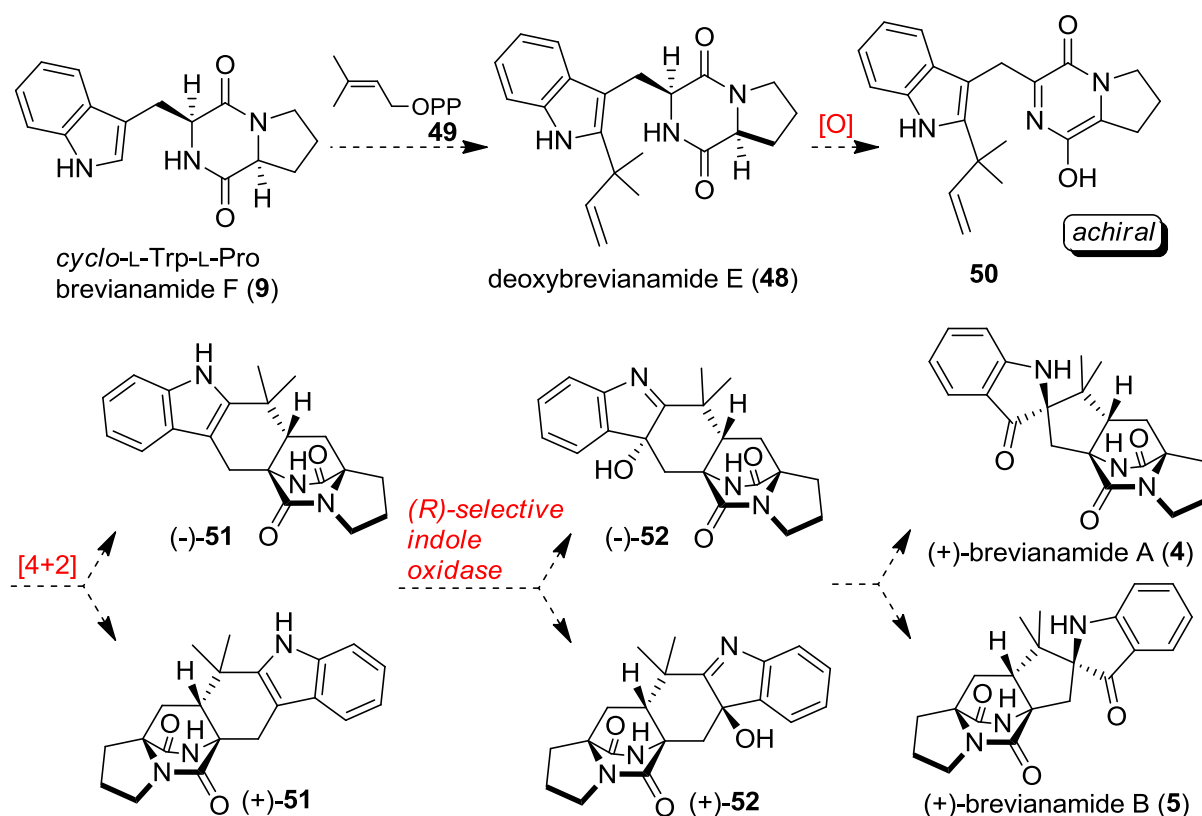
Scheme 1.1

Birch *et al.* proposed a biosynthetic pathway of brevianamide B (**5**) as shown in Scheme 1.2.^{35b} The proposed biosynthesis was based on feeding experiments with ¹⁴C and ³H-labelled compounds and previous reports by Steyn *et al.*³⁶



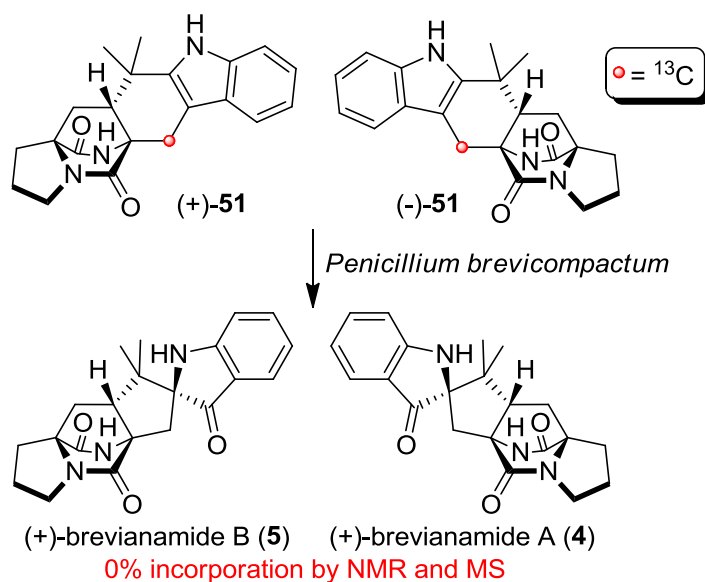
Scheme 1.2

In similar fashion, Williams *et al.* proposed a biosynthetic pathway towards brevianamide A (**4**) and B (**5**) (Scheme 1.3).³⁷ This proposal involves a reverse prenylation of brevianamide F (**9**), followed by oxidation and enolisation to furnish azadiene **50**. Cycloaddition of the achiral **50** would lead to formation of racemic **51** which could undergo an oxidation by an (*R*)-selective indole reduction to give two optically pure, diastereomeric hydroxyindolenines **52**. Finally, stereospecific pinacol-type ring construction would provide the optically pure brevianamides.



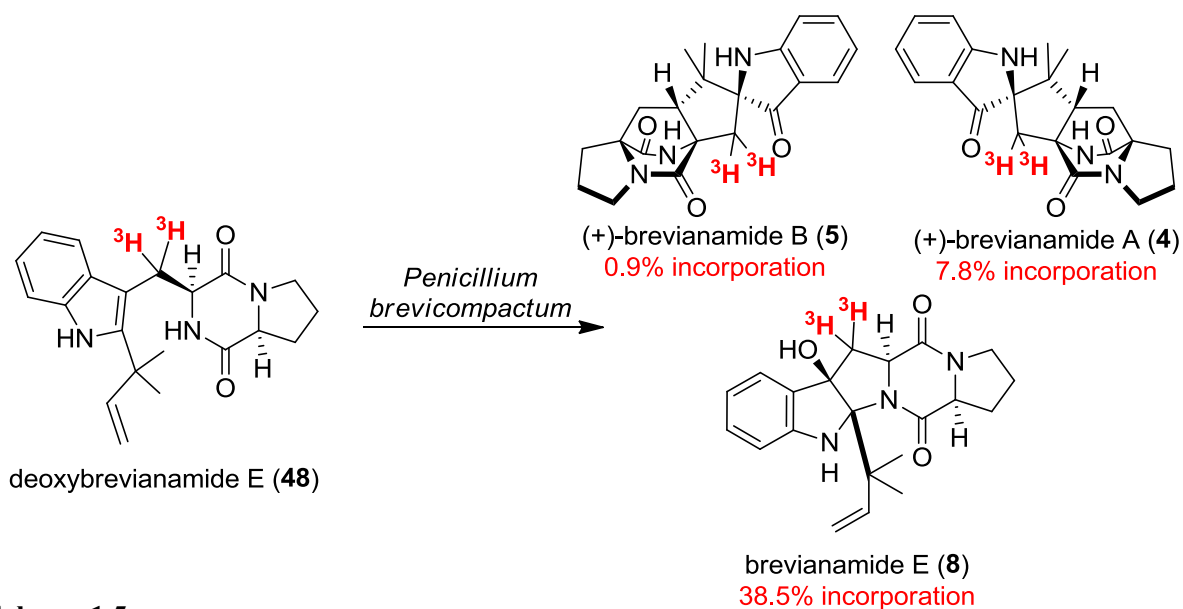
Scheme 1.3

In order to explore this proposed biosynthetic pathway, Williams and co-workers synthesised a racemic mixture of ¹³C-labeled cycloadducts **51** (Scheme 1.4).³⁸ Feeding cultures of *Penicillium brevicompactum* with **51** and further analysis of the extracts by NMR and MS showed 0% incorporation into the natural brevianamides A (**4**) and B (**5**).



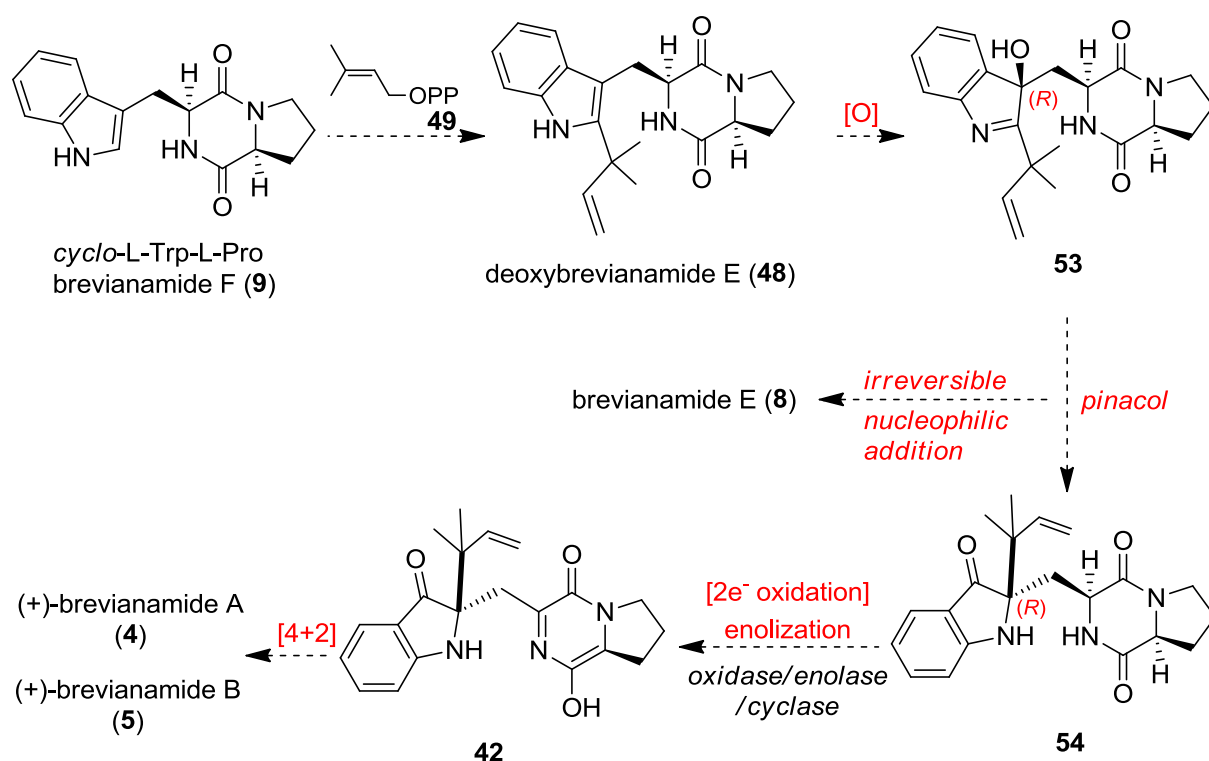
Scheme 1.4

After these results Williams and co-workers envisioned an alternative biosynthetic pathway which involved a tritium-labelled deoxybrevianamide E (**48**) derivative as the initial precursor (Scheme 1.5).³⁸ When cultures of *Penicillium brevicompactum* were fed with **48** incorporation was observed into **4**, **5** and **8** with the most efficient incorporation into brevianamide E. The cultures were then re-fed with brevianamide E (**8**) but in that case they did not observe significant incorporation into brevianamide A (**4**) and B (**5**). This observation suggests that brevianamide E (**8**) is a dead-end, shunt metabolite in this biogenetic pathway.



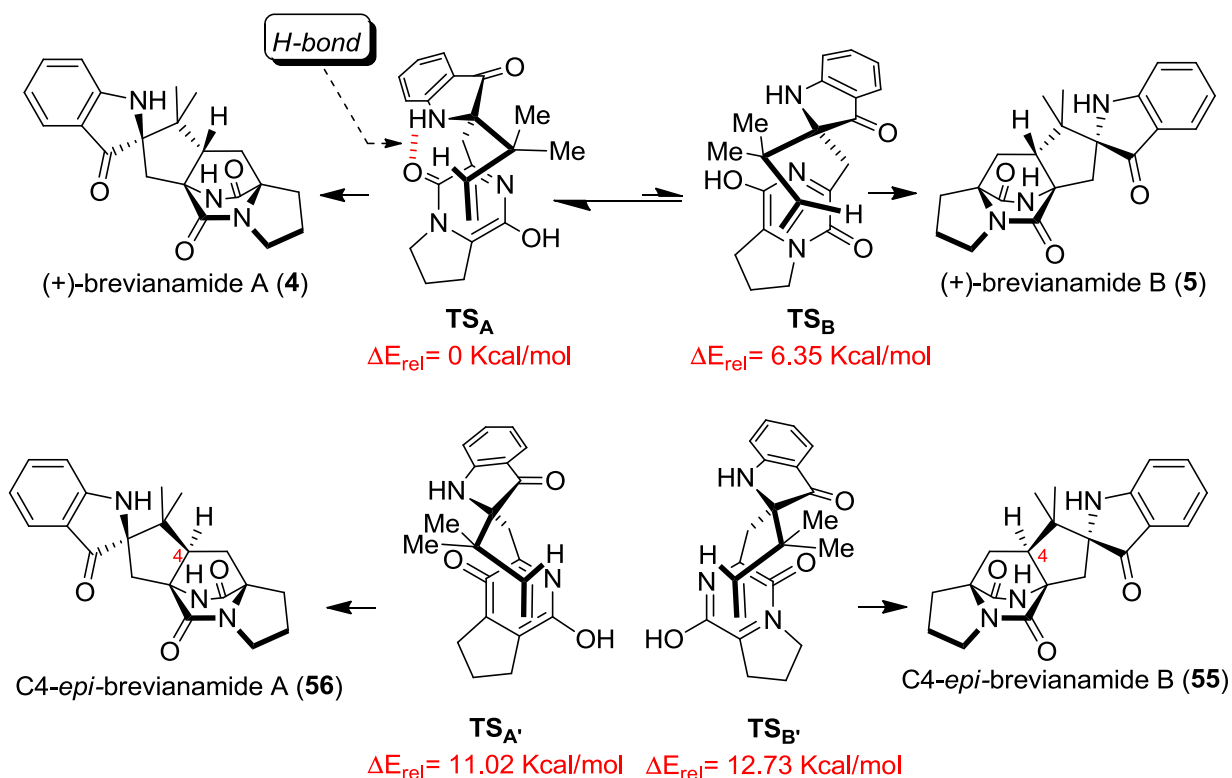
Scheme 1.5

With these results in hand, a new biosynthetic pathway was suggested (Scheme 1.6). As previously described, brevianamide F (**9**) could give deoxybrevianamide E (**48**) via a reverse prenylation. (*R*)-selective oxidation at the 3-position of the indole gives an (*R*)-hydroxyindolenine **53** which undergoes either irreversible nucleophilic addition of the tryptophyl amide nitrogen, generating brevianamide E (**8**), or a stereospecific pinacol-type rearrangement to **54**. Intermediate **54** could undergo two-electron oxidation of the tryptophyl α -carbon, followed by enolisation and intramolecular hetero Diels-Alder reaction to give brevianamide A (**4**) and B (**5**).



Scheme 1.6

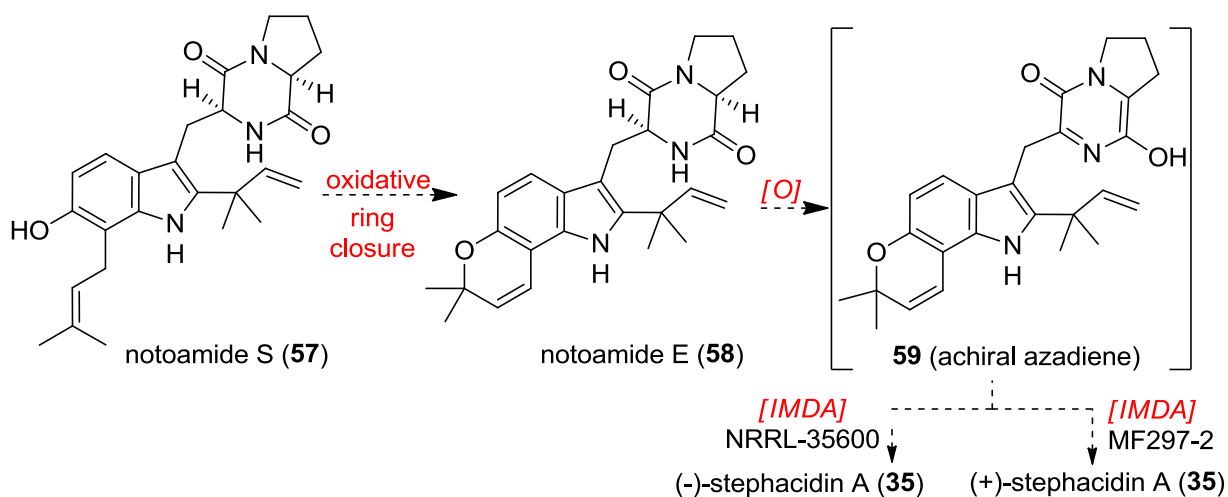
Ab initio calculations were then carried out in order to find further support and explain the outcome of these results (Scheme 1.7). Analysis of calculations showed that the conformers which lead to formation of the natural product had the lowest energy transition-state TS_A and TS_B . Moreover, TS_A was even lower than TS_B due to the hydrogen bonding. The fact that **55** and **56** were not detected in the crude extracts from fungus could be due to the high transition-state energy of $TS_{A'}$ and $TS_{B'}$.



Scheme 1.7

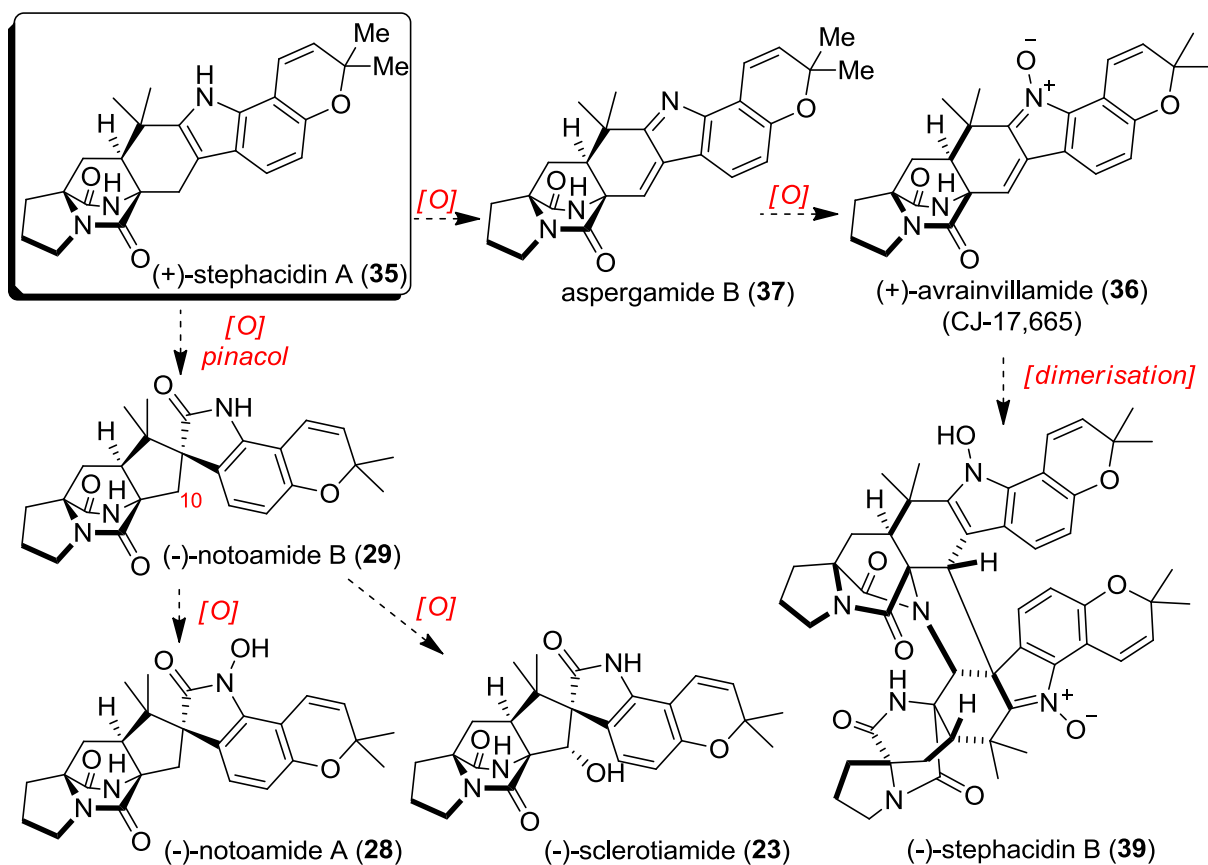
1.4 Stephacidins – The biosynthetic studies

The fascinating molecular architecture of stephacidin B (**39**) provided a new level of complexity within the family of prenylated indole alkaloids. In many cases in biogenesis of prenylated indole alkaloids, Nature can assemble libraries of natural products from only limited panels of starting materials such as tryptophan, proline and isoprene units. Considering the structural similarities, it was initially suggested that stephacidins, avrainvillamide, notoamides, and sclerotiamide consist of natural products with common biosynthetic origins. Williams was also interested to investigate the biogenesis of this family of prenylated indole alkaloids. In recent biosynthetic research, he proposed that oxidative ring closure of notoamide S (**57**) followed by oxidation - tautomerization could generate key *achiral* azadiene species **59** (Scheme 1.8).³⁹ It is known that azadiene species can undergo cycloaddition reactions and presumably **59** could lead to stephacidin A (**35**) in the respective producing organism such as metabolite *Aspergillus* sp. MF297-2⁴⁰ and NRRL 35600.⁴¹



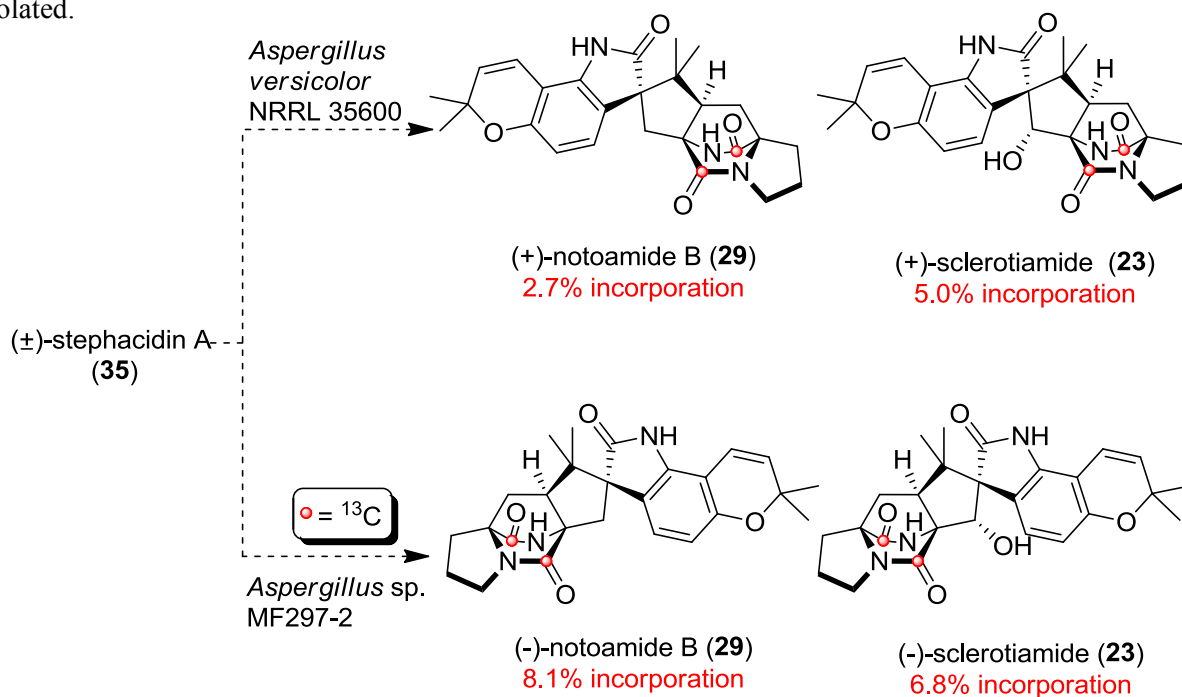
Scheme 1.8

It was also proposed that a face-selective oxidative rearrangement of the 2,3-disubstituted indole (35) would possibly generate notoamide B (29). As Scheme 1.9 shows, notoamide B (29) could undergo a second face-selective oxidation at C10 position to give sclerotiamide (23).⁴²



Scheme 1.9

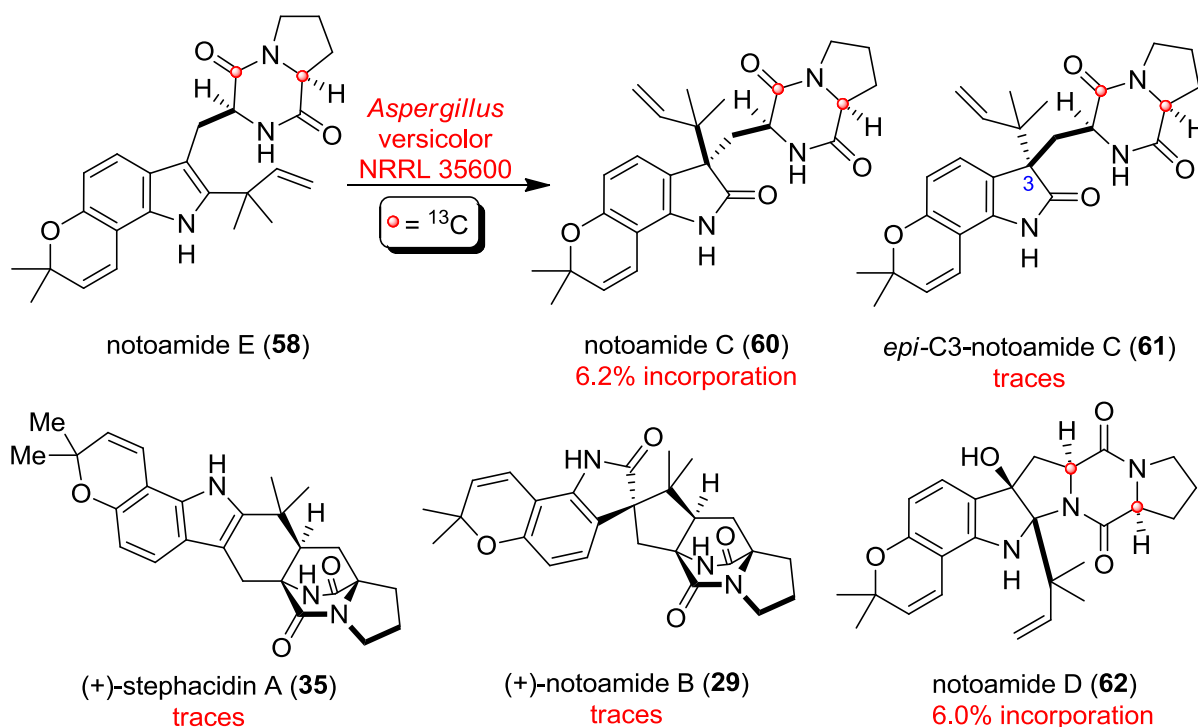
In order to provide new evidence for the biogenesis of notoamide B (**29**) and sclerotiamide (**23**), Williams and co-workers synthesised a ^{13}C labelled analogue of racemic stephacidin A (**35**) (Scheme 1.10).⁴² The racemic mixture was added to cultures of *A. versicolor* NRRL 35600 and the fungal's extracts were then investigated further. Analysis of the samples showed 2.7% intact-incorporation of the labelled (-)-stephacidin A (**35**) into (+)-notoamide B (**29**) and 5.0% incorporation into the metabolite (+)-sclerotiamide (**23**). Unreacted (+)-stephacidin A (**35**) was also isolated. In a similar way racemic stephacidin A (**35**) was also added to the marine-delivered *Aspergillus* sp. MF297-2. The ^{13}C -incorporation into (-)-notoamide B (**29**) was 8.1% and 6.8% into the known metabolite (-)-sclerotiamide (**23**). Similarly with the previous experiment, unreacted (-)-stephacidin A (**35**) was also isolated.



Scheme 1.10

Feeding experiments of *Aspergillus versicolor* NRRL 35600 with synthetic ^{13}C -labeled notoamide E (**58**) showed ^{13}C incorporation into three minor metabolites, **60**, **61**, and **62** (Scheme 1.11).⁴³ In contrast with previous studies,⁴⁴ traces of unlabelled (-)-stephacidin A (**35**) and (+)-notoamide B (**29**) were also detected. It was also reported that the amount of notoamide E (**58**) in *Aspergillus versicolor* affected the ratio of minor and major metabolites. For example, normal feeding conditions of

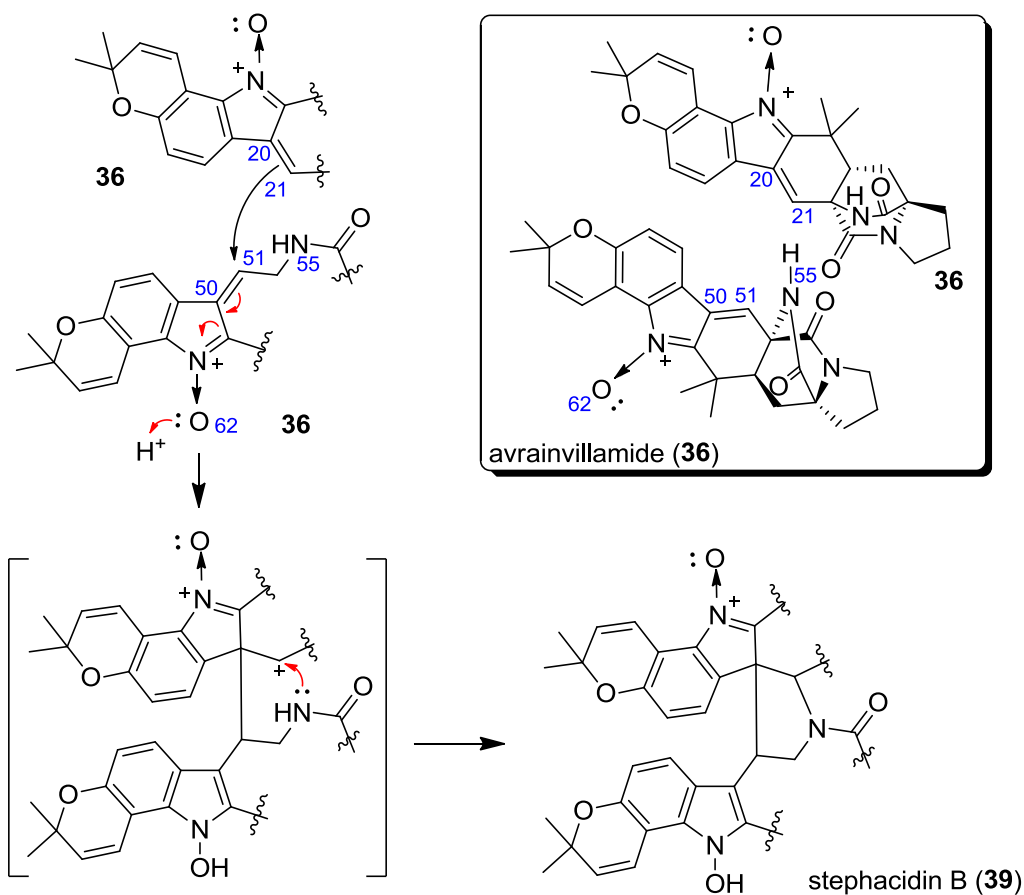
Aspergillus versicolor with notoamide E (**58**), resulted in production of **60**, **61**, and **62** in trace amounts with stephacidin A (**35**) and notoamide B (**29**) being the major metabolites. When an excess of notoamide E (**58**) was added **60**, **61**, and **62** were the major metabolites. This suggests that addition of notoamide E (**58**) inhibits or diverts the enzymatic machinery which is responsible for the biosynthesis of bicyclo[2.2.2]diazaoctane metabolites.



Scheme 1.11

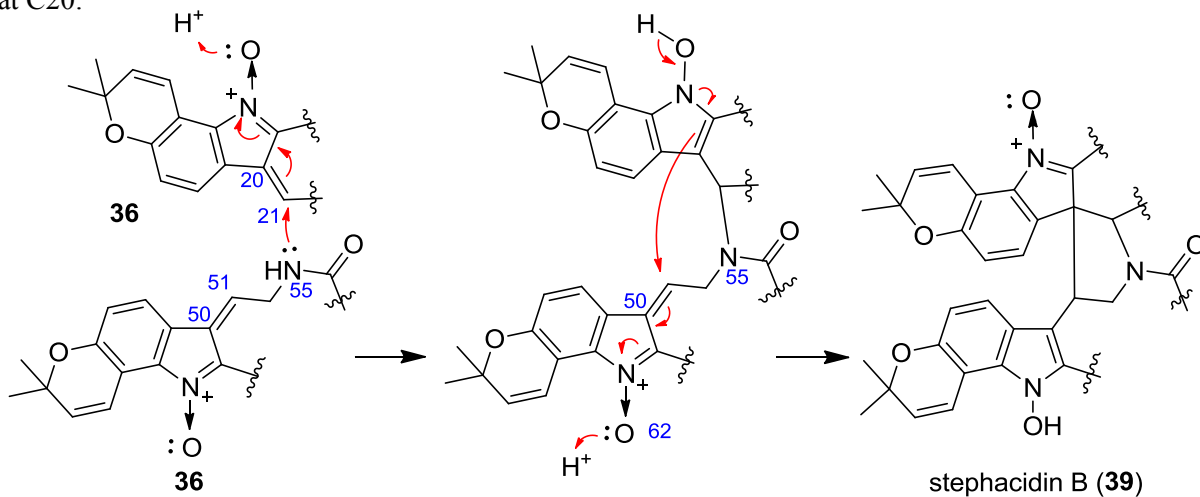
1.5 Avrainvillamide, stephacidin B – The dimerization step

Qian–Cutrone *et al.* from Bristol-Myers Squibb pointed out that Stephacidin B (**39**) probably represents a dimer of avrainvillamide (**36**) (Scheme 1.12).²⁶ They suggested that a protonation at O62 in the monomeric unit could promote a nucleophilic attack at C51 from the C20–C21 double bond of another avrainvillamide unit. Finally N55 could then attack at C21 to form the central 5-membered ring of stephacidin B (**39**).



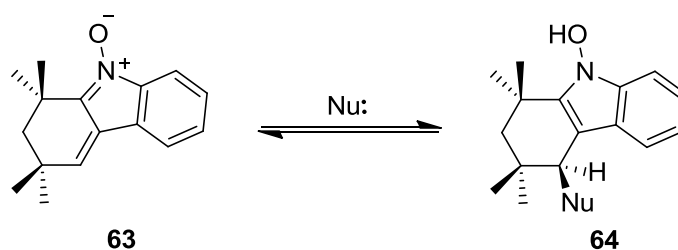
Scheme 1.12

It is also more likely, that the dimerization pathway occurred *via* a double Michael addition rather than the generation of secondary carbocation as an intermediate as previously reported (Scheme 1.13).⁴⁵ Nucleophilic attack of the amidic N55 at the nitron Michael acceptor followed by a subsequent attack of the upper donor to the lower nitron Michael acceptor were the key step to furnish the *spiro*-system at C20.



Scheme 1.13

Based on previous studies,^{45b} Myers and co-workers described the interconversion between the monomer avrainvillamide (**36**) and stephacidin B (**39**) in solution as a reversible process. Myers reported that avrainvillamide (**36**) could be transformed into stephacidin B (**39**) in the presence of triethylamine. The same observation was also reported when a solution of avrainvillamide (**36**) in DMSO-*d*₆-CD₃CN was concentrated in *vacuo*. The dimerization reaction could also occur during the purification process using a preparative TLC method. When pure synthetic stephacidin B (**39**) in MeCN-water was concentrated, a 2:1 mixture of avrainvillamide (**36**) and stephacidin B (**39**) was observed. Moreover, it was also shown that stephacidin B (**39**) was stable in a solution of DMSO-*d*₆-CD₃CN, but when powdered 3 Å molecular sieves were added then a retrodimerisation occurred to give a mixture of **36** and **39**.⁴⁶ Comparison of samples of avrainvillamide (**36**) in solid state and solution showed that the natural product was stable only in solid form and this implies that dimerization could only occur in solution.⁴⁷ The above observations could also be supported by other reports in the literature which describe the ability of saturated indolic nitrones to dimerize.⁴⁸ Further studies by Myers *et al.* showed that **63** in methanol-*d*₄ could undergo a reversible 1,5-addition of solvent to the α,β -unsaturated nitrone group (Scheme 1.14).^{45b} It was also reported that the equilibrium between **63** and **64** exhibited a significant temperature dependence.



Scheme 1.14

Nu= OCD₃, SPh, SC₆H₄OCH₃

Analysis by HPLC shown a half-life 10 minute at 37 °C of stephacidin B (**39**) to avrainvillamide (**36**) which supported that a retrodimerisation process could also occur in cell culture media.⁴⁹ Considering the experimental observations of the equilibrium, Myers and Herzon cast some doubt over which of the alkaloids is responsible for the potent biological activity.

1.6 Avrainvillamide, stephacidin B – Biological activity

The initial biological studies on stephacidins by Qian-Cutrone and co-workers showed that both natural products display potent *in vitro* cytotoxicity against a panel of tumor cell lines (Table 1.4).²⁶ Stephacidin B (**39**) shows significant ability to inhibit the growth of the testosterone-dependent prostate cancer cell line LNCaP at nanomolar concentration. Due to the fact that both compounds were not mediated by p53, mdrl, bcl2, tubulin or topoisomerase II-mediated it was suggested that cytotoxic activity arose by a novel mechanism of action.

Cell-line	Histotype	Characteristic	IC ₅₀ (35)	IC ₅₀ (39)
PC3	prostate	Testosterone-independent	2.10	0.37
LNCaP	prostate	Testosterone-sensitive	1.00	0.06
A2780	ovarian	Parental	4.00	0.33
A2780/DDP	ovarian	Mutp53/bcl2+	6.80	0.43
A2780/Tax	ovarian	Taxol-resistant	3.60	0.26
HCT116	colon	Parental	2.10	0.46
HCT116/mdr	colon	Overexpress mdrl	6.70	0.46
HCT116/topo	colon	Resistance to etoposide	13.10	0.42
MCF-7	breast	Estradiol-sensitive	4.20	0.27
SKBR3	breast	Estradiol- independent	2.15	0.32
LX-1	lung	Sensitive	4.22	0.38

Table 1.4 *In Vitro* Cytotoxicity of (+)-stephacidin A (**35**) and (-)-stephacidin B (**39**), IC₅₀ in μ M

Myers and co-workers investigated further the biological activity of both enantiomers of stephacidin B (**39**) and avrainvillamide (**36**) against four different cancer cell lines (Table 1.5).⁴⁹ It was shown that stephacidin B (**39**) exhibits similar activity with its monomer (**36**) when corrected for stoichiometry (i.e., solutions of **39** were twice as potent as equimolar solutions of **36**). It was also reported that both of the enantiomeric series were similarly active against the specific cell lines.

	Natural enantiomers		Unnatural enantiomers	
Cell line	steph. B (39)	avrainvillamide (36)	ent-steph. B (39)	ent-avrainvil. (36)
LNCaP	135 nM (40-231)	241 nM (159-323)	952 nM (638-1266)	1514 nM (1243-1786)
β T-549	346 nM (321-372)	621 nM (548-694)	550 nM (488-611)	786 nM (717-855)
T-47D	91 nM (30-152)	205 nM (110-299)	942 nM (583-1301)	1485 nM (1305-1655)
MALME-3M	289 nM (108-469)	406 nM (206-607)	987 nM (727-1247)	1854 nM (1750-1957)

Table 1.5 Measured IC₅₀ values for (±)-stephacidin B (**39**) and (±)-avrainvillamide (**36**)

Further evidence supporting that the biological activity of stephacidin B (**39**) arises from the nitron moiety of avrainvillamide (**36**) were also reported by Myers *et al.* (Figure 1.9).⁴⁹ Synthetic analogues **63** and **65** share the structural features of stephacidin B (**39**) and avrainvillamide (**36**) but are incapable of dimerization. Both nitron derivatives **63** and **65** exhibit potent cytotoxicity on LNCaP and T-47D cancer cell lines. These results strongly suggested that avrainvillamide (**36**) was responsible for the biological activity *in vivo*.

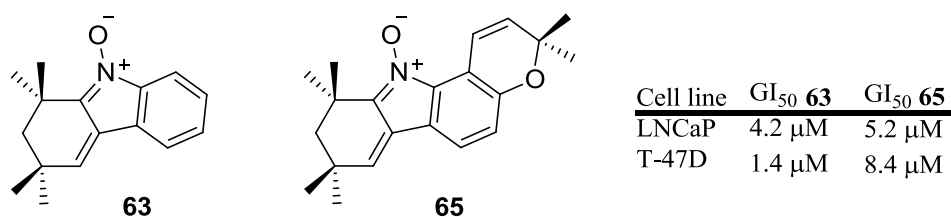


Figure 1.9 Structures of synthetic analogues of avrainvillamide

In their studies Myers and co-workers also examined the possible biological binding targets of the corresponding cancer cell lines. This part was investigated by affinity-isolation experiments with cell lysates from LNCaP cancer cells.⁴⁹⁻⁵⁰ Thus, lysates were treated with activity-based probe **65** and streptavidin-agarose, followed by subsequent purification to isolate several cysteine-containing proteins as possible targets (heat-shock protein 60 -HSP60-, exportin 1 -XPO1, glutathione reductase -

GR-, peroxiredoxin 1 -PRX1-). Compounds **66** and **67** sharing a bicyclo[2.2.2]diazaoctane core were also tested in similar experiments, acting as molecular probes (Figure 1.10). Both compounds showed growth-inhibition potencies against T-47D and LNCaP cancer cell lines. Compound **67** proved to be a more efficient binder to the phosphoprotein nucleophosmin which is an overexpressed protein in many human tumors with an important role in cancer progression.⁵¹ The ability of **67** to bind in a more efficient way than **66** was also proved by the results of competition experiments between **66**, **67** and nucleophosmin. Fluorescence microscopy experiments of dansyl-substituted probe **68** demonstrate that the probe partially localized in the nucleoli of T-47D cells. Compound **67** was also used in order to provide new evidence about the source of binding in nucleophosmin. Studies showed that, when cysteine residues (cys²⁷⁵) were exchanged with mutant alanine, the nucleophosmin binding to **67** was significantly reduced.

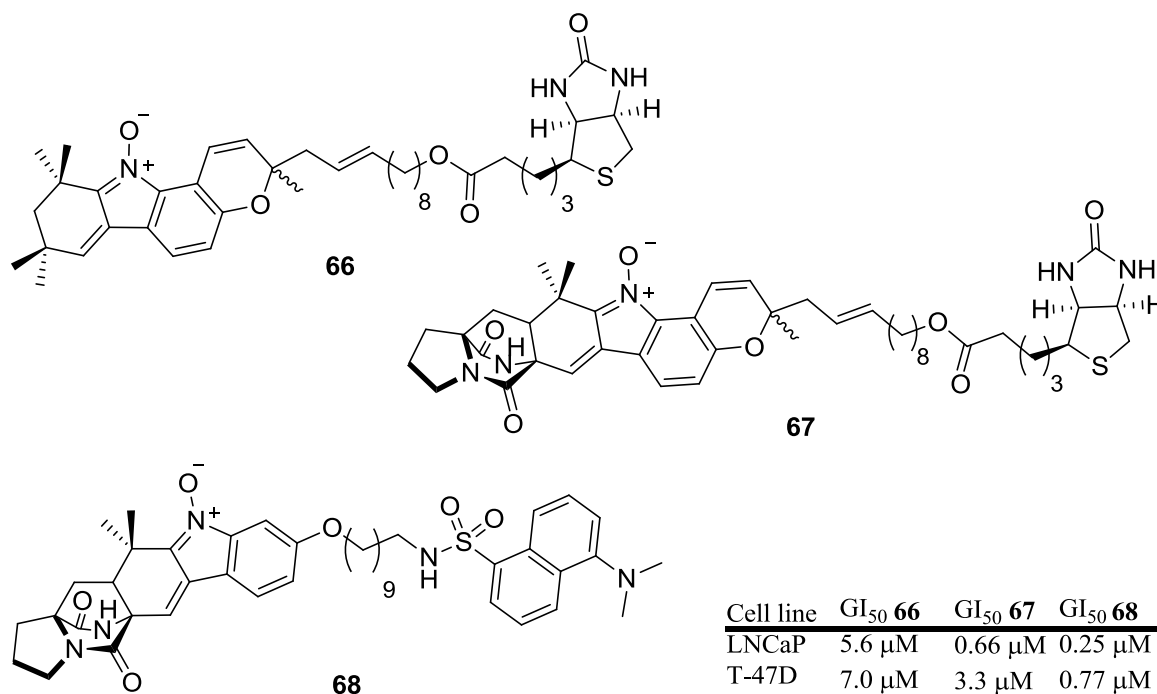


Figure 1.10 Structures of synthetic analogues of avrainvillamide

Finally, it was demonstrated that changes in the chromene moiety could affect the biological activity.⁵⁰ Examination of the synthetic analogues **70**, **71** and **72** showed lower activities compare with **67** and **68** (Figure 1.11). The only case where the biphenyl moiety did not affect the inhibition of the molecule was observed with compound **69**.

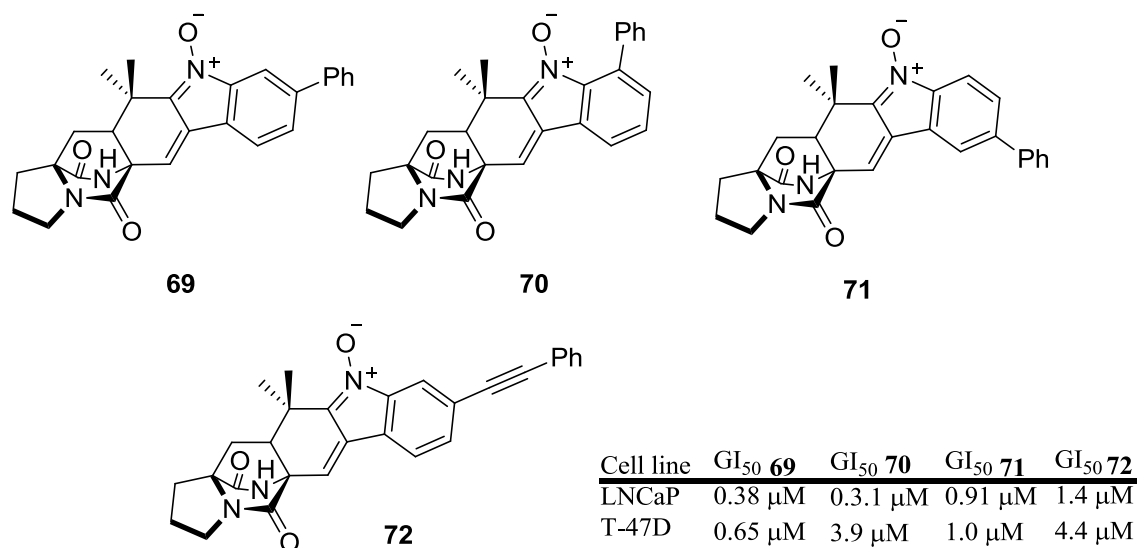


Figure 1.11 Structures of synthetic analogues of avrainvillamide

The unusual structures and in some cases potent biological activity have made the prenylated alkaloid family important and challenging targets for synthetic and biosynthetic studies. Since the first isolation of brevianamide A (**4**), there has been significant progress towards giving access to these synthetically complex structures. However, much work is left to be done before we have a full understanding of the biosynthetic pathways.

Chapter 2

Synthesis of fused DKP and MKP

2.1 Marcfortines, paraherquamides and asperparalines

Marcfortines A–C (**25–27**), paraherquamides A (**10**), C (**12**), E (**14**), F (**20**) and asperparalines A (**32**) and B (**33**) constitute part of an interesting class of structurally related prenylated alkaloids, sharing a bicyclo[2.2.2]diazaoctane core system equipped with *spiro*-oxindole or *spiro*-succinimide units (Figure 2.1).

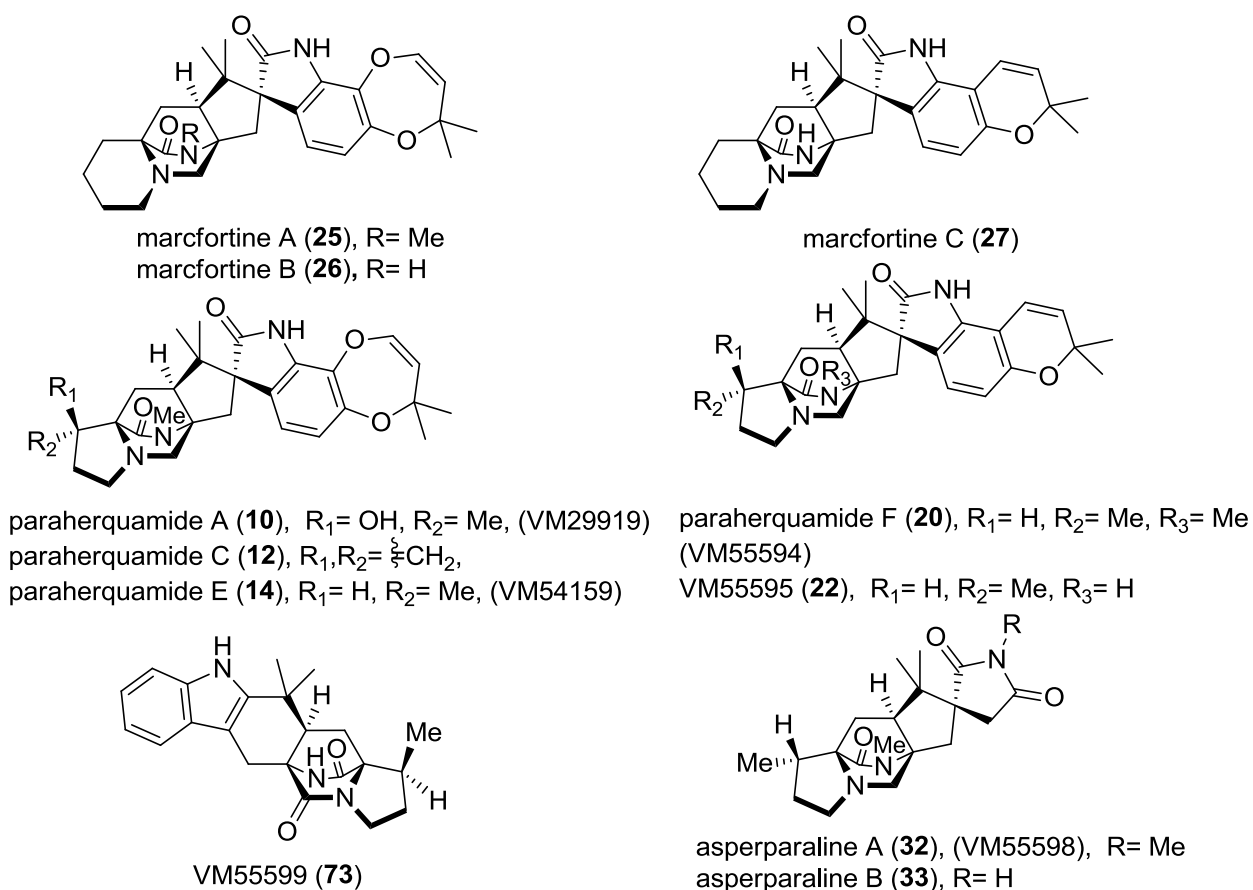
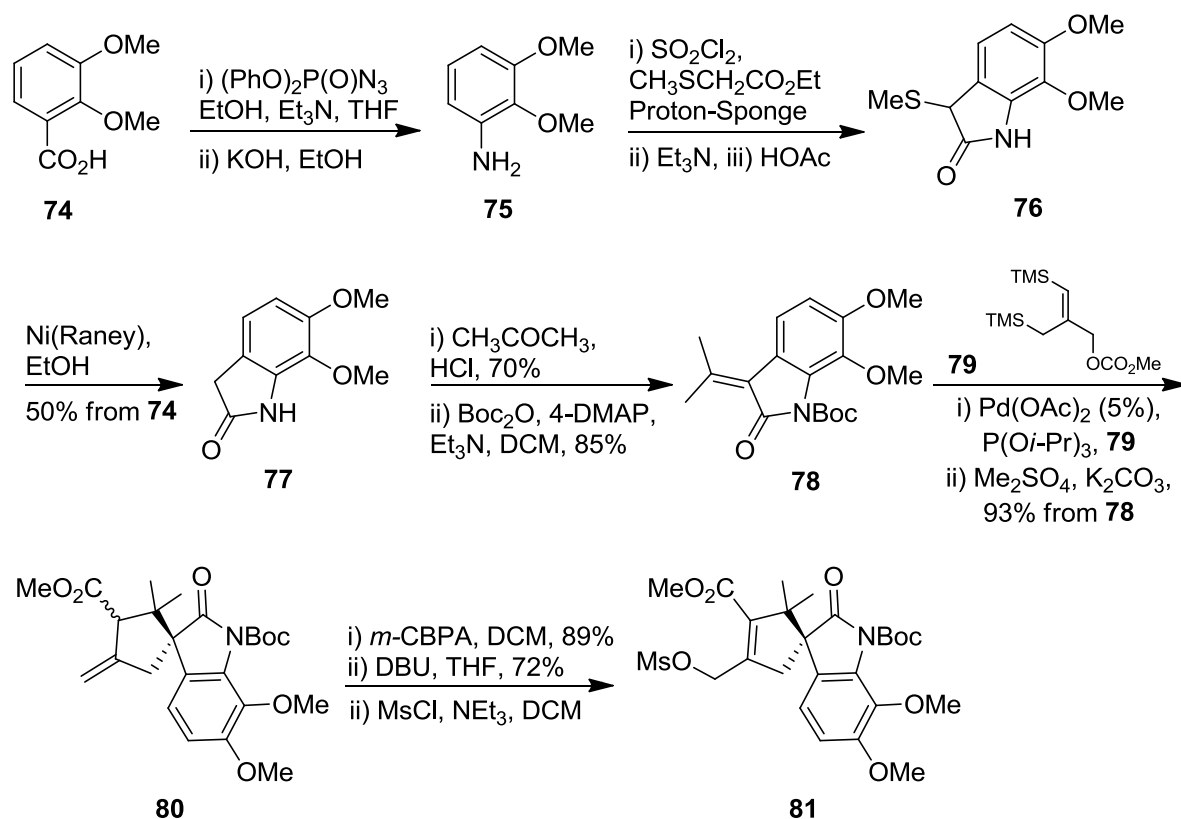


Figure 2.1 Structures of the paraherquamides, marcfortines and asperparalines

Another common structural feature of paraherquamides and asperparalines includes an interesting β -methylproline motif which can be delivered biosynthetically from isoleucine. Unlike with paraherquamides and asperparalines, marcfortine A (**25**) and B (**26**) possess an unsubstituted six-membered ring instead of proline, which initially can be delivered from pipecolic acid.

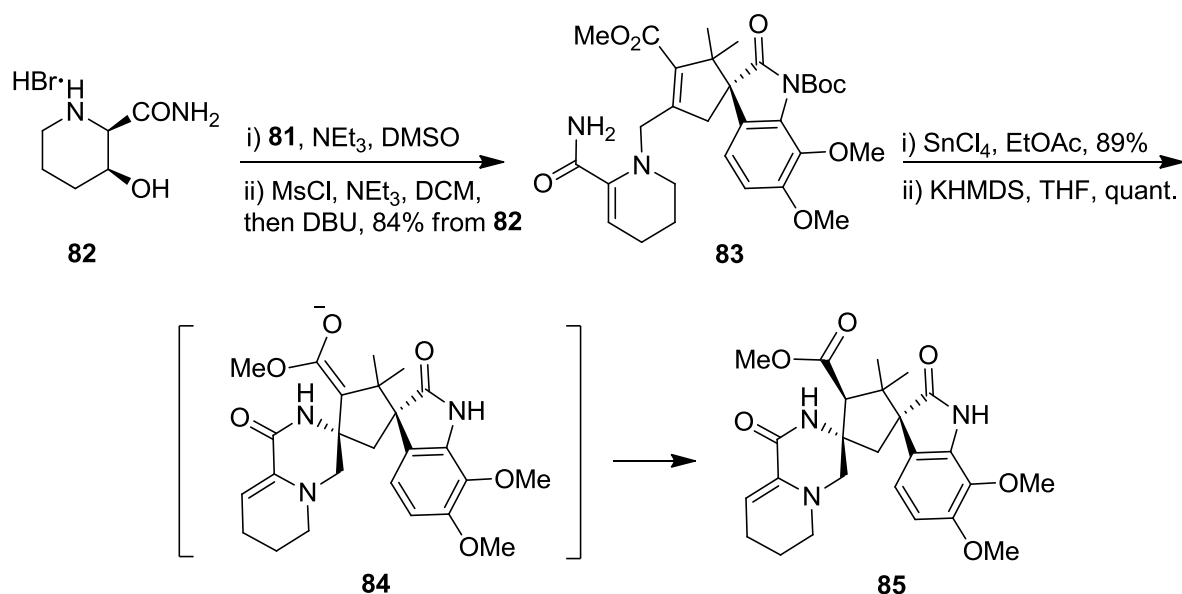
2.2 Synthesis of the pipecolate moiety

Trost and co-workers became interested in this subclass of prenylated indolic alkaloids as their previous research on trimethylenemethane (TMM) [3+2]-cycloadditions was able to assemble the common structural features of these natural products.⁵² In the first total synthesis of (\pm)-marcfortine B (**26**), the core ring system was delivered by an alkylation of 2-hydroxy-pipecolic amide (**82**) and oxindole (**81**), followed by an intramolecular Michael-Addition and a radical ring closure (Scheme 2.2).⁵³ Thus, 2,3-dimethoxybenzoic acid **74** was converted to aniline **75** via a Yamada modification of the Curtius rearrangement followed by hydrolysis of the resulting urethane (Scheme 2.1).⁵⁴ In the presence of sulfuryl chloride, aniline **75** was chlorinated and then reacted with ethyl (methylthio)acetate. The heterocyclic ring of **76** was formed after rearrangement in the presence of triethylamine followed by acetic acid. Desulfurization of oxindole **76** followed by condensation and Boc protection led to formation of the TMM-acceptor **78**. Similarly with previous studies⁵⁵ by Trost *et al.* a spirocyclic carboxyl acid was generated by carboxylative cycloaddition of **78** and **79**. The corresponding acid was then converted to the corresponding methyl ester **80**. Epoxidation of the exomethylene double bond of **80** followed by subsequent exposure to DBU yielded an allylic alcohol which was then transformed to mesylate **81**.



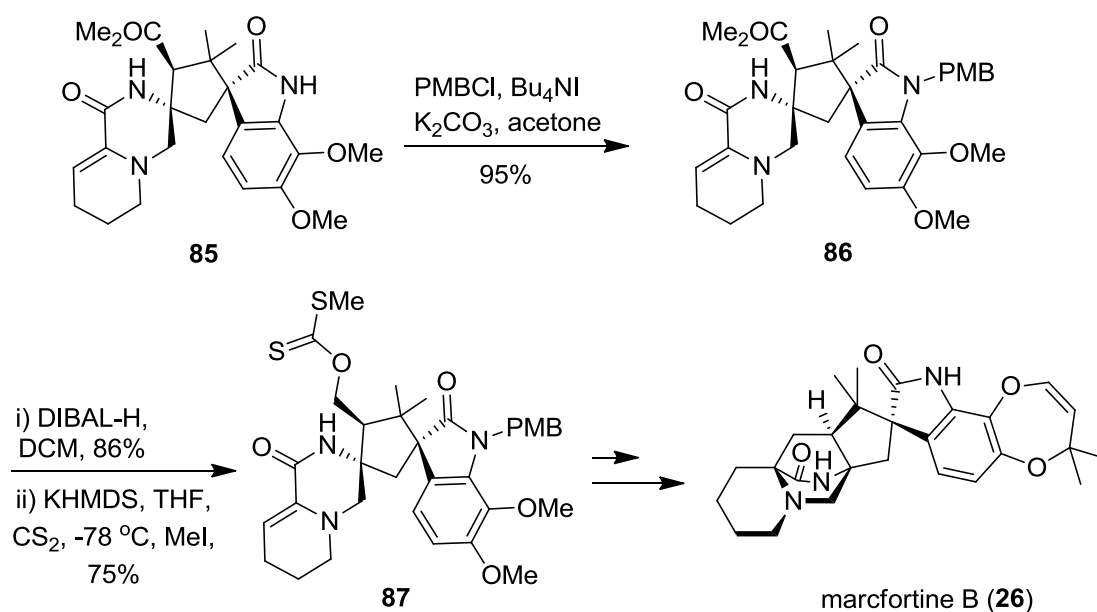
Scheme 2.1

N-Alkylation of **82** with **81** followed by elimination of the secondary alcohol of the piperidine ring yielded the α,β -unsaturated amide **83** in 84% overall yield (Scheme 2.2). It was shown that *N*-Boc deprotection of the *spiro*-oxindole **83** prior to Michael-addition was necessary in order to avoid decomposition during the cyclisation step. Michael-addition of the free oxindole resulted in formation of only one diastereomer of **85** due to the efficient shielding of the *re*-face by the aromatic portion of the Michael acceptor. The corresponding enolate **84** was protonated by the amide hydrogen atom to deliver the *trans* relationship into the ester **85**. The validity of their explanation for the observed stereocontrol was supported when the reaction was repeated on the *N*-methylated amide derivative of **83** and they obtained exclusively the other epimeric ester.



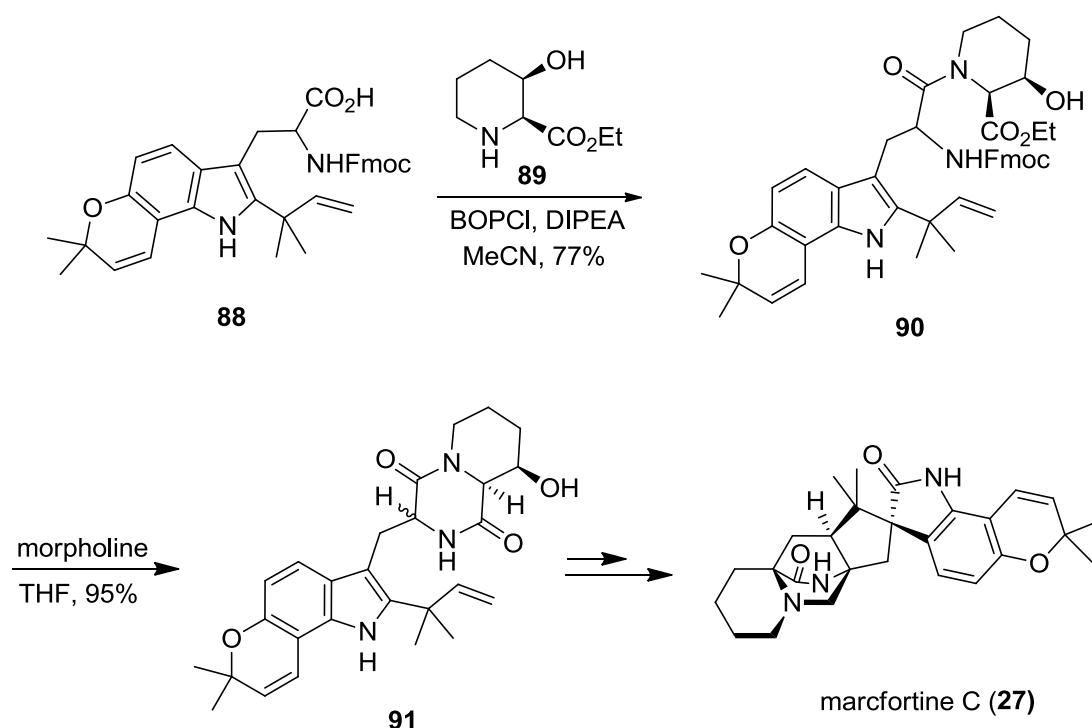
Scheme 2.2

In order to improve the solubility of compound **85**, oxindole unit was protected with *p*-methoxy benzylbromide (Scheme 2.3). Chemoselective reduction of ester **86** with DIBAL, followed by conversion of the corresponding alcohol to its xanthate ester gave **87**. The key step for the synthesis of marcfortine B (**26**) involved a radical cyclisation and is being discussed in detail in Chapter 4.⁵³



Scheme 2.3

In the synthesis of (±)-marcfortine C (**27**), Williams and co-workers chose a DKP (**91**) equipped with a fused pipecolate unit as a key intermediate to access the natural product (Scheme 2.4).⁵⁶ In order to prepare intermediate **91**, peptide coupling was applied to tryptophan derivative **88** and pipecolic acid ethyl ester **89**. The resulting diastereomeric mixture of amides **90** was then treated with a solution of morpholine in THF to promote *N*-Foc deprotection and an intramolecular cyclisation between the free amine and the ester group occurred to give the desired DKP **91** as a mixture of diastereoisomers.

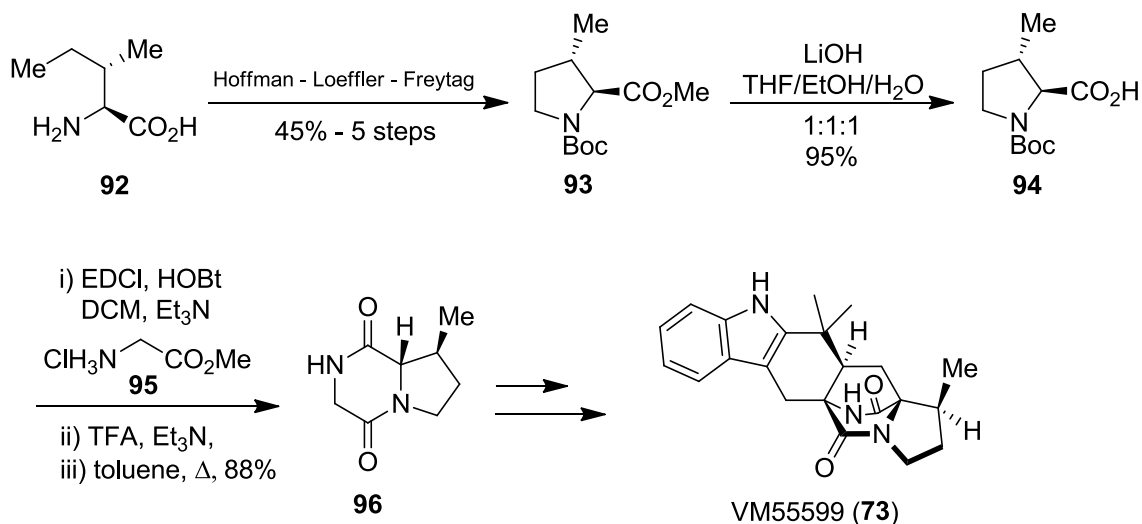


Scheme 2.4

2.3 Synthesis of β -methylproline moiety

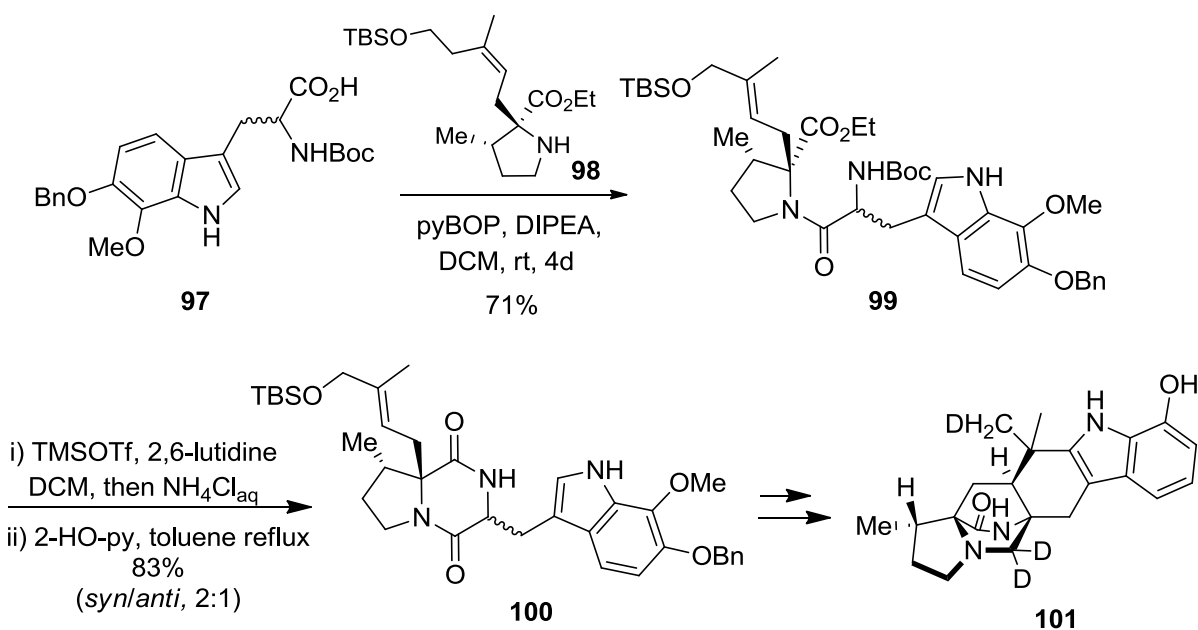
The methyl group in the β -methylproline moiety of VM55599 (**73**) is disposed *syn* to the bridging unit. In all the other isolated prenylated alkaloids the observed stereochemistry in the β -methylproline moiety is *anti*. In extensive investigation on the biosynthetic proposal of VM55599 (**73**) and paraherquamide A (**10**), Williams established the unknown absolute configuration of VM55599 (**73**).⁵⁷ For the asymmetric total synthesis of **73**, Williams and co-workers envisioned installing the β -methylproline ring in such a manner that the stereogenic centre at β -position would not be perturbed.

Enantiopure β -methylproline **93** was delivered in five steps using the Hoffman – Loeffler – Freytag sequence,⁵⁸ starting from (*S*)-isoleucine (L-Ile) (**92**) (Scheme 2.5). Hydrolysis of proline **93** with LiOH gave acid **94** which was then coupled with glycine methyl ester hydrochloride to furnish the corresponding peptide. Treatment with TFA effected removal of Boc group and the crude material was heated in toluene to afford the desired DKP **96**.



Scheme 2.5

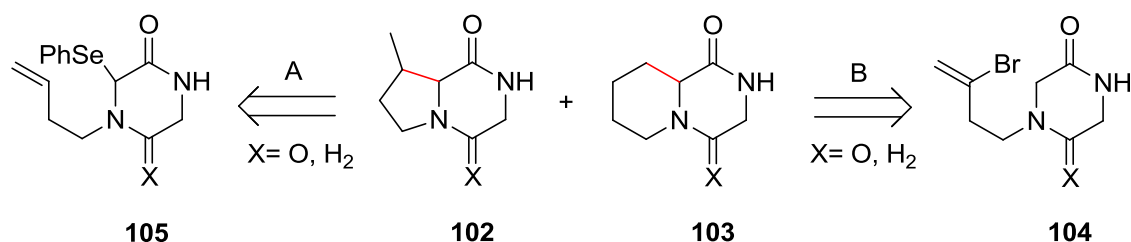
Williams and co-workers also synthesised a deuterium-labelled derivative to investigate biosynthesis of paraherquamides. DKP **100** was synthesised starting from enantiopure proline derivative **98** (Scheme 2.6). Peptide coupling of **98** with a modified tryptophan **97** furnished peptide **99**. Selective removal of Boc group followed by thermal cyclisation of the corresponding amine gave **100** as a 2:1 (*syn:anti*) mixture of diastereomers.



Scheme 2.6

2.4 Retrosynthetic plan

Our interest to deliver new approaches for the synthesis of prenylated indole alkaloids prompted us to investigate the possibility of assembling the bicyclic fused system of these natural products via a radical approach. Thus, our retrosynthetic plan for the fused bicyclic DKPs or partially reduced derivatives (MKPs) **102** and **103** involved a key disconnection of the C–C bond as Scheme 2.7 shows. According to disconnection A the desired products **102** and **103** could be delivered via an intramolecular radical cyclisation of a precursor equipped with a leaving group at the α -amidic position (**105**). Alternatively, the same C–C bond could be formed by radical translocation and cyclisation of **104**.



Scheme 2.7 Retrosynthetic plan of the radical key step

Firstly, we were interested in investigating the regioselectivity of the radical cyclisation reaction on simple DKP and MKP substrates. The aim of this project included the application of this methodology to enantiopure substrates such as **106** and **107** and further investigation of the stereoselectivity of the outcome (Figure 2.2). This strategy in combination with established work⁵⁹ from our lab on construction of the bicyclo[2.2.2]diazaoctane framework would allow access to other important members of this alkaloid family.

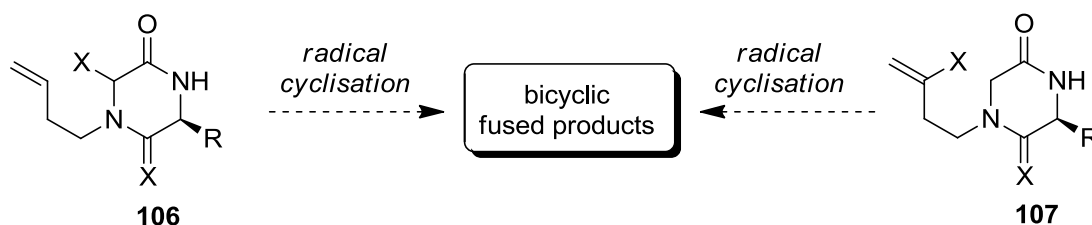
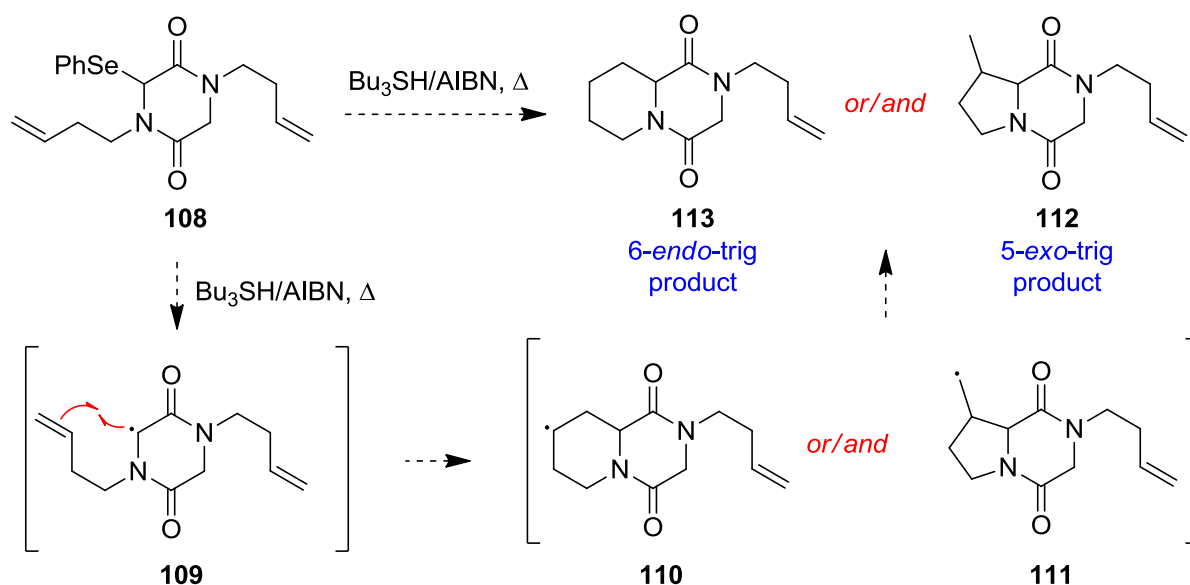


Figure 2.2 Radical cyclisation of enantiopure DKP and MKP substrates

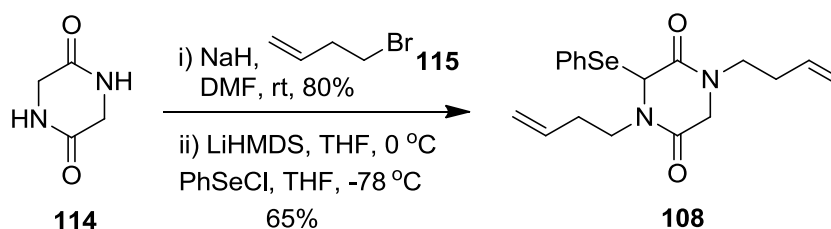
2.5 Radical cyclisation of DKP and MKP substrates

The first example investigated involved DKP **108**, which contains a phenylselenenyl group (Scheme 2.8). In the presence of tributyltin hydride and AIBN, captodative radical **109** would be formed by homolytic cleavage of the phenylselenenyl group. The corresponding radical species could then react with the double bond in the *N*-substituent via a 6-*endo*-trig or 5-*exo*-trig cyclisation to give **112** and **113**.



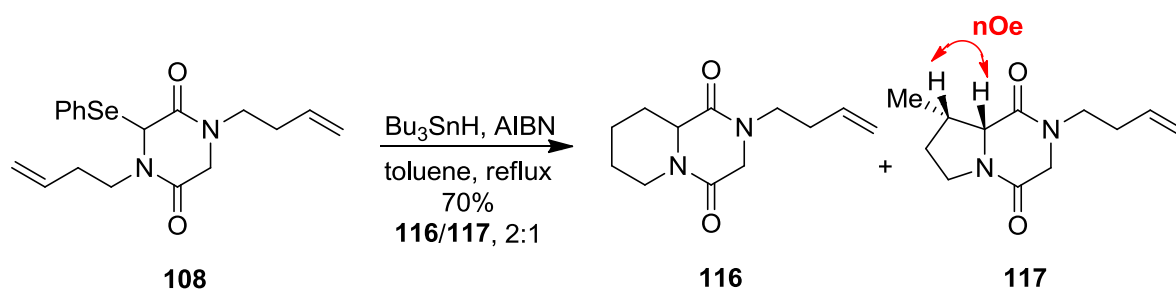
Scheme 2.8

The radical precursor **108** was easily synthesised in two steps via a double *N*-alkylation of glycine anhydride **114** followed by introduction of the phenylselenenyl group (Scheme 2.9).



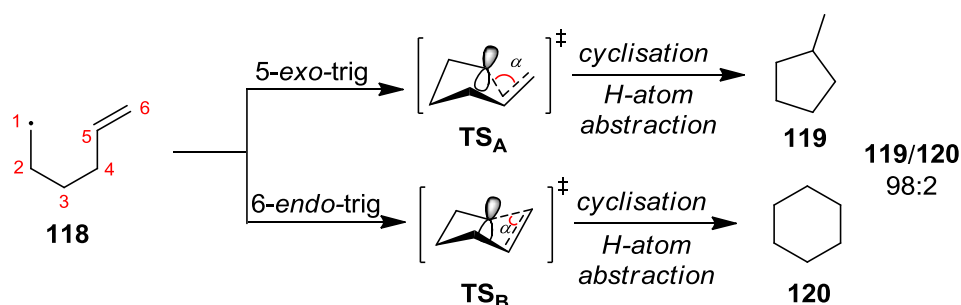
Scheme 2.9

Compound **108** in toluene was treated with tributyltin hydride and AIBN over 8 hours (Scheme 2.10). After purification of the crude material we were able to obtain DKPs **116** and **117** in 2:1 ratio and 70% overall yield. We were pleased to confirm by nOe studies that the β -methyl on the proline unit was placed with the same stereochemistry as that most of reported prenylated indole alkaloids. Surprisingly the major product of this reaction was the thermodynamic product **116** from 6-*endo*-trig cyclisation rather than the kinetic product **117** from 5-*exo*-trig cyclisation as Baldwin rules suggest.⁶⁰



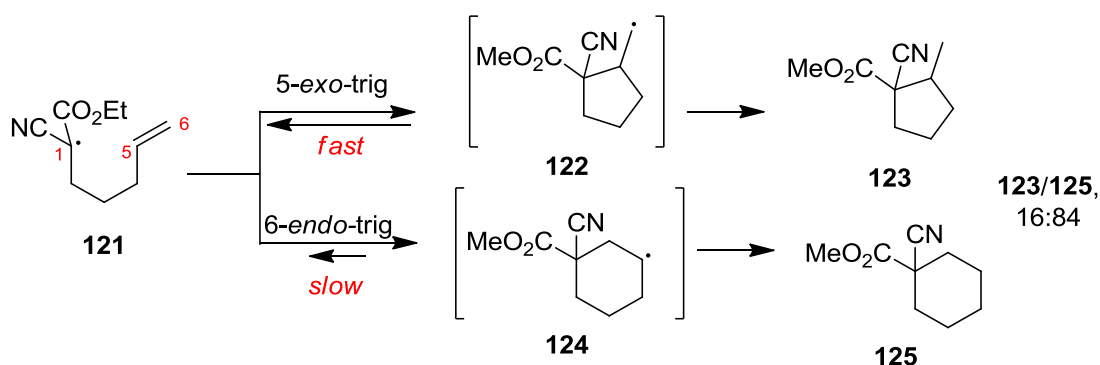
Scheme 2.10

Frontier orbital theory can explain much of the selectivity in radical reactions.⁶¹ Beckwith has pointed out the stereoelectronic effects which can contribute to the regioselectivity of radical cyclisation.⁶² It is known that radical centres attack at an obtuse Bürgi-Dunitz-like angle⁶³ the carbon atom with the largest LUMO coefficient. The intramolecular radical cyclisation of **118** proceeds via an unsymmetrical 6-membered chair-like transition state (Scheme 2.11). The most preferable approach occurs via TS_A (5-*exo*-trig) where the angle α is similar to the value of the Bürgi-Dunitz angle. Thus, due to better LUMO-SOMO orbital overlap, 5-*exo*-trig product (**119**) forms faster than the thermodynamically more stable 6-*endo*-trig product (**120**).^{60-61,62a,64} The 6-*endo*-trig pathway is not explicitly disfavoured but it is usually more strained than the corresponding 5-*exo*-trig.



Scheme 2.11

There are number of cases where the 6-*endo*-trig product is favoured.^{64b,65} One example involves substrates with *Z*-substituents^{64b,66} (electron-withdrawing groups), such as **121** (Scheme 2.12).⁶⁷ The 5-*exo*-trig cyclisation of the stabilised radical **121** occurs faster than the 6-*endo*-trig and gives primary radical **122**. Under the reaction conditions the 5-*exo*-trig process could be reversible and the latter of **122** could open again to give the thermodynamically preferred secondary radical **124**.



Scheme 2.12

Radicals adjacent to Z-substituents (**121**, Scheme 2.12) (carbonyl, cyano, nitro, carboxyl, metals and metalloids such as silyl groups) are electrophilic radicals with low-energy SOMO orbital (Figure 2.3). In that case, SOMO orbital will interact with HOMO orbital of alkene. Alternatively, when radicals adjacent with X-substituents (methoxy, amino, alkyl) or hydrogen atoms (**118**) (Scheme 2.11), the π -bond will interact more with LUMO orbital of the alkene (Figure 2.3). Finally, when the radical centre is substituted by an aryl group then the substituents to the aromatic ring are able to influence the interaction between the SOMO and HOMO or LUMO of alkene.⁶⁸

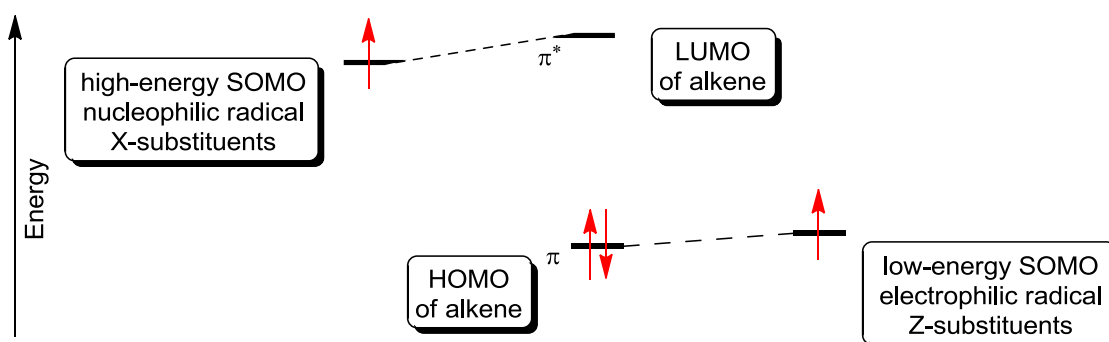
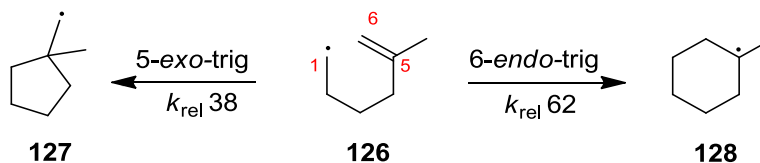


Figure 2.3 Frontier orbital interaction of an electrophilic and nucleophilic radical with alkene

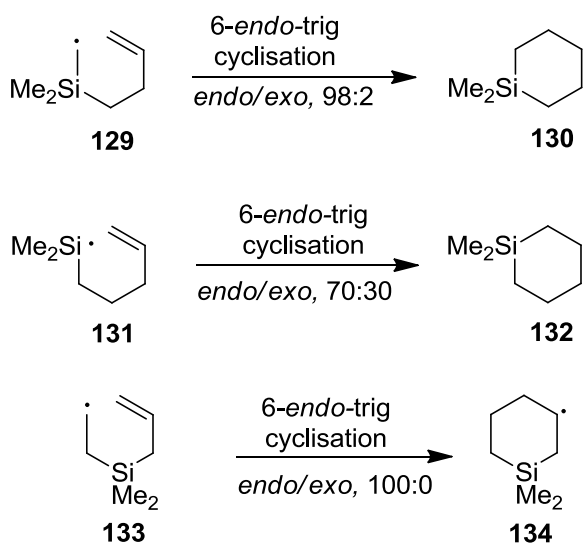
Radical cyclisation of 1,1 disubstituted terminal olefins such as **126** could also lead to 6-endo-trig products (Scheme 2.13) due to steric effects. Addition of radical **126** occurs faster via 6-endo-trig pathway by a factor of 1.6 ($k_{\text{rel-endo}}/k_{\text{rel-exo}}$) to give the more stabilized radical **128**.⁶⁹ When substituents

are placed on the terminal carbon (C6) of the double bond, the 5-*exo*-trig cyclisation is favoured compared to the 6-*endo*-trig process.⁷⁰



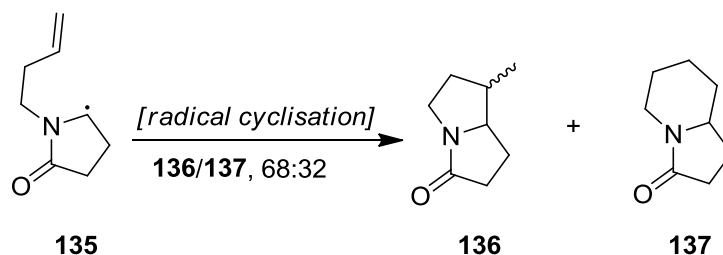
Scheme 2.13

Another category in which 6-*endo*-trig is favoured, involves silicon-containing radicals such as **129**,⁷¹ **131**^{70b,70c,71} and **133**⁷¹ (Scheme 2.14). The regioselective outcome in that case could arise by the presence of Si–C bond. The relatively long length of the Si–C bond reduces the strain of the 6-*endo*-trig transition state and allows better orbital overlapping. Moreover, the silicon group in radical **129** consists of a Z-substituent which will promote a 6-*endo*-trig addition.



Scheme 2.14

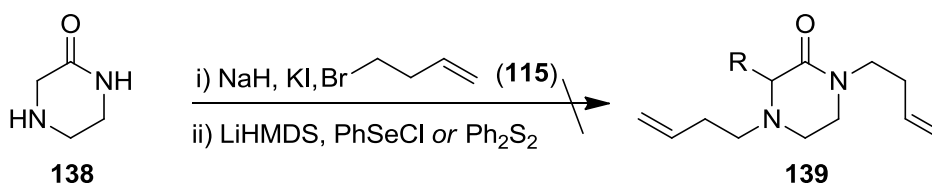
In a similar manner, radical cyclisation of substrates, such as **135**, containing amido groups also leads to formation also of the *endo* products **137** (Scheme 2.15).⁷² These examples are important for comparison with our substrate, DKP **108** (Scheme 2.10), in which we were also observed formation of 6-*endo* product.



Scheme 2.15

We believed that regioselectivity in cyclisation of **108** (Scheme 2.10) was mainly affected by the geometrical restriction of the DKP ring which has four sp^2 and two sp^3 centres. The nature of the sp^2 nitrogen centre increases the planarity of the *N*-substituent while the presence of carbonyl groups also contributes to the ring's low flexibility. Careful examination of molecular models showed that the terminal double bond is disposed at a disfavoured distance from the radical centre which would probably contribute to an inefficient SOMO-HOMO overlapping.

In order to examine the contribution of steric effects of the DKP core on the regioselectivity for this reaction we decided to synthesise the MKP analogue **139** (Scheme 2.16). Compound **139** possesses only one carbonyl group which would enable a more flexible transition state and would possibly allow a more efficient overlapping between the orbitals. Double *N*-alkylation of **138** with 4-bromo-1-butene gave the corresponding *N*-alkylated MKP in 52% yield but unfortunately the following substitution step with phenylselenenyl chloride or diphenyl disulfide was not successful.

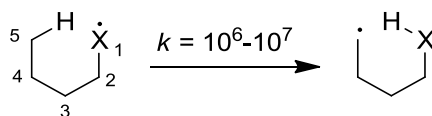


Scheme 2.16

Another possible synthetic way to generate radical centres at positions where the introduction of a group such as a halogen atom or SPh or SePh is restricted, involves intramolecular hydrogen-atom translocation (HAT). Position five from the radical centre is usually favoured for H-atom transfer due

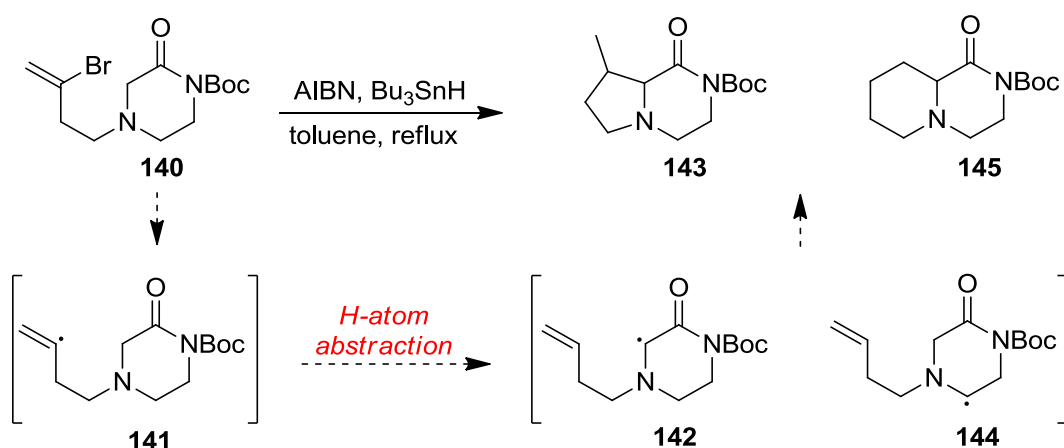
to favoured distance and angle of X – H – C (180°) which allows such a process (Scheme 2.17).⁷³

When 1,5-H abstraction could not occur then 1,6 or 1,7 abstractions maybe be observed.



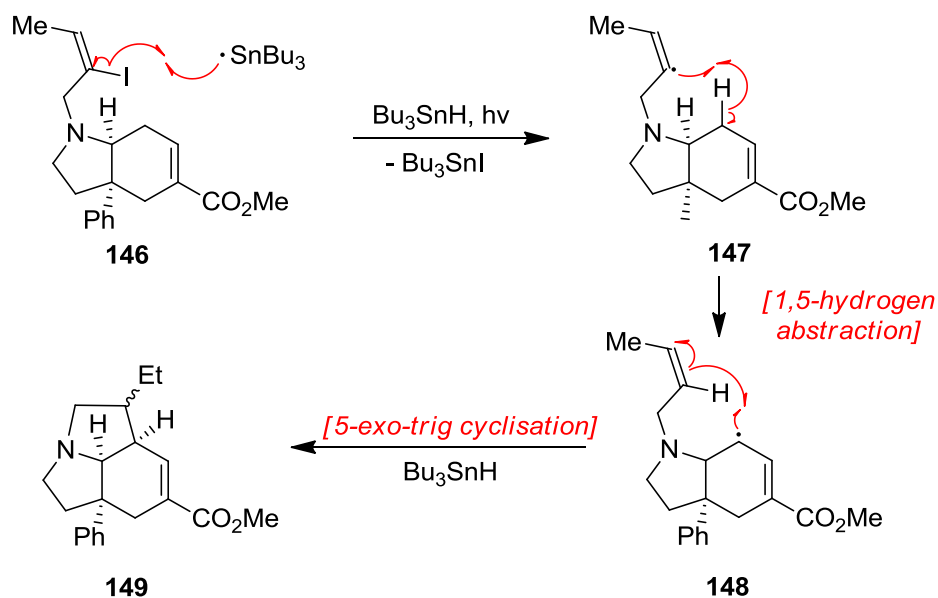
Scheme 2.17

Given the failure of the preparation of **139**, an alternative precursor compound **140** was prepared (Scheme 2.18). Unlike DKP **139**, the mechanism for radical cyclisation of **140** would involve generation of an alkenyl radical centre (**141**) which would translocate to generate a new radical centre (**142**) and/or, (**144**). We expected that the abstraction of the hydrogen atom would occur on C5 position from the alkenyl radical and exclusively α -position to the amide, to give a more stable captodative radical **142**.



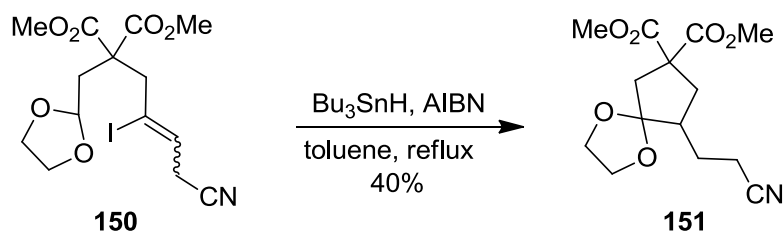
Scheme 2.18

Parsons⁷⁴ (Scheme 2.19) and Curran⁷³ (Scheme 2.20) thoroughly investigated the process of vinyl radical translocation initiated using vinyl halides. For example, iodine atom abstraction from **146** generated radical species **147** which subsequently translocated via 1,5-H atom abstraction to give **148** (Scheme 2.19). The new radical centre then reacted with the double bond to furnish compound **149** via a 5-*exo*-trig cyclisation.



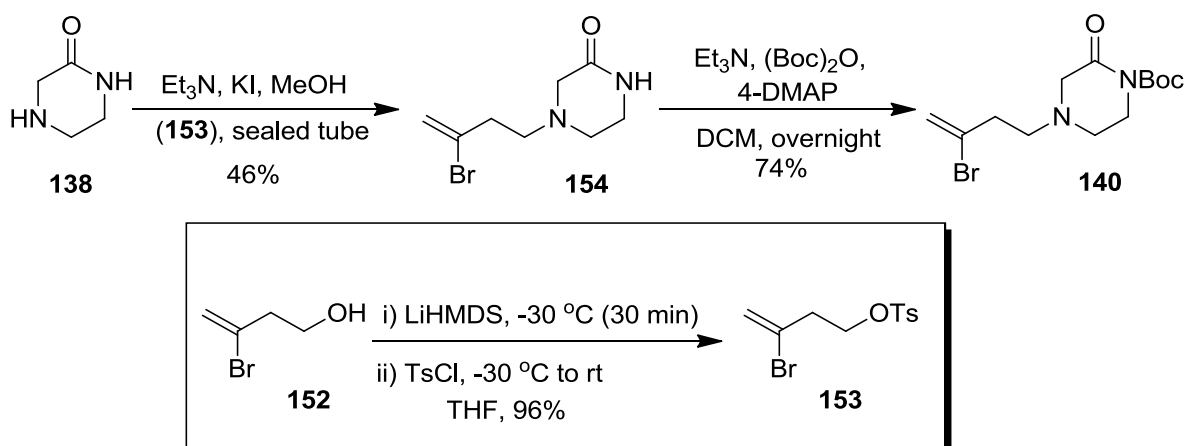
Scheme 2.19

In similar fashion, Curran and co-workers obtained *spiro*-system **151** through a straightforward route from the precursor **150** (Scheme 2.20). This process involved formation of a vinyl radical followed by 1,5-hydrogen abstraction and finally 5-*exo*-trig cyclisation.^{73b}



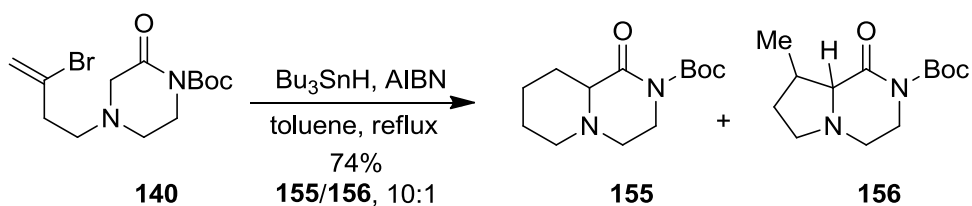
Scheme 2.20

Synthesis of the desired compound **140** started with *N*-alkylation of the commercially available oxopiperazine (**138**) to furnish compound **154** (Scheme 2.21). Protection of the amide **154** with a Boc group led to formation of the radical precursor **140**.



Scheme 2.21

Radical cyclisation of **140** under the standard conditions gave a 10:1 mixture of *endo* (**155**) and *exo* (**156**) products (Scheme 2.22). The unexpected by high regioselectivity in favour of the *endo* product presumably arises from a combination of steric and electronic factors. Although due to the structural and mechanistic differences between DKP **108** and MKP **140**, it is difficult to identify the contribution of the individual effects on the selectivity outcome.

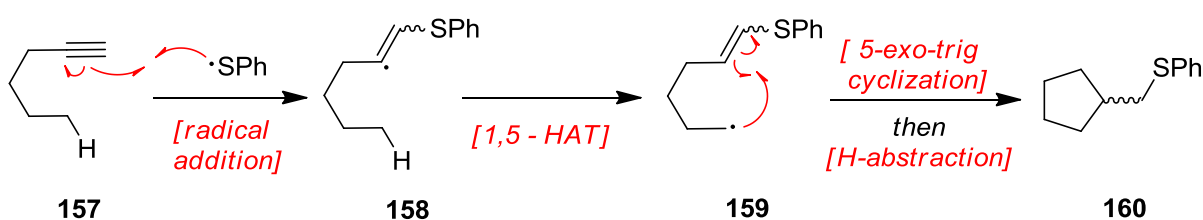


Scheme 2.22

After this unexpected highly regioselective synthesis of a 6,6-fused MPK (**155**) we wanted to investigate the possibility of a radical cyclisation with 5-*exo* cyclisation selectivity. We thought that this might be possible by using an alternative way to generate the intermediate alkenyl radical by radical addition of sulfanyl radical onto a terminal alkyne group.

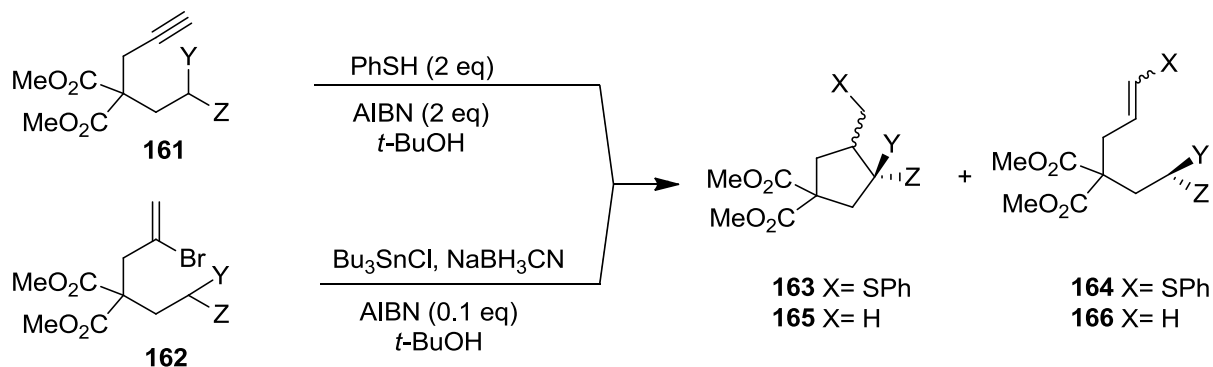
2.6 Radical cyclisation –The thiophenol mediated approach

Intermolecular addition of radicals onto terminal alkynes offers an efficient method to generate alkenyl radical centres suitable for 1,5-hydrogen translocation. To date, a wide selection of radical species (tin, thiol and phosphate radicals) have been used, with the recent attention of tin-free procedures which involve thiophenol-mediated hydrogen transfer-cyclisations (Scheme 2.23).⁷⁵ Addition of sulfanyl radical, generates an alkenyl radical (**158**) which subsequently translocates, usually through a 1,5-hydrogen atom translocation (**159**), followed by radical cyclisation to give the final products (**160**).



Scheme 2.23

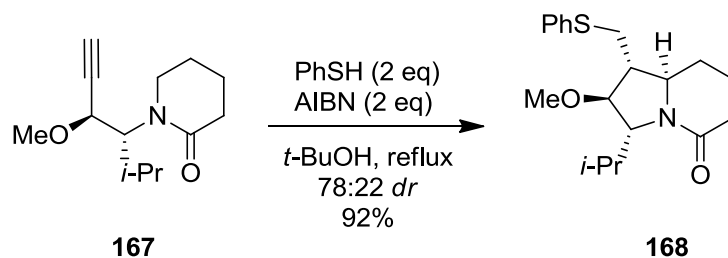
Extensive research carried out by Renaud and co-workers revealed further synthetic application of this method.^{75l-o} In many cases it had been shown that the thiophenol-mediated abstraction-cyclisation process was an efficient method to minimize the amount of directly reduced products (Table 2.1).^{75m}



Substrates 161 or 162 Y,Z	PhSH 163/164 (% yield)	Bu ₃ SnH 165/166 (% yield)
OCH ₂ CH ₂ O	100:0 (90%)	58:42 (81%)
OTBS, H	100:0 (89%)	88:12 (87%)
PhS, H	100:0 (88%)	—
Ph, H	100:0 (85%)	78:22 (76%)
CO ₂ Et, H	100:0 (57%)	76:24 (83%)
Me, Me,	100:0 (83%)	87:13 (65%)

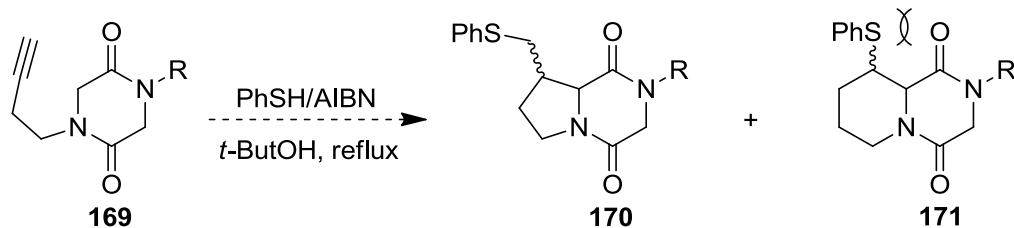
Table 2.1 Comparison of thiophenol-mediated with tin-initiated approach

After examination of the literature, we were pleased to find a structurally related example described by Renaud.⁷⁵ⁿ According this report, piperidinone **167** was reacted under the typical conditions to give **168** in 92% yield and 78:22 diastereoselectivity (Scheme 2.24).



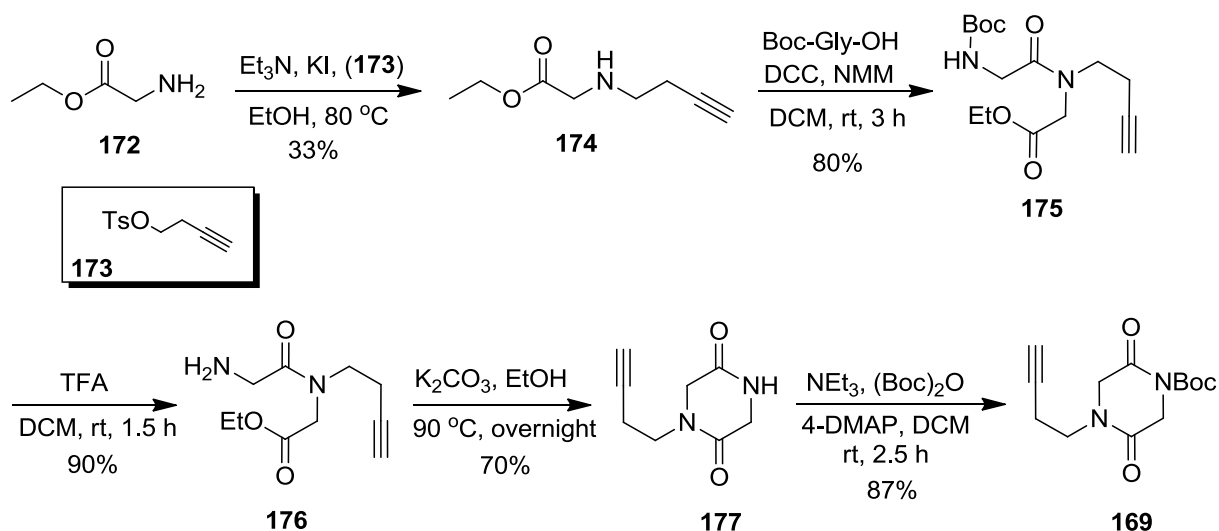
Scheme 2.24

With this in mind and considering the possible steric effects between thiophenyl and carbonyl group we were confident that radical cyclisation of DKP **169** would lead selectively to the 5-*exo* product **170** (Scheme 2.25). Thus, DKP **169** was chosen as the first target compound to test the proposed plan.



Scheme 2.25

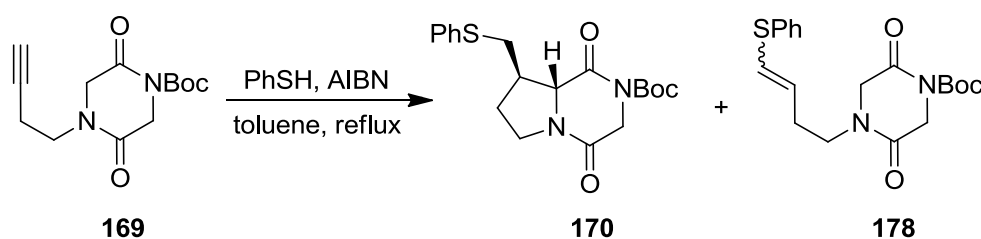
Preparation of the precursor **169** involved *N*-alkylation of the commercially available glycine ethyl ester **172**, followed by peptide coupling with Boc protected glycine to furnish the corresponding amide **175** (Scheme 2.26). Deprotection of the Boc group under acidic conditions followed by treatment with potassium carbonate gave the non-symmetrical DKP **177**. Finally the desired radical precursor was synthesised after protection of the amide function with a Boc group. With DKP **169** in hand, we were now ready to set about the radical cyclisation following Renaud's protocol.



Scheme 2.26

Addition of 2.0 equivalents PhSH and 2.0 equivalents AIBN over 20 hours to a toluene solution of **169** at 80 °C led to the formation of fused *bis*-cyclic DKP **170** as well as the reduced product **178** in 1:2 ratio (Table 2.2 entry 1). The fact that we were not able to isolate the 6-*endo* product (**171**) confirmed our expectations for the regioselectivity of the reaction. Unlike Renaud's reports,^{75m} we obtained a high yield of the reduced product **178** (65% yield). Further investigation was then carried out in order

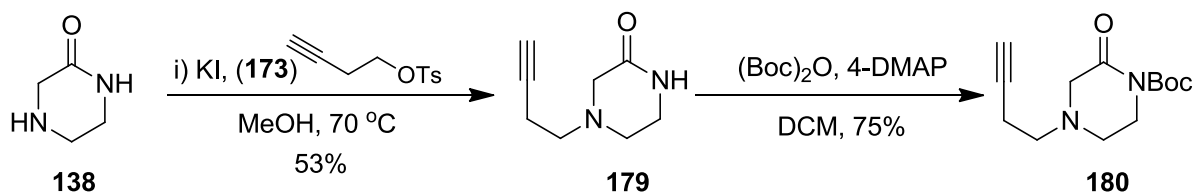
to minimize formation of **178**, which involved attempts at lower concentration or with faster addition of the reagents. It was shown that the reaction was complete with less than 2.0 equivalents of AIBN and 2.0 equivalents PhSH. The optimum conditions involved, addition of 1.3 equivalents of AIBN and 1.3 equivalents of PhSH over 3 hours at reflux to furnish the final products as a 1.0:1.6 mixture of **170** and **178** (Table 2.2 *entry 2*). The rate of the reduction process appeared to be higher than the cyclisation step, something which could arise from the additional steric effect by the presence of the thiophenyl group.



	PhSH (eq)	AIBN (eq)	addition of PhSH/AIBN	Yield	170 / 178
<i>entry 1</i>	2.0	2.0	20 h	65%	1:2
<i>entry 2</i>	1.3	1.3	3 h	70%	1.0:1.6

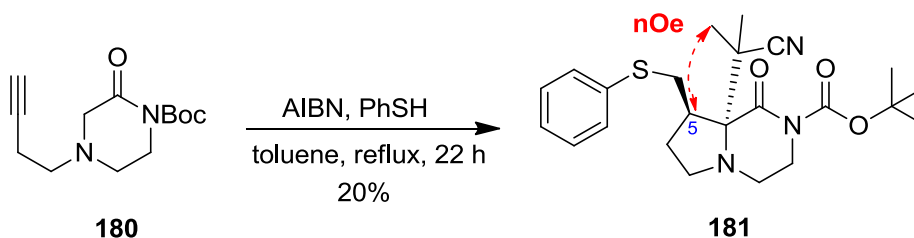
Table 2.2 Thiophenol-mediated cyclisation reaction of **169**

Since we were able to obtain only the 5-*exo* product **170** we were also interested to investigate how the MKP analogue would react and what the regioselectivity would be under the same conditions. Thus, compound **180** was chosen as the final substrate on which to apply the thiol-mediated radical cyclisation (Scheme 2.27). Precursor **180** was successfully prepared through *N*-alkylation of commercially available 2-oxopiperazine **138** with tosylate **173** followed by Boc protection of the resulting ketopiperazine **179**.



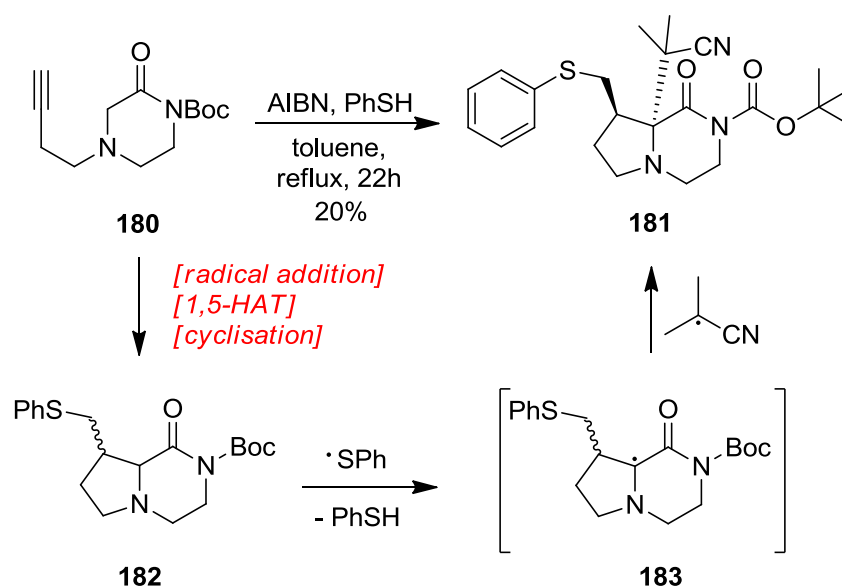
Scheme 2.27

When cyclisation of ketopiperazine **180** was attempted in *t*-BuOH/toluene at reflux we did not observe formation of cyclisation products but we only recovered the starting material. Another attempt of the reaction in toluene under reflux, showed formation of compound **181** in 20% yield within a complex mixture of unidentified products (Scheme 2.28). nOe studies showed correlation between the methyl groups and H5 which has *anti* stereochemistry to the thiophenyl group. This proves that addition of the cyanopropyl radical occurred *anti* to thiophenyl group due to the steric hindrance on the opposite face.



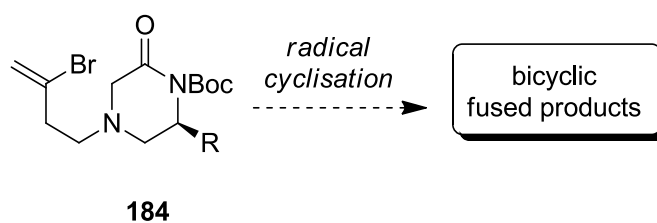
Scheme 2.28

It is possible that the major product **181** of this reaction was generated through an additional hydrogen atom abstraction of the cyclised products. As Scheme 2.29 shows, a second sulfanyl radical could abstract the α -hydrogen atom of the amide **182** to generate a captodative radical centre **183**. Addition of the cyanopropyl radical generated by the excess of AIBN would give the observed bicyclic product **181**. In many examples in the literature it has been reported that sulfanyl radical can directly abstract α -amidical hydrogen atoms, which supports our explanation.^{75n,76}



Scheme 2.29

Thus, all of our work with thiophenol-mediated hydrogen transfer-cyclisation both for DKPs and MKPs led to the formation of the 5-*exo* products in low yields. Due to the low yield of these reactions we would not be in a position to apply this reaction in more complex systems. However the highly 6-*endo* regioselective radical cyclisation of MKP **140** (Scheme 2.21) could possibly give more interesting results under further investigation of radical cyclisation employing enantiopure precursors such as **184** (Scheme 2.30).



Scheme 2.30

Unfortunately, preparation of MKP **184** would involve a more complex synthetic approach thus, we diverted our interest to the exploration of different methodologies within the area of prenylated indole alkaloids. Our next targets involved formal synthesis of stephacidin A (**35**) and new methods to access the hexacyclic bicyclo[2.2.2]diazaoctane framework.

Chapter 3

Towards stephacidin A

3.1 Previous syntheses

Stephacidins (**35**), (**39**) and avrainvillamide (**36**) are important representative members of prenylated indole alkaloids which have been a vibrant source of inspiration for the synthetic chemist over the last few decades (Figure 3.1). Stephacidin A (**35**) and B (**39**) were isolated from fungal strain *Aspergillus ochraceus* WC76466 in 2001 and were shown to exhibit a potent *in vitro* cytotoxicity against various human tumor cell lines.^{26,31} The absolute configuration of stephacidin A (**35**) was not reported in the original isolation. Due to the intriguing structural architecture, the biological activity and the need to determine the absolute stereochemistry of stephacidin A (**35**), these molecules have been adopted as challenging targets for several synthetic groups. To date three synthetic approaches towards stephacidin A (**35**) have been reported, first by Baran *et al.*^{47,77} and later from Williams *et al.*⁷⁸

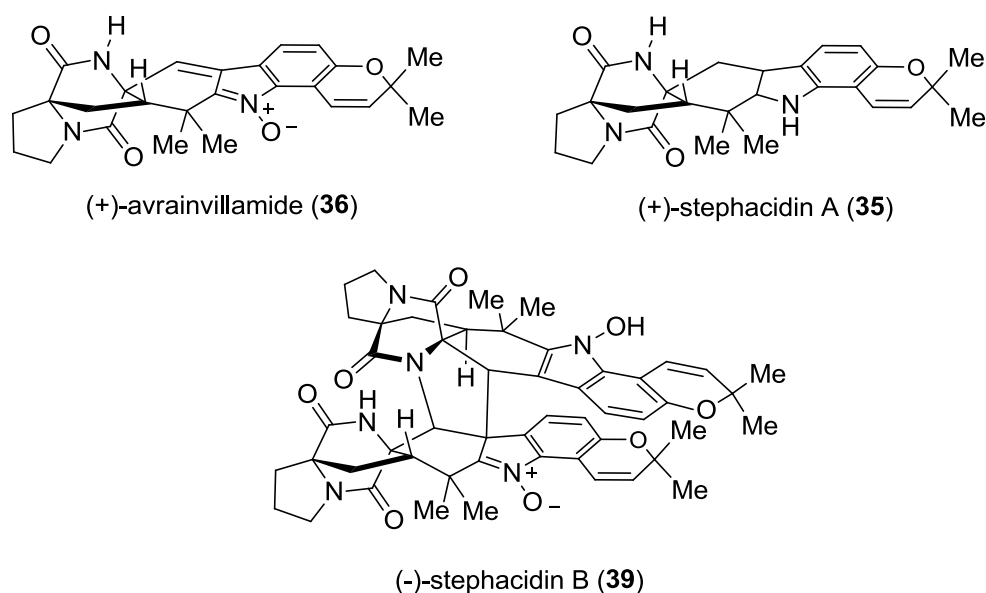


Figure 3.1 Structures of the stephacidins and avrainvillamide

First enantioselective total synthesis of unnatural (-)-stephacidin A

Baran and co-workers in 2005 were the first to demonstrate an enantioselective total synthesis of (-)-stephacidin A (**35**) via a novel *bis*-oxidative enolate coupling reaction.⁷⁷ As shown in Figure 3.2 the core skeleton of the bridged DKP was generated by a metal-mediated enolate coupling of a DKP precursor followed by a formal ene reaction and 1,2-rearrangement.

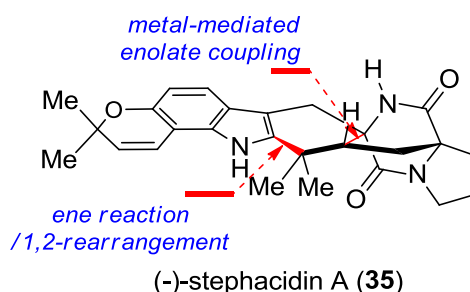
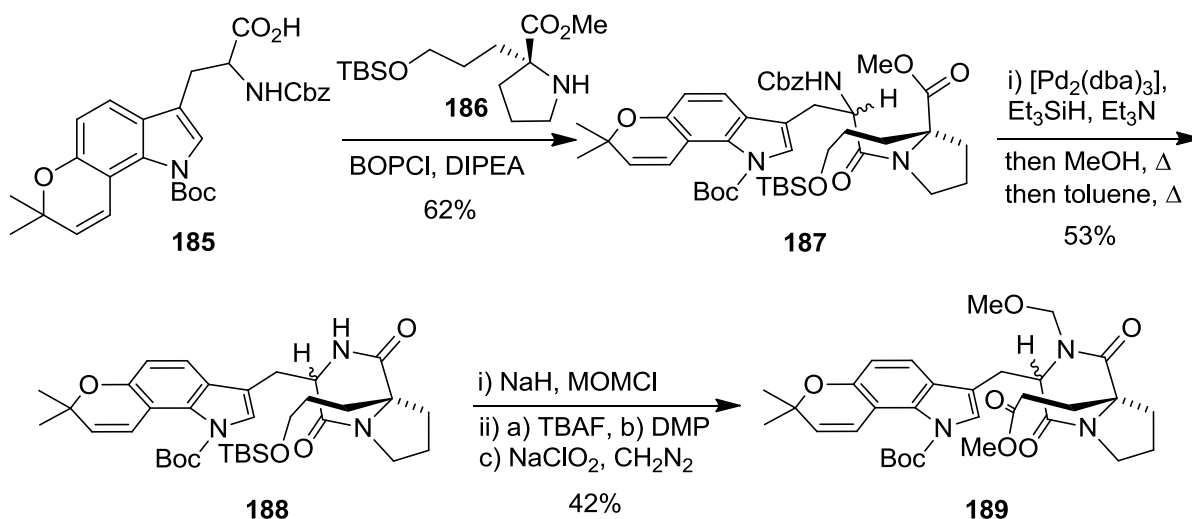


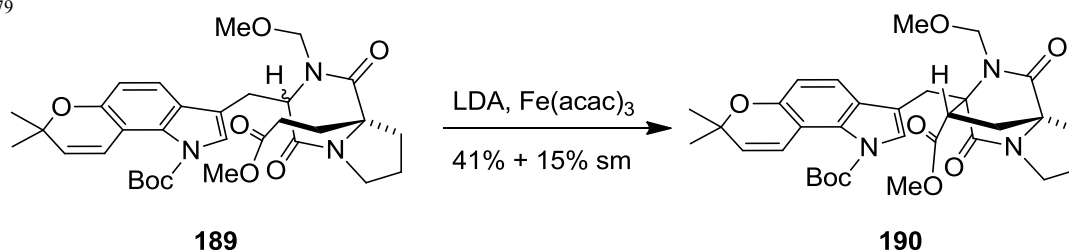
Figure 3.2 Key disconnections of stephacidin A (**35**)

In their synthetic approach the racemic tryptophan derivative **185** was chosen as the starting material and it was coupled with an enantiomerically pure L-proline derivative **186** to give a mixture of diastereomeric amides **187** in 62% yield (Scheme 3.1). Chemoselective *N*-Cbz deprotection followed by thermal cyclisation led to DKP **188**. Amide **188** was protected with a MOM group followed by TBS removal to give the corresponding alcohol which was then oxidised to furnish ester **189**.



Scheme 3.1

The key step for the synthesis of the bridged DKP core structure involved an intramolecular oxidative heterocoupling of two carbonyl enolates. After extensive investigation on model systems, Baran and co-workers reported the first example of this type of intramolecular coupling. Among all the oxidants which were investigated, $\text{Fe}(\text{acac})_3$ and $\text{Cu}(\text{II})$ salts furnished the highest yields of 19-39% and 41% respectively. The optimum conditions involved the addition of 2.2 eq of LDA to a solution of **189** followed by addition of 2.2 eq solid $\text{Fe}(\text{acac})_3$ to give **190** in 41% as a single diastereoisomer (Scheme 3.2).⁷⁹



Scheme 3.2

The authors suggest that the key reaction occurred in high yield possibly due to unique selectivity of the iron oxidant. Four possible scenarios are suggested for the bond formation in which the iron oxidant could selectively oxidise one of the enolate species (Figure 3.3).⁷⁹ The remaining enolate could then be combined with the new radical centre and generate a ketyl-type radical anion which could be further oxidised to give the final product.

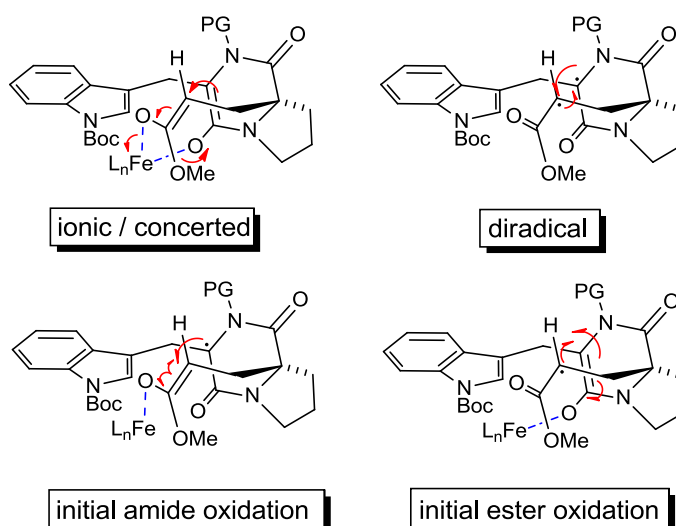


Figure 3.3 Possible scenarios for bond formation

The selectivity outcome was rationalised by a chelated transition state between the enolate and the oxidant (Figure 3.4). Williams in his research had also related the stereoselectivity on similar reactions to the presence or absence of metal chelation (tight ion pairing).⁸⁰

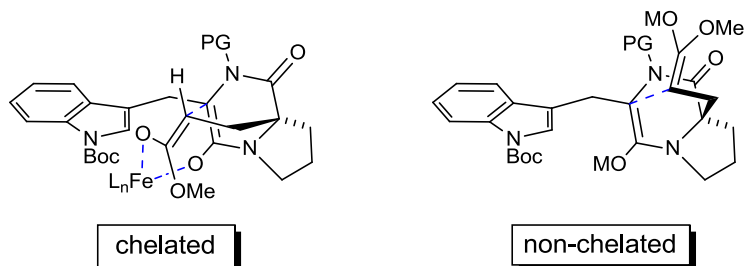
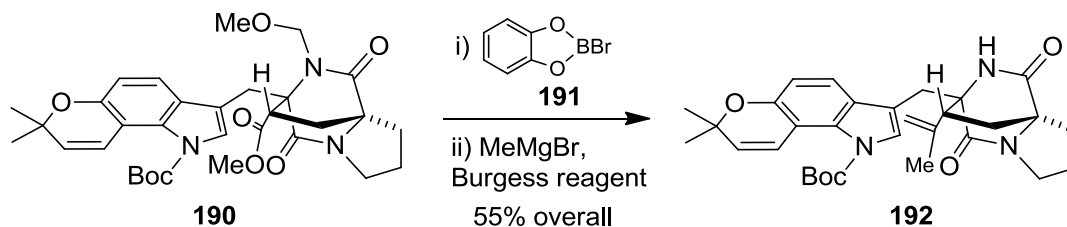


Figure 3.4 Metal chelation

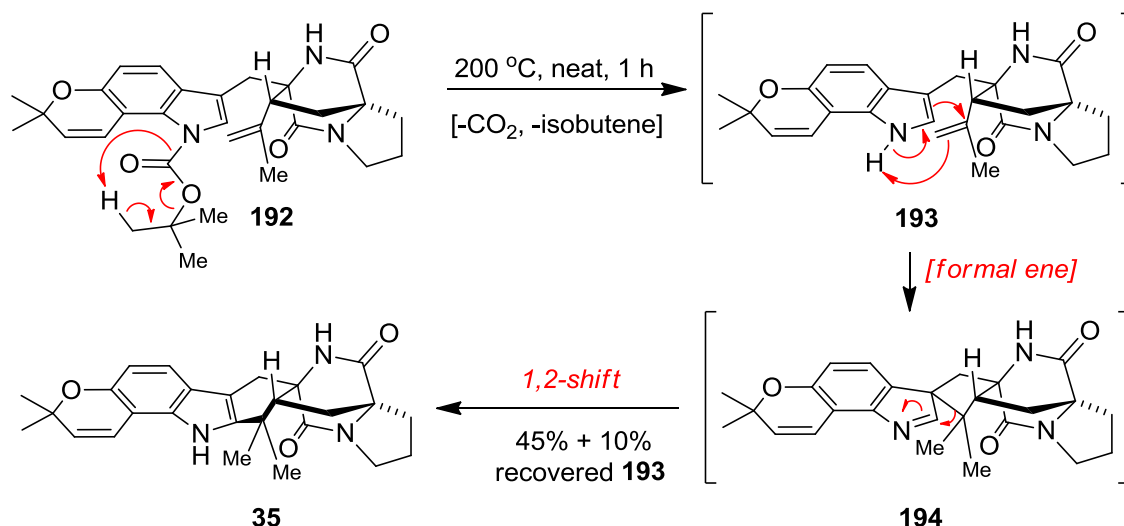
Removal of the *N*-MOM group of **190** with *B*-bromocatecholborane (**191**) followed by Grignard reaction with methylmagnesium bromide and dehydration of the corresponding tertiary alcohol gave **192** in 55% overall yield (Scheme 3.3).



Scheme 3.3

The final step of the synthesis involved formation of the last six-membered ring which would lead to the desired heptacyclic core. Although acid treatment proved to be ineffective for this step as the pyran ring is sensitive under acidic conditions, when neat **192** was heated at 200 °C for 1 h the favoured product **35** was formed in 45% yield (Scheme 3.4). It was suggested that the last cyclisation firstly involved a thermal Boc removal to give **193** followed by a formal ene reaction to afford spirocyclic compound **194** and finally 1,2-alkyl shift to furnish **35**. In comparison with the isolation reports it was confirmed that synthetic **35** had identical spectral properties with the natural product. However only the relative configuration of **35** could be confirmed at that time as the optical rotation of the natural

product was not reported. A few years later in 2009, Baran's research group reported an improved synthesis of α,β -unsaturated nitrones relevant to the stephacidins.⁸¹



Scheme 3.4

First enantioselective total synthesis of the natural (+)-stephacidin A – Determination of the absolute configuration

In 2005, Baran, in collaboration with Fenical *et al.* re-isolated natural stephacidin A (**35**) and measured the optical rotation of the natural product.⁴⁷ It was proved that natural stephacidin A (**35**) exhibit the opposite CD data to that exhibited by synthetic **35** (Figure 3.5).

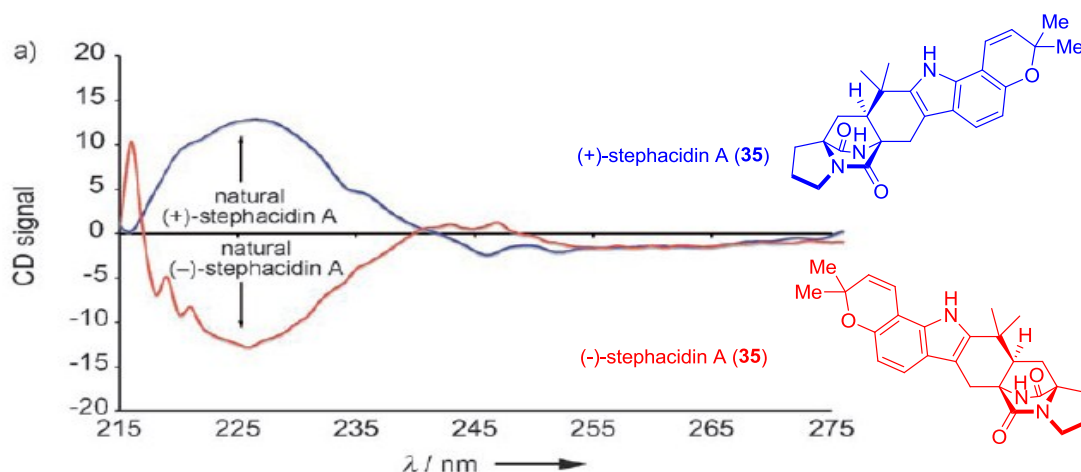
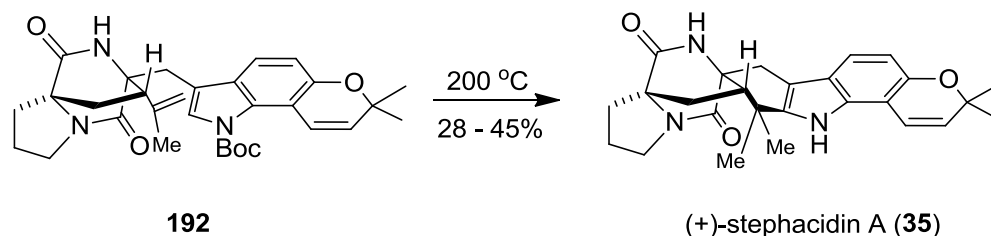


Figure 3.5 CD measurements of natural and synthetic stephacidins A

As a consequence, Baran repeated the synthesis starting with D-proline to give the enantiopure natural product (+)-stephacidin A (**35**) in 18 steps and overall synthetic yield of 0.5% from commercially available material (Scheme 3.5). Having the correct enantiomer in hand they also proceeded toward the enantioselective total synthesis of avrainvillamide (**36**) and stephacidin B (**39**).



Scheme 3.5

Biomimetic total synthesis of (±)-stephacidin A: the Diels-Alder approach

The most extensive work in the area of synthesis and biosynthesis of prenylated indole alkaloids has been carried out by Williams. Williams and co-workers have achieved several total syntheses of these natural products and also verified the biosynthetic proposal of a Diels-Alder reaction, originally described by Birch and Sammes.^{16,35} Even though this elegant biomimetic Diels-Alder approach has proved to be difficult for enantioselective synthesis of these compounds, Williams and co-workers applied this approach to the total synthesis of (±)-stephacidin A (**35**).^{78a}

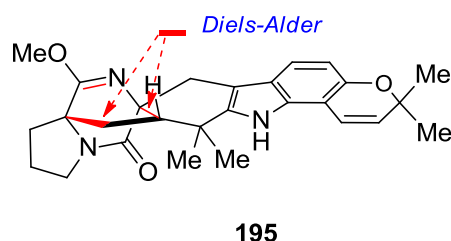
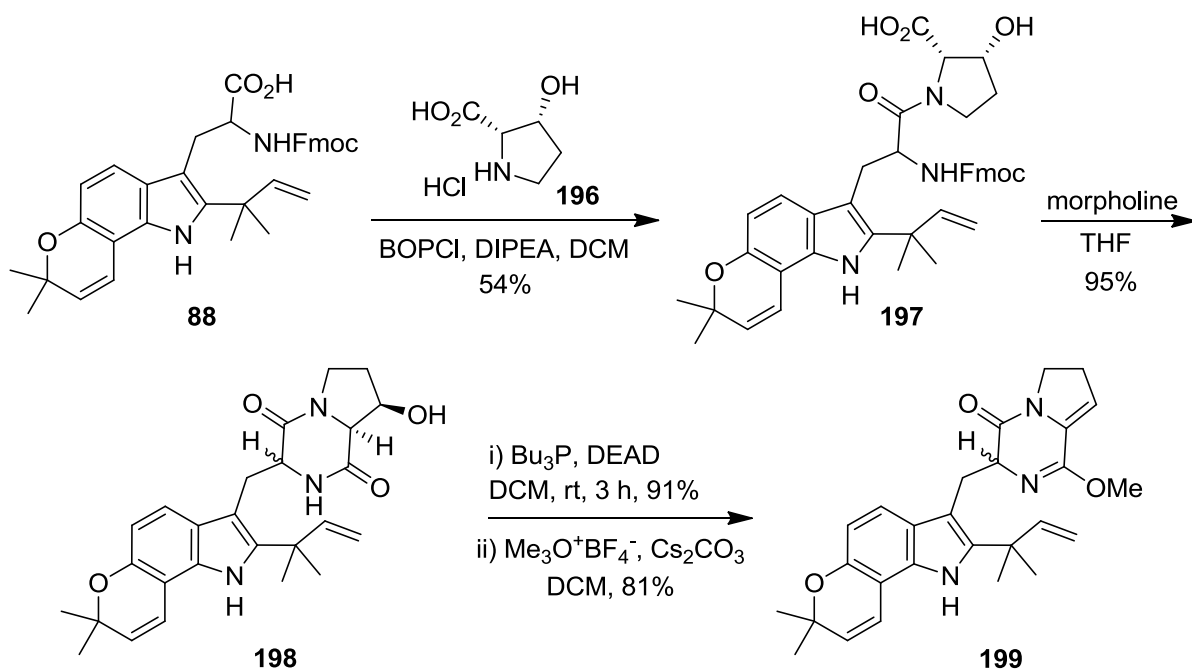


Figure 3.6 Key disconnections of bridged lactim ether **195**

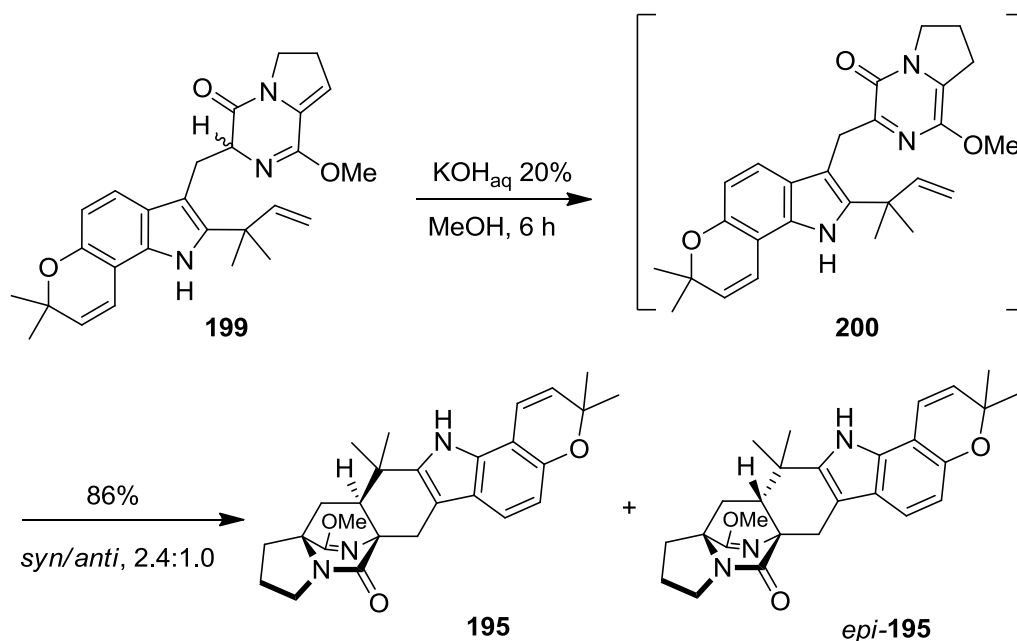
L-Proline derivative **196** was coupled with compound **88** to give amide **197** as a mixture of diastereomers in 54% yield and 1:1 ratio (Scheme 3.6). Treatment of **197** with morpholine resulted in removal of the Fmoc protective group and the resulting amine underwent an intermolecular cyclisation

to form DKP **198** as 1:1 mixture of diastereomers. Mitsunobu-type elimination of water followed by treatment with $\text{Me}_3\text{O}^+\text{BF}_4^-$ and Cs_2CO_3 generated Diels-Alder precursor **199**.



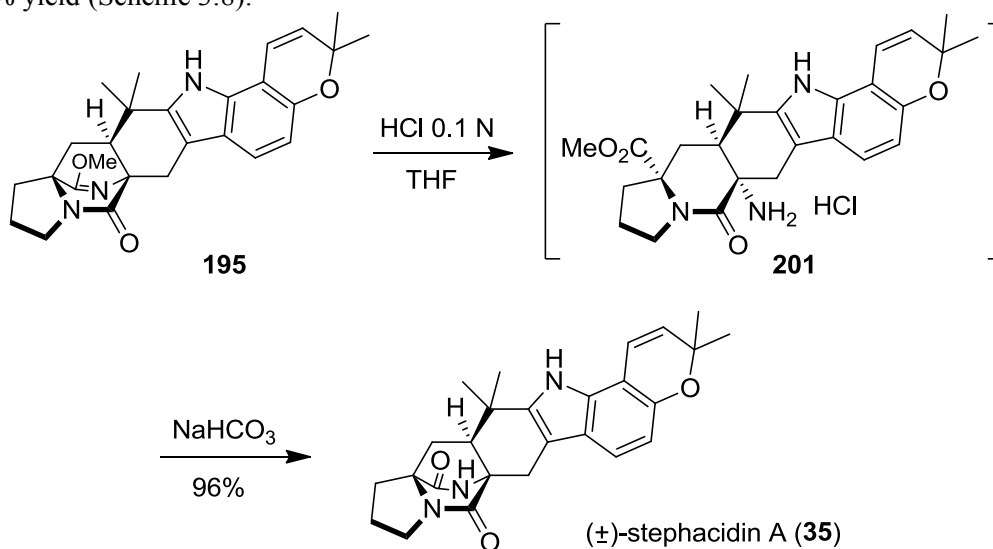
Scheme 3.6

A Diels-Alder reaction under the optimum conditions which had previously been described was then attempted.⁸² Under basic conditions, **199** formed azadiene **200** which spontaneously underwent an intramolecular Diels-Alder reaction to give selectively compounds **195** and *epi*-**195** in a 2.4:1.0 ratio (*syn/anti*) and 86% yield (Scheme 3.7).



Scheme 3.7

Lactim ether **195** was hydrolysed in the presence of HCl in THF to afford a ring-opened amino ester **201** which then cyclised on the treatment with NaHCO_3 to give the corresponding (\pm)-stephacidin A (**35**) in 96% yield (Scheme 3.8).

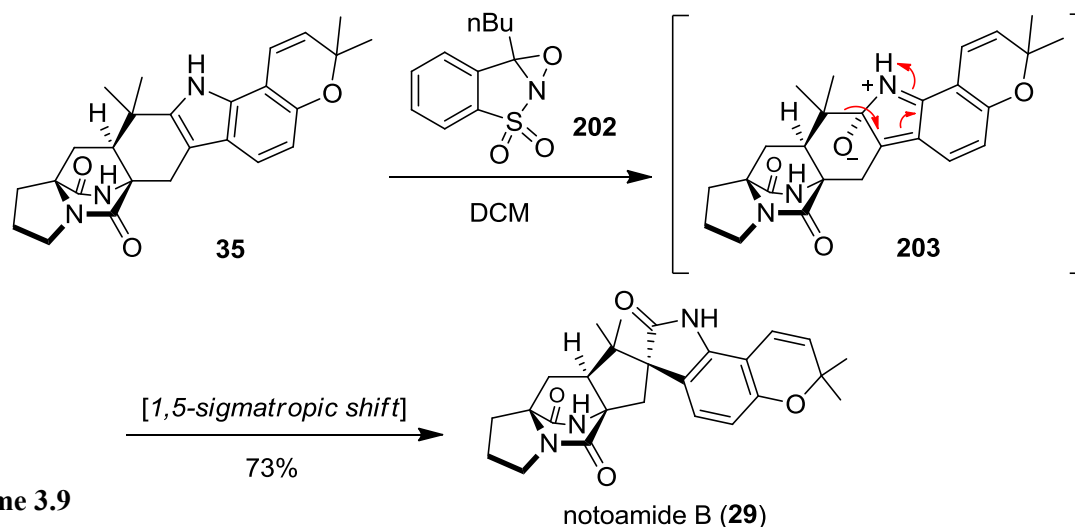


Scheme 3.8

Intermediate **203** was generated by a stereoselective oxidation of **35** using an excess of oxaziridine **202** followed by epoxide opening (Scheme 3.9). This oxidation step involves an epoxidation of a 2,3-disubstituted indole from the less hindered α -face. A pinacol [1,5]-sigmatropic rearrangement then

takes place to form another biologically active natural product notoamide B (**29**) in 73% yield.

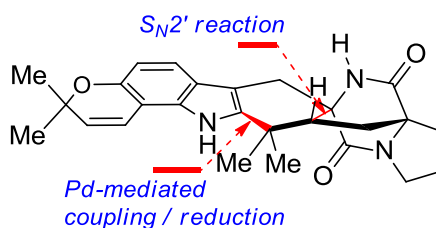
Williams' synthesis of stephacidin A (**35**) was achieved in 17 synthetic steps and 5.0% overall yield.



Scheme 3.9

Asymmetric, stereocontrolled total Synthesis of (-)-stephacidin A: the S_N2' alkylation approach

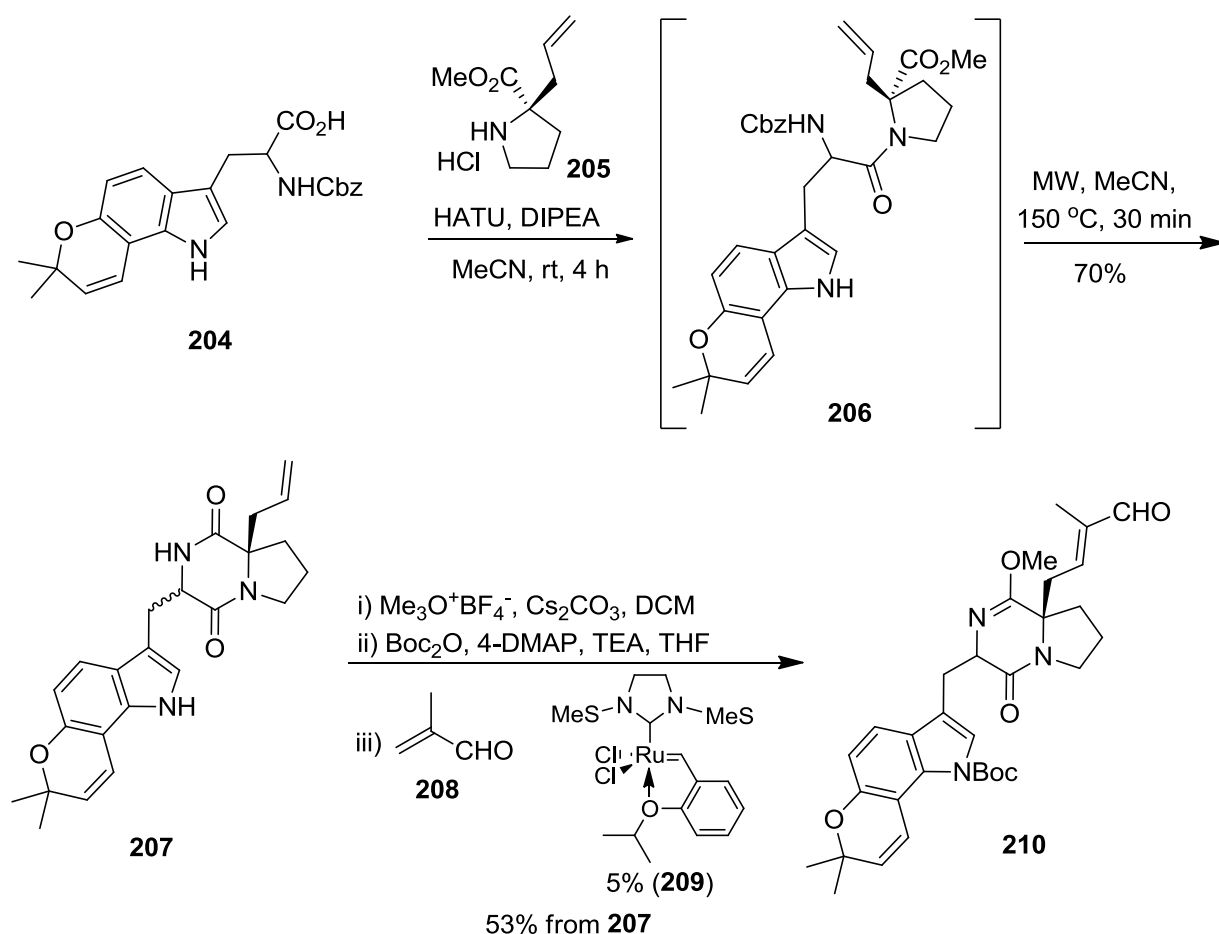
Williams published an asymmetric total synthesis of (-)-stephacidin A (**35**), (+)-stephacidin B (**39**) and (+)-notoamide B (**29**).^{78b} The advantage of this approach was the high selectivity of the S_N2' key step cyclisation reaction in the formation of the bridged DKP skeleton (Figure 3.7). The heptacyclic core was generated by a Pd-mediated coupling reaction between the isoprene functional group and the indole moiety of a DKP derivative.



(-)-stephacidin A (**35**)

Figure 3.7 Key disconnections of stephacidin A (**35**)

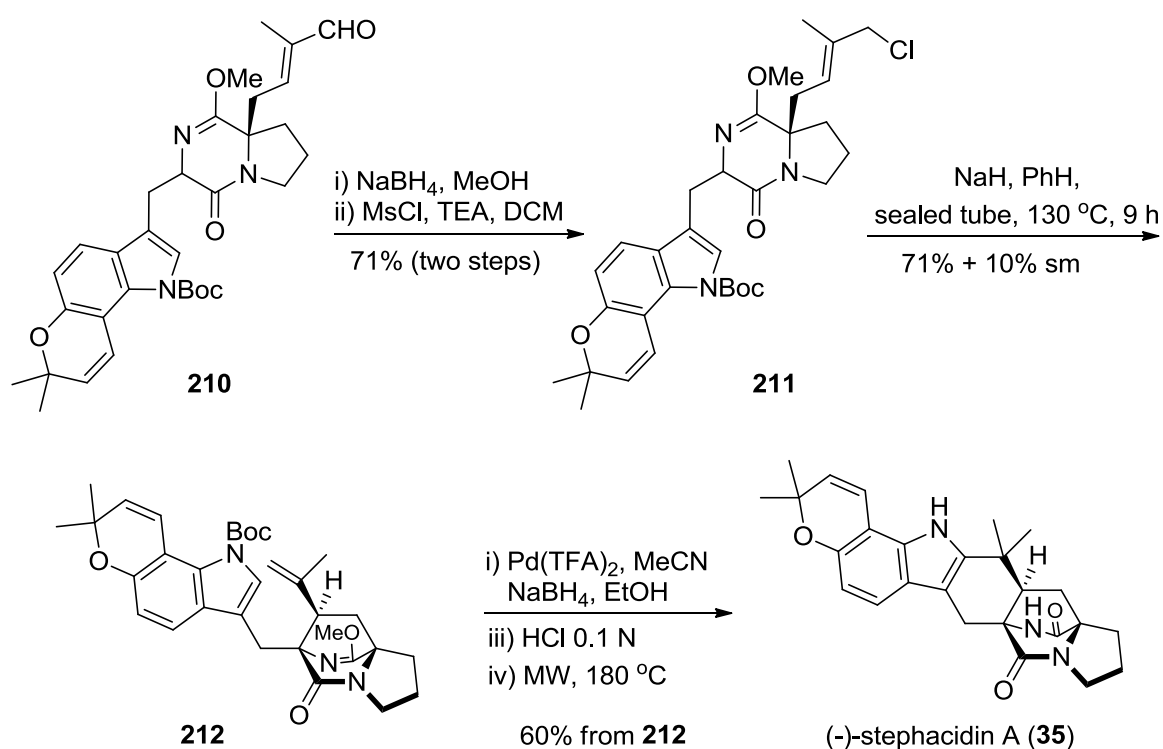
Proline derivative **205** was coupled with tryptophan **204** to afford peptide **206** and then the crude mixture was heated in a microwave to remove the Boc group and form DKP **207** in 70% overall yield (Scheme 3.10). Over the next three steps, the amide functional group was protected as lactim ether and the nitrogen of the indole moiety with a Boc group, before cross-metathesis with Hoveyda-Grubbs 2nd generation catalyst was carried out to give formyl DKP **210**.



Scheme 3.10

Formyl DKP **210** was reduced to the allylic alcohol which was then transformed into the desired allylic chloride **211** in 71% yield over two steps (Scheme 3.11). As previously described,⁸³ a cyclisation with *syn* selectivity could occur when NaH was added to a solution of this type of substrates in benzene. Repeating the standard conditions, Williams and co-workers were pleased to

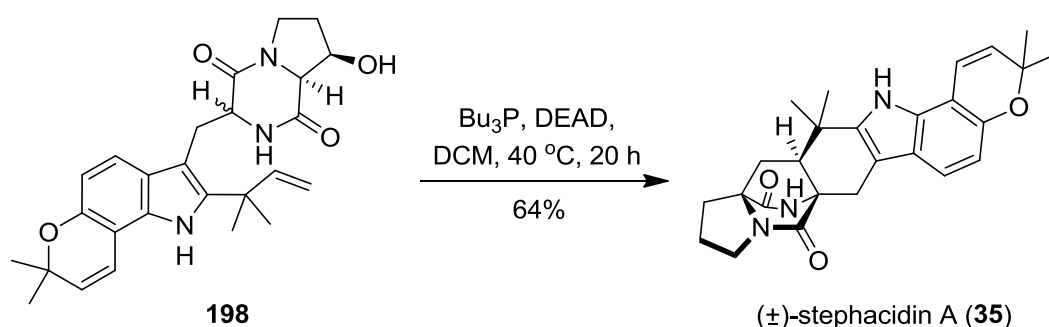
isolate the bridged product **212** as a single diastereoisomer in 60% yield. As described earlier, the diastereoselective outcome arises through a tight ion-pair-driven closed transition state. To perform the second cyclisation it was necessary to develop a different methodology in the absence of acids as the pyran ring is sensitive to these conditions. After extensive investigation they found that the optimum conditions involved addition of 5.0 equivalents of $\text{Pd}(\text{TFA})_2$ to a solution of **212** in MeCN. The resulting alkyl-palladium intermediate was then reduced using NaBH_4 and the double cyclised product was obtained after treatment with aqueous HCl at low concentration (0.1 N). Finally, the Boc group was removed under thermal conditions and (-)-stephacidin A (**35**) was isolated in 60%. Thus (-)-stephacidin A (**35**) was prepared in 6% overall yield from commercially available materials and in 17 total steps.



Scheme 3.11

Improved total synthesis of (±)-stephacidin A: Mitsunobu conditions for intermolecular Diels-Alder reaction

Williams in 2007 also published an improved biomimetic total synthesis of (±)-stephacidin A (**35**) in 14 steps and overall yield of 11%.^{78c} It was observed that a Diels-Alder reaction occurred during elimination of the hydroxyl group DKP **198** when the reaction was left longer (Scheme 3.12). After purification (±)-stephacidin A (**35**) and its epimer in a 2.4:1.0 ratio were isolated in 64% yield. The new general protocol lacked the need for amide protection and deprotection steps and it is closer to the biosynthetic pathway that Nature chooses in order to make these natural products.



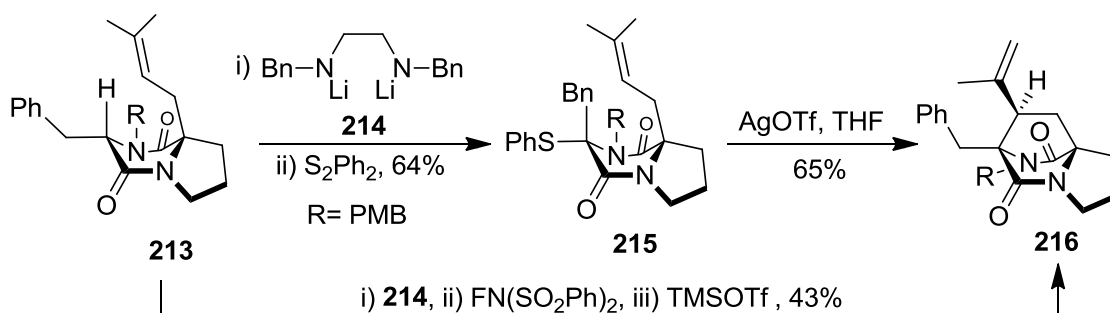
Scheme 3.12

Isolation of the antipodal (-)-stephacidin A

In 2008 Williams reported for the first time the isolation of the antipode (-)-stephacidin A from *Aspergillus versicolor* NRRL 35600.³² This report was published seven years after the original paper for the isolation of (+)-stephacidin A (**35**) and 3 years after Baran's group reported the synthesis of the unnatural product. The isolation of the both antipodal natural products such as stephacidins and notoamides supports the proposal that the biosynthetic path for these natural products involves a Diels-Alder reaction.

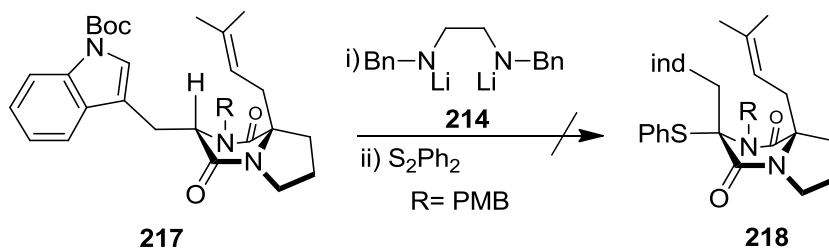
3.2 Previous work by Simpkins' group - Studies towards complex bridged alkaloids

Previous work in our group carried out by M. Pichowicz,⁸⁴ showed a promising cyclisation of a highly substituted DKP substrate to access the bridged DKP core present in the prenylated alkaloid natural products. Synthesis of the unsymmetrical DKP **213** (Scheme 3.13) was achieved in 5 steps and involved peptide coupling of two amino acid derivatives and several protection/deprotection modifications.^{84b} Enolisation of the DKP **213** proved to be problematic as various bases such as LDA, LiHMDS, KHMDS, *n*-BuLi did not give successful results and only *bis*-amine **214** gave reasonable yields. Treatment of **213** with 1.1 equivalents of base **214** at -78 °C followed by addition of diphenyl sulfide after 1 h gave DKP **215** as a single diastereoisomer in 64% yield (Scheme 3.13). The stereochemical assignment was secured by X-ray crystallography and the SPh substituent was found to be *anti* to the prenyl group and on the more concave face of the bicyclic system. The stereoselective outcome was been explained by hindrance of the convex face which is shielded by the prenyl group. Thus the electrophile approaches *anti* to the prenyl group. Since DKP substrates are known for their ability to generate cationic intermediates, compound **215** was treated with AgOTf in an attempt at a cationic cyclisation. The resulting carbocation was trapped by the double bond of the prenyl group to give bridged DKP **216** as a single diastereoisomer in 65% yield. A direct cyclisation was also effected by enolisation of **213** followed by electrophilic fluorination and then treatment with TMSOTf to afford **216** in 43% in a one pot process. After the successful cyclisation of the model system it was attempted to extend this approach towards brevianamide F.



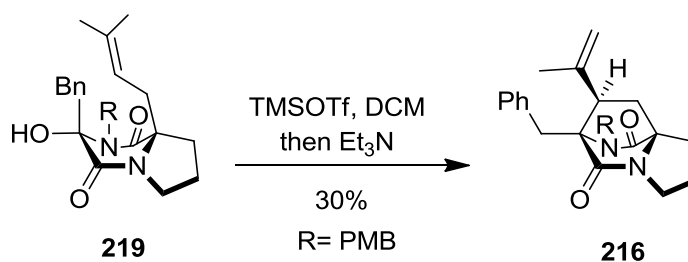
Scheme 3.13

It was proposed that the indole moiety might trap the intermediate isoprenyl carbocation involved in these cyclisation, leading to another cyclisation. DKP **217** was straightforwardly synthesised following a similar approach to that for compound **213**.^{84b} Unfortunately enolisation of **217** using the previous reported conditions was unsuccessful and the cationic cyclisation methodology could not be applied to this system (Scheme 3.14). At this point an alternative approach needed to be investigated.



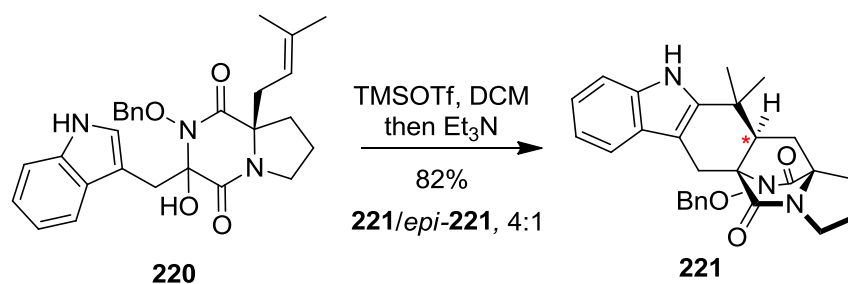
Scheme 3.14

The modified synthetic plan, which was carried out by F. Frebault, involved introduction of a different functional group to trigger the cationic cyclisation.^{59a} A hydroxyl group seemed to be a suitable candidate for this proposal and so hydroxyl-DKP **219** was chosen as the ideal precursor (Scheme 3.15). DKP **219** was easily synthesised and when it was treated with TMSOTf at 0 °C it gave compound **216** in 30% yield.



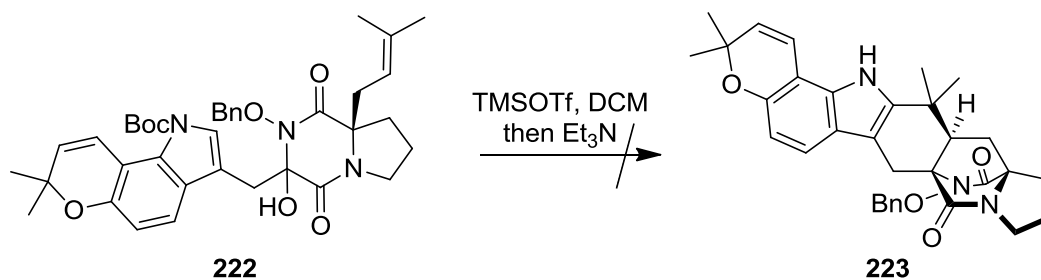
Scheme 3.15

Having shown that a cationic cyclisation could occur, starting with a hydroxy-DKP, the next step was to synthesise DKP **220**.^{59a} The presence of the indole was crucial in order to undergo a cationic cascade and afford the hexacyclic bridged DKP in a single step. DKP **220** was synthesised in 4 steps and when it was treated with TMSOTf, **221** and *epi*-**221** in a 4:1 ratio were isolated in 82% combined yield (Scheme 3.16).



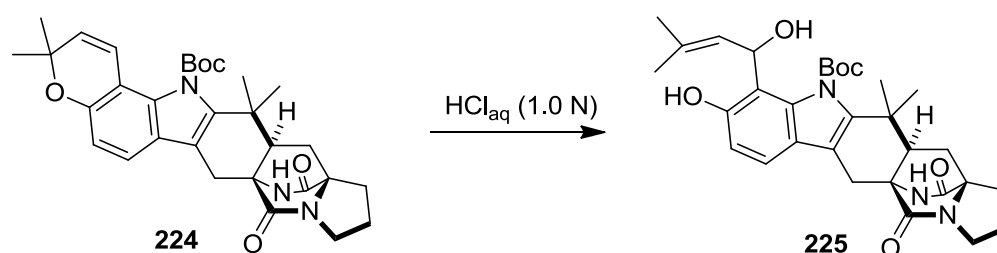
Scheme 3.16

In comparison to previous reported approaches to access the bicyclo[2.2.2]diazaoctanecore ring system, only the Diels-Alder approach leads to the formation of two new C–C bonds in a single step (Scheme 3.7). However the Diels-Alder methodology does not enable enantiomeric control and leads to racemic mixtures. On the other hand Williams' S_N2' cyclization reaction and Baran's oxidative enolate coupling undergo reactions with higher stereoselectivity, however in these approaches there is a stepwise formation of the final products. Simpkins' cationic cyclisation occur a double cyclisation of the hydroxy-DKP leading to the final products in one pot and with reasonable stereocontrol. *Ent*-malbrancheamide B (**41**) and *ent*-brevianamide B (**5**) were synthesised by applying this new methodology to some modified precursors.⁵⁹ Unfortunately, this reaction could not be used for the synthesis of stephacidin A (**35**) due to the high acid sensitivity of the pyran ring of compound **222** and **223** (Scheme 3.17). The triflic acid generated during the reaction promotes decomposition of the starting material and the products. Several Lewis and Brønsted acids were also tested (TFA, HCl, TiCl_4) but with no success. Unfortunately F. Frebault was not able to isolate the monocyclised products and complete the synthesis via a stepwise cyclisation process.



Scheme 3.17

Previous studies have shown that the presence of an electron donating oxygen atom on the indole made the molecule sensitive to acidic conditions. Williams had also reported^{78b} the sensitivity of the pyran ring in a similar substrate during acidic work-up of **224** (Scheme 3.18).

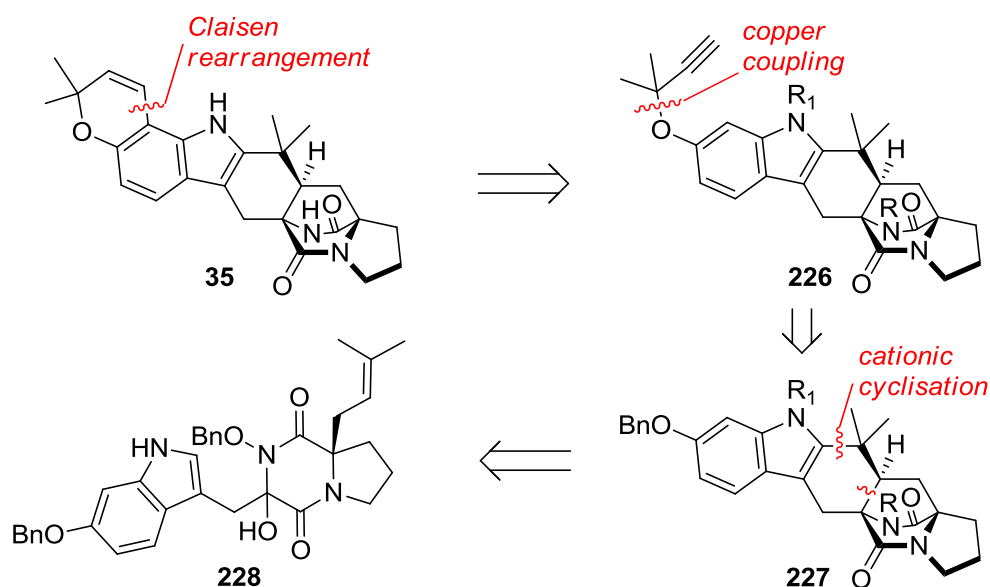


Scheme 3.18

As we were not able to synthesise the heptacyclic core structure via a cationic cascade cyclisation it was necessary to devise an alternative route in order to complete the synthesis of stephacidin A (**35**).

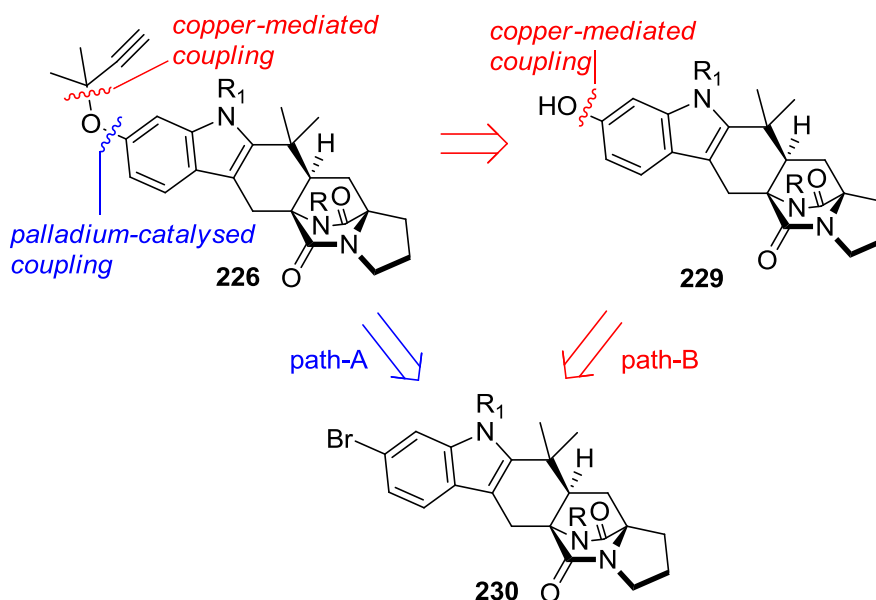
3.3 Investigating the new strategy

In order to overcome the acid sensitivity of the pyran-containing intermediates it was decided to develop a new synthetic route which involved introduction of the pyran ring at a late stage of the synthesis. The feasibility of two new approaches was initially explored by choosing compound **227** (Scheme 3.19) and **230** (Scheme 3.20) as potential precursors. For the first approach, *O*-benzyloxyindole bridged DKP **227** would be synthesised via a cationic cascade reaction of **228** as previously described by our group (Scheme 3.19). Deprotection of the OBn protecting group followed by formation of the ether via a copper-mediated coupling would lead to compound **226**. Finally, intermediate **226** could undergo an aromatic Claisen rearrangement^{78b} according to previous reports to furnish the final target of the synthesis **35**.



Scheme 3.19 Retrosynthetic analysis of **35**

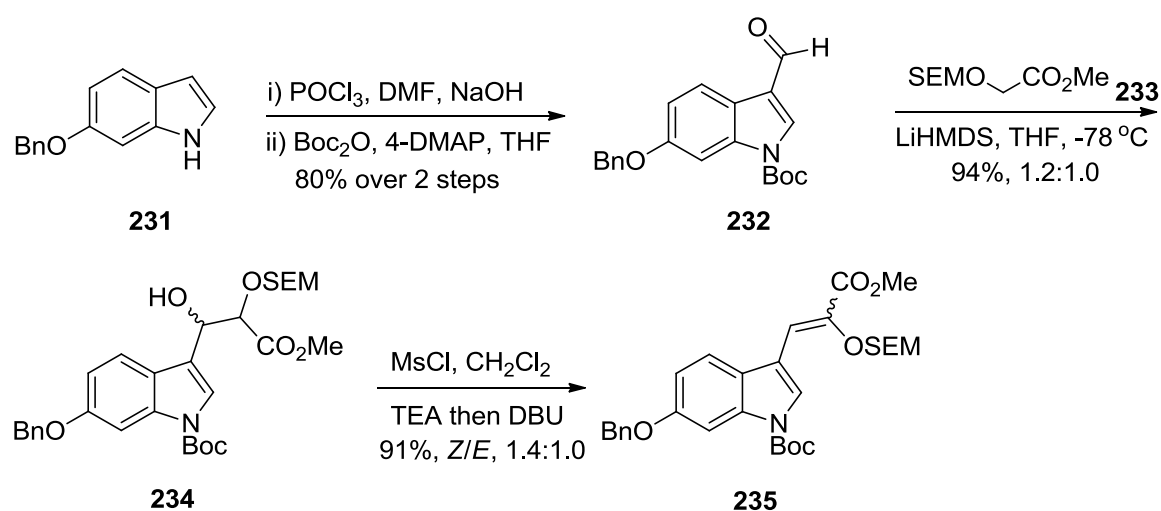
Alternatively, synthesis of compound **226** could also be achieved from **230** as the primary precursor, which could also be prepared by cationic cyclisation of a bromo modified DKP derivative (Scheme 3.20). Furthermore, there are two distinct pathways by which **230** can be converted via the phenolic derivative **229** (path-B) or directly to **226** (path-A). Path-A involves a Pd-coupling reaction of bromoindole analogue **230**, whereas path-B would involve a copper catalysed aryl hydroxylation of **230** followed by another metal-catalysed coupling to furnish **226**.



Scheme 3.20 Retrosynthetic analysis of **226**

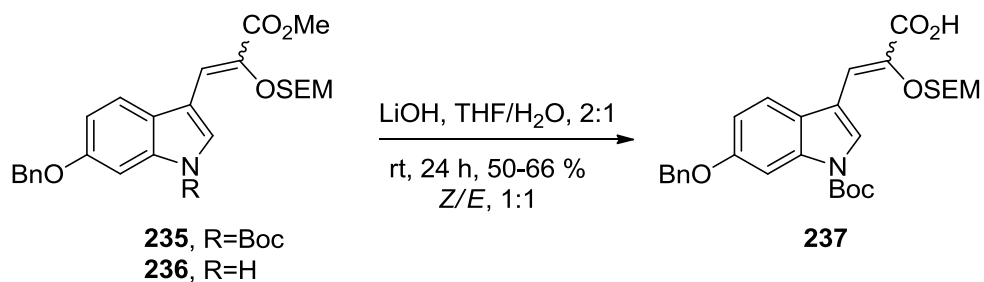
3.4 Synthesis of 6-benzyloxy-hydroxy-DKP precursor

Vilsmeier formylation of the commercially available 6-benzyloxyindole **231** with POCl₃ in DMF followed by *N*-Boc protection gave formyl indole **232** (Scheme 3.21).⁸⁵ Aldol condensation of **232** gave alcohol **234** in a ratio of 1.2:1.0 and 94% yield.^{59b} The mixture of alcohols were then dehydrated after treatment with MsCl, TEA and DBU to obtain α,β -unsaturated esters **235** as a 1.4:1.0 mixture of stereoisomers. The variation of diastereoselectivity in these reactions confirms the results of previous studies within our research group of structurally similar substrates.^{59b}



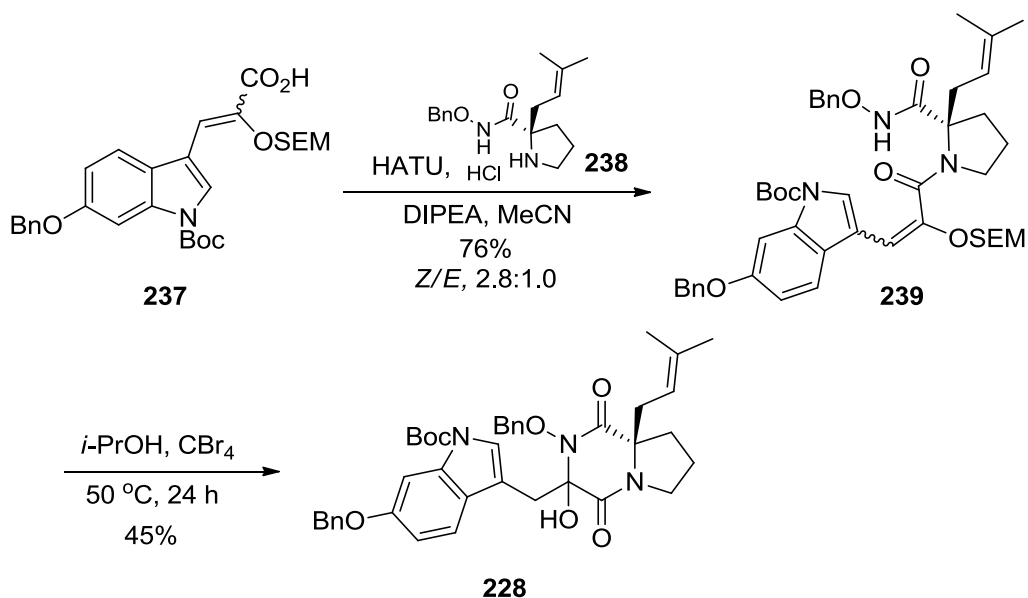
Scheme 3.21

Ester **235** was treated with 5.0 eq of LiOH in THF/H₂O this allowed the formation of 1:1 mixture of **237** (in a range of 50 - 66% yield) with the minimum formation of amine **236** (Scheme 3.22) and recovery of starting material. It was important to avoid formation of the **236** derivative due to difficulties during the purification process. Previous work in our laboratory had shown that hydrolysis of esters similar to **235** has proved problematic.^{59b} In order to improve the yield of this step several modifications of the experimental process were attempted but with no success. Finally, following the procedure originally described by Boger,⁸⁶ ester **235** was treated with 3.0 N LiOH in THF/MeOH/H₂O (3/2/1). In this case loss of the Boc group during the first 2 h of the reaction was observed.



Scheme 3.22

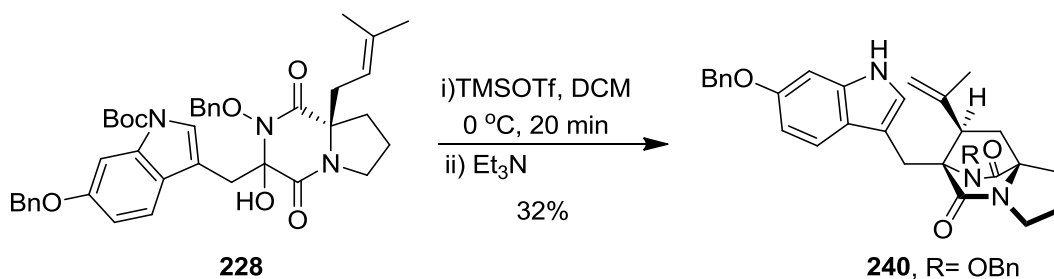
Acid **237** was coupled with enantiopure proline derivative **238** in the presence of HATU and DIPEA to afford a 2.8:1.0 mixture of amide **239** and 76% yield (Scheme 3.23). We were also able to observe changes in the diastereoselectivity during the peptide coupling as previously studies reports.^{59b} Preparation of hydroxy-DKP **228** involved OSEM deprotection of the enol followed by an intramolecular cyclization. The deprotection was facilitated by treatment of **239** with CBr₄ in dry *i*-PrOH at 50 °C. After 24 h DKP derivative **228** was obtained as a single diastereoisomer in 45% yield.



Scheme 3.23

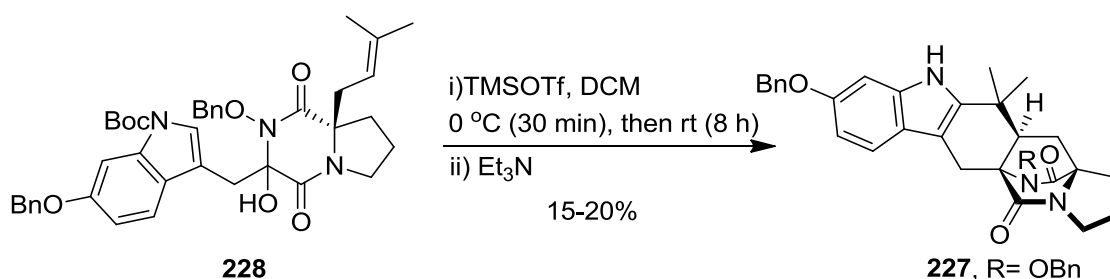
3.5 Cationic cyclisation of 6-benzyloxy-hydroxy-DKP

With DKP **228** in hand we were now ready to investigate the cationic cascade cyclization (Scheme 3.24). Treatment of **228** with 2.0 eq of TMSOTf at 0 °C followed by quenching with Et₃N after 30 min a new, more polar product, showed by TLC analysis. Upon purification of the reaction mixture we were able to obtain a 32% yield of the monocyclised product **240**.



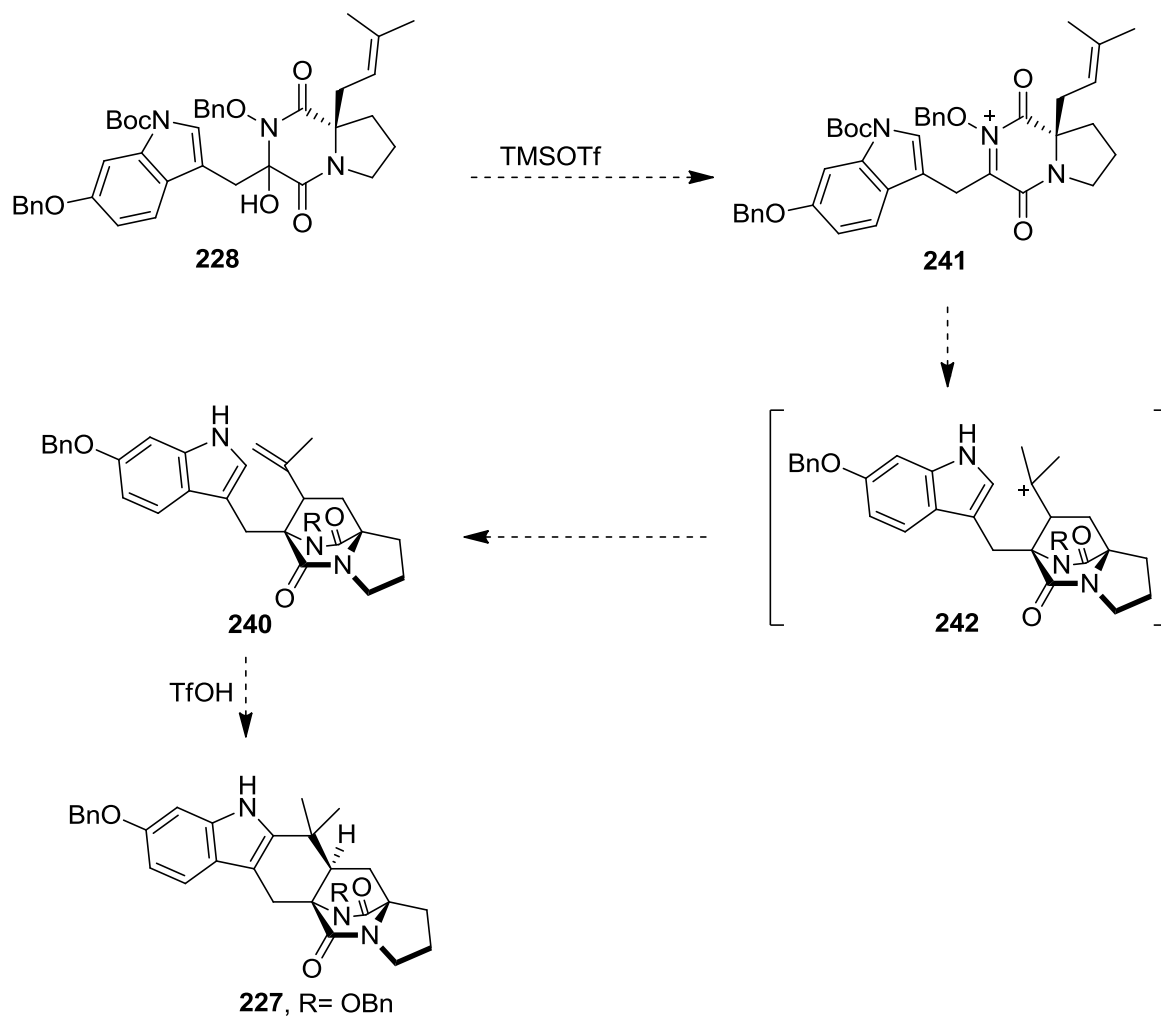
Scheme 3.24

Unfortunately, when the reaction was left for longer in the presence of TMSOTf we were able to obtain only 15-25% of the double cyclised product **227** (Scheme 3.25). The cyclisation attempt was followed by degradation of the starting material and/or products.



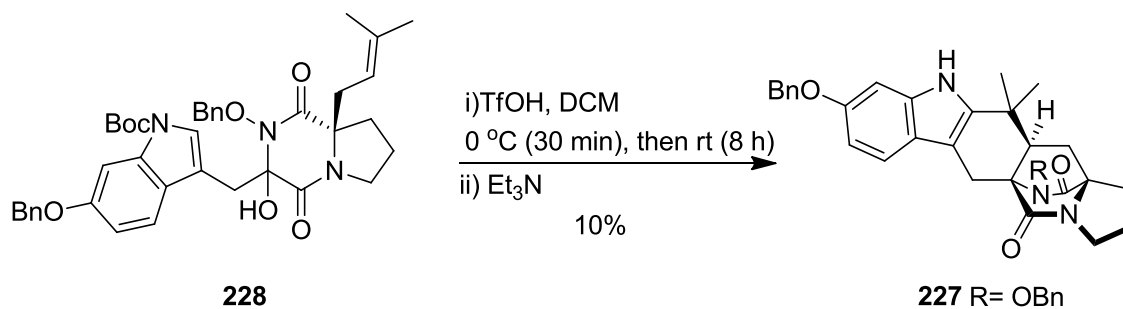
Scheme 3.25

During our investigations for the optimal conditions we observed that concentration of the reaction mixture had critical effect on the reaction rate. Surprisingly, concentration of the reaction mixture was also affecting the rate for the intramolecular cyclisation step, from intermediate **242** towards **227** (Scheme 3.26). Considering this, it is possible that the presence of another equivalent of acid (triflic acid) could initiate the second cyclisation and furnish **227**.



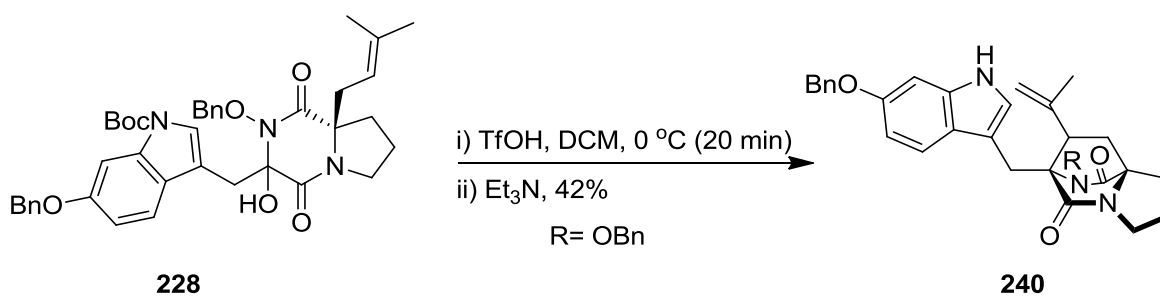
Scheme 3.26

Having evidence that the presence of acid could be vital for the completion of the reaction we were keen to repeat the reaction using directly triflic acid instead of TMSOTf. Unfortunately, treatment of **228** with 1.0-2.5 equivalents of triflic acid at 0 °C led to partial formation of the desired products as well as degradation (Scheme 3.27). In order to avoid degradation of the product, the reaction was then repeated at lower temperature (8 h at -50 °C to -40 °C for the first cyclisation, then 10 h at rt) but also in this case the yield was low.



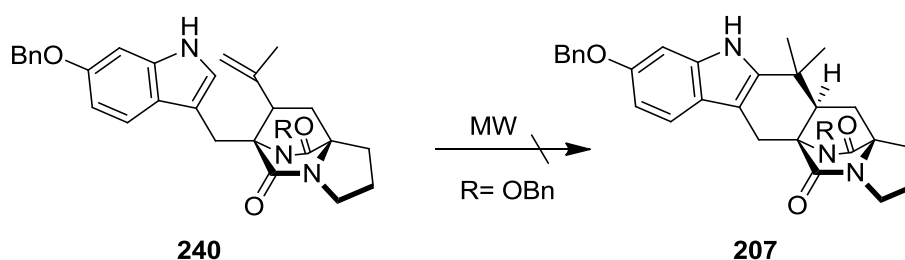
Scheme 3.27

Finally, when DKP **228** was allowed to stir in the presence of triflic acid for 20 min and then treated with triethylamine we were able to isolate the monocyclised product **240** in 42% (Scheme 3.28).



Scheme 3.28

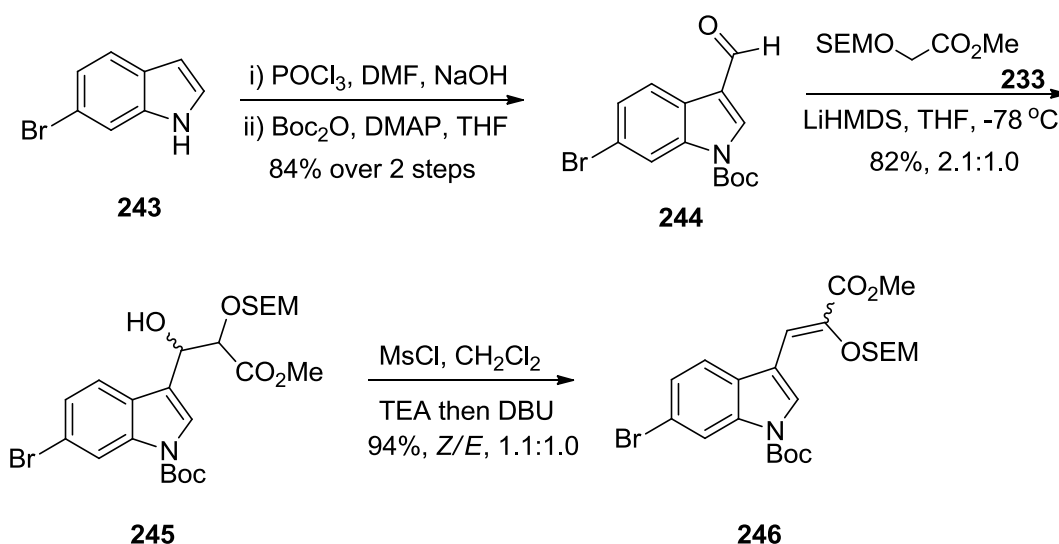
With small quantities of **240** in hand, the second cyclisation in the absence of acid was then attempted. These types of isoprene bridged DKP are known to undergo an ene reaction followed by a 1,2-shift when they are heated.^{77,87} Unfortunately, when solution of **240** in toluene was heated in microwave, left the starting material unchanged, while heating neat **240** at 200 °C resulted in complete degradation of the starting material (Scheme 3.29).



Scheme 3.29

3.6 Synthesis of DKP precursor of 6-bromoindole-hydroxy-DKP

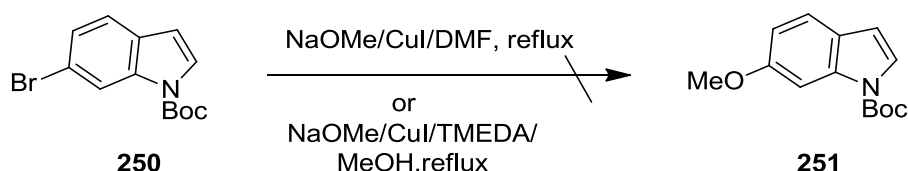
It is worth mentioning that similarly with preparation of **228** and other structurally related substrates the diastereoselectivity of the reactions towards **249** also varied.^{59b} The route towards DKP **249** began with formylation of 6-bromoindole (**243**) followed by *N*-Boc protection to afford indole **244** (Scheme 3.30). Aldol condensation using the same procedure as before and then dehydration of the hydroxy esters gave SEM enol ester **246** as a mixture of stereoisomers (*Z/E*, 1.1:1.0) and 94% yield.



Scheme 3.30

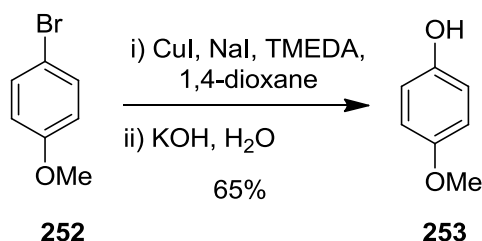
Hydrolysis of ester **246** in the presence of LiOH followed by peptide coupling led to the formation of amide **248** as a single diastereoisomer (Scheme 3.31). Finally derivative **248** was then SEM-deprotected to yield compound **249** which is the precursor for the key cationic cyclisation step.

optimum synthetic route and conditions by testing a cheap model system. Commercially available *N*-Boc-6-bromoindole was considered a suitable substrate for our research. Firstly methoxylation of 6-bromoindole was tested according literature reported examples.⁸⁸ Copper-mediated coupling of *N*-Boc-6-bromoindole **250** in dry DMF and excess of NaOMe/CuI after 48 h showed only Boc-deprotection of the starting material (scheme 3.33). Deprotection of the indole nitrogen was also observed when the reaction was repeated in MeOH in the presence of TMEDA.



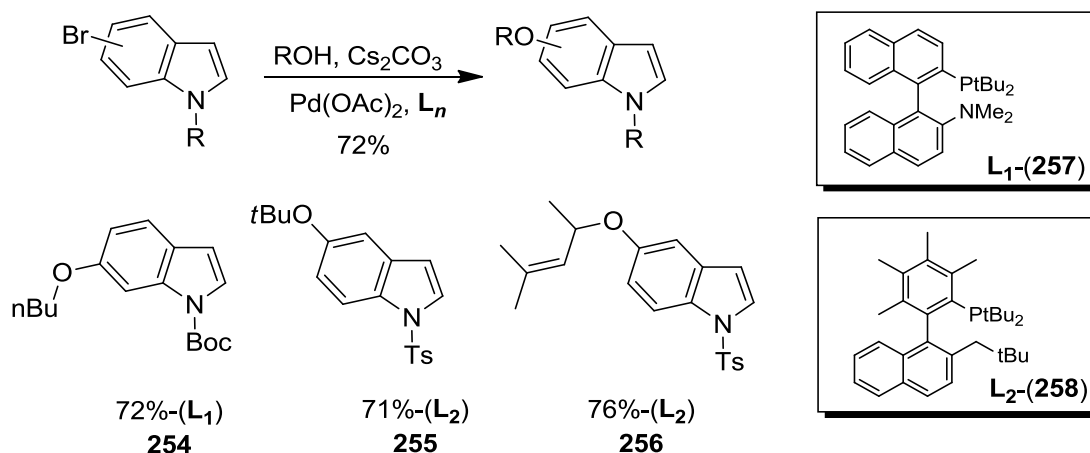
Scheme 3.33

Aryl bromides are known to give phenol products via copper-catalysed coupling.⁸⁹ Despite the lack of examples of indole derivatives in the literature we were keen to investigate this possibility in our substrates. First a literature example was tested in order to verify the experimental procedure as it is shown in Scheme 3.34.^{89a} Treatment of **252** with copper iodide, sodium iodide and TMEDA in 1,4-dioxane followed by addition of KOH in degassed H₂O gave the desired phenol **253** in 65% yield. Unfortunately, when the same conditions were applied to *N*-Boc-6-bromoindole, only starting material was recovered.



Scheme 3.34

We then turned our attention to Pd-catalysed C–O bond formation of aryl bromides with primary/secondary alcohols as developed by Buchwald *et al.*⁹⁰ We were pleased to find that among the test substrates, bromoindoles were also reported to undergo this type of transformation (Scheme 3.35).



Scheme 3.35 Literature examples of Pd-catalysed C–O bond formation indole substrates⁹⁰

Buchwald reports the use of non-commercial complex ligands for coupling reaction with indole substrates (Scheme 3.35).⁹⁰ As we were not certain of the unique utility of these ligands we firstly decided to test the reaction with commercially available ligands. Test reactions of 6-bromoindole were then attempted with various palladium catalysts ($\text{Pd}(\text{OAc})_2$, $\text{Pd}(\text{dba})_3 \cdot \text{CHCl}_3$,) and the in presence of ligands **259–262** (Figure 3.8). The Pd-mediated coupling reactions attempts were preceded with either commercially available alcohols (*n*-BuOH, 2-methyl-3-butyn-2-ol) under basic condition (Cs_2CO_3) or salts such as sodium 2-methyl-3-butyn-2-oxide.

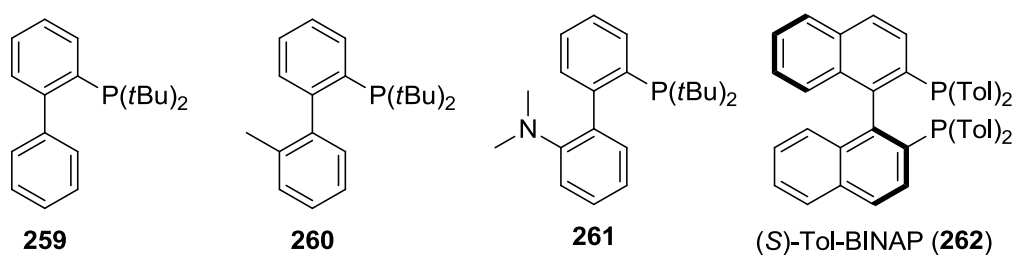
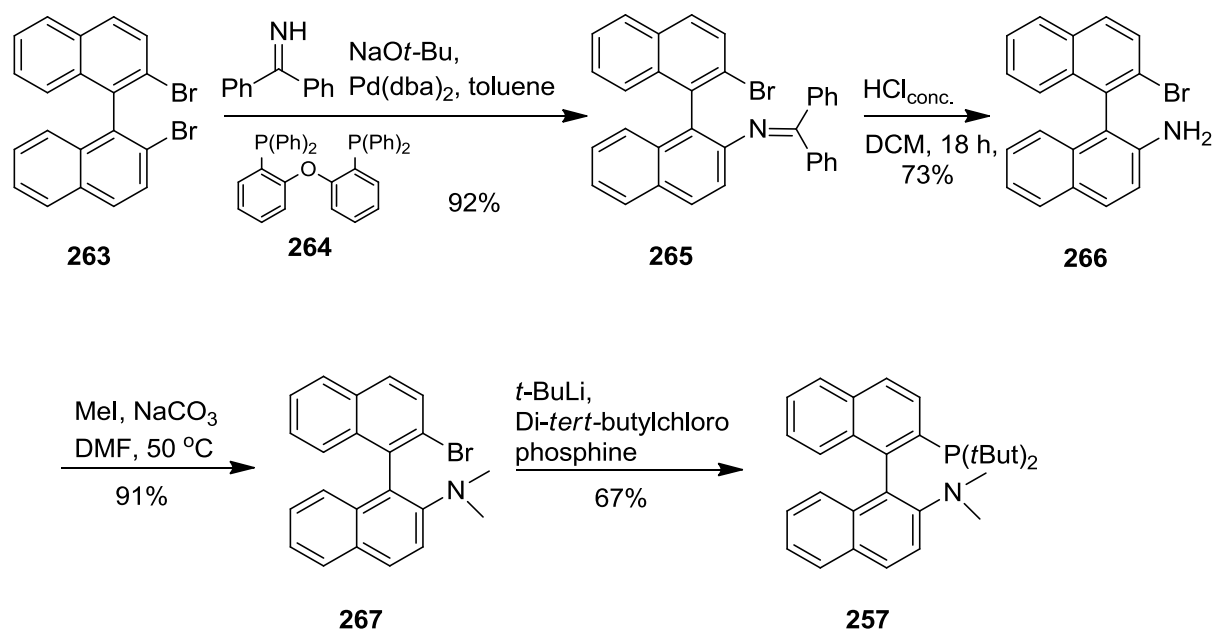


Figure 3.8 Structure of Pd-ligands

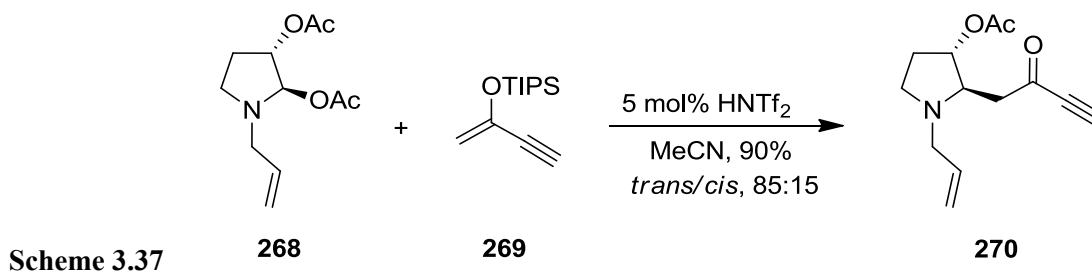
Unfortunately we were not able to obtain any of the desired products and as a consequence we turned our attention to the synthesis of the ligands that Buchwald reported (Scheme 3.36).⁹¹ The lack of experimental procedures and characterisation data⁹¹ for the intermediates made this synthesis very difficult to accomplish. We were only able to proceed to compound **266** in 45% overall yield from **263**, but despite our attempts we were not able to repeat the methylation step of this synthesis and synthesise **267**.



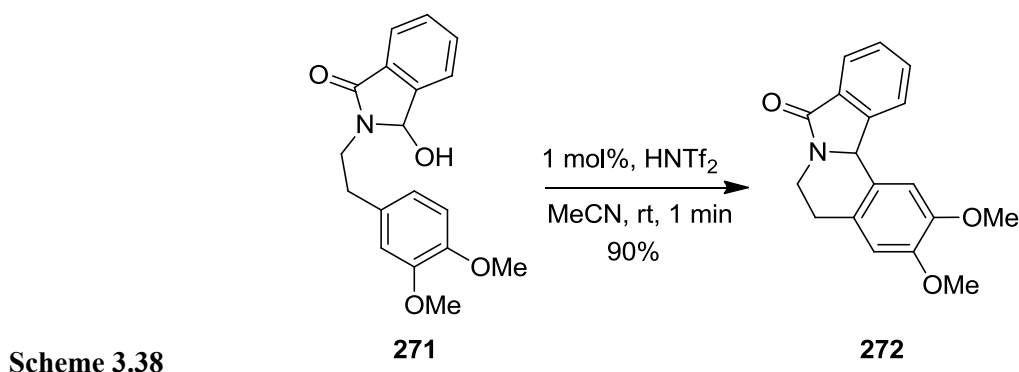
Scheme 3.36⁹¹ The Buchwald synthesis of ligand

3.8 Progress toward stephacidin A

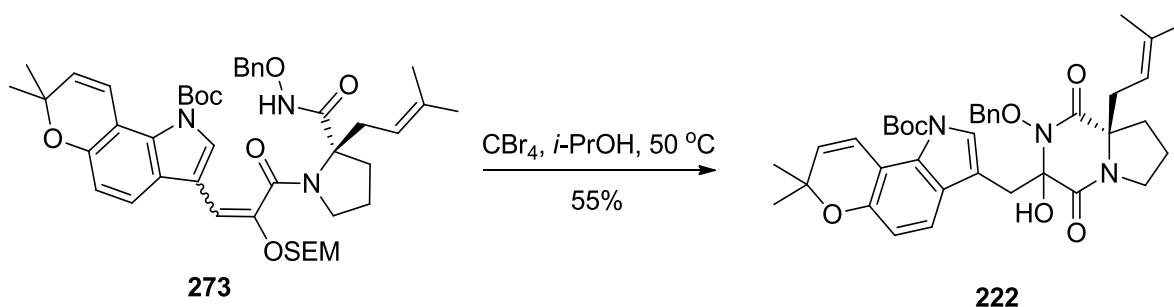
Despite our efforts to develop a new strategy towards stephacidin A (**35**), our attempts were not successful at this stage. After examination of the literature, we found that Dala and co-workers have developed a highly efficient α -amino alkylation reaction of silicon-based nucleophiles by *N*-acyliminium ion assisted by the catalytic system of $\text{HNTf}_2/\text{Me}_3\text{SiNTf}_2$.⁹² The strong oxophilic Lewis acid $\text{Me}_3\text{SiNTf}_2$ was synthesised *in situ* by photodesilylation of the precatalyst HNTf_2 with with silyl enol ether **269** (Scheme 3.37).



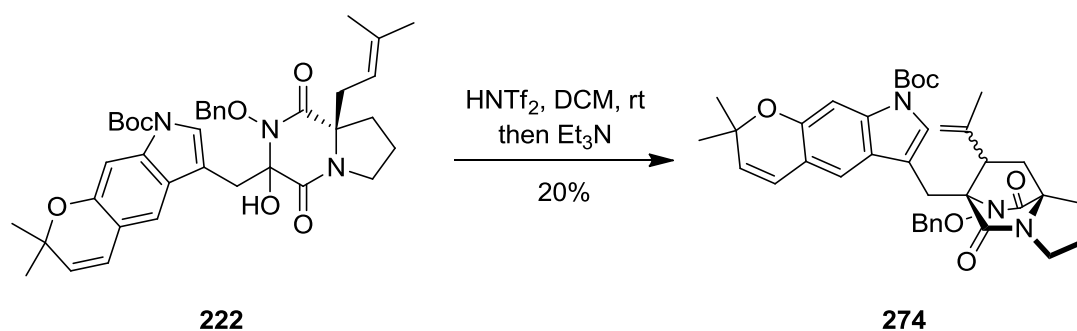
An intramolecular Friedel-Craft type cyclisation of hydroxylactam **271** in presence of 1 mol% of HNTf₂ was also reported (Scheme 3.38).⁹³ Considering the extremely poor nucleophilicity of HNTf₂ (which could provide long-lived cations) and its lower acidity than TfOH, this encouraged us to investigate the possibility of a cationic cyclisation initiated by catalytic acid.



We were hoping that the low concentration of this acid in solution would promote a cyclisation of the DKP precursor rather than the degradation reaction. Besides, it is known that advanced intermediates of stephacidin A (**35**) are stable to 0.1 N solution of HCl.^{78b} From an advanced intermediate (**273**), we prepared the desired hydroxy-DKP **222** (Scheme 3.39) and we were now poised to apply cyclisation under HNTf₂ catalyst.

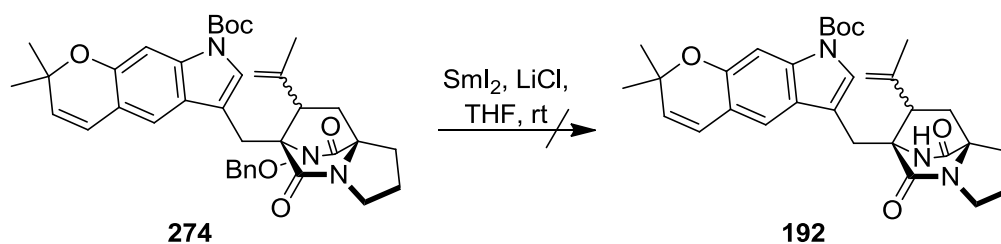


To a solution of **222** in dry DCM was added 5% mol of 0.5M solution of HNTf₂ in DCM and the reaction mixture was stirred at rt (Scheme 3.40). TLC analysis of the reaction mixture after 2 h showed that the starting material was left unchanged, and it proved possible to drive the reaction to completion only by addition of 1 equivalent of HNTf₂. After purification of the new polar spot by flash column chromatography followed by HPLC, we were pleased to confirm formation of the bridged DKP **274** by NMR analysis, albeit in very modest yield.



Scheme 3.40

With DKP **274** in hand, we were now in a position to set about the formal synthesis of (-)-stephacidin A (**35**). Deprotection of the DKP-amide by oxidative cleavage using freshly prepared SmI₂⁹⁴ would lead to compound **192** which is described by Baran and co-workers in the total synthesis of stephacidin A (**35**).⁷⁷ When the optimum conditions were applied in solution of **274** in THF a new more polar spot was observed by TLC analysis (Scheme 3.41). Despite our efforts and due to the insufficient amount of product, we were not able to provide clean NMR data and compare them with literature.



Scheme 3.41

Even though we were not able to complete the formal synthesis, it has been shown that a stepwise cyclisation was possible to give an advanced intermediate for stephacidin A (**35**). It was clear to us that the present cationic cyclisation key-step promoted by acids had limitations in the synthesis of complex and sensitive natural products belonging to this family. For these reasons we focused our efforts to developing a new radical-based methodology for construction of the core ring system which could be applied in the synthesis of various natural products including stephacidin A (**35**).

Chapter 4

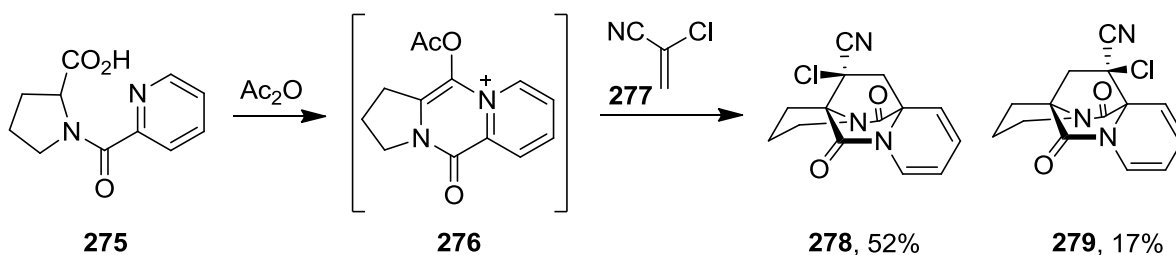
Studies of cyclisation reaction of prenylated DKP

4.1 Synthetic approaches to the bicyclo[2.2.2]diazaoctane ring system.

The bicyclo[2.2.2]diazaoctane core ring system is common to a number of biological highly active secondary metabolites isolated from various species of fungi. Over the last three decades intense research efforts have been made to prepare the basic skeleton for the diverse family of prenylated indole alkaloids. Major synthetic strategies employed intramolecular S_N2' cyclisation, biomimetic Diels-Alder reaction, radical cyclisation and a one-pot cationic approach.

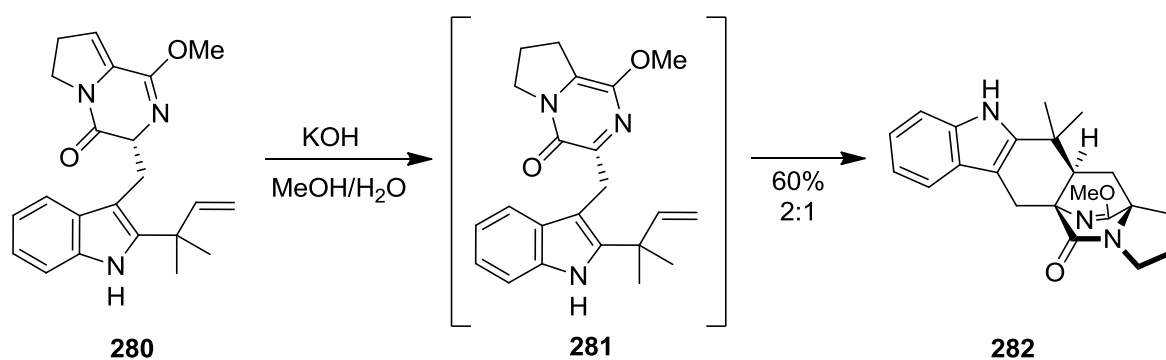
4.2 Biomimetic Diels-Alder approach

An interesting by-product was reported by Fabre *et al.* during their studies on 1,3-dipolar cycloaddition of prolines.⁹⁵ When proline **275** was treated with acetic anhydride, azadiene **276** was formed and spontaneously reacted with 2-chloroacrylonitrile to give cycloadducts **278** and **279** (Scheme 4.1).



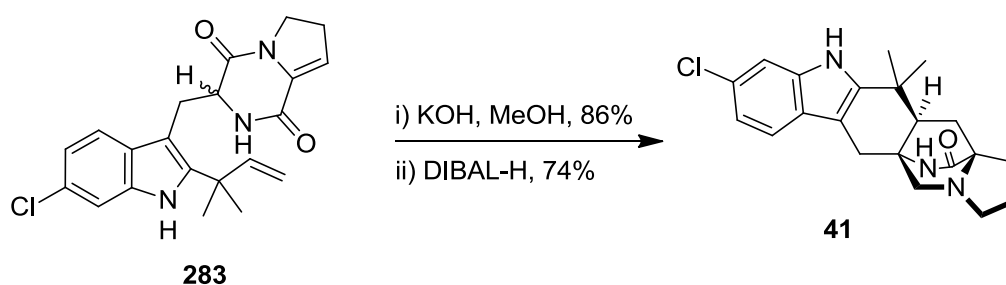
Scheme 4.1

The first application of the biomimetic Diels-Alder reaction to this family of alkaloids was in the total synthesis of (±)-brevianamide B (**5**) by Williams (Scheme 4.2).⁸² Lactim ether **280** was tautomerized to the azadiene **281** under basic conditions followed by an intramolecular Diels-Alder reaction to give **282** as a 2:1 ratio of diastereomers. Very similar synthetic approaches were also applied to the synthesis of racemic VM55599 (**73**),⁹⁶ stephacidin A (**35**) and notoamide B (**29**).^{78a}



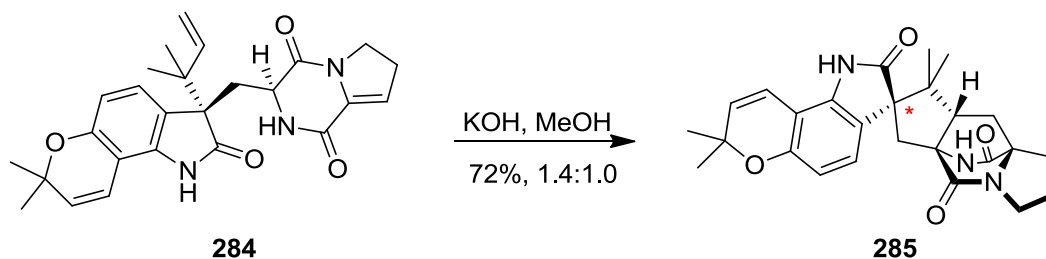
Scheme 4.2

For the synthesis of malbrancheamide B (**41**), DKP **283** was prepared for use in the key intramolecular Diels-Alder reaction (Scheme 4.3).⁹⁷ Addition of aqueous KOH to a solution of **283** followed by a selective reduction of tertiary amide using an excess of DIBAL gave the final heptacyclic product **41**.



Scheme 4.3

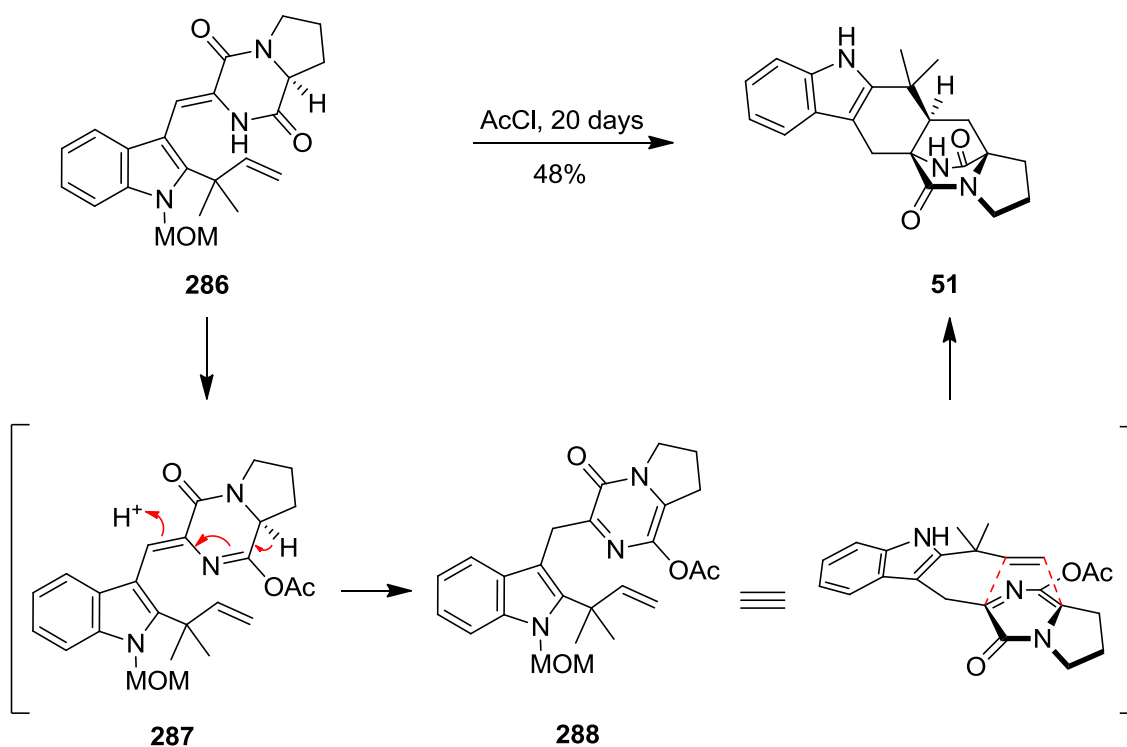
This methodology was also applied to the synthesis of *spiro*-oxindole structures common to a number of highly biologically active natural products.^{15a} As Scheme 4.4 shows, oxindole **284** was chosen as a precursor for the key step towards (-)-versicolamide B. Under basic conditions DKP **284** undergoes an intramolecular Diels-Alder reaction to give *spiro*-oxindole **285** and its diastereomeric cycloadduct in a 1.4:1.0 ratio and 72% yield.



Scheme 4.4

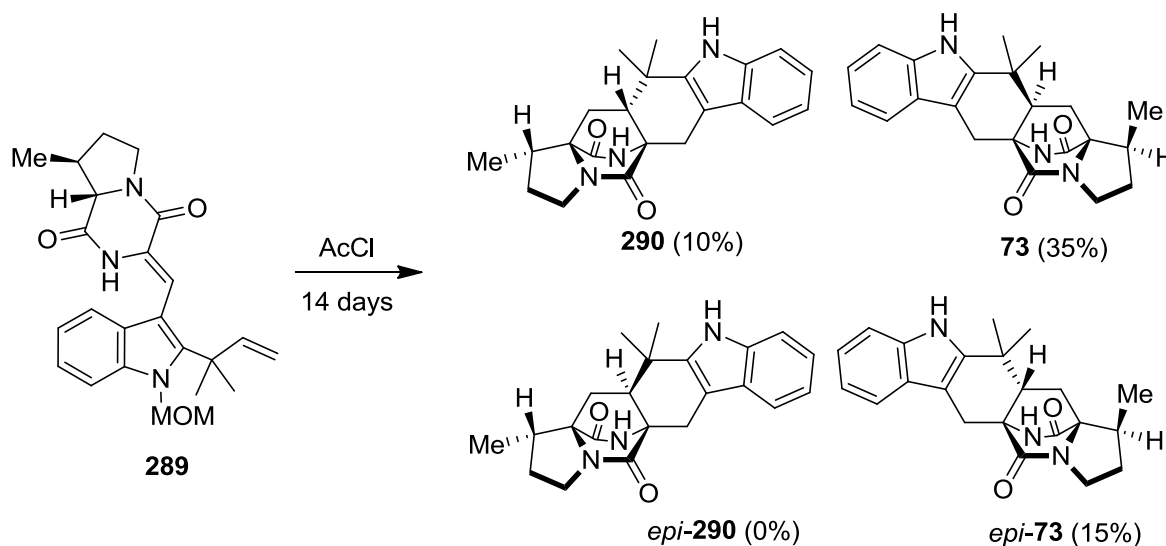
From *ab initio* calculations it has been shown that the Diels-Alder reaction of an oxindolic azadiene leads to *anti*-cycloadducts due to a particularly stable transition state.⁹⁸ On the other hand, an indolic azadiene reacts though roughly equally stable *syn*- and *anti*-transition states.

A Diels-Alder reaction under neutral conditions was introduced by Liebscher and co-workers,⁹⁹ who developed a shorter synthesis to access precursor **286**. The unsaturated compound **286** was treated with neat acetyl chloride for 20 days leading the formation of bridged DKP **51** as a single diastereomer (Scheme 4.5).



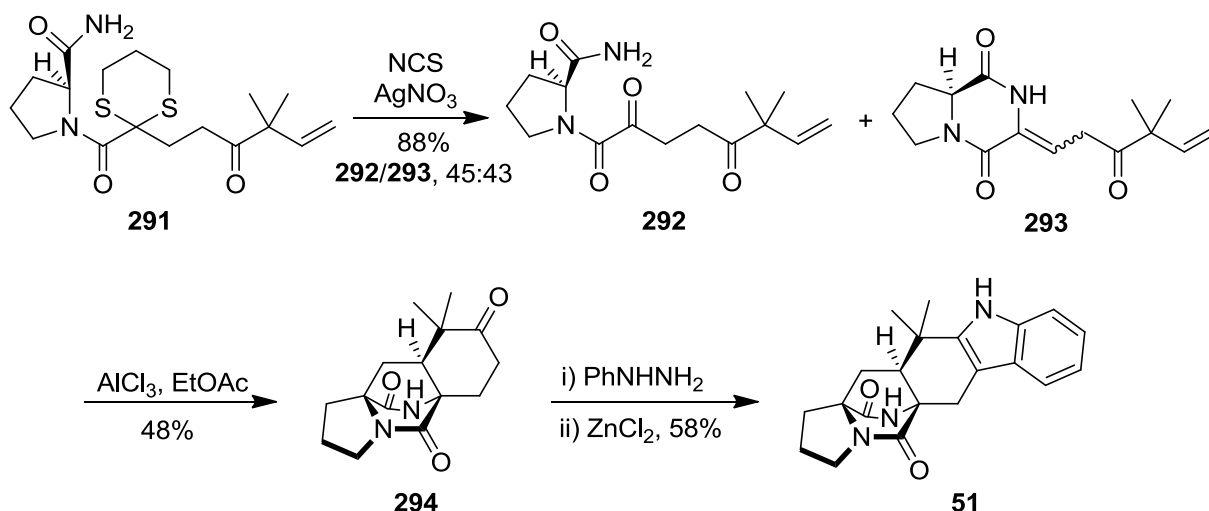
Scheme 4.5

Liebscher's protocol was also applied to the synthesis of *Z*-unsaturated DKP **289** in the first asymmetric total synthesis of (-)-VM55599 (**73**) by Williams (Scheme 4.6).⁵⁷ Diels-Alder reaction of **289** gave a mixture of diastereoisomers with **73** as the major cycloadduct. The authors suggest that the key intermediate **289** undergoes an intramolecular Diels-Alder reaction via three of the four possible transition states. Cycloadduct **73** was reduced by an excess of DIBAL-H to give enantiopure (-)-VM55599 (**73**) in 68% yield and the absolute stereochemistry of the natural product was also determined.



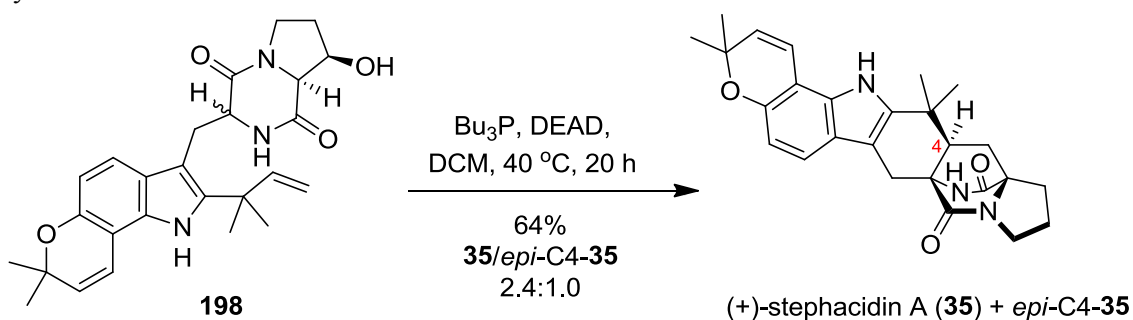
Scheme 4.6

A highly *anti*-selective Diels-Alder was later introduced for the synthesis of racemic brevianamide B (**5**) (Scheme 4.7).¹⁰⁰ Amide **292** and DKP **293** which were generated by dithiane group removal from **291**, were treated with excess of AlCl₃ to give exclusively cycloadduct **294**. Fischer indole synthesis of **294** gave **51** in 58% yield.



Scheme 4.7

Finally, Williams also reported that **198** undergoes a Mitsunobu-type elimination and Diels-Alder reaction to give the bicyclo[2.2.2]diazaoctane core.^{56,78c} As shown in Scheme 4.8 when DKP **198** was treated with an excess of PBu_3 and DEAD it formed cycloadduct **35** and its epimer in 2.4:1.0 ratio and a total yield of 64%.

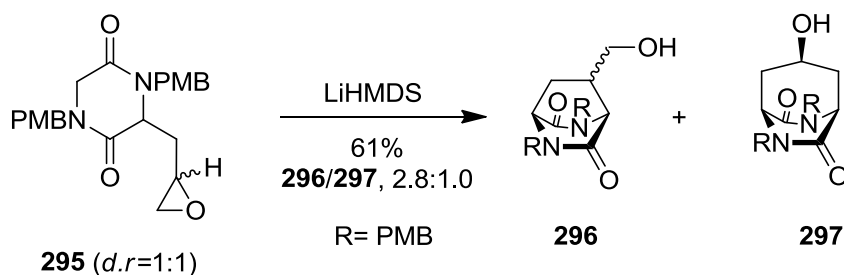


Scheme 4.8

4.3 Intramolecular $\text{S}_{\text{N}}2'$ cyclisation approach

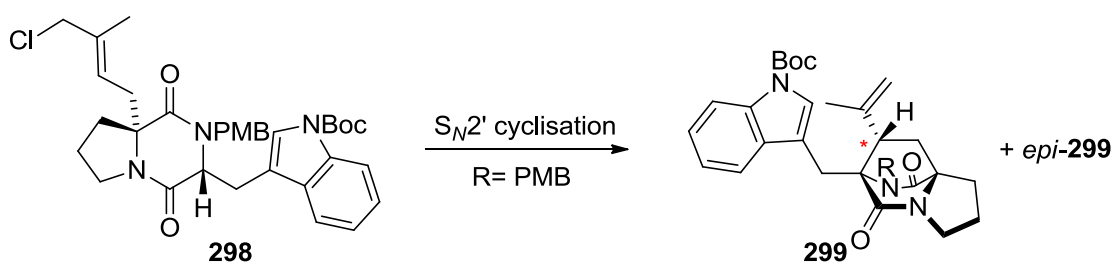
Before Williams' research group focused their efforts on the biomimetic Diels-Alder approach they developed an intramolecular $\text{S}_{\text{N}}2'$ cyclization reaction. In their first attempt a 1:1 mixture of diastereoisomeric epoxides **295** were ring-opened by a nucleophilic attack of an enolate which was

produced by addition of LiHMDS (Scheme 4.9).¹⁰¹ The epoxide ring opening gave a 2.8:1.0 mixture of **296** and **297** in 61% combined yield.



Scheme 4.9

In the synthesis of brevianamide B (**5**), Williams and co-workers introduced a chloro-alkyl group in order to avoid formation of a seven-membered ring akin to product **297**.⁸³ In the key step, DKP **298** (Table 4.1) underwent intramolecular S_N2' cyclisation to give **299** and its epimer in a 2:1 ratio and 62% yield. Surprisingly when benzene was used as a solvent they obtained *epi*-**299** as the major product (ratio 3:97, 82% yield). In contrast with the previous example, the reaction in the presence of 18-crown-6 in benzene gave as a major product **299** in a 4:1 ratio and 56% yield.



Base	Solvent	299 : <i>epi</i> - 299 (yield)
NaH	DMF	2:1 (62%)
NaH	benzene, Δ	3:97 (82%)
NaH	benzene, Δ (18-crown-6)	4:1 (56%)

Table 4.1 Intramolecular S_N2' cyclisation of **298**

A possible reason for the different diastereoselectivities is the ability of DMF and 18-crown-6 to solvate the sodium cation of the enolate anion.⁸³ Without a solvent effect there is a tight intramolecular interaction which promotes an ion pair-driven closed transition state which leads to the *syn* product (B in Figure 4.1). Alternatively, the presence of DMF or 18-crown-6 can break open this closed transition

state to affect the cyclisation from the other face of the allylic π -system and lead to the *anti*-product (A in Figure 4.1).

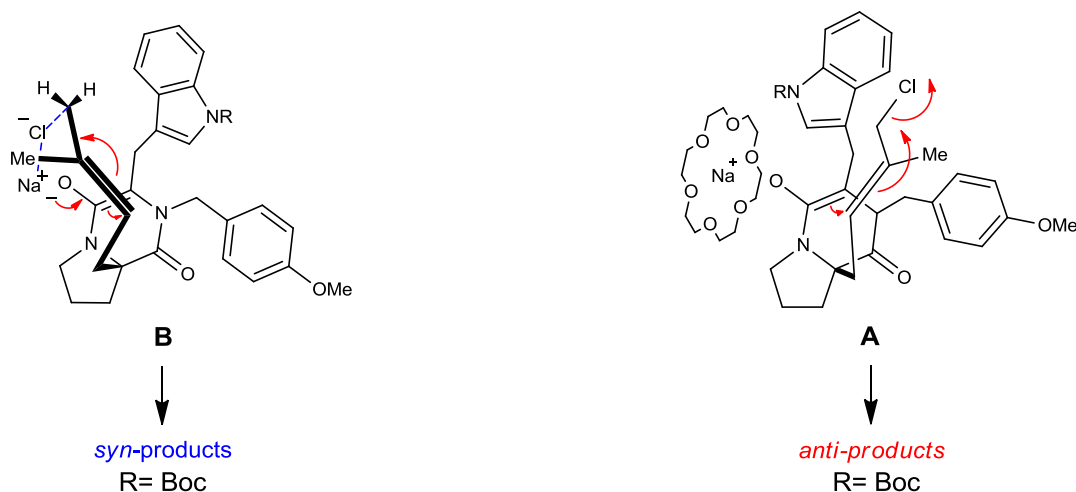


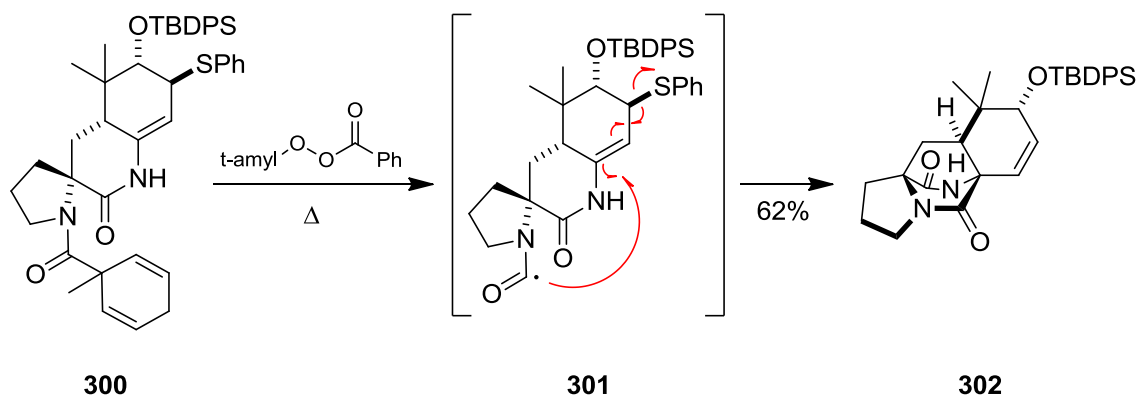
Figure 4.1⁸³ Transition states of enolate **298**

Using the same strategy, Williams and co-workers applied the selective intramolecular S_N2' cyclization reaction in order to synthesise the structurally similar natural products paraherquamide **A** (**10**)¹⁰² and **B** (**11**),¹⁰³ stephacidin **A** (**35**) and **B** (**39**), and avrainvillamide (**36**).^{78b}

4.4 Radical cyclisation approach

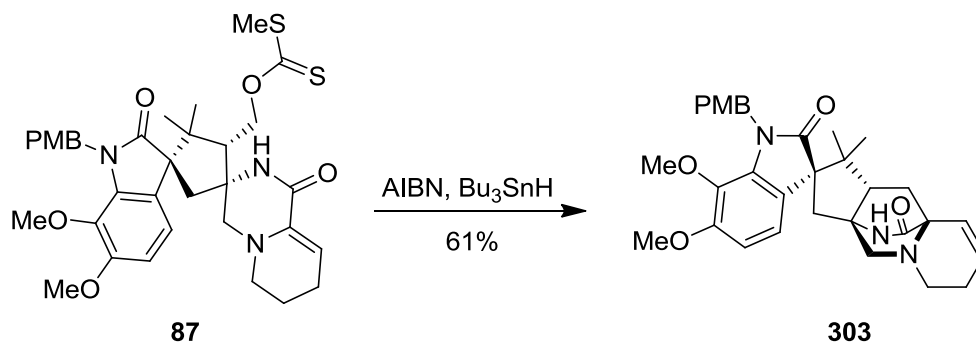
Free radical chemistry is one of the most powerful tools in organic synthesis and it can provide new cascade reactions towards moderately complex and densely functionalised natural products. Several groups working on the synthesis of the bicyclo[2.2.2]diazaoctane core have based their retrosynthetic plans around multiple key bond disconnections which could be formed using radical chemistry.

In their synthetic approach towards avrainvillamide (**36**) and stephacidin **B** (**39**), Myers and co-worker proved that the bicyclo[2.2.2]diazaoctane core could arise via an aminoacyl radical cyclisation of **300** (Scheme 4.10).⁴⁶ When **300** was heated in presence of *tert*-amyl peroxybenzoate, amino acyl radical **301** was generated and cyclisation occurred onto the more substituted carbon of the enamine double bond. After addition a thiophenyl radical was expelled to give **302**.



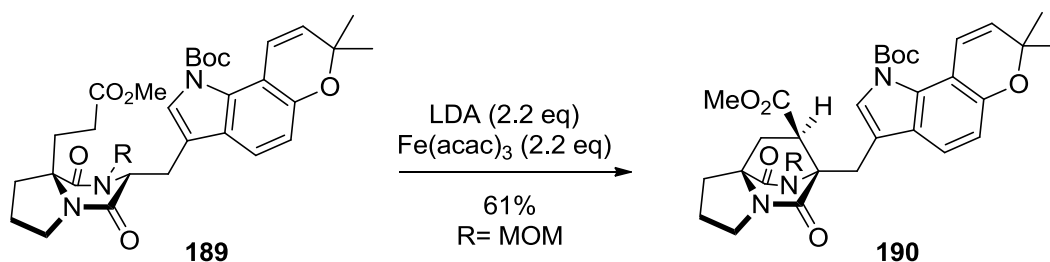
Scheme 4.10

One year later a concise synthesis of (\pm)-marcfortine B (**26**) was reported by Trost *et al.*⁵³ The synthetic route involved a [3+2] cycloaddition (TMM) and a radical cyclisation reaction to form the core framework of the natural product. Having in hand the *spiro*-oxindole **87** (eleven steps), a radical cyclisation was then performed to give the more advanced hexacyclic intermediate **303** (Scheme 4.11).



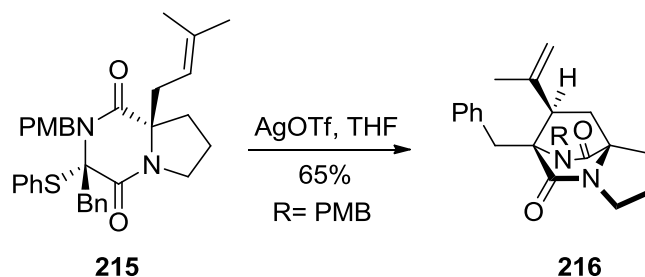
Scheme 4.11

Baran's group was also attracted to the complexity of these natural products and for several years focused their research in this area. In their efforts to synthesise of the stephacidins, they demonstrated an interesting oxidative enolate coupling of **189** to **190** (Scheme 4.12).^{47,77,79}



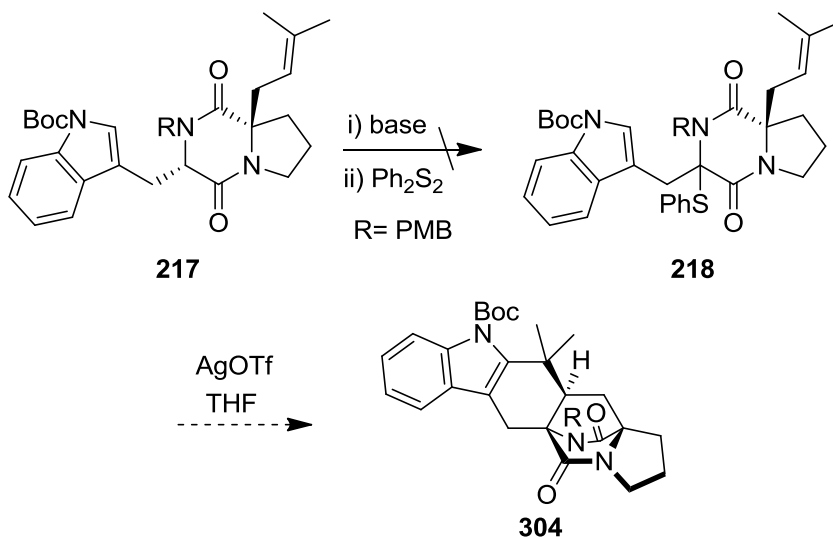
Scheme 4.12

Previous work in our group showed that a cationic cyclisation route could also be applied to the synthesis of these bridged DKP structures.^{59,84} DKP **215** underwent cationic cyclisation in the presence of AgOTf to give exclusively bridged DKP **216** (Scheme 4.13).



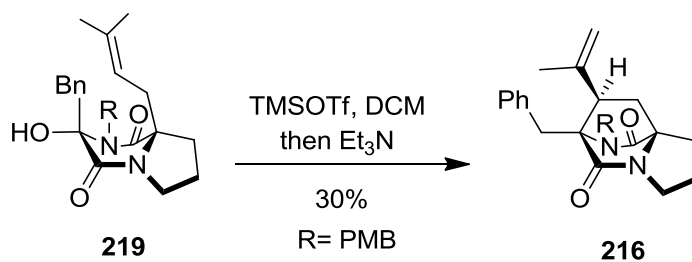
Scheme 4.13

With the first successful example of cationic cyclisation in hand, Simpkins and co-workers were now keen to explore a cationic cascade reaction. DKP **218** was then attempted to be synthesised but unfortunately installation of a thiophenyl group proved to be problematic^{59a,84b,104} (Scheme 4.14) and so an alternative approach was then applied.



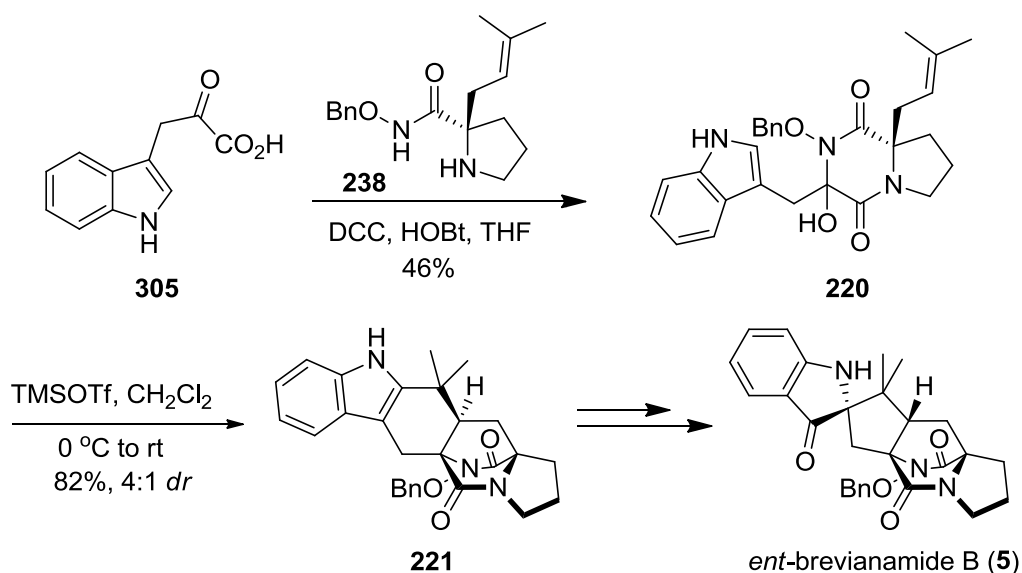
Scheme 4.14

The new strategy proposed that a hydroxyl-DKP such as **219** (Scheme 4.15) could possibly undergo a cationic cyclisation in the same fashion as **215** (Scheme 4.13) and furnish the same products. Thus, treatment of **219** with TMSOTf led to formation of bridged product **216** in 30% yield (Scheme 4.15).



Scheme 4.15

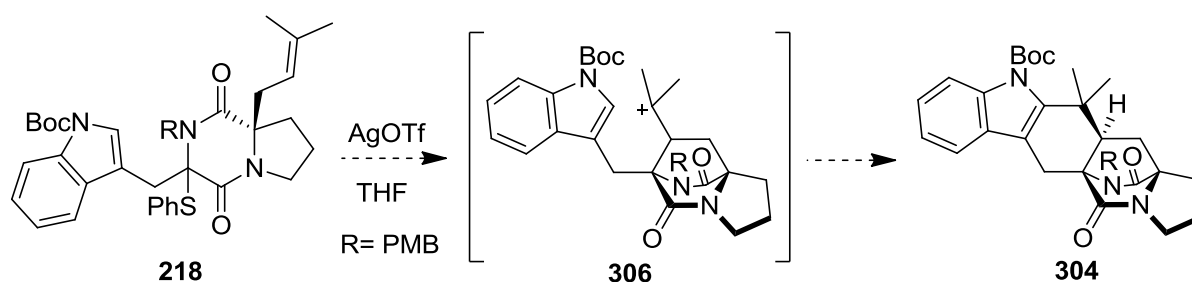
A new access to indole alkaloids could be possibly achieved by combination of cationic reaction of hydroxy-DKPs with the indole-capture step already described by Williams.^{80,83} *O*-benzyl proline hydroxamic acid **238** was coupled with indole puruvic acid **305** to give DKP **220** in 46% yield (Scheme 4.16). Treatment of **220** with TMSOTf gave a 4:1 mixture of heptacyclic product **221** and *epi*-C4-**221**. Based on this successful double cyclisation, total syntheses of *ent*-brevianamide B (**5**)^{59a} and *ent*-malbrancheamide B^{59b} (**41**) was also achieved.



Scheme 4.16

4.5 Investigation of a new strategy towards stephacidins

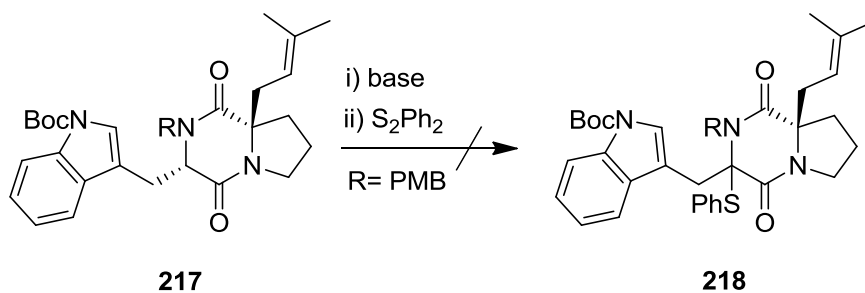
Unfortunately, the previously described cationic cascade cyclisation strategy (Scheme 4.16) could only be applied on acid-stable substrates such as **220**. Thus, this methodology could not be used for the synthesis of stephacidins or other relevant natural products. For that reason, we decided to put effort into the synthesis of sulfenyl-DKP **218** (Scheme 4.17).^{84b,85,108} This strategy was combining a non-acidic cationic reaction of sulfenyl-DKP **215** (Scheme 4.13) and the indole-capture step of intermediate **306** to give **304** (Scheme 4.17).



Scheme 4.17

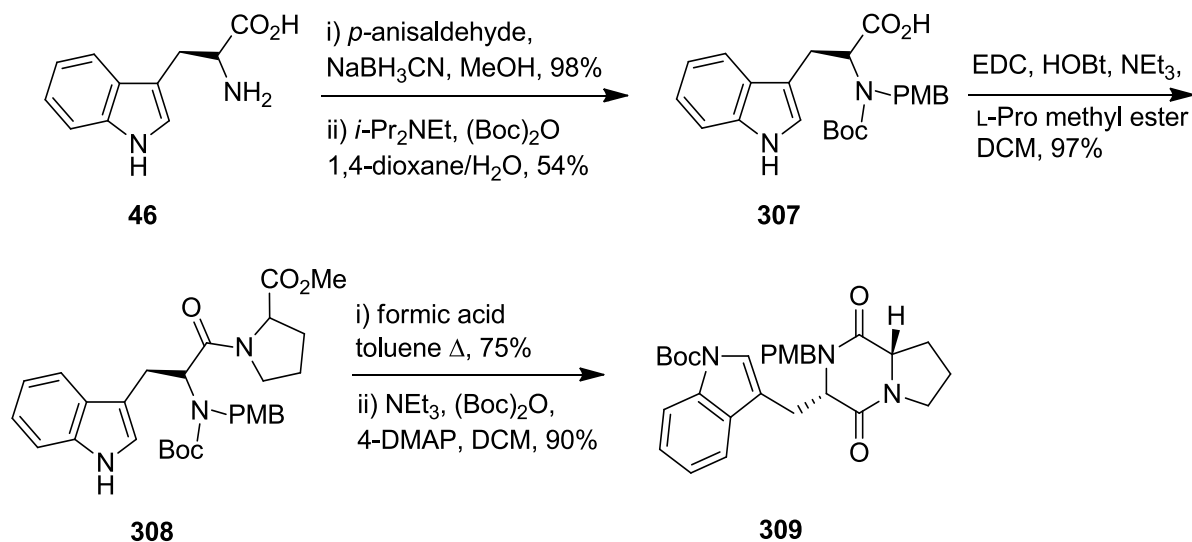
4.6 Synthesis of the DKP precursor – The sulfenylation reaction

Previous studies of the sulfenylation step in our group involved an extensive screening of different bases (LDA, LiHMDS, KHMDS, *n*-BuLi, NaH) but there was no examination about the time which the enolate was forming.^{84b} All attempts involved treatment of **217** with 1.0 to 2.5 eq of base at -78 °C and stirring at this temperature for a further hour before the electrophile was added (Scheme 4.18). We believed that the long enolate formation could be one of the possible reasons we could not obtain the desired **218**. In order to investigate this possibility we decided to re-synthesize DKP **217** and optimise the condition in order to obtain the desired precursor **218**.



Scheme 4.18

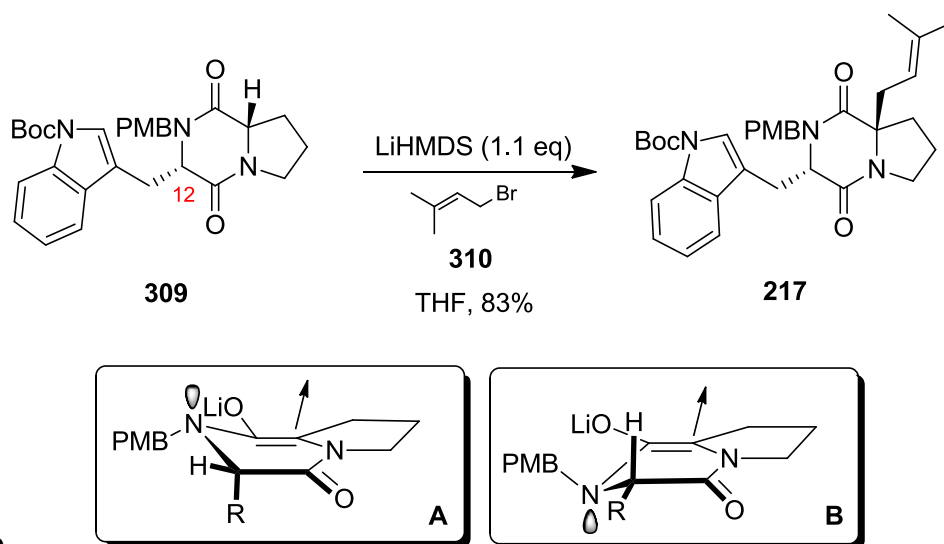
Commercially available L-tryptophan **46** was doubly *N*-protected and subsequently coupled with enantiopure L-proline methyl ester to afford amide **308** (Scheme 4.19). Deprotection of the Boc group under acidic conditions, thermally induced cyclisation of the crude material followed by *N*-Boc protection gave the desired DKP **309**.



Scheme 4.19

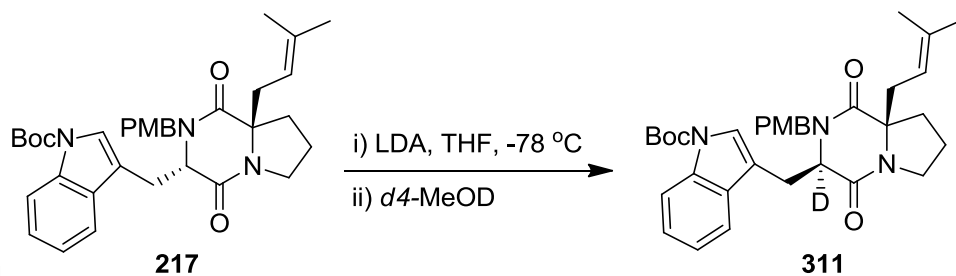
DKP **309** was treated with 1.1 eq of LiHMDS and the reaction mixture was left to stir at -78°C for 1 h followed by addition of prenyl bromide in dry THF to furnish the corresponding prenylated DKP derivative **217** (Scheme 4.20). This highly stereoselective enolate substitution with overall retention at the proline α -centre led smoothly to formation of only one diastereoisomer **217**. The alkylation proceeded with a high level of facial selectivity due to the pseudo-axial group located at C12 as

conformation A in Scheme 4.20 shows.^{84b,104-105} In the case of small R groups such as methyl this argument is less convincing. In that case, the steric shielding afforded by a small substituent in a 1,4-arrangement is not reasonable to explain the high stereoselectivity. In this case, conformation B seems reasonable due to the weak 1,2-torsional strain and it is possible the alkylation to occur from the top face as well-established work for various lactams enolates tend to react *anti* to the pyramidalised nitrogen lone pair.¹⁰⁶



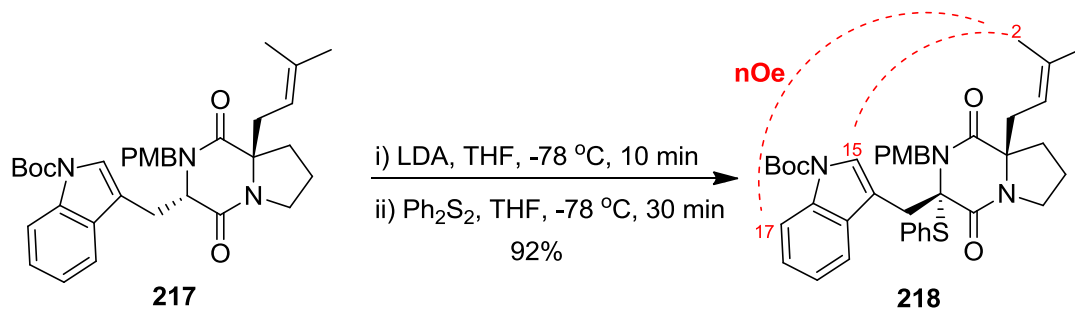
Scheme 4.20

With **217** in hand, we were about to investigate the optimum conditions of the sulfenylation step. Firstly, we examined whether we would be able to form the enolate of **217** and then report the optimum conditions. It was crucial to know how fast we could have full conversion of the starting material to the enolate form in order to obtain the desired product. Thus, solution of **217** in dry THF was prepared and 1.7 eq of LDA (1.0 M in hexane/THF) was added slowly at -78 °C (Scheme 4.21). After 5 min, 1 mL of the reaction solution was transferred via syringe to a dry flask containing 2 mL of *d*4-MeOD. The same procedure was repeated at 30 min, 1 h and 2 h after the addition of the base. Monitoring the reaction by TLC we observed an additional more polar spot in all of these batches. By NMR studies we were delighted to find that we had full incorporation of deuterium at C12, 5 minutes after addition of base and that the new spot we observed was due to formation of the deuterated-(C12)-epimer **311**.



Scheme 4.21

Simpkins and Pichowicz showed that the stereoselective outcome on enolisation of DKPs could arise by hindrance of the convex face which is shielded by the prenyl group.^{84b} The resulting steric effects promote an *anti*-electrophilic approach to the prenyl group. It is worth to note that we were able to monitor the enolate formation by TLC analysis due to different R_f of **311** and compound **217**. Having defined the optimum conditions for the enolate formation we were now poised to investigate the sulfenylation step in the synthesis of the important sulfide **218**. Repeating the reaction under the same conditions, DKP **217** was treated with 1.4 eq of LDA (0.8 M in THF/hex) at $-78\text{ }^\circ\text{C}$ and the reaction mixture was left to stir at this temperature (Scheme 4.22). Monitoring the progress of the reaction by TLC after 10 min we observed full conversion to the *epi*-**217** and then a solution of Ph_2S_2 in dry THF was added. After 30 min TLC monitoring showed no remaining *epi*-**217** but instead a new spot appeared. Examination of the crude ^1H NMR spectrum showed no starting material or its corresponding epimer and the compound was the desired sulfide. After purification and assignment we were delighted to report that the crucial precursor sulfide **218** was formed in 92% as a single diastereoisomer.



Scheme 4.22

nOe studies showed a correlation between H2 with H15 and H17 and as a result we were able to establish the complete stereochemistry relative to the unchanged α -centre of the proline. We were subsequently able to grow crystals from MeOH and secure the relative configuration by X-ray crystallography. The structure shows clearly that the substitution of the SPh unit is *anti* to the prenyl group and on the more concave face to the bicyclic system. The crystal system of this compound was orthorhombic and it contained one molecule of methanol per DKP unit which forms a hydrogen bond (Figure 4.2).

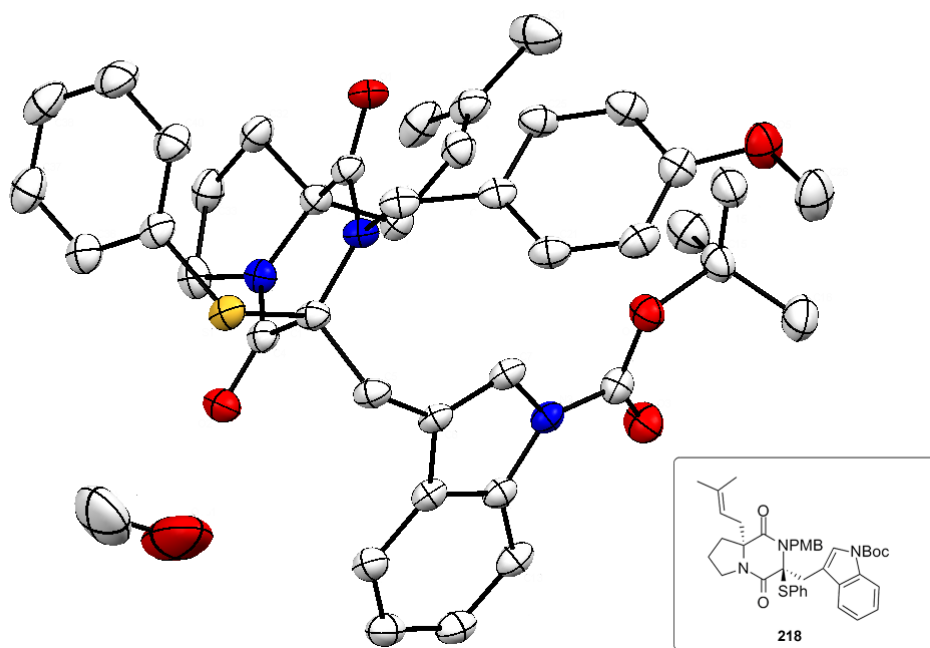
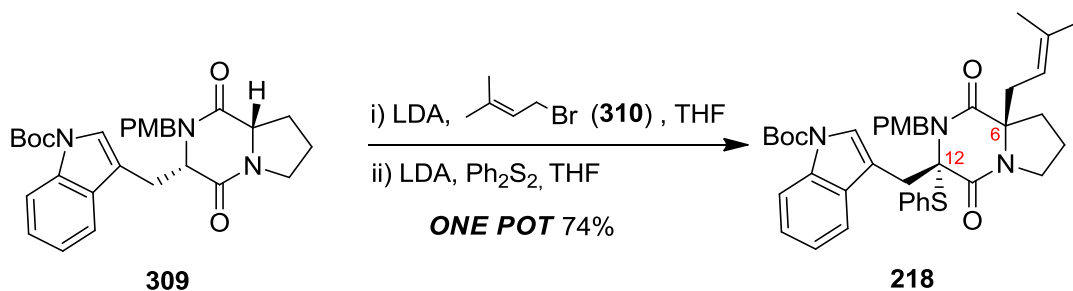


Figure 4.2 Crystal structure of sulfide **218**

4.7 A new stereospecific alkylation – Sulfenylation reaction

Before we examined the possible synthetic applications of sulfide **218** we were keen to investigate an stereoselective double enolate substitution reaction. Our proposal involved a stereospecific introduction of a prenyl unit to the proline α -centre (C6) controlled by the presence of the indole substituent (Scheme 4.23). This prenyl substituent could now control the geometry of the newly formed stereogenic centre at C12 if a second equivalent of base was added followed by Ph_2S_2 . Indeed, addition of 1.1 eq of LDA (0.8 M) to a solution of **309** in dry THF, stirring for 10 min at -78°C followed by addition of 1.0 eq of prenyl bromide showed a new spot on the TLC plate. The reaction mixture was stirred for 30 min before another 1.1 eq of LDA was added at -78°C . After 10 min 2.5 eq of Ph_2S_2 was added and the mixture quenched and purified to obtain **218** as a single diastereoisomer. This method proved to be effective for giving concise access to sulfide **218** in less steps with control of the stereochemistry of the centres at C12 and C6 without using the Seebach protocol¹⁰⁷ in our synthesis.

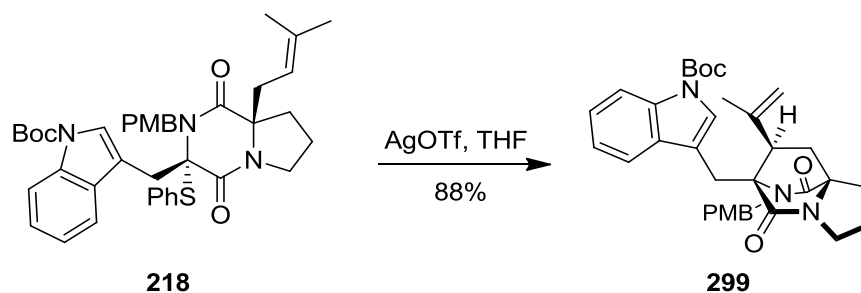


Scheme 4.23

4.8 The cationic cyclisation

With **218** in hand, we were now ready to explore the cationic cascade cyclisation which could be initiated by addition of AgOTf as previously described (Scheme 4.17). We were hoping that the carbocation formed from the isoprene could be trapped by the indole unit to form the desired bicyclo[2.2.2]diazaoctane core ring system. Sulfide **218** was diluted in dry THF and then 1.5 eq of

AgOTf was added at -10 °C for 1 hour before the reaction was quenched. Surprisingly after purification we only isolated bridged DKP **299** (Scheme 4.24). The reaction was repeated with 4.0 eq of AgOTf and overnight stirring but in that case we obtained the Boc-deprotected derivative of **299**. Finally we also attempted to increase the nucleophilicity at the position 3 of the indole by removing the Boc group and therefore increasing the possibility of a trapping by the indole moiety of the tertiary carbocation intermediate. Thus, treatment of sulfide **218** with potassium carbonate in a mixture of methanol and water afforded the unprotected indole derivative but our attempts at cyclisation failed to give the desired product.



Scheme 4.24

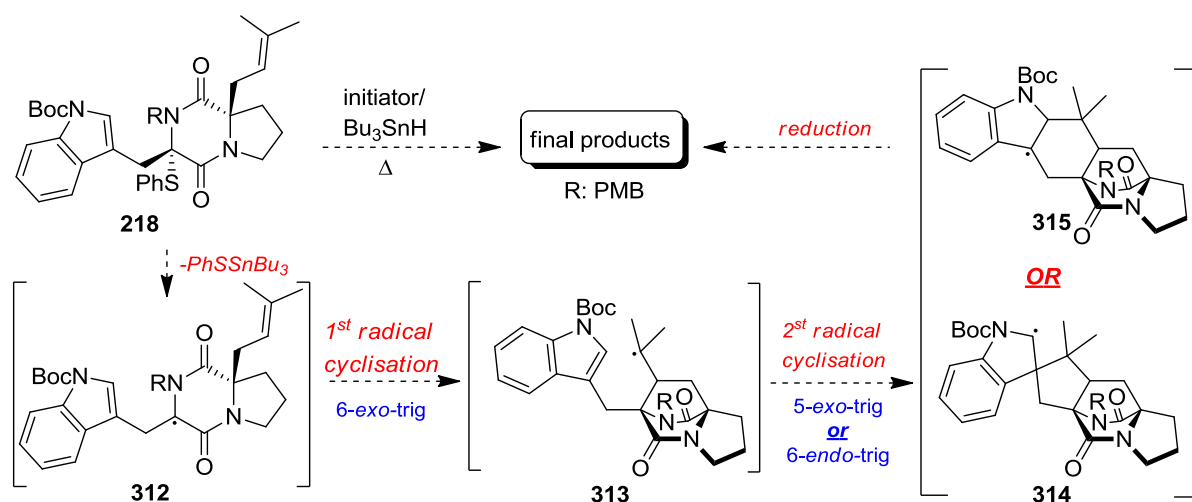
These results provided additional evidence which suggests that in the absence of acid this type of cationic reaction undergoes only the first cyclisation and leads into products such as **299** (Scheme 4.24). When the reaction occurs under acidic conditions another molecule of acid is possible to trigger the second cyclisation and lead to double cyclised products such as **227** in Scheme 3.26.

Following these results we turned our attention to a different approach driven by that fact that an S–C bond is relatively weak and reactive under radical conditions.

4.9 The radical cascade cyclisation

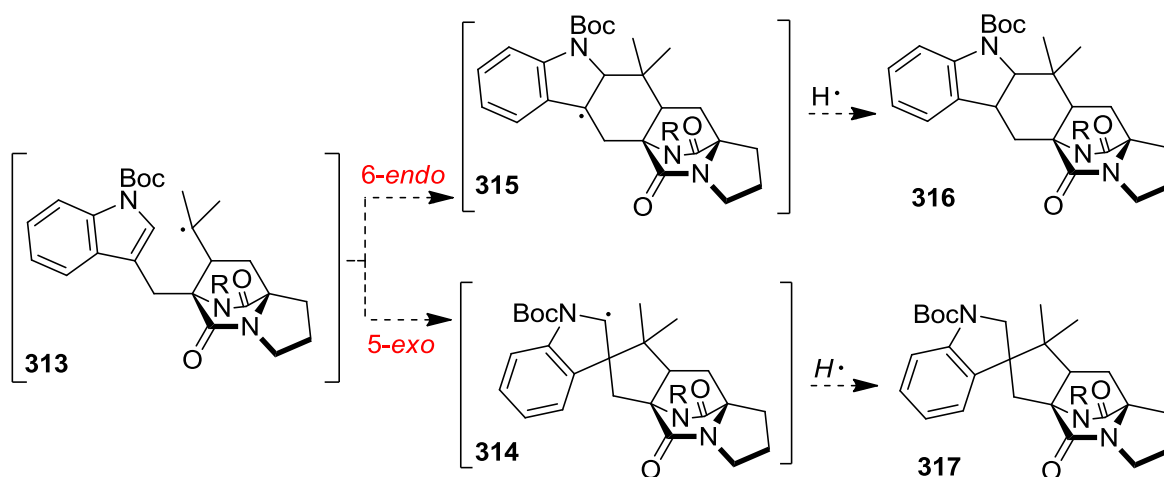
It is well known that a carbonyl group has a remarkable influence on the stability of an α -radical centre.¹⁰⁸ Moreover, thiophenyl groups along with halides are commonly used to initiate radical reaction by homolytic cleavage using a free radical source.¹⁰⁹ As there is a lot prior art in respect of

radical addition to indole substrates,¹¹⁰ sulfide **218** was a suitable substrate to undergo a radical cascade cyclisation in a parallel fashion to the cationic proposal. As Scheme 4.25 shows, a homolytic cleavage of the SPh unit could generate a captodative α -amide radical **312** which could cyclise in 6-*exo*-trig fashion to generate a new tertiary radical centre **313**.



Scheme 4.25

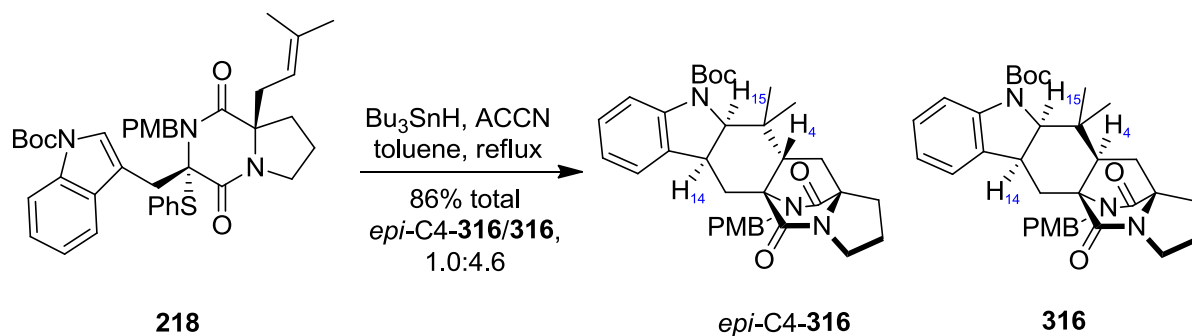
The new radical centre could take part in a second cyclisation onto the indole appendage via an 5-*exo*-trig process to give **314** or via an 6-*endo*-trig to generate **315** (Scheme 4.26). It is well known that 5-*exo* products are usually favoured over the thermodynamically more stable 6-*endo* due to the fact that 5-*exo*-trig cyclisations are faster than 6-*endo*-trig cyclisation.^{59-60,61a,63} Both **314** and **315** are well stabilised radical species but we believed that the regioselective outcome would be driven by the extended aromatic conjugation of intermediate of **315** and the steric effects from the *gem*-dimethyl group of **314** during the reduction step so that indoline **316** would be the final product.



Scheme 4.26

If our proposal proved viable then we would be able to demonstrate a completely new approach to access the desired bicyclo[2.2.2]diazaoctane core ring system in the absence of acids. This would be the first double radical cyclisation towards this type of natural products. It is worth mentioning that only Myers⁴⁶ and Trost⁵³ was able to demonstrate a radical approach towards the bicyclo[2.2.2]diazaoctane framework, although these approaches did not involve a cascade radical cyclisation.⁴⁶ Moreover, Baran also attempted to access similar structures via radical cyclisation with no success.^{47,77,79}

With **218** in hand, we were now poised to secure experimental support for such a radical approach. Bu_3SnH and ACCN were added via syringe pump over 5 h to a solution of **218** in toluene under reflux (Scheme 4.27). After completion of the addition, the reaction mixture was purified using flash column chromatography and we were delighted to isolate indolines *epi*-C4-**316** and **316** in 1.0:4.6 ratio and combined yield 86%.



Scheme 4.27

NMR studies of the major product **316** showed a characteristic doublet at 4.06 ppm with J value of 8.2 Hz which was assigned to H15 (Figure 4.3). H14 appeared in the spectra as a multiplet at 3.36 ppm and finally H4 appeared as a doublet of doublet (coupling with H5) at 1.89 ppm and with J values of 10.6 and 5.4 Hz.

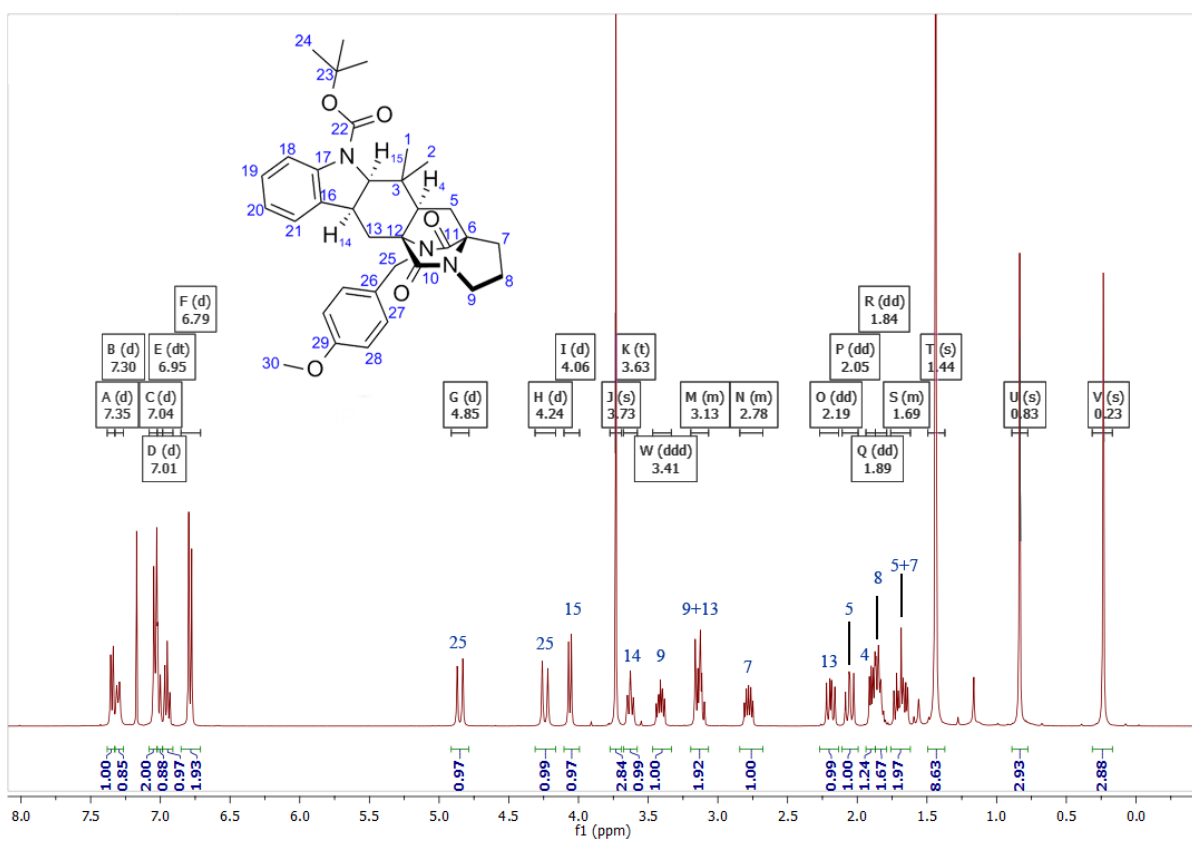


Figure 4.3 ^1H -NMR spectrum of indoline **316**

nOE studies also showed that the major component was the *syn* product with the H4 facing down and on the same side as PMB group (Figure 4.4).

Indolines	H15	H14	H4	PMB
<i>epi</i> -C4- 316	H14	H15	-	-
316	H14, H4	H15	H15	H4

Table 4.2 nOe correlations of indolines **316** and *epi*-**316**

The correct stereochemistry at C4 is

very important as most natural products of this family possess this specific configuration at this centre.

In indoline **316** hydrogen atoms H15, H14 and H4 are facing up and are *anti* to the PMB group.

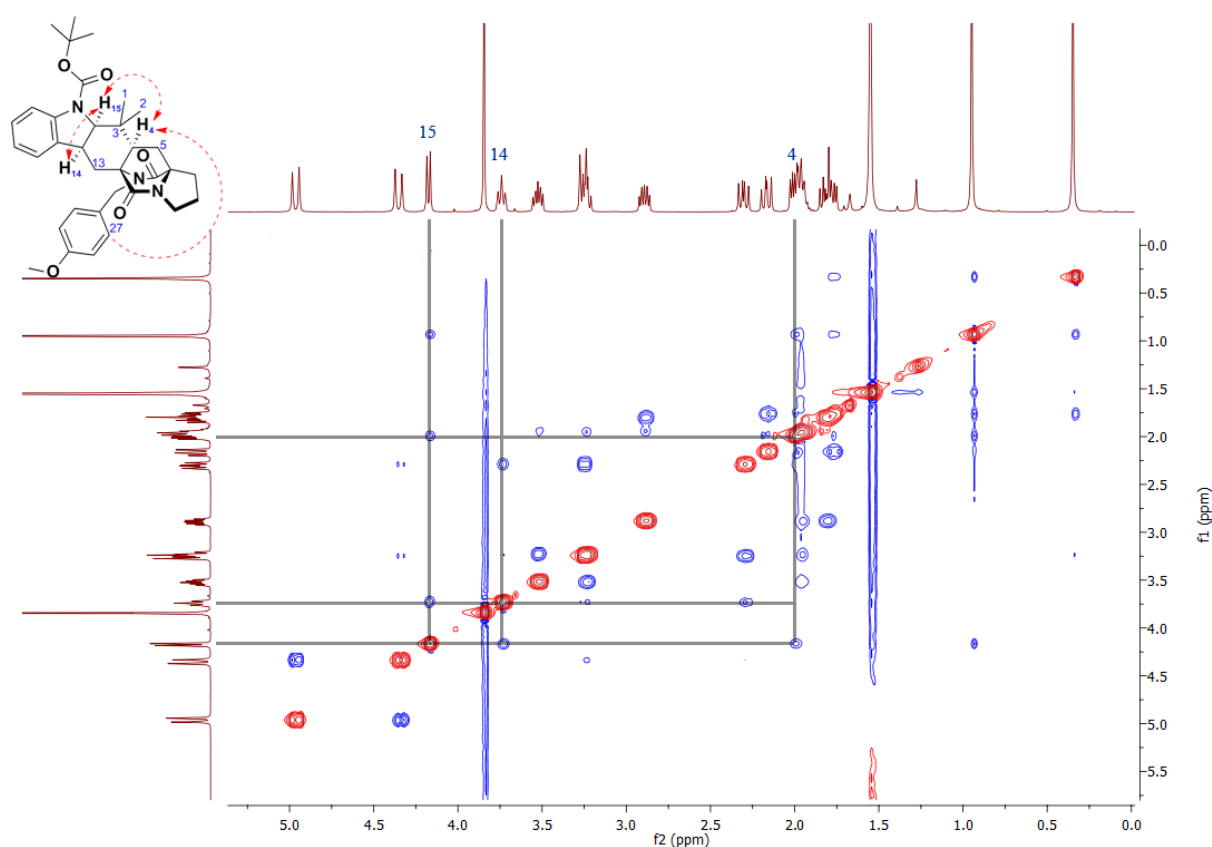
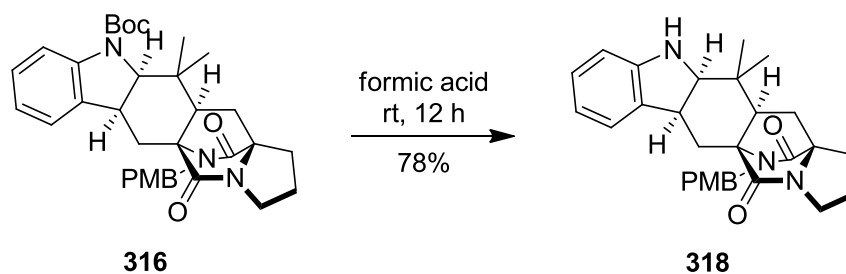


Figure 4.4 nOe spectrum of **316**. nOe correlations of H15 with H14/H4 and H27 with H4

In addition it is worth mentioning that we did not observe any of the possible *spiro*-products **317** (Scheme 4.26) which could be formed via 5-*exo*-trig cyclisation. Thus, our initial proposal proved to be correct and a new synthetic tool was now available to access the bicyclo[2.2.2]diazaoctane core structure.

We also tried to confirm our assignment by X-ray crystallography but with no success in growing crystals. We were hopeful though, that the *N*-deprotected material **318** might furnish good quality crystals. For that reason indoline **316** was stirred overnight in formic acid and after purification we obtained indoline **318** (Scheme 4.28).



Scheme 4.28

When indoline **318** was diluted in MeOH, crystals started to form spontaneously. After 2 weeks of slow evaporation we were pleased to observe sizable and good quality crystals of the product which confirmed our assignment. X-ray crystallography showed that hydrogen atoms H4, H14, H15 being all *syn* to the PMB group (Figure 4.5). The crystal system of **318** was monoclinic and possessed two MeOH units per molecule.

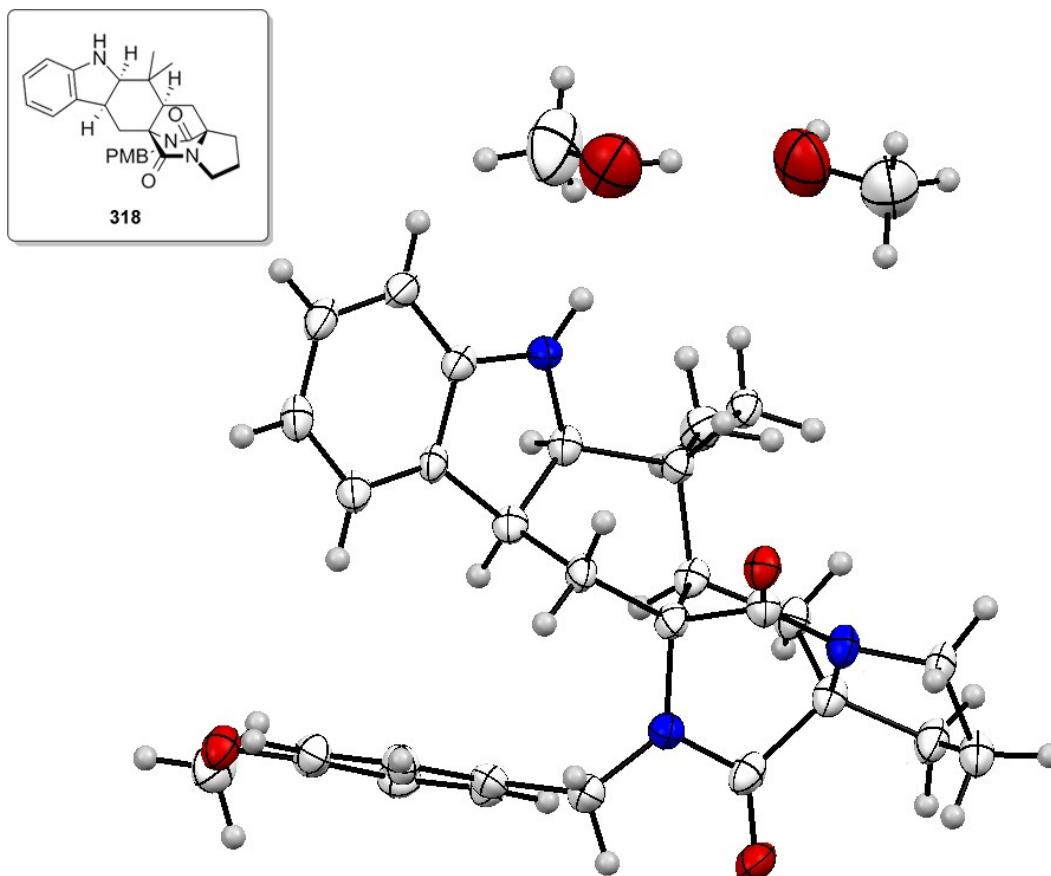


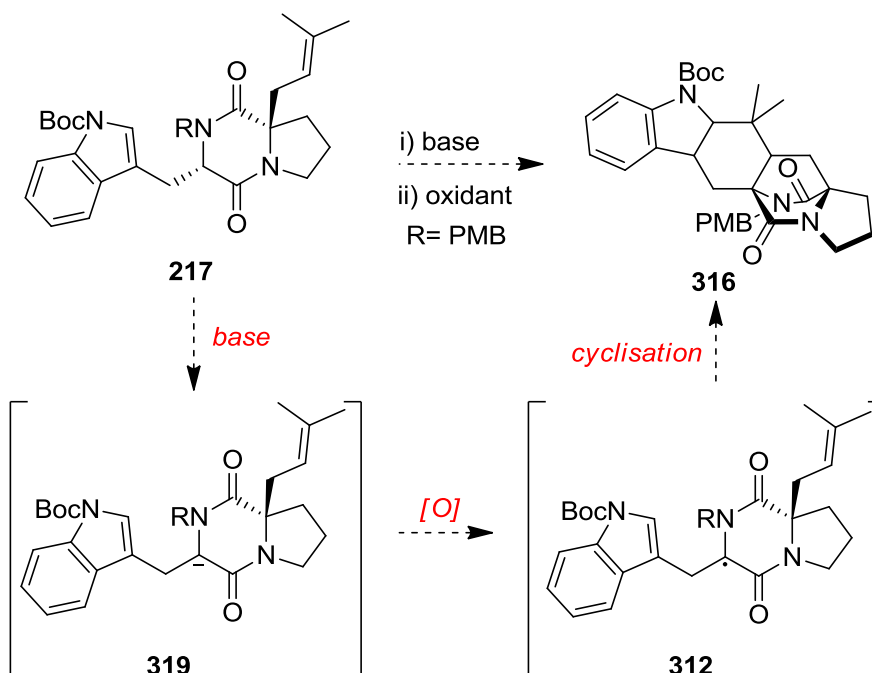
Figure 4.5 Crystal structure of indoline **318**

We also tried to cleave the PMB group using standard methods for this function but with no success. For example indoline **318** on treatment with PTSA in toluene¹¹¹ at reflux resulted only in degradation of the starting material. The same result was observed when TFA was added to **318** in anisole,¹¹² whereas CAN left starting material untouched.¹¹³

4.10 The oxidative radical cyclisation reaction

At this stage, we decided to investigate further other possible synthetic applications towards bridged DKPs. Taking advantage of the acidic nature of H12 we were now interested to attempt a direct generation of a radical centre via an oxidation of the corresponding enolate. As Scheme 4.29 shows, intermediate **217** was chosen as the starting material to explore this proposal. Treatment of **217** with base should deprotonate C12 to form enolate **319**. Oxidation of the corresponding enolate would generate radical intermediate **312** followed by radical cyclisation to give **316**. Unlike the previous

approaches, this alternative way to access the bridged DKPs avoids the need for installation of an initiating group in order to trigger the cyclisation reaction.

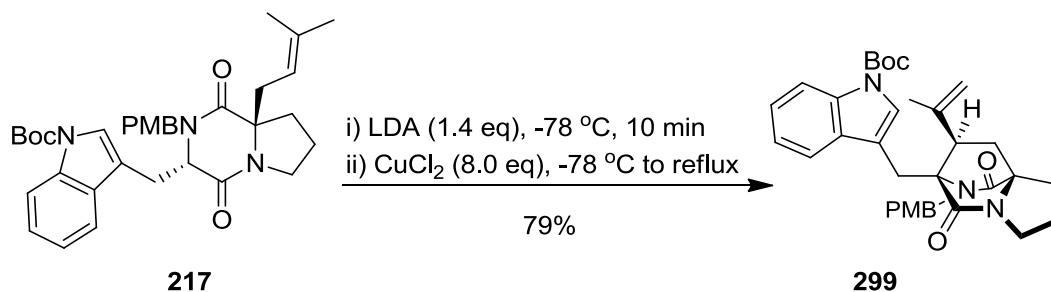


Scheme 4.29

There are numerous examples of oxidative dimerization reactions of enolates using mild oxidants. Most commonly, lithium enolates have been combined with different oxidants such as FeCl_3 , Cu(II) salts or I_2 ,¹¹⁴ while other metal ions such as Na ,¹¹⁵ K ,^{114h,114i} Si ,¹¹⁶ Ti ,¹¹⁷ or Sn ¹¹⁸ have been used less frequently.

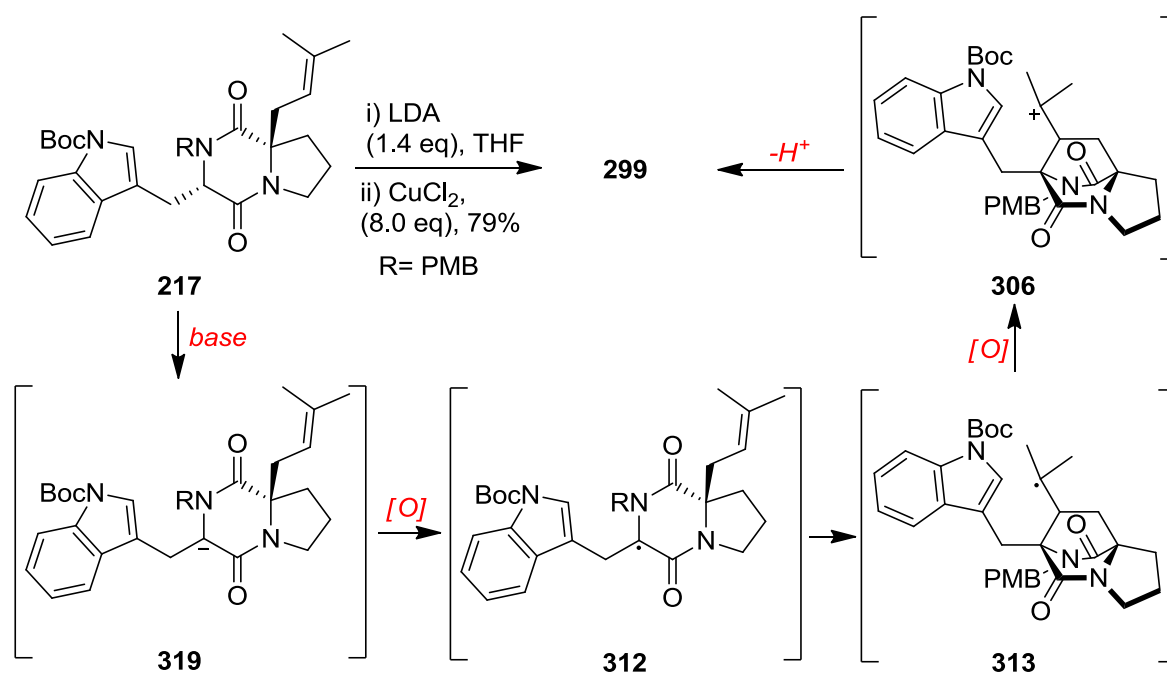
After an examination of the literature we were now ready to try an oxidative radical cyclisation on DKP **217**. One of the inherent difficulties with this chemistry was the in-soluble nature of the oxidising reagents in common organic solvents. Considering the sensitivity of an enolate solution to moisture, we tried to address this problem by connecting an addition funnel pre-charged with the oxidant inside, prior to the addition of the base. Compound **217** was treated with 1.4 eq of LDA at -78°C and stirred for 10 min before 8.0 eq of copper dichloride were added portion-wise over the period of 10 min (Scheme 4.30). After completion of the addition the reaction colour remained green-

blue. TLC analysis showed full conversion of the starting material to a more polar spot which was different to the expected indoline **316** (Scheme 4.29). After purification of the crude material we obtained the monocyclised product **299**.



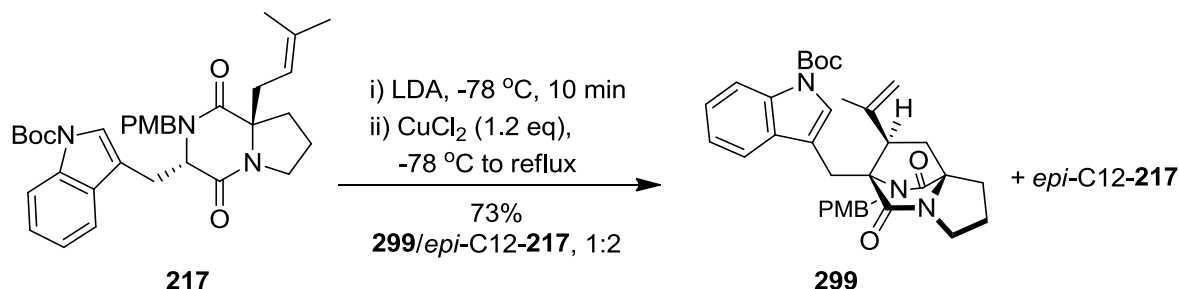
Scheme 4.30

This unexpected result could be explained by a further oxidation step of the radical intermediate **313** which could lead to **306** due to the excess of oxidant (Scheme 4.31). According to our previous results we showed that the cationic cyclisation when carried out in the absence of acid terminates after the first cyclisation. Notably, this reaction fails when using Fe(acac)₃ and ferricinium hexafluorophosphate oxidants which are known to give radicals from enolates.⁷⁷



Scheme 4.31

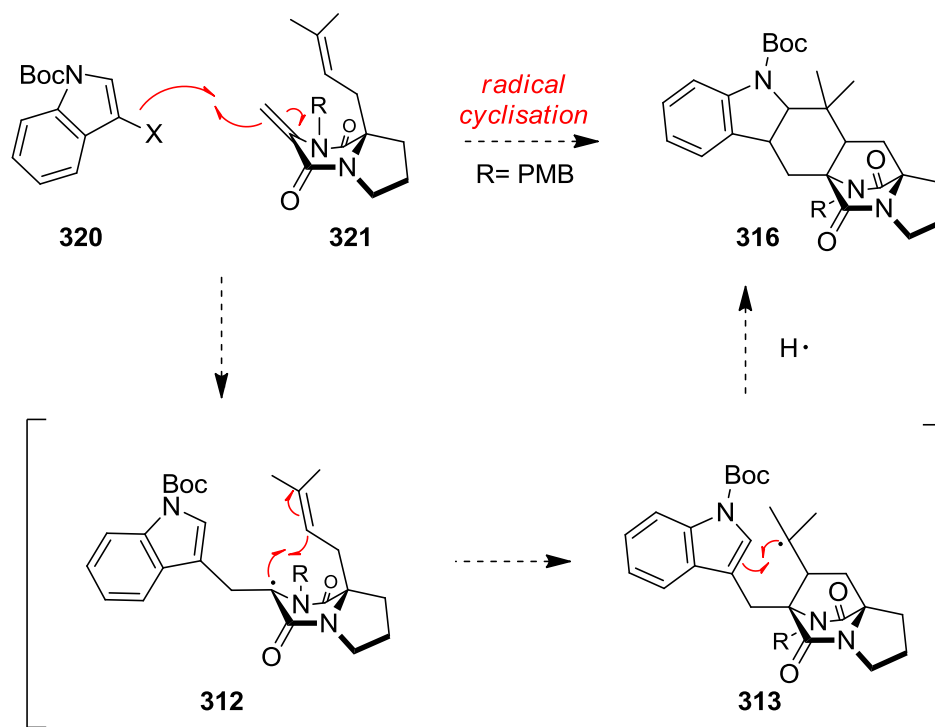
In order to address this problem we repeated the reaction with 1.2 equivalents of oxidant but unfortunately we were only able to obtain a mixture of *epi*-C12-**217** and the bridged DKP **299** with no observation of the desired indoline (Scheme 4.32).



Scheme 4.32

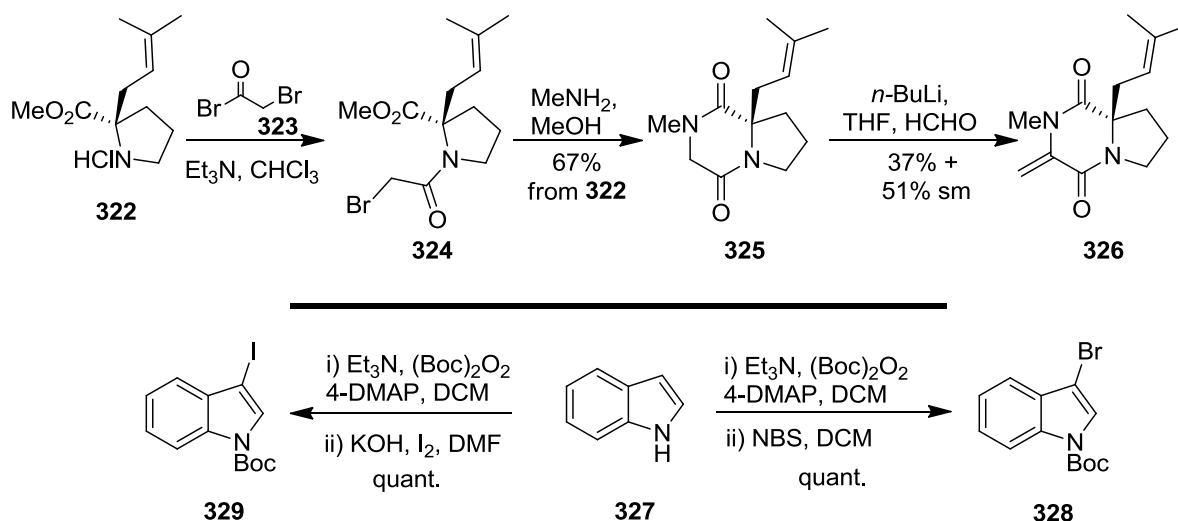
4.11 An inter/intra-molecular radical attempt

As we abandoned our efforts to achieve cascade cyclisation on DKP **217**, we turned our attention to a different approach in order to generate intermediate **312** (Scheme 4.33). This proposal involved an intermolecular radical addition of an indole radical source such as **320** onto an exo-methylene DKP **321**. The corresponding intermediate **312** would be identical with the intermediate generated via the radical cyclisation (Scheme 4.26) or via oxidative radical cyclisation (Scheme 4.31). As Scheme 4.33 shows intermediate cyclisation of **312** could lead to indoline products **316** via a double radical cyclisation forming three new C–C bonds and two new rings in one pot. Since many of these natural products only differ in the substitution on the indole ring the application of such an approach would allow the rapid synthesis of a variety of these natural products in a highly convergent fashion.



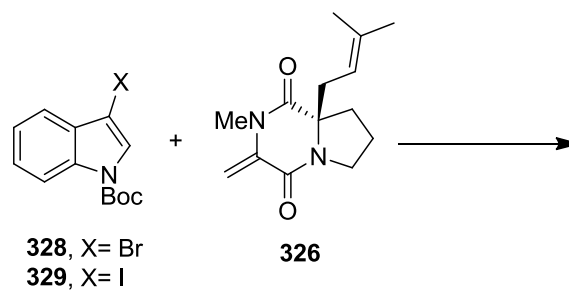
Scheme 4.33

In order to demonstrate the feasibility of this proposal, *exo*-methylene DKP was first synthesised starting from methylester **322** as the hydrochloride salt (Scheme 4.34).¹¹⁹ Compound **322** was acylated with bromoacetyl bromide to give **324**. Addition of methylamine¹²⁰ to a solution of **324** in methanol afforded DKP **325**, which was then treated with *n*-BuLi and formaldehyde to give the radical precursor **326**. Iodination or bromination steps starting from cheap and commercially available tryptophan led to iodoindole derivative **329** and bromoindole substrate **328**, respectively. Both of the halo-indole compounds were tested in these radical cyclisation attempts.



Scheme 4.34

With gram quantities of **326**, **328** and **329** in hand, we were now poised to engage them in the intermolecular radical procedure. In our first attempt (entry 1, Table 4.3), **326** and **328** were charged into a two neck round bottom flask in degassed toluene and a solution of ACCN and Bu₃SnH was added over 8 h via syringe pump. After completion of the addition and examination of the crude ¹H NMR spectrum only reduction of the halide was observed. The reaction was performed at a higher concentration with faster addition of the initiator and tin reagent but unfortunately this gave no result other than reduction of starting material (entry 2, Table 4.3). Finally **326** and **329** were treated with *bis*(tributyltin) and exposed to UV light at 80 °C for several hours while fresh tin reagent was added every 2 h (entry 3, Table 4.3). Unfortunately we were unable to obtain any of the desired products apart from reduction of **329**.



	sm 1	sm2	concentration of reaction mixture	reagents	addition time of reagents	product
<i>entry 1</i>	326	328	0.35 M	Bu ₃ SnH/ACCN in toluene	8 h (110 °C)	recovery of 326 and 328
<i>entry 2</i>	326	328	0.60 M	Bu ₃ SnH/ACCN in toluene	3 h (110 °C)	reduction of 328
<i>entry 3</i>	326	329	0.35 M	(Bu ₃) ₂ Sn ₂ in toluene	every 2 h, UV light (80 °C)	reduction of 329

Table 4.3 Radical cyclisation of **326**

Having already delivered a new synthetic tool for the synthesis of the complex bicyclo[2.2.2]diazaoctane core it was now envisaged to apply these methodologies towards a synthesis of the stephacidin B model system.

Chapter 5

Synthesis of indolines via radical cyclisation approach

5.1 Stephacidins, avrainvillamide and aspergamide A

Stephacidins (**35**), (**39**), avrainvillamide (**36**) and aspergamide A (**38**) are structurally related prenylated indole alkaloids at different oxidation states. As Figure 5.1 shows, stephacidin A (**35**) has the lowest oxidative state among this group of natural products and can deliver through sequential oxidation steps aspergamide A (**38**) and avrainvillamide (**36**) respectively. In the presence of a weak base or acid, avrainvillamide (**36**) can be dimerised to furnish the most advanced and structurally complicated alkaloid, stephacidin B (**39**). The unprecedented structural architecture of stephacidin B (**39**) has been the subject of intense synthetic endeavours by several groups. Herein we present the previous syntheses by other groups and our recent progress towards a stephacidin B model system.

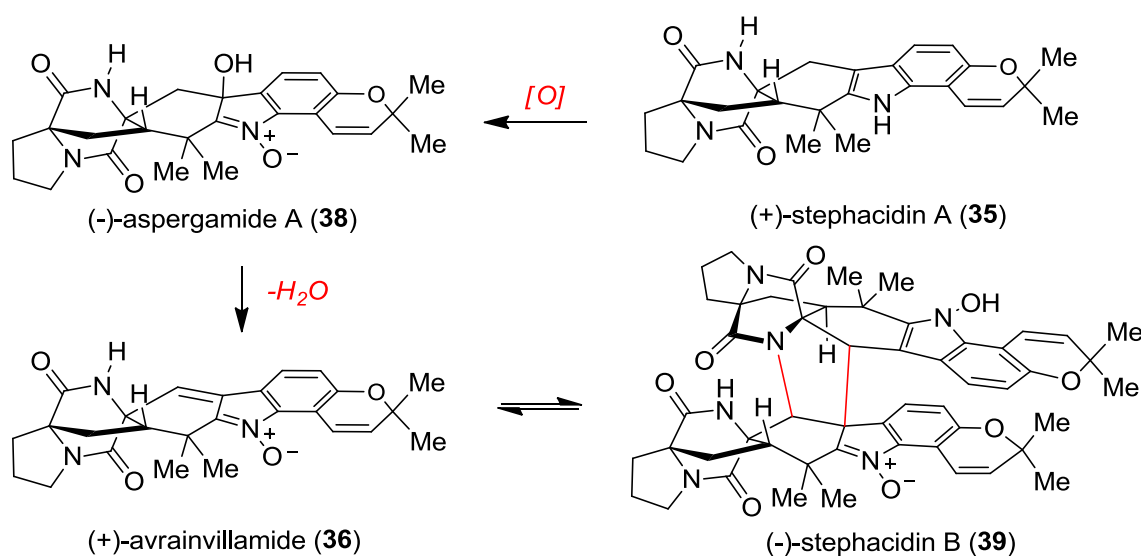
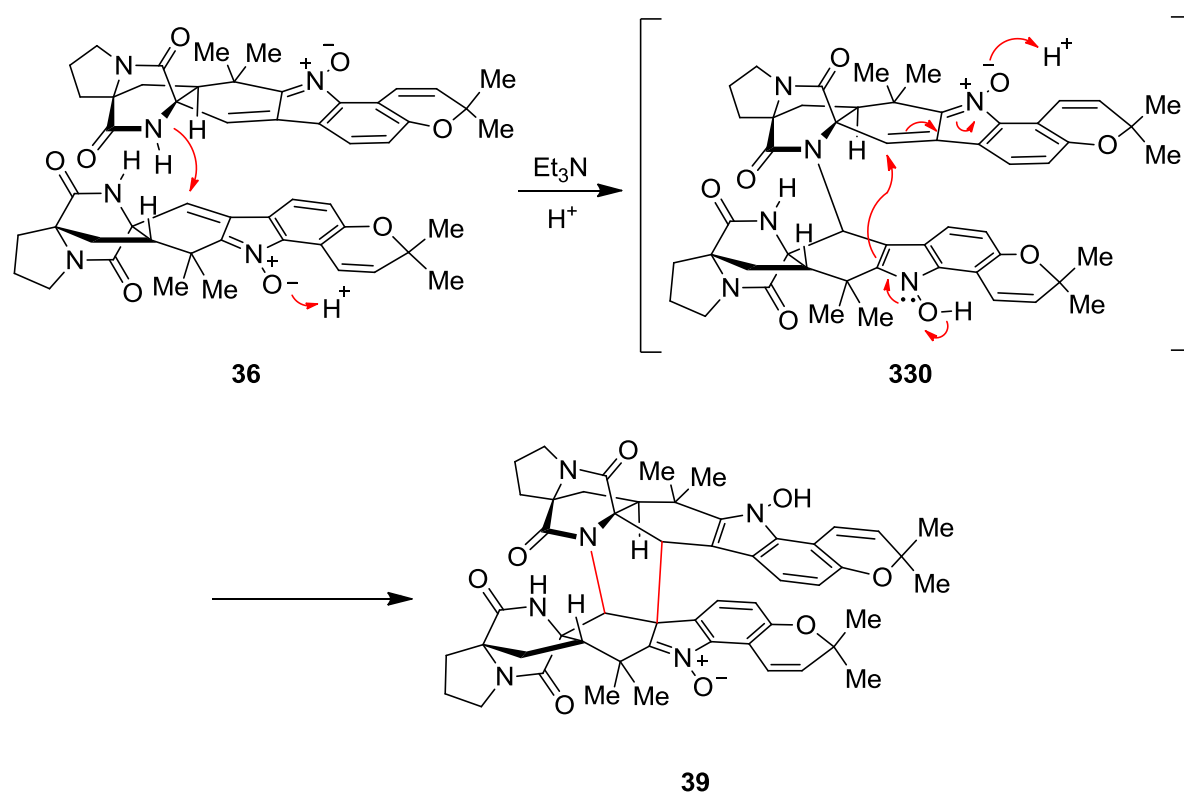


Figure 5.1 Oxidation state of stephacidins, aspergamide A and avrainvillamide

5.2 Previous syntheses of stephacidin B and avrainvillamide

Avrainvillamide (**36**) was first isolated in 2000 by Fenical and co-workers from the *Aspergillus* strains³⁰ and a year after by Sugie *et al.* who described it as CJ-17,665.^{7c} Qian-Cutrone and co-workers in 2001 reported the isolation³¹ of stephacidin B (**39**) from the fungal species *Aspergillus ochraceus* WC76466 and a year later they unambiguously elucidated its structure by a combination of NMR spectroscopy and X-ray crystallography studies.²⁶ Nussbaum *et al.* proposed that the biosynthetic pathway of stephacidin B (**39**) could involve a formal double 1,5-Michael addition sequence between the nitrono moieties and nearby amide nitrogen of avrainvillamide (**36**).^{45a} This not only implies that the vinyl nitrones could serve as unusual Michael acceptors in this system, but also that the dimerization might be reversible. To date, three distinct approaches^{46-47,121} have been reported using various strategies and synthetic manipulations. Later on it was shown that avrainvillamide (**36**) was in equilibrium with stephacidin B (**39**) in the presence of either Et₃N, silica or even on slow evaporation in DMSO. Likewise a retrodimerisation could also occur when molecular sieves were added to a solution of **39** in d₆-DMSO/CD₃CN.⁴⁷



Scheme 5.1

First enantioselective total synthesis of (+)-stephacidin B

In a conceptually different approach among all the other strategies for assembling the bicyclo[2.2.2]diazaoctane core ring system, Myers and Herzon suggested that the key disconnection could be an intramolecular radical cyclisation of an aminoacyl derivative (Figure 5.2).⁴⁶ A Pd-mediated Ullman-like cross coupling, followed by reduction of the corresponding nitroarene would enable access to the heptacyclic (-)-avrainvillamide (**36**).

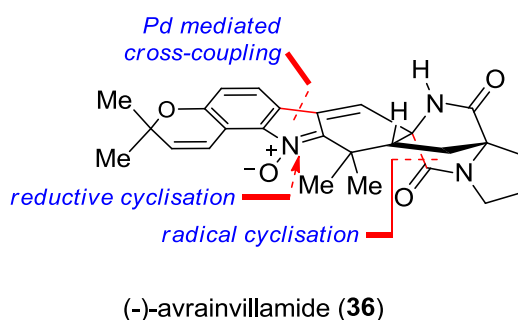
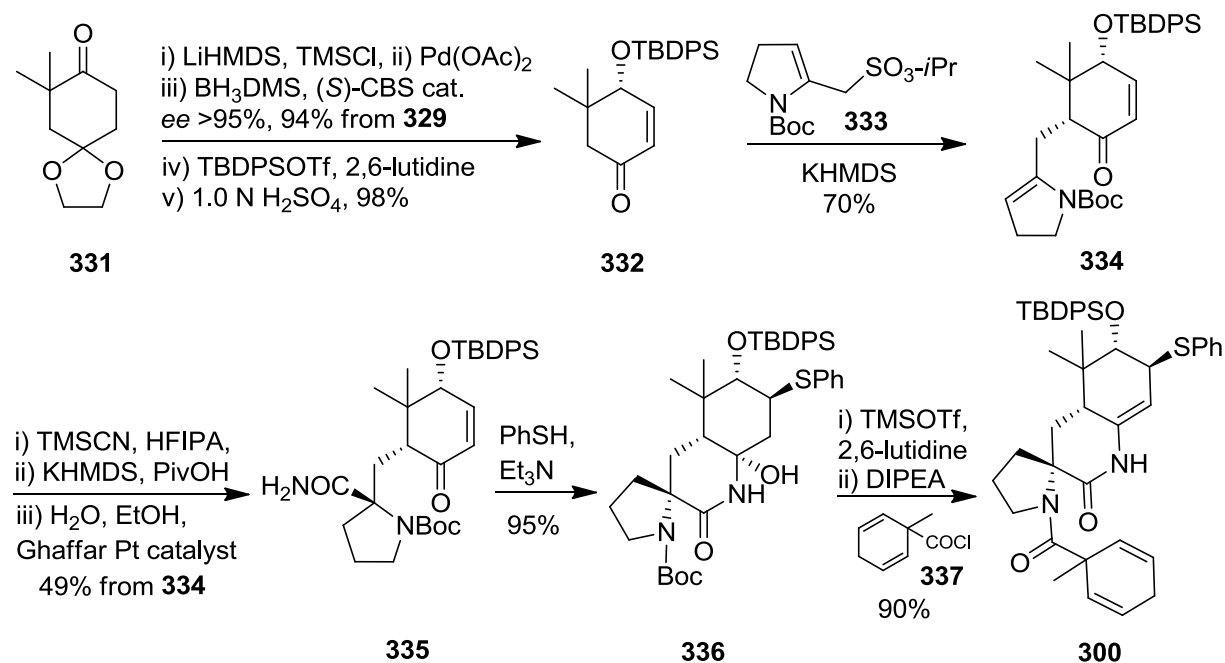


Figure 5.2 Key disconnections of avrainvillamide (**36**)

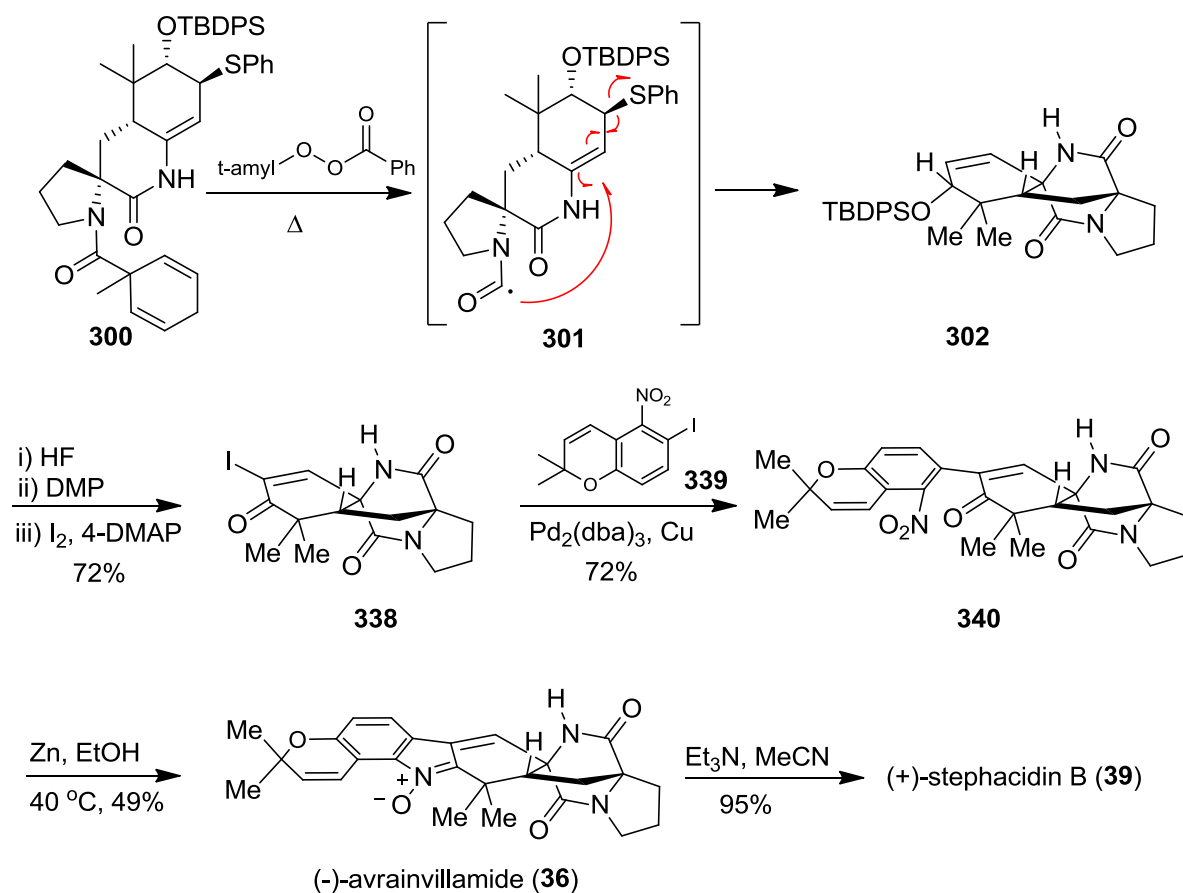
Starting from cyclohexanone derivative **331** (Scheme 5.2),¹²² the trimethylsilyl enol ether was generated and was then transformed into the corresponding α,β -unsaturated ketone. The ketone was reduced enantioselectively using the Corey-Bakshi-Shibata (CBS) catalytic protocol to give (*R*)-allylic alcohol in 95% *ee* and 96% yield. The introduction of the new stereocentre of **332** was crucial because this centre was subsequently relayed to all others within stephacidin B (**39**). However due to the fact that the absolute configuration of stephacidin B (**39**) and avrainvillamide (**36**) were not known at that time, it was decided to use the (*S*)-CBS catalyst in this synthesis. The next manipulations included formation of a silyl ether and ketal hydrolysis to give ketone **332**, which was then treated with KHMDS and the corresponding enolate was alkylated with **333**, to form the *trans* coupling product **334** as a single diastereoisomer. Compound **334** was subjected to a Strecker-like addition of hydrogen cyanide, an epimerization in the presence of base and pivalic acid and finally a transformation of the corresponding nitrile group, to give primary amide **335**. After treatment with thiophenol and Et₃N, **335** underwent a conjugate Michael-type addition of the thiophenol group as well as cyclic hemiaminal

formation to afford tricyclic product **336**. Dehydration of the cyclic hemiaminal **336**, Boc cleavage followed by acylation of the pyrrolidine ring with 1-methyl-2,5-cyclohexadiene-1-carbonyl chloride **337** furnished intermediate **300** and this set the stage for a radical-mediated elaboration of the DKP ring.



Scheme 5.2

As the key step, heating a solution of **300** and *tert*-amyl peroxybenzoate in *tert*-butyl benzene generated bridged DKP **302** (Scheme 5.3). This is formed via an amino-acyl radical intermediate which proceeds to attack the more substituted carbon of the enamide C–C double bond. Transformation of **302** into vinyl iodide **338** followed by an Ullmann-type coupling gave **340**. Finally **340** was subjected to a zinc-mediated reductive coupling to furnish (+)-avrainvillamide (**36**) (4.2% overall yield, 17-steps), which spontaneously dimerised to **39** during the purification step.



Scheme 5.3

Enantioselective total synthesis of avrainvillamide and (-)-stephacidin B

As has been already described in Chapter 3 (Scheme 3.4), Baran and co-workers were the first group to report the enantioselective total synthesis of (-)-stephacidin A (**35**).⁷⁷ Later on, Myers reported the first synthesis of (+)-avrainvillamide (**36**) and (-)-stephacidin B (**39**) and a few months later Baran's group also reported their approach towards (+)-avrainvillamide (**36**) and (-)-stephacidin B (**39**).⁴⁷

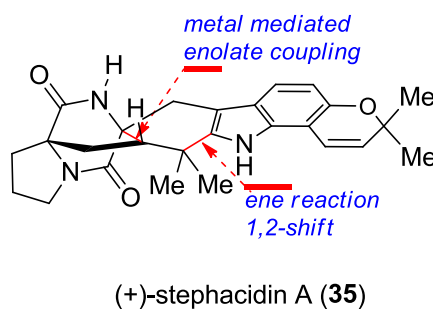
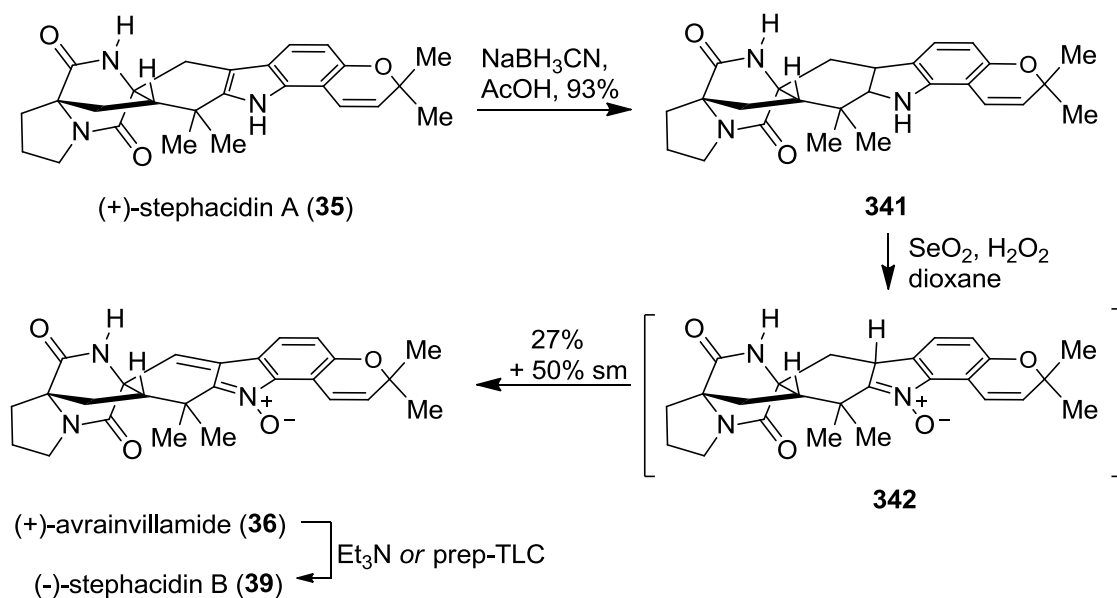


Figure 5.3 Key disconnections of stephacidin A (**35**)

Chemoselective Gribble reduction¹²³ of the indole C2–C3 π -bond of stephacidin A (**35**) led to a mixture of indolines **341**, which was then oxidised to deliver (+)-avrainvillamide (**36**) (Scheme 5.4).⁴⁷



Scheme 5.4

Asymmetric, stereocontrolled total synthesis of the stephacidins.

In 2007, having already investigated biomimetic and enantioselective approaches to access several of the prenylated indole alkaloids, Williams reported an asymmetric synthesis of stephacidins and notoamide B (**29**).¹²¹ The key steps around which the synthesis was based involved an intramolecular $\text{S}_{\text{N}}2'$ cyclisation reaction to generate the bridged DKP core and a Pd-mediated coupling to generate the heptacyclic structure (Figure 5.4).

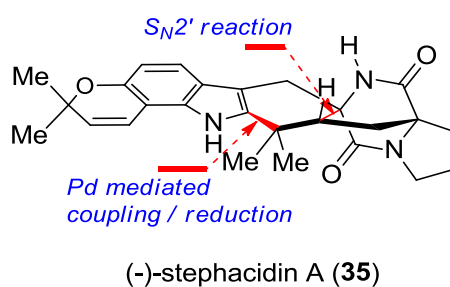
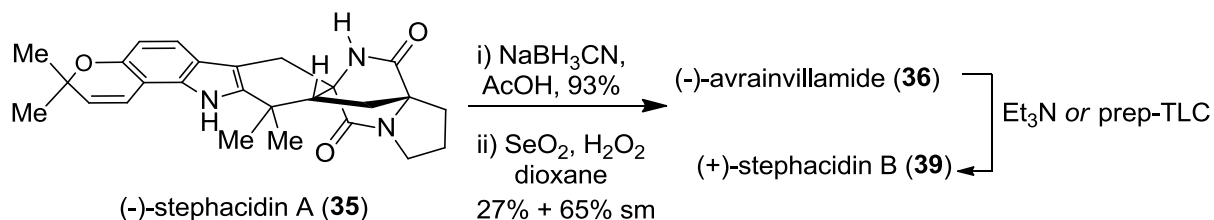


Figure 5.4 Key disconnections of stephacidin A (**35**)

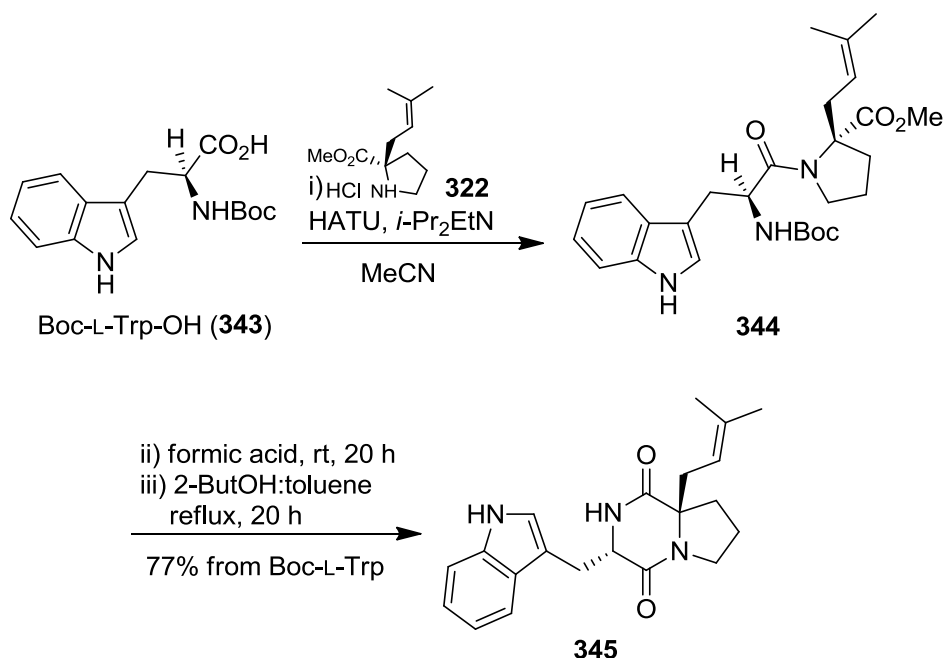
As has been described in Chapter 3 (Scheme 3.11), (-)-stephacidin A (**35**) was synthesised in 6% over 17 synthetic steps. Having in hand the enantiopure (-)-stephacidin A (**35**), Williams and co-worker applied Barans procedure to access (-)-avrainvillamide (**36**) and its epimer stephacidin B (**39**).



Scheme 5.5

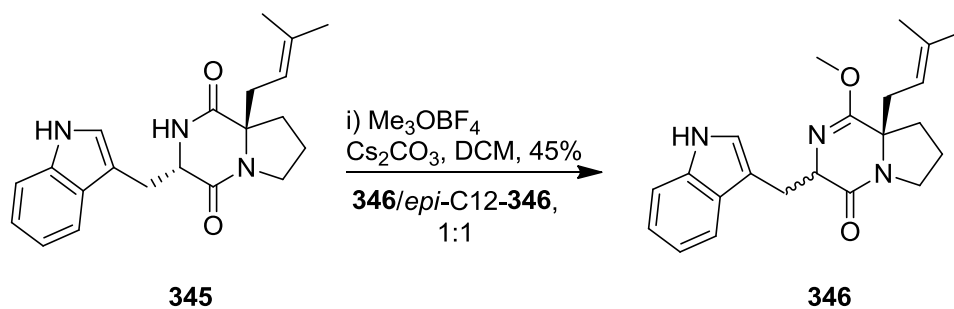
5.3 Synthesis of the radical precursor

As our initial attempts to remove the *N*-PMB group from indoline **318** (Scheme 4.28) failed, we decided to investigate the synthesis of a modified radical precursor possessing an easier to remove group on the amide. Moreover, this new approach should involve a protecting unit which could be easily removed under neutral or even mildly acidic conditions in order to deliver a suitable synthesis for acid sensitive substrates such as the stephacidins. It has been shown by others that amides in similar substrates could be reversibly masked as lactim ethers and hydrolysed under mild acidic solutions.^{32,96,121} In order to explore this scenario, DKP **345** was smoothly synthesised in three steps starting from commercially available Boc-L-Trp-OH (Scheme 5.6). Compounds **342** and **343** were subjected to peptide coupling in the presence of HATU and DIPEA to give amide **344**. Deprotection of the Boc group under acidic conditions and then thermally induced cyclisation of the crude material gave the desired DKP **345** in 77% overall yield from Boc-L-Trp.



Scheme 5.6

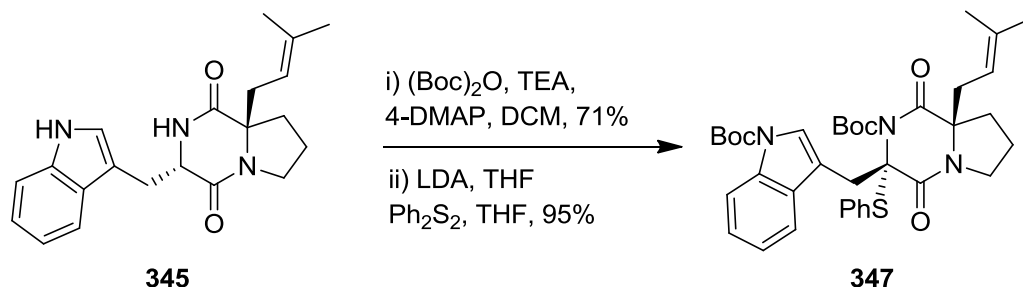
Compound **345** was then treated with Cs₂CO₃ and trimethyloxonium tetrafluoroborate in DCM to give a 1:1 mixture of **346** and *epi*-C12-**346** (Scheme 5.7).¹⁰² Formation of the epimer at the C12 centre would not affect our strategy as both of the epimers would lead to the same diastereoisomer after the sulfenylation step. Nevertheless due to the low yield of the reaction we turn our attention in an alternative approach.



Scheme 5.7

Given the failure for the synthesis of **346** in a high yield an alternative synthetic plan (Scheme 5.8) was then drawn up which involved double *N*-Boc protection¹²⁴ of both the secondary amide and indole nitrogen. Such an approach would provide the desired radical precursors in fewer synthetic steps and we also anticipate that the bulky Boc groups would control the stereoselectivity in the key step. DKP **345** in the presence of TEA (1.5 eq), (Boc)₂O (3.0 eq) and catalytic 4-DMAP gave the desired doubly

N-Boc protected derivative. This corresponding DKP was then treated with LDA under the standard conditions for the sulfenylation step and we obtained the radical precursor **347** in 5 steps and 52% overall yield starting from commercially available material.

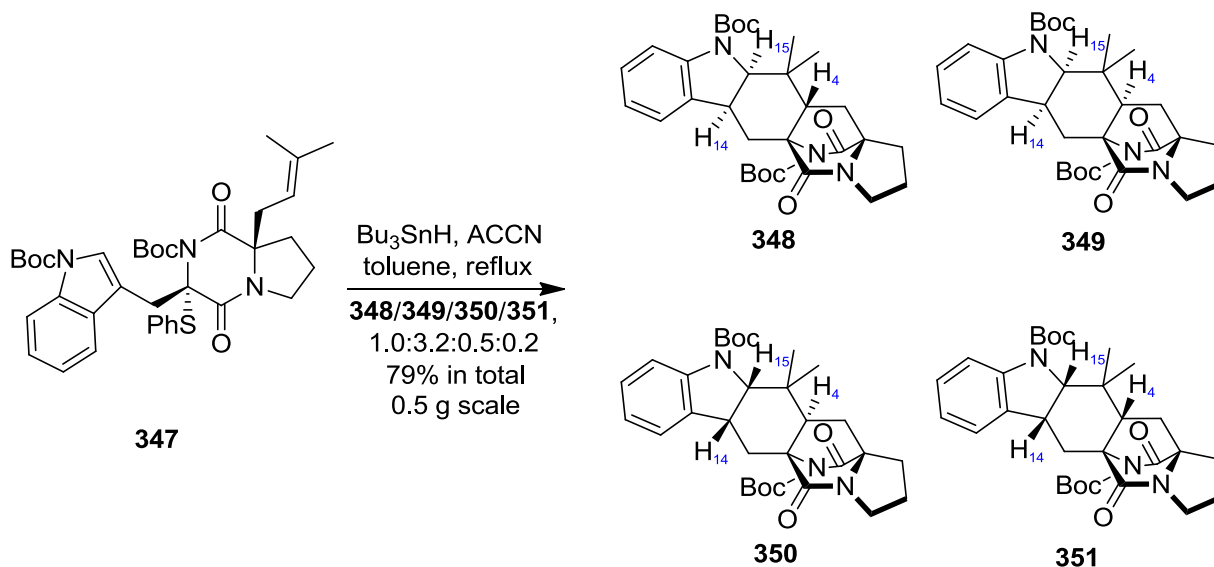


Scheme 5.8

5.4 The radical cyclisation step

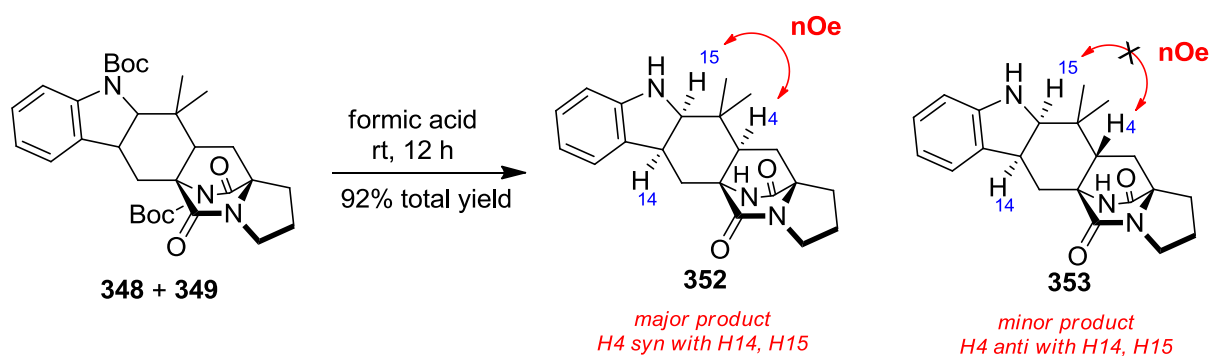
The stage was now set for the critical radical cyclisation, which sets the relative stereochemistry at C4 during formation of the bicyclo[2.2.2.]diazaoctane core skeleton. Based on the precedent from our indoline synthesis, **347** was treated with a solution of Bu_3SnH (0.06M in toluene) and ACCN (0.01M in toluene) over 8 h, at 120 °C (Scheme 5.10). The crude material was purified and three new and more polar fractions were isolated. After purification we were able to obtain **348/349/350/351** in 1.0:3.2:0.5:0.2 ratio and 79% total yield in which indolines **348** and **349** formed an inseparable mixture. NMR studies and mass spectrometry of the isolated compounds showed that all of the components were diastereoisomers of an indoline core. In theory four possible structures could be generated from this radical reaction. The diastereoisomers would share H4 *anti* or *syn* with respect to the *N*-Boc group on the bridged DKP core and H14 and H15 would be both *anti* or *syn* to H4. Unlike with the PMB series, the nOe studies of these products did not show a correlation between H4 and the Boc group of the amide. Molecular modelling showed that the molecule prefers a conformation that positions the *tert*-butyl group remote from the bridged DKP core and at a distance longer than 5 Å that

corresponds to the maximum distance for a nOe correlation. Unfortunately we also failed to grow crystals of these compounds and establish their complete configuration by X-ray.



Scheme 5.10

It had been demonstrated from previous work in our group that, nOe-correlation on the deprotected derivative between the amide NH and H4 was possible. With this in mind we proceeded to deprotect of these indoline derivatives under acidic conditions. The mixture of **348** and **349** was treated with formic acid to furnish the unprotected indolines **352** and **353** (Scheme 5.11). These compounds had an extremely similar R_f but we were able to separate them by preparative TLC purification. During subsequence NMR studies we faced several difficulties due to the low solubility of the compounds in NMR solvents and the dependency of the spectra on the concentration of the samples. nOe studies showed that for **352** the H4, H14 and H15 protons were placed on the same face but unfortunately we could not confirm the stereochemistry at C4 as the peak of the NH was broad and it did not shown correlations. nOe spectra for the minor indoline **353** were also low quality but we were able to confirm that H4 was *anti* to H14 and H15.



Scheme 5.11

When each of the substances **352** and **353** were diluted in MeOH we were pleased to observe crystals of both of the indolines form after slow evaporation. The orthorhombic crystal system of structure **352** clearly shows that the hydrogen atom H4 was placed on the same side as the NH and being *syn* to the hydrogen atoms H14 and H15 (Figure 5.5).

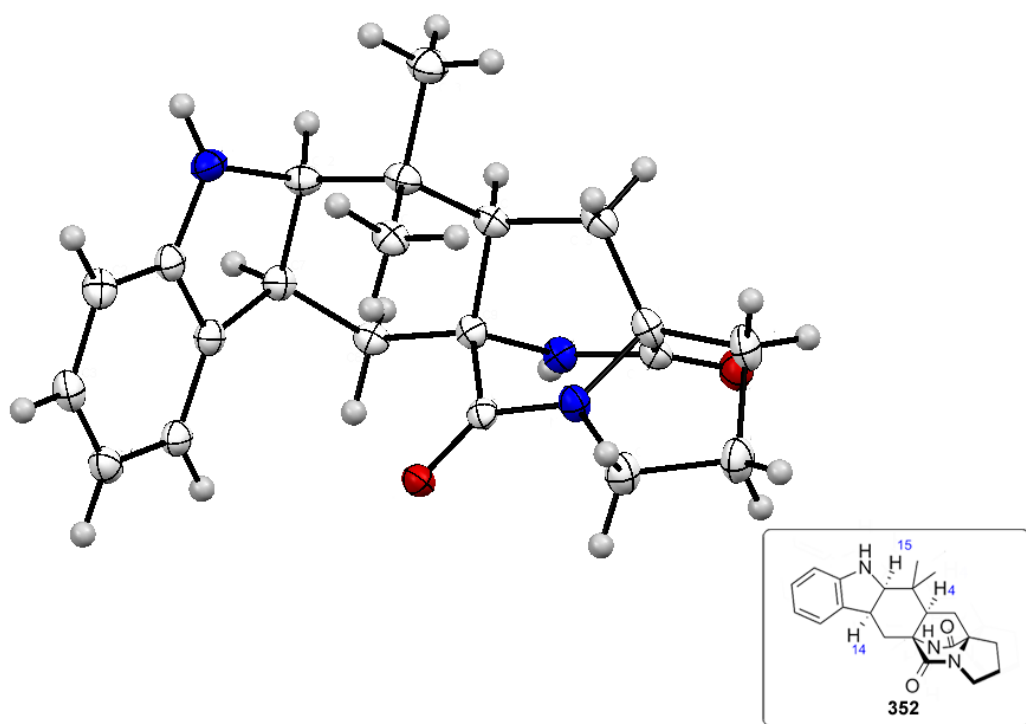


Figure 5.5 Crystal structure of indoline **352**

The crystal system of **353** was also orthorhombic with H4 *anti* to proline and NH amide and also to H14 and H15 (Figure 5.6). Moreover C8 was disordered over two positions at a refined occupancy ratio of 0.74 (1):0.26 (1).

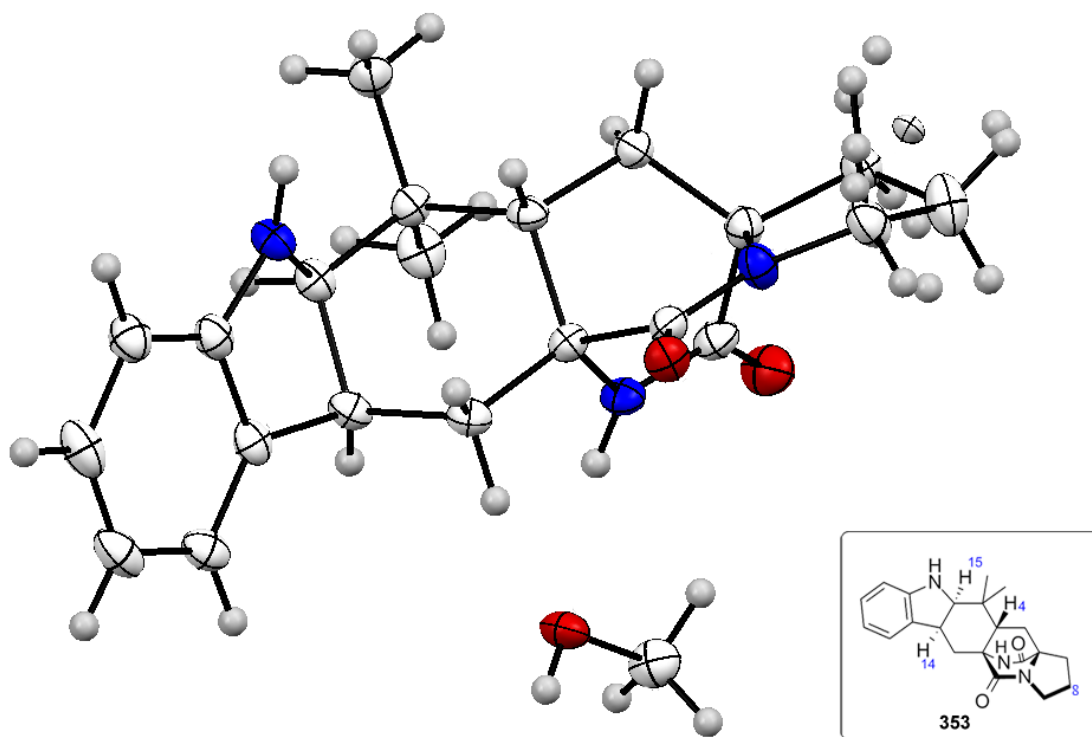
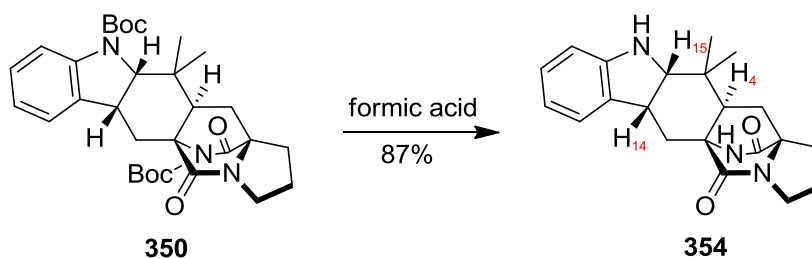


Figure 5.6 Crystal structure of indoline **353**

In the meantime we also analysed compounds **350** and **351** by nOe studies which showed that **350** had H4 *anti* to H14, H15 and **351** possessed H4 *syn* to H14, H15. Unfortunately in that case, nOe correlation between amide and H4 did not provide to us convincing information about the stereochemistry at C4. Having already assigned the *cis* **352** we could conclude that of **351** also had H4, H14 and H15 placed on the same side but *anti* to the amide. As a consequence our interest was now the assignment of indoline **350**. Deprotection of substrate **350** was allowed by treatment with formic acid and after purification of the crude material by flash column chromatography we obtained indoline **354** in good yield (Scheme 5.12).



Scheme 5.12

NMR studies shown, hydrogen atom H4 appeared at 2.47 ppm in the proton NMR spectra and H14 and H15 were overlapping with H9_{a,b} at 3.56 and 3.39 ppm respectively (Figure 5.7). Unlike with the previous indoline derivatives we did not observe any solubility problems with this sample. Moreover the signal for the NH peak of the amide was less broad this time with clear correlations in the nOe experiments. Upon studying the nOe spectra we were able to observe correlations between the amide NH and H4 and no signal between the protons H4 with H15 and H14 (Figure 5.8).

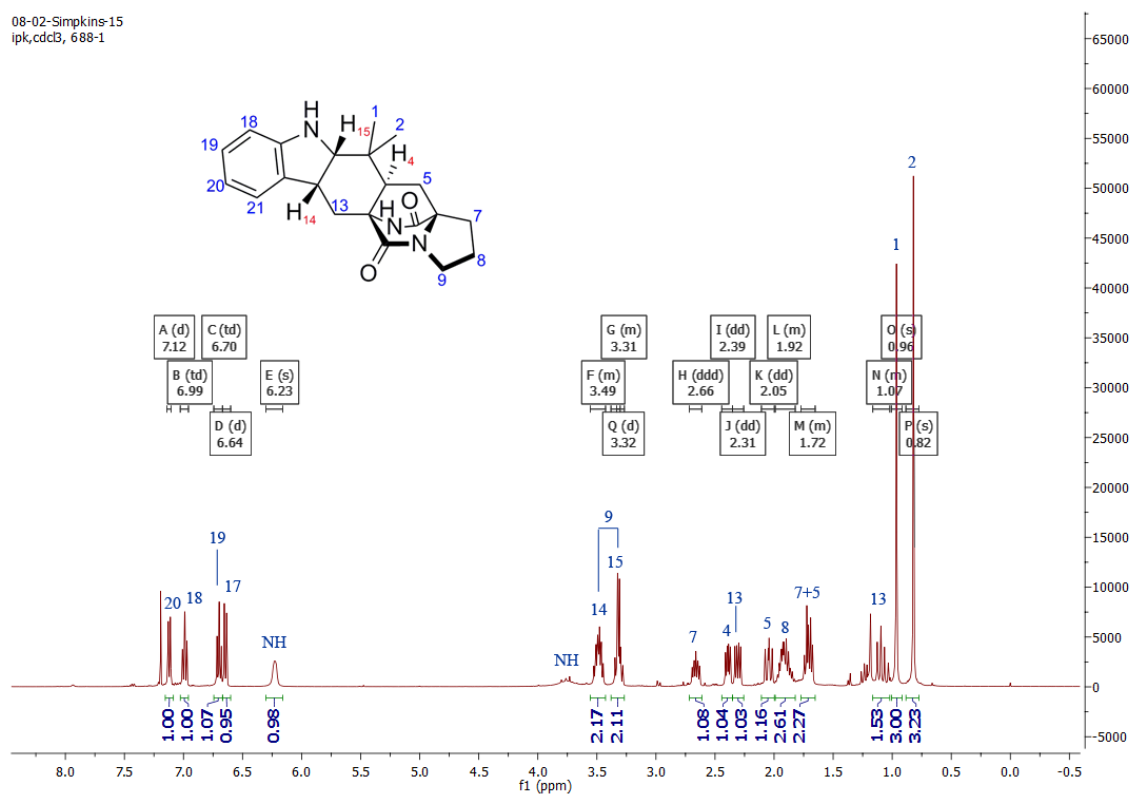


Figure 5.7 ¹H-NMR spectrum of indoline **354**

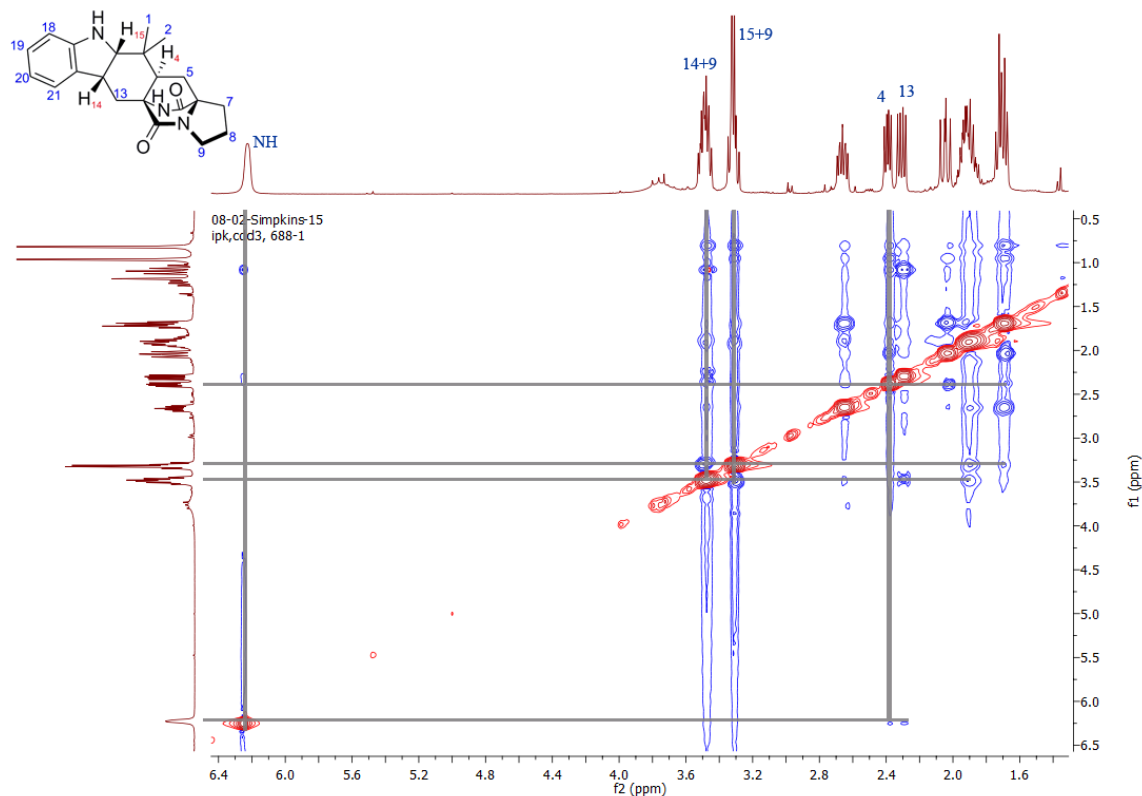
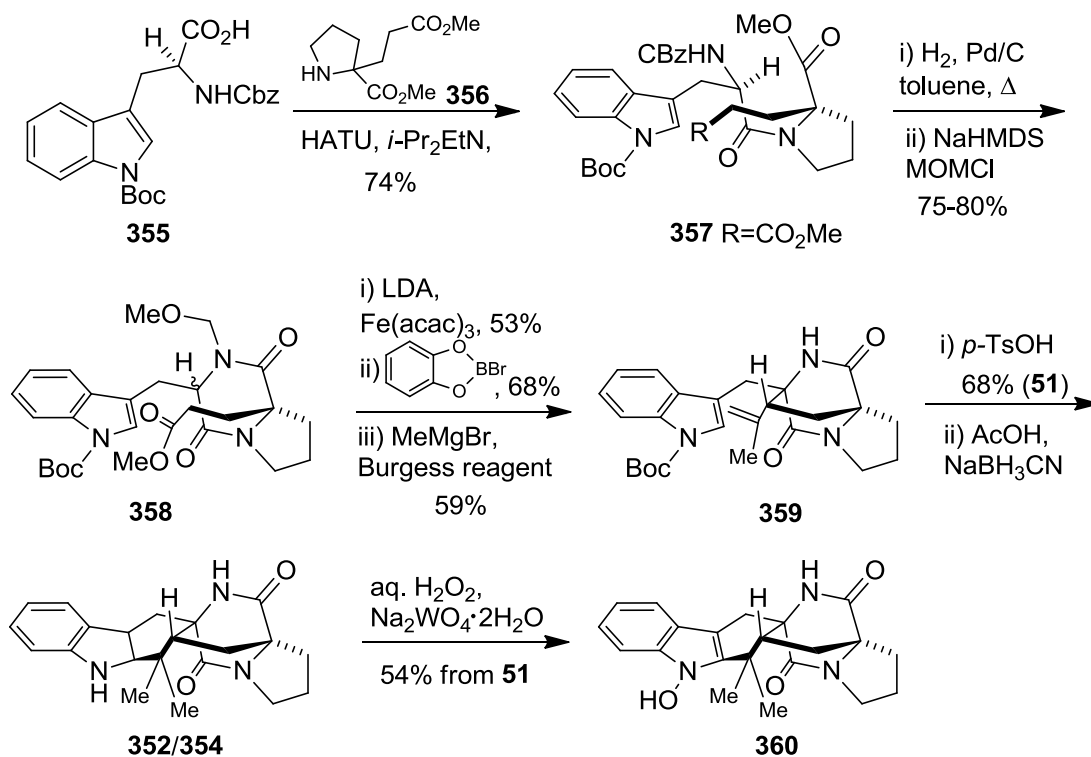


Figure 5.8 nOe spectrum of indoline **354**. nOe correlations of H15 with H14 and NH with H4

As we were able to achieve a full assignment for compound **354** we could also report that the selectivity at the C4 centre for the radical cyclisation was 3:1. The lower selectivity at C4 from these results shows the effect of the Boc group. The conclusion to be drawn from the overall results is that PMB is the protective group which leads to highly selective cyclisations but there are difficulties in the process of deprotection.

Baran's group were the first which synthesised indolines **352/354** in 8 steps and 6% overall yield starting from **355**.⁷⁹ Baran *et al.* began with indole **355** (Scheme 5.13) which was coupled with a racemic mixture of proline derivative **356** to give an inseparable mixture of diastereomeric amides **357** in 74% yield. Chemoselective Cbz-deprotection was then applied to the mixture followed by thermal cyclisation to furnish the corresponding DKP as 1:1 mixture of diastereoisomers and 87% total yield. The two diastereoisomers were then protected in separate steps to give **358** in 86% and 92% yield. Intramolecular oxidative heterocoupling of **358**, *N*-MOM removal followed by a Grignard reaction

and dehydration of the corresponding alcohol gave **359**. A second cyclisation which led to the hexacyclic core **352/354** then occurred by treatment with acid. Gribble reduction led cleanly to the indoline which was used in an oxidation step to give **360**.



Scheme 5.13

Our approach to access indoline derivatives **352/354** occurs in 6 steps and with an overall yield of 28%. The key step in our strategy was a cascade radical reaction in which the poly-substituted DKP **347** underwent a double cyclisation to form two new rings of the final hexacyclic product in a 3:1 ratio with the major product possessing the desired configuration at C4.

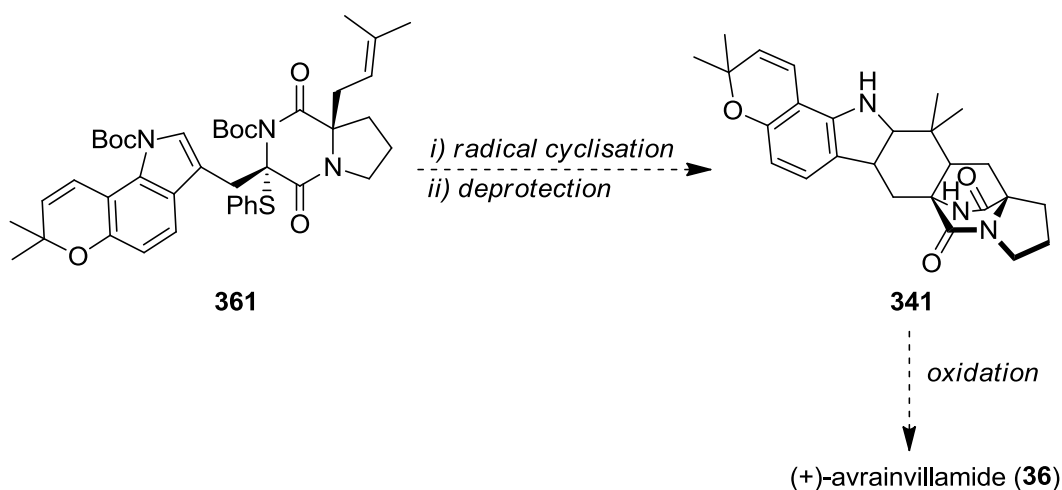
5.5 Summary and future work

This work has highlighted the utility of a radical cyclisation strategy for assembling the bicyclo[2.2.2]diazaoctane framework. The final products and key precursors in a stephacidin B model

system, indolines **352/354**, were previously synthesised by Baran⁷⁹ *et al.* in 8 steps (6% overall yield) and delivered the hexacyclic core structure in two separate cyclisation steps.

We were pleased to report a new synthetic way to access these valuable materials in only 6 steps and 28% overall yield via a concise radical manipulation of poly-substituted DKP precursor **352/354**. In our approach the final hexacyclic core structure arises from a cascade radical cyclisation which involves formation of two new C–C bonds and two new rings. According to our synthesis, oxidation of indolines **352/354** followed by dimerization would lead to the corresponding stephacidin B model system in only 8 steps.

It is hoped that in similar fashion, avrainvillamide (**36**) and stephacidin B (**39**) could be synthesised via radical cyclisation of sulfide **361** (Scheme 5.14). Oxidation of the resulting indoline **341** will allow access to avrainvillamide (**36**) and via a dimerization to stephacidin B (**39**).



Scheme 5.14

Stephacidin B (**39**) has a unique structure with some intriguing biological activity and it has been a vibrant synthetic challenge for several groups. Other interesting targets in this family include prenylated alkaloids equipped with a *spiro*-oxindole motif such as marcfortine C (**27**), (+)-versicolamide B (**362**), notoamides B (**29**) and N (**31**) (Figure 5.9).

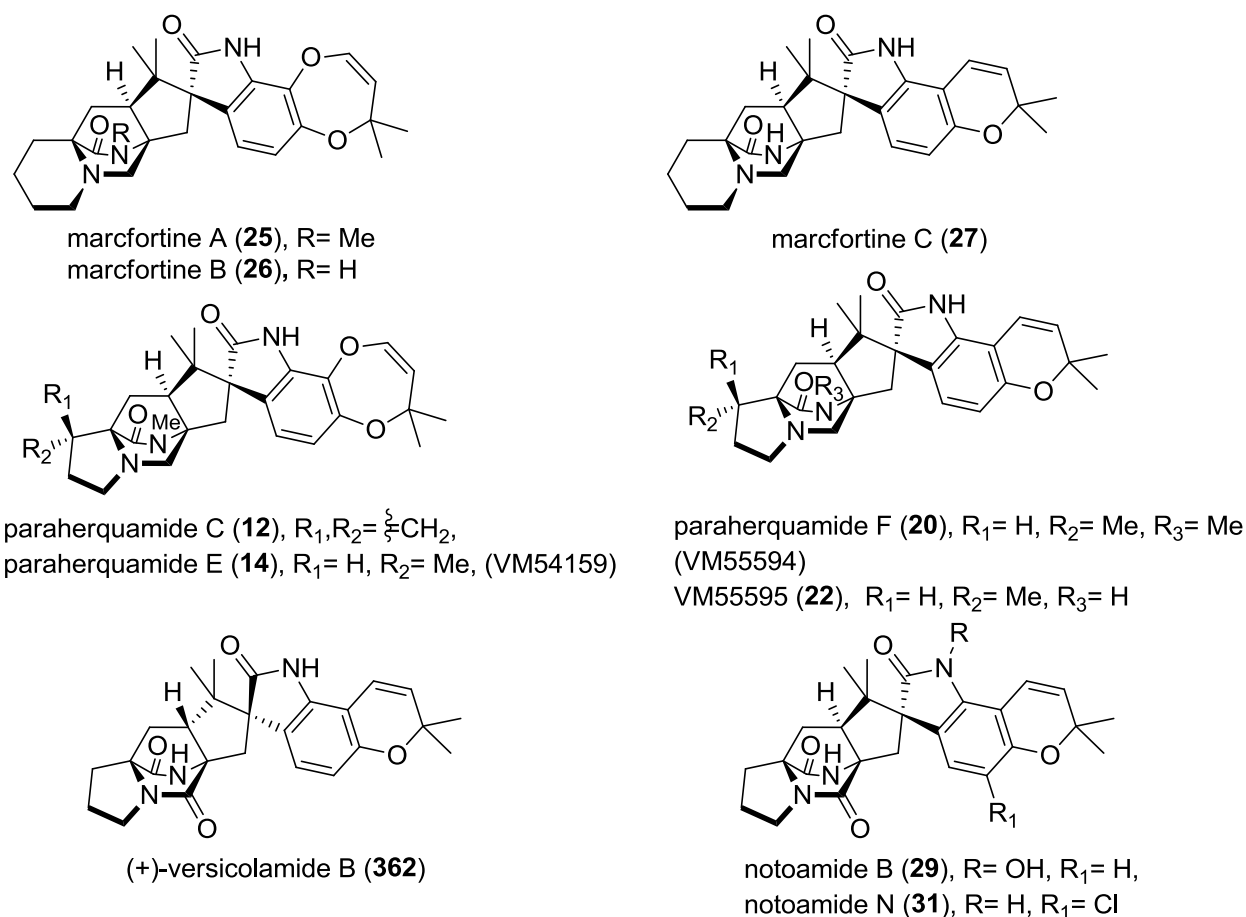
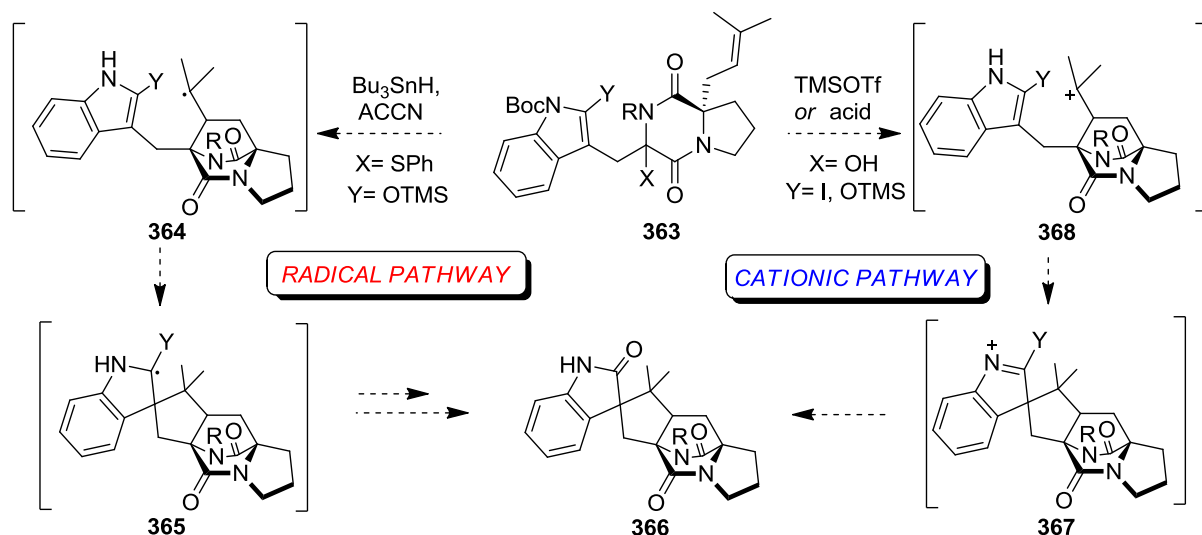


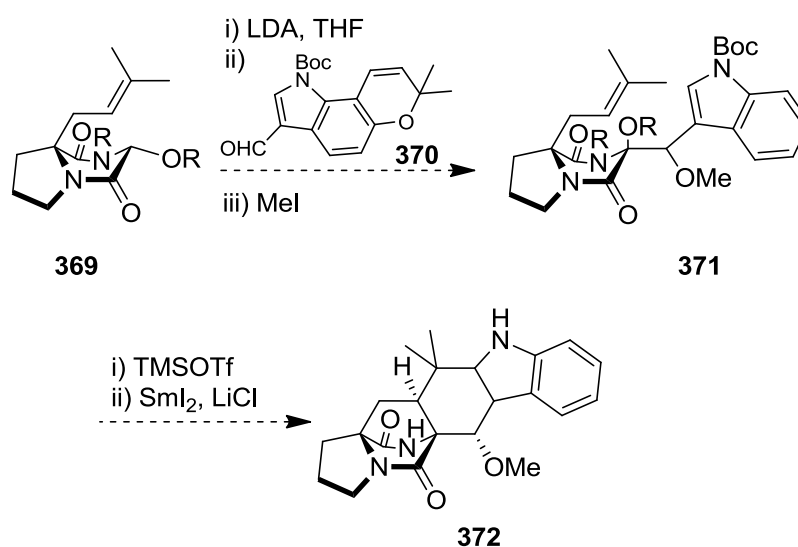
Figure 5.9 Structures of the marcfortines, paraherquamides, notoamides and versicolamide B

Intramolecular cyclisation of a DKP precursor (**363**) which is equipped with a substituted indole unit at the 2-position would possibly allow to the spiro-oxindole framework as Scheme 5.15 shows. This process could rely on either cationic or radical intermediates. The cationic pathway of this proposal suggests that the precursor **363** must possess, in addition to the hydroxyl group, an indole ring with a substituent like an iodine atom or *O*-silyl group at the 2-position. Thus, under acidic conditions or the established conditions with TMSOTf, **363** could generate a *spiro*-intermediate such as **367** which upon hydrolysis would give the desired *spiro*-oxindole core skeleton **366**. Alternatively, if a thiophenyl group is introduced onto the *O*-silylated indole substrate **363** could initiate a radical cyclisation to furnish *spiro*-indoline **366** after removal of the silyl group.



Scheme 5.15

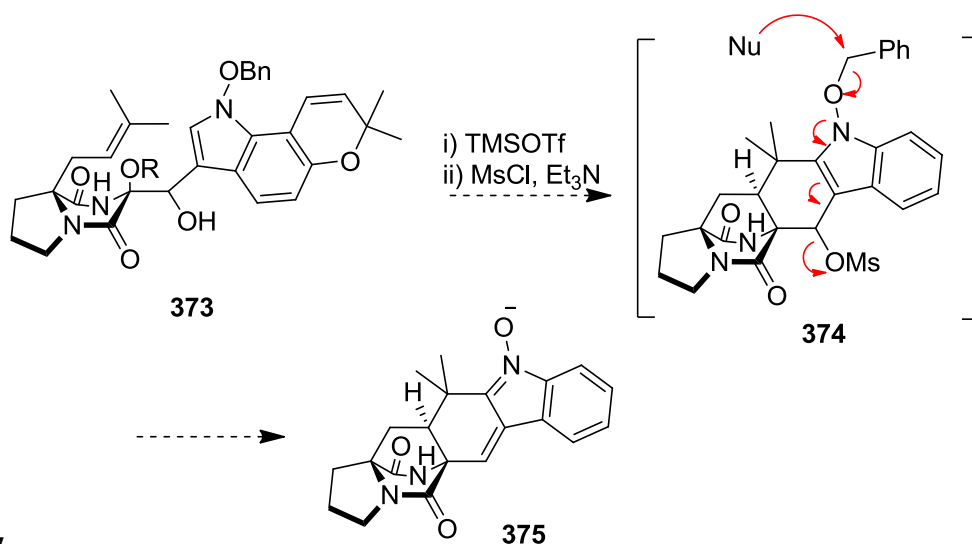
Another desirable and interesting area for exploration lies on the rapid synthesis of the poly-substituted DKP substrates such as **371** (Scheme 5.16). Acylation or aldol coupling are some of the possible approaches to access the DKP core of key precursors in a more efficient and direct fashion. Model system (**372**) of notoamide F could be synthesised by an aldol coupling of **369** and **370** followed by cationic cyclisation and a deprotection step (Scheme 5.16).



Scheme 5.16

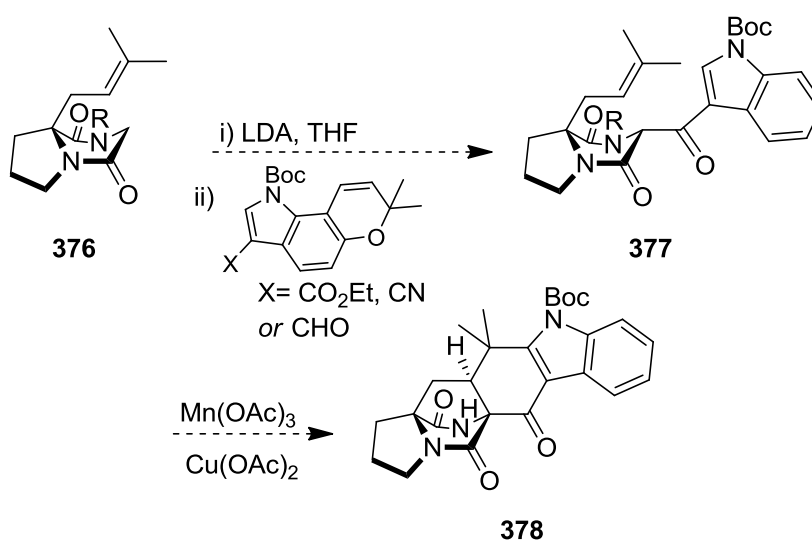
From DKP **373** it might also be possible to achieve a short access to indole nitrones derivatives like avrainvillamide such as **375** (Scheme 5.17). Cationic cyclisation of DKP **373** followed by subsequent

activation of the hydroxyl as a mesyl group would generate intermediate **374**. Nucleophilic addition on the *N*-benzyloxy group of **374** would form the nitron unit and will trigger the elimination of the mesyl group to give **375**.



Scheme 5.17

It might also be possible to assemble core structures similar to notoamide I as indicated in Scheme 5.18. Following the procedure described by Snider *et al.*,¹²⁵ we believe that substrate **377** could be cyclised via a cationic/radical pathway to give notoamide I in one pot. Alternatively, installation of a thiophenyl function would possibly allow the cyclisation to proceed through radical intermediates.



Scheme 5.18

Chapter 6

Experimental

6.1 General procedures

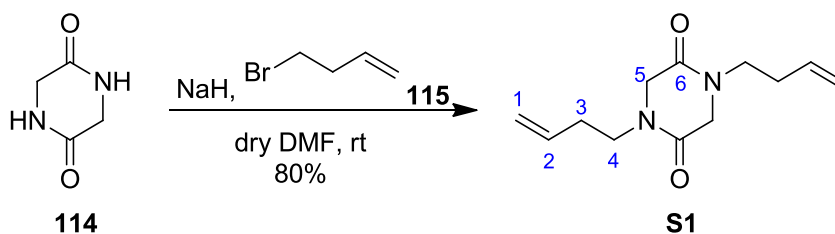
All glassware was flame-dried under a steady flow of nitrogen or oven-dried at 100 °C overnight before use and all reactions were performed under an atmosphere of nitrogen or argon unless otherwise stated. All other solvents and reagents were used as received from commercial suppliers unless otherwise stated. Pet. ether refers to the fraction boiling between 40 °C and 60 °C. Dry-purified solvents collected and transferred under Ar by a Pure Solv-MD Solvent Purification System (alumina columns) from Innovative Technology.¹²⁶ Solvents and solutions for radical reactions were degassed before use by bubbling a steady stream of dry N₂ gas through them for 45 minutes. Reaction progress was monitored by thin layer chromatography (TLC) performed on aluminium or plastic plates coated with kieselgel F254 with 0.2 mm thickness. Visualisation was achieved by a combination of ultraviolet light (254 nm) and ethanolic phosphomolybdic acid (PMA), acidic potassium permanganate or anisaldehyde. Flash column chromatography was performed using silica gel 60 (230-400 mesh, Merck and co.). All reaction temperatures refer to values recorded for an external bath and room temperature implies temperatures in the range 18-25 °C.

Solution infra-red spectra were recorded using a Perkin Elmer 100-series FTIR spectrometer using chloroform as solvent. Neat infra-red spectra were also recorded using a Perkin Elmer 100-series FTIR spectrometer. Wavelengths (ν) are reported in cm⁻¹. Optical rotations were recorded as dilute solutions in the indicated solvent in a 25 mm glass cell using a JASCO DIP370 digital polarimeter at 294 nm. Mass spectra were obtained using a VG Micromass 70E or VG Micron Autospec spectrometer, using electrospray ionisation (ESI) with *meta*-nitrobenzyl alcohol as matrix. All ¹H-NMR and ¹³C-NMR

experiments were recorded using Bruker AC300, AV300, AV400 and DMX500 NMR spectrometers. Chemical shifts (δ) are quoted in ppm and coupling constants (J) are quoted in Hz. The 7.27 ppm resonance of residual CHCl_3 and 77.1 ppm resonance of CDCl_3 were used as internal references, (MeOD signal as reference, ^1H = 3.31 ppm, ^{13}C = 49.0 ppm, benzene- d_6 signal as reference, ^1H = 7.16 ppm, ^{13}C = 49.0 ppm). The following abbreviations apply: (br) broad, (s) singlet, (d) doublet, (t) triplet, (q) quartet, (m) multiplet, (dd) double doublet, etc. The chemical shifts of multiplets corresponding to a single proton are quoted as a point, representing the centre of the multiplet. When signals for two or more protons overlap, a range is quoted. Required assignments were confirmed by two-dimensional homonuclear (^1H - ^1H) and heteronuclear (^1H - ^{13}C) correlation spectroscopy on a Bruker AV400 spectrometer. Single crystal data collection at room temperature and structural solutions were performed by Dr Louise Male at the University of Birmingham. Tetrahydrofuran (THF) was distilled immediately prior to use from sodium and benzophenone.

6.2 Experimental

1,4-di(but-3-en-1-yl)piperazine-2,5-dione (S1)

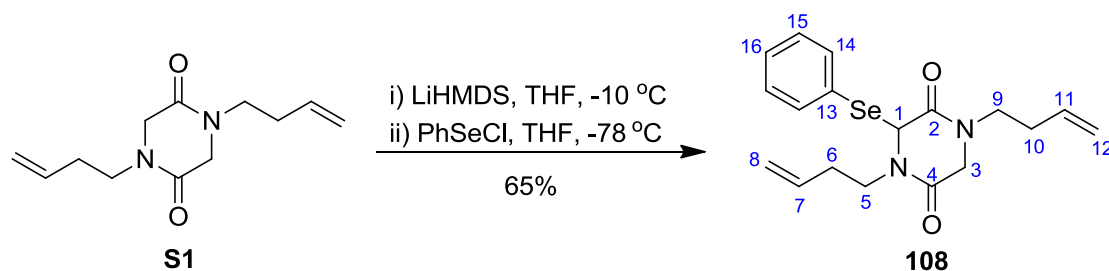


NaH (705 mg, 17.6 mmol, 2.2 equiv) as dispersion in mineral oil, was washed with Pet. ether ($3 \times 5\text{ mL}$) and added to a round bottom flask along with DMF (15 mL). The mixture was cooled to 0°C , glycine anhydride **114** (934 mg, 8.2 mmol) was added and stirred for 30 min before 4-bromobut-1-ene **115** (2.16 mL, 21.3 mmol, 2.6 equiv) was added dropwise. The reaction mixture was stirred for 5 h and then the excess NaH was quenched by careful addition of saturated $\text{NH}_4\text{Cl}_{\text{aq}}$ solution (20 mL). The

mixture was separated and the aqueous phase was extracted with EtOAc (3 × 20 mL). The combined organic extracts were washed with a saturated solution of CaCl_{2aq} (2 × 20 mL), water (20 mL) and brine (7 mL) and then dried over MgSO₄ and evaporated under reduced pressure. The crude material was purified by flash column chromatography on silica gel (eluent: Pet. ether/EtOAc, 1:2) to give **S1** (1.56 g, 7.02 mmol, 80%) as a white solid.

R_f: 0.32 (EtOAc/MeOH, 9:1); mp: 84-86 °C; FTIR (ATR) ν_{max} 1654, 1477, 1433, 1327, 1189, 1152, 997, 914, 843, 776; ¹H NMR (300 MHz, CDCl₃) δ 5.76 (ddt, *J* 17.0, 10.1, 6.9, 2H, H₂), 5.15 – 5.06 (m, 4H, H₁), 3.96 (s, 4H, H₅), 3.47 (t, *J* 7.0, 4H, H₄), 2.34 (q, *J* 7.0, 4H, H₃) ppm; ¹³C NMR (75 MHz, CDCl₃) δ 163.3 (C₆), 134.2 (C₂), 117.4 (C₁), 50.0 (C₅), 45.1 (C₄), 31.1 (C₃) ppm; HRMS (ESI) calculated for C₁₂H₁₈N₂NaO₂ [M+Na]⁺ 245.1266, found 245.1269.

1,4-di(but-3-en-1-yl)-3-(phenylselanyl)piperazine-2,5-dione (**108**)

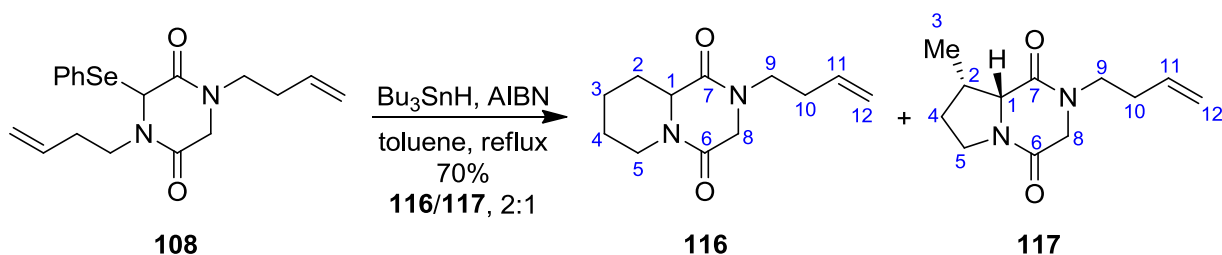


LiHMDS (6.2 mL of 0.51 M solution in THF, 3.18 mmol, 1.2 equiv) was added to a solution of **S1** (590 mg, 2.65 mmol) in dry THF (12 mL) at -10 °C. After the reaction mixture was stirred for 1 h, it was cooled to -78 °C and a solution of PhSeCl (1.0 g, 5.3 mmol, 2.0 equiv) in dry THF (4 mL) was added. The mixture was then allowed to warm to rt and stirred for 5 h before being quenched with saturated NH₄Cl_{aq} (8 mL) and extracted with EtOAc (2 × 10 mL). The extracted organic layers were washed with brine (8 mL), dried over MgSO₄ and the solvent was evaporated under reduced pressure. The crude material was purified by flash column chromatography on silica gel (eluent: Pet. ether/EtOAc, 12:1) to give **108** (652 mg, 1.72 mmol, 65%) as a yellow solid.

R_f: 0.35 (Pet. ether/EtOAc, 9:1); mp: 64-66°C; FTIR (ATR) ν_{max} 3071, 2924, 1655, 1461, 1437, 1302, 1258, 1192, 1151, 1021, 998, 911, 794, 741, 672; ¹H NMR (500 MHz, CDCl₃) δ ppm 7.61 (dd, *J* 8.0, 1.1, 2H, H14), 7.49 – 7.43 (m, 1H, H16), 7.33 – 7.30 (m, 2H, H15), 5.79 – 5.66 (m, 2H, H7, H11), 5.20 (s, 1H, H1), 5.12 – 5.01 (m, 4H, H8, H12), 4.11 (ddd, *J* 13.9, 7.2, 7.1, 1H, H5a), 3.43 (d, *J* 15.0 1H, H3a), 3.41 – 3.34 (m, 1H, H9a), 3.16 – 3.11 (m, 2H, H5b, H9b), 2.54 (d, *J* 15.0, 1H, H3b), 2.39 – 2.35 (m, 2H, H6), 2.27 – 2.20 (m, 1H, H10a), 2.18 – 2.11 (m, 1H, H10b); ¹³C NMR (126 MHz, CDCl₃) δ 164.0 (C4), 163.0 (C2), 138.0 (2 C14), 133.9 (C7), 133.9 (C11), 129.90 (C16), 128.9 (2 C-15), 124.5 (C13), 117.5 (C8), 117.2 (C12), 60.1 (C1), 49.0 (C3), 45.5 (C9), 43.6 (C5), 31.0 (C6), 30.8 (C10) ppm; HRMS (ESI) calculated for C₁₈H₂₂N₂NaO₂Se [M+Na]⁺ 401.0744, found 401.0739.

General procedure for radical cyclisation

Fused DKP (116) and (117)



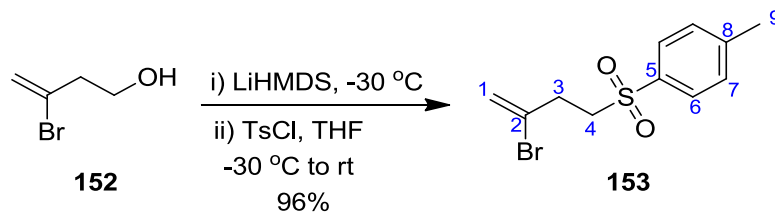
In a two neck flask connected with a condenser, 1,4-di(but-3-enyl)-3-(phenylselenenyl)piperazine-2,5-dione (**108**) (110 mg, 0.29 mmol) was dissolved in degassed toluene (9.6 mL) under inert atmosphere. The mixture was warmed to reflux and solution of AIBN 0.003 M (4.7 mg, 0.029 mmol, 0.1 equiv) and Bu₃SnH 0.036 M (94 μ L, 0.35 mmol, 1.2 equiv) in degassed toluene were added over 8 h via syringe pump. After completion of the addition the mixture was allowed to cool to rt and the solvent was evaporated under reduced pressure. The crude material was purified by flash column

chromatography on silica gel (eluent: Pet. ether/EtOAc, 70/1) to give **116** (30 mg, 46%) as a colourless oil and **117** (15 mg, 24%) as a colourless oil.

116: R_f: 0.4 (EtOAc/MeOH, 9:1); ν_{\max} (CHCl₃)/cm⁻¹ 2971, 2935, 1650, 1464, 1329, 1184, 993, 914, 732; ¹H NMR (500 MHz, CDCl₃) δ 5.75 (ddt, *J* 17.1, 10.2, 6.9, 1H, H11), 5.12 – 5.04 (m, 2H, H12), 4.65 (dt, *J* 13.0, 2.5, 1H, H5a), 3.98 (d, *J* 17.5, 1H, H8a), 3.92 (d, *J* 17.5, 1H, H8b), 3.81 (d, *J* 11.5, 1H, H1), 3.58 – 3.45 (m, 1H, H9a), 3.40 – 3.35 (m, 1H, H9b), 2.50 (td *J* 13.0, 2.5, 1H, H5b) 2.39 – 2.29 (m, 3H, H10 + H2a), 2.00 – 1.97 (m, 1H, H3a), 1.72 – 1.70 (m, 1H, H4a), 1.55 (qt, *J* 13.0, 3.5, 1H, H3b), 1.44 (qt, *J* 13.0, 3.5, 1H, H4b), 1.42 (qd, *J* 12.5, 3.5, 1H, H2b) ppm; ¹³C NMR (126 MHz, CDCl₃) δ : 165.2 (CO), 161.6 (CO), 134.4 (C11), 117.5 (C12), 59.3 (C1), 49.4 (C8), 45.1 (C9), 42.4 (C5), 31.4 (C2), 31.0 (C10), 24.5 (C4), 24.4 (C3); HRMS (ESI) calculated for C₁₂H₁₈N₂NaO₂ [M+Na]⁺ 245.1266, found 245.1268.

117: R_f: 0.2 (EtOAc/MeOH, 9:1); ν_{\max} (CHCl₃)/cm⁻¹ 3504, 2971, 2934, 1652, 1463, 1329, 1151, 915, 731; ¹H NMR (500 MHz, CDCl₃) δ : 5.72 (ddt, *J* 17.1, 10.1 7.0, 1H, H11), 5.11 – 5.04 (m, 2H, H12), 4.12 (d, *J* 4.5, 1H, H1), 4.08 (d, *J* 16.5, 1H, H8a), 3.86 (d, *J* 16.5, 1H, H8b), 3.74 (dt, *J* 11.0, 8.0, 1H, H5a), 3.57 (dt, *J* 13.5, 7.0, 1H, H9a), 3.50 (t, *J* 11.0, 1H, H5b), 3.40 (dt, *J* 13.5, 7.0, 1H, H9b), 2.77 – 2.73 (m, 1H, H2), 2.33 (q, *J* 7.0, 2H, H10), 2.08 – 2.00 (m, 1H, H4a), 1.73 (dd, *J* 12.6, 8.0, 1H, H4b), 0.90 (d, *J* 7.0, 3H, H3) ppm; ¹³C NMR (126 MHz, CDCl₃) δ 165.3 (CO), 162.7 (CO), 134.5 (C11), 117.5 (C12), 62.9 (C1), 51.4 (C8), 45.0 (C9), 43.2 (C5), 35.1 (C2), 31.4 (C10), 29.5 (C4), 13.6 (C3) ppm; HRMS (ESI) calculated for C₁₂H₁₈N₂NaO₂ [M+Na]⁺ 245.1266, found 245.1268.

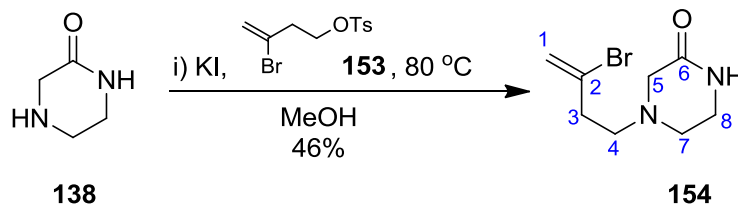
1-((3-bromobut-3-en-1-yl)sulfonyl)-4-methylbenzene (153)



LiHMDS 1.0 M in THF (7.95 mL, 7.95 mmol, 1.2 equiv) was added slowly to a solution of **152** (1.0 g, 6.62 mmol) in dry THF (30 mL) at -30 °C. The reaction mixture was stirred for 30 min at -30 °C and then solution of TsCl (1.6 g, 8.60 mmol, 1.3 equiv) in dry THF (4 mL) was added. After stirring for 20 min. the ice-bath was removed and the reaction mixture was left to warm to rt and stirred for further 20 min. To the mixture was added diethyl ether (30 mL) and the organic layer washed with saturated $\text{NH}_4\text{Cl}_{\text{aq}}$ (20 mL) and brine (2 \times 20 mL). The combined organic layers were dried over MgSO_4 , and concentrated. The crude material was purified by flash column chromatography on silica gel (eluent: Pet. ether/EtOAc, 20:1 to 5:1) to give **153** (2.0 g, 6.39 mmol, 96%) as a colourless oil.

R_f: 0.58 (Pet. ether/EtOAc, 2:1); ν_{max} (CHCl_3)/ cm^{-1} 2929, 1631, 1597, 1356, 1174, 1145, 1096, 976, 903, 814, 771; ^1H NMR (300 MHz, CDCl_3) δ : 7.77 (d, *J* 8.0, 2H, H6), 7.33 (d, *J* 8.0, 2H, H7), 5.63 (s, 1H, H1a) ppm 5.45 (s, 1H, H1b) 4.16 (t, *J* 6.0, 2H, H4) 2.72 (t, *J* 6.0, 2H, H3) 2.42 (s, 3H, H9) ppm; ^{13}C NMR (75 MHz, CDCl_3) δ : 145.0 (C8+C5), 132.7 (C2), 129.8 (2C7), 127.9 (2C6), 120.1 (C1) 67.2 (C4), 40.7 (C3), 21.6 (C9) ppm; HRMS (ESI) calculated for $\text{C}_{11}\text{H}_{13}\text{BrNaO}_3$ $[\text{M}+\text{Na}]^+$ 326.9666, found 326.9665.

4-(3-bromobut-3-en-1-yl)piperazin-2-one (**154**)

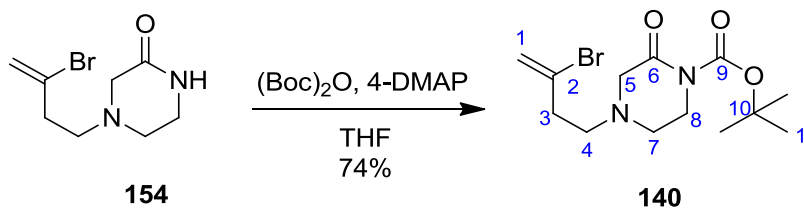


Potassium iodide (182 mg, 1.58 mmol) was added to a solution of 2-oxopiperazine **138** (315 mg, 3.15 mmol, 2.0 equiv) and **153** (962 mg, 3.15 mmol, 2.0 equiv) in MeOH (7 mL) at rt. The reaction mixture was heated at 80 °C and stirred for 48 h. After cooling the reaction mixture to rt the solvents were evaporated under reduced pressure and the crude material was purified by flash column chromatography on silica gel (EtOAc/MeOH, 1:0 to 8:2) to give **154** (340 mg, 46%) as an orange solid.

R_f: 0.42 (EtOAc/MeOH, 8:2); mp: 95-97 °C; ν_{max} (CHCl₃)/cm⁻¹ 3189, 3068, 2933, 2828, 1658, 1501, 1419, 1358, 1326, 1161, 1105, 1010, 976, 896, 856; ¹H NMR (300 MHz, CDCl₃) δ 6.92 (s, 1H, NH), 5.56 (s, 1H, H1a), 5.36 (s, 1H, H1b), 3.26 (s, 2H, H8), 3.08 (s, 2H, H5), 2.81 – 2.39 (m, 6H, H7, H4, H3); ¹³C NMR (75 MHz) δ 169.9 (C6), 131.5 (C2), 118.2 (C1), 56.7 (C7), 55.5 (C4), 49.0 (C5), 41.2 (C3), 38.9 (C8); HRMS (ESI) calculated for C₈H₁₃N₂ONaBr 255.0109, found [M+Na]⁺ 255.0115.

General procedure for amide *N*-Boc protection

tert-butyl 4-(3-bromobut-3-en-1-yl)-2-oxopiperazine-1-carboxylate (**140**)

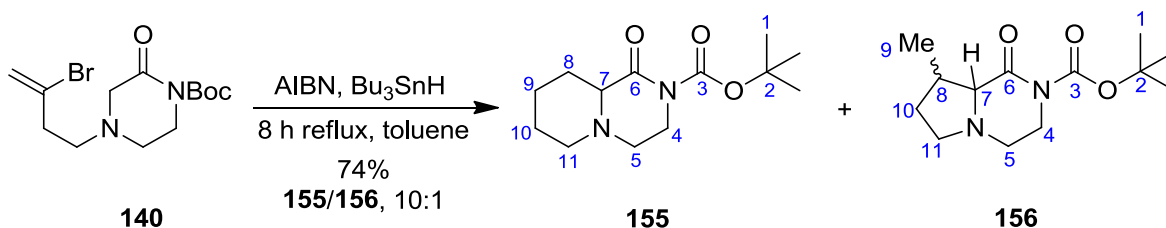


(Boc)₂O (457 mg, 2.1 mmol, 1.6 equiv), 4-DMAP (29 mg, 0.26 mmol, 0.2 equiv) were added to a solution of **154** (300 mg, 1.29 mmol) in THF (10 mL). The reaction mixture was stirred at rt for 5 h

and then diethyl ether (20 mL) was added. The mixture was washed with saturated $\text{NH}_4\text{Cl}_{\text{aq}}$ (20 mL) and brine (1×10 mL) and the combined organic layers were dried over MgSO_4 , and concentrated. The crude material was purified by flash column chromatography on silica gel (eluent: EtOAc) to give **140** (319 mg, 74%) as a yellow foam.

R_f: 0.73 (EtOAc/MeOH, 8:2); ν_{max} (CHCl_3)/ cm^{-1} 2980, 2930, 1736, 1464, 1368, 1294, 1198, 1151, 1024, 910, 776; ^1H NMR (400 MHz, CDCl_3) δ 5.52 (d, J 1.8, 1H, H1a), 5.43 (d, J 1.8, 1H, H1b), 3.67 – 3.62 (m, 2H, H8), 3.24 (s, 2H, H5), 2.72 – 2.68 (m, 2H, H7), 2.62 – 2.56 (m, 4H, H4, H3), 1.40 (s, 9H, H11); ^{13}C NMR (75 MHz, CDCl_3) δ 167.3 (C6), 151.6 (C9), 131.3 (C2), 118.2 (C1), 83.4 (C10), 59.1 (C5), 55.1 (C4), 49.7 (C7), 45.6 (C8), 38.8 (C3), 28.0 (C11); HRMS (ESI) calculated for $\text{C}_{13}\text{H}_{21}\text{N}_2\text{O}_3\text{NaBr}$ $[\text{M}+\text{Na}]^+$ 355.0633, found 355.0640.

monoketopiperazines (**155**) and (**156**)



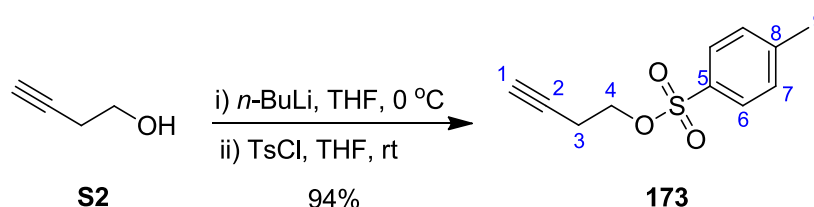
The general procedure for radical cyclisation of ketopiperazines (page 126) was followed using **140** (74 mg, 0.22 mmol) in 8 mL degassed toluene, 0.009 M AIBN (10 mg, 0.07 mmol, 0.3 equiv), 0.033 M Bu_3SnH (67 μL , 0.26 mmol, 1.8 equiv). AIBN and Bu_3SnH were added over 8 h via syringe pump to a solution of **140** at reflux. The crude material was purified by flash column chromatography on silica gel (eluent: Pet. ether/EtOAc, 5:1 to 1:1) to give **155** (38 mg, 68%) as a colourless oil and **156** (4 mg, 7%) as a colourless oil.

155: R_f: 0.2 (Pet. ether/EtOAc, 2:1); ν_{max} (CHCl_3)/ cm^{-1} 2933, 1762, 1656, 1460, 1327, 1145, 1106, 896, 850; ^1H NMR (500 MHz, CDCl_3) δ : 3.75 – 3.59 (m, 2H, H4), 2.97 – 2.83 (m, 2H, H11a, H5a),

2.53 (dd, J 11.0, 2.5, 1H, H7), 2.45 (td, J 12.0, 4.5, 1H, H5b), 2.33 (brd, J 13.0, 1H, H8a), 2.07 (td, J 11.5, 3.0, 1H, H11b), 1.86 (brd, J 13.0, 1H, H9a), 1.65 – 1.59 (m, 1H, H10a), 1.60 – 1.52 (m, 1H, H10b), 1.53 (s, 9H, H1), 1.43 (qd, J 13.0, 3.5, 1H, H8b), 1.34 – 1.24 (m, 1H, H9b) ppm: ^{13}C NMR (126 MHz, CDCl_3) δ : 169.4 (C6), 152.3 (C3), 83.0 (C2), 67.6 (C7), 56.0 (C11), 51.5 (C5), 45.3 (C4), 28.0 (C1), 27.7 (C8), 25.0 (C10), 24.3 (C9); HRMS (ESI) calculated for $\text{C}_{13}\text{H}_{22}\text{N}_{22}\text{NaO}_3$ $[\text{M}+\text{Na}]^+$ 277.1528, found 277.1522.

156: Rf: 0.12 (Pet. ether/EtOAc, 1:2); ν_{max} (CHCl_3)/ cm^{-1} 2983, 2920, 2850, 1719, 1469, 1293, 1151, 1025, 911, 851, 751; *traces - not enough for NMR assignment*; HRMS (ESI) calculated for $\text{C}_{13}\text{H}_{22}\text{N}_{22}\text{NaO}_3$ $[\text{M}+\text{Na}]^+$ 277.1528, found 277.1520.

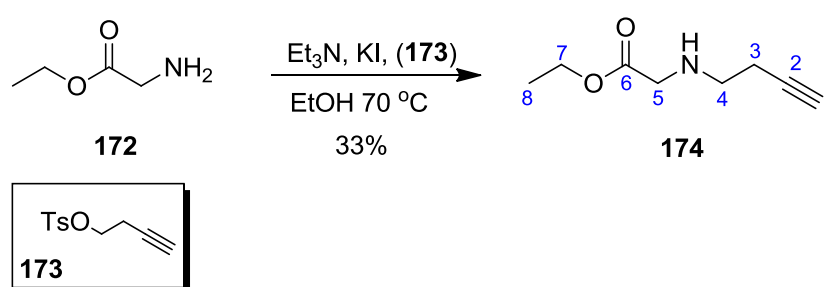
but-3-yn-1-yl 4-methylbenzenesulfonate (173)¹²⁷



$n\text{-BuLi}$ (4.6 mL, 2.5 M in hexane, 11.2 mmol, 2.0 equiv) was added slowly to a solution of but-3-yn-1-ol **S2** (0.5 mL, 5.75 mmol) in dry THF (12 mL) at 0 °C. The reaction mixture was stirred for 30 min at 0 °C and then solution of TsCl (2.84 g, 17.2 mmol, 3.0 equiv) in dry THF (4 mL) was added. After stirring for 5 min the ice-bath was removed and the reaction mixture was left to warm to rt and stirred for further 4 h. To the mixture diethyl ether (15 mL) was added and the organic layer washed with saturated $\text{NH}_4\text{Cl}_{\text{aq}}$ (2×6 mL) and brine (2×6 mL). The combined organic layers were dried over MgSO_4 , and concentrated. The crude material was purified by flash column chromatography on silica gel (eluent: Pet. ether/EtOAc, 15:1 to 5:1) to give **173** (2.44 g, 10.9 mmol, 94%) as a colourless oil;

R_f: 0.68 (Pet. ether/EtOAc, 1:1); ¹H NMR (300 MHz, CDCl₃) δ: 7.81 (d, *J* 8.2, 2H, H6), 7.34 (brd, *J* 8.2, 2H, H7), 4.11 (t, *J* 7.0, 2H, H4), 2.56 (t, *J* 7.0, 2H, H3), 2.46 (s, 3H, H9), 1.98 (t, *J* 3.0, 1H, H1) ppm; ¹³C NMR (75 MHz, CDCl₃) δ: 145.2 (C5), 132.9 (C8), 130.1 (2C7), 128.2 (2C6), 78.6 (C2), 71.0 (C1), 67.6 (C4), 21.8 (C9), 19.6 (C3) ppm; HRMS (ESI) calculated for C₁₁H₁₂NaO₃S [M+Na]⁺ 247.0405, found 247.0409.

ethyl 2-(but-3-yn-1-ylamino)acetate (**174**)

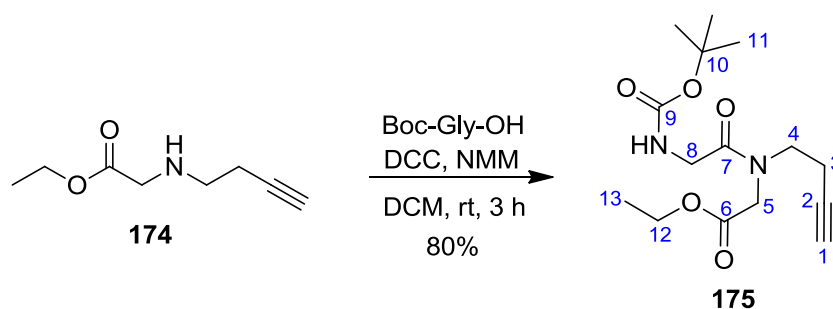


KI (904 mg, 5.6 mmol, 0.2 equiv) and Et₃N (3.4 mL, 24.5 mmol, 0.6 equiv) were added to a solution of glycine ethyl ester hydrochloride **172** (5.2 g, 37.6 mmol) in EtOH (80 mL) and a white suspension was observed. After 5 min, but-3-ynyl 4-methylbenzenesulfonate **173** (4.22 g, 56.4 mmol, 1.5 equiv) was added slowly and the reaction mixture stirred at 80 °C overnight. To the mixture EtOAc, diethyl ether 8:2 (30 mL) were added and the mixture was extracted with saturated NH₄Cl_{aq} (2 × 20 mL) and brine (2 × 20 mL). The aqueous phase was extracted with EtOAc, diethyl ether 8:2 (2 × 20 mL). The combined organic layers were dried over MgSO₄, and concentrated. The crude material was purified by flash column chromatography on silica gel (eluent: Pet. ether/EtOAc, 2:1 to 0:1) to give **174** (954 mg, 6.15 mmol, 33%) as a yellow oil.

R_f: 0.14 (Pet. ether/EtOAc, 2:1); ν_{max} (CHCl₃)/cm⁻¹ 3292, 2982, 2914, 2843, 1733, 1467, 1372, 1185, 1147, 1026, 762; ¹H NMR (300 MHz, CDCl₃) δ 4.00 (q, *J* 7.1, 2H, H7), 3.24 (s, 2H, H5), 2.60 (t, *J* 6.7, 2H, H4), 2.19 (td, *J* 6.7, 2.6, 2H, H3), 1.84 (t, *J* 2.6, 1H, H1), 1.67 (s, 1H, NH), 1.08 (t, *J* 7.1, 3H,

H8); ^{13}C NMR (101 MHz, CDCl_3) δ 172.0 (C6), 82.0 (C2), 69.4 (C1), 60.6 (C7), 50.5 (C5), 47.6 (C4), 19.6 (C3), 14.1 (C8); HRMS (EI) calculated for $\text{C}_8\text{H}_{13}\text{NO}_2$ $[\text{M}]^+$ 155.0946, found 155.0949, m/z (EI) 155 (7) $[\text{CH}_3\text{CH}_2\text{COCH}_2\text{NH}-\text{CH}_2\text{CH}_2\text{CCH}]^+$, 116 (94) $[\text{CH}_3\text{CH}_2\text{COCH}_2\text{NHCH}_2]^+$, 88 (6) $[\text{CH}_3\text{CH}_2\text{COCH}_2]^+$, 82 (100) $[\text{CH}_2\text{NHCH}_2\text{CH}_2\text{CCH}]^+$.

ethyl 2-(*N*-(but-3-yn-1-yl)-2-((*tert*-butoxycarbonyl)amino)acetamido)acetate (175**)**

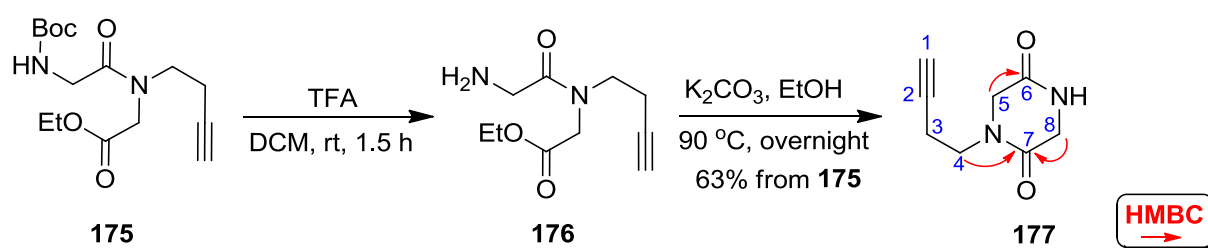


To a round bottom flask Boc-Gly-OH (1.18 g, 6.76 mmol, 1.1 equiv), and ethyl 2-(but-3-ynylamino)acetate **174** (954 mg, 6.15 mmol) were dissolved in DCM (40 mL). To the mixture was then added NMM (743 μL , 6.76 mmol, 1.1 equiv) and solution DCC (6.15 mL, of 1.0 M in DCM, 6.15 mmol). A precipitate formed within minutes and the reaction mixture was stirred at rt. After 3 h the solids were filtered off and washed with DCM (20 mL). The filtrate solution was then evaporated to dryness. The crude was purified by flash column chromatography on silica gel (eluent: Pet. ether/EtOAc, 1:1) to give **175** (1.53 g, 80%) as a pale yellow oil. The compound was obtained as an inseparable mixture (1.0:1.5*) of rotamers.

R_f: 0.4 (Pet. ether/EtOAc, 1:1); ν_{max} (CHCl_3)/ cm^{-1} 3427, 3302, 2979, 2935, 1743, 1708, 1657, 1461, 1366, 1200, 1161, 1027, 961, 918, 964, 731; ^1H NMR (400 MHz, CDCl_3) δ 5.35 (s, 1H, NH), 5.33 (s, 1H, NH*), 4.16 – 4.05 (m, 4H, H12, H12*), 4.05 – 3.99 (m, 6H, H5, H5*, H8*), 3.79 (d, J 4.3, 2H, H8), 3.46 (t, J 6.7, 2H, H4), 3.41 (t, J 6.7, 2H, H4*), 2.44 – 2.32 (m, 4H, H3, H3*), 1.96 (t, J 2.6, 1H, H1*), 1.89 (t, J 2.6, 1H, H1), 1.34 (s, 18H, H11, H11*), 1.19 (dt, J 8.3, 7.2, 6H, H13, H13*); ^{13}C

NMR (101 MHz, CDCl₃) δ 169.3 (2CO), 168.9 (2CO), 168.7 (2CO), 81.7 (C2), 80.11 (C2*), 79.8 (C10, C10*), 71.4 (C1*), 70.2 (C1), 62.0 (C12), 61.5 (C12*), 50.0 (C5), 48.0 (C5*), 47.2 (C4), 46.6 (C4*), 42.2 (C8, C8*), 28.41 (3C11, 3C11*), 18.8 (C3*), 17.8 (C3), 14.2 (C13, C13*); HRMS (ESI) calculated for C₁₅H₂₄NaN₂O₅ [M+Na]⁺ 335.1583, found 335.1579.

1-(but-3-yn-1-yl)piperazine-2,5-dione (**177**)



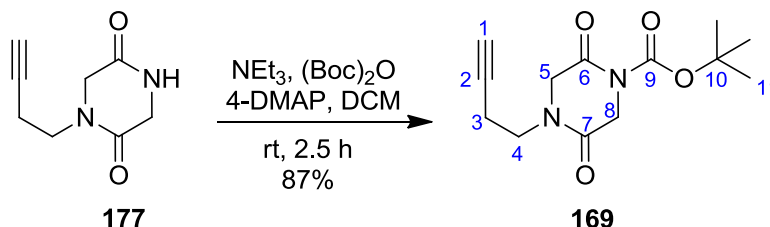
Deprotection: TFA (5.46 mL, 73.8 mmol, 15.0 equiv) was added to a solution of ethyl 2-(N-(but-3-ynyl)-2-(*tert*-butoxycarbonylamino)acetamido)acetate **175** (1.5 g, 4.92 mmol) in DCM (30 mL) and stirred for 1.5 h. The reaction mixture was washed with a saturated NH₄Cl_{aq} solution (20 mL) and brine (20 mL), dried over MgSO₄ and concentrated. The deprotected amide was confirmed by HRMS (ESI) calculated for C₁₀H₁₇N₂O₃ 213.1239, found [M]⁺:213.1233. R_f: 0.23 (EtOAc/MeOH 9/1). The crude was carried through to the next step without any purification; **Intramolecular cyclization:** The crude material **176** (937 mg, 4.42 mmol) was diluted in EtOH (30 mL) and K₂CO₃ (4.80 g, 35.3 mmol, 8.0 equiv) was added and stirred overnight at 90 °C. The crude was filtrated and purified by flash column chromatography on silica gel (eluent with EtOAc/MeOH, 15:1) to give **177** (513 mg, 3.1 mmol in 63% overall yield) as a white solid.

R_f: 0.23 (EtOAc/MeOH, 9:1); mp: 77-79 °C; ν_{\max} (CHCl₃)/cm⁻¹ 1669, 1575, 1430, 1203, 1173, 1119, 834, 801, 721; ¹H NMR (300 MHz, MeOD) δ 4.89 (s, 1H, NH), 4.14 (s, 2H, H5), 3.96 (s, 2H, H8), 3.55 (t, *J* 6.9, 2H, H4), 2.51 (td, *J* 6.9, 2.7, 2H, H3), 2.36 (t, *J* 2.7, 1H, H1); ¹³C NMR (101 MHz,

MeOD) δ 168.3 (C6), 166.6 (C7), 81.8 (C2), 71.5 (C1), 51.4 (C5), 46.5 (C4), 45.6 (C8), 17.5 (C3);

HRMS (EI) calculated for $C_8H_{10}N_2O_2$ $[M]^+$ 166.0742, found 166.0737.

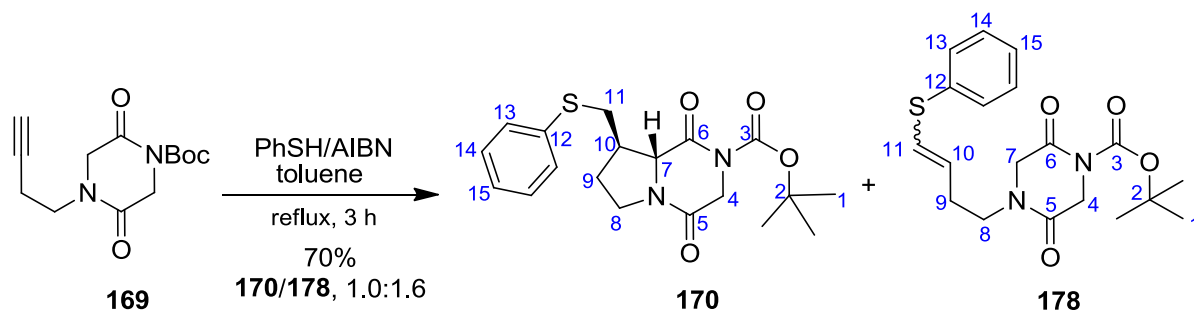
***tert*-butyl 4-(but-3-yn-1-yl)-2,5-dioxopiperazine-1-carboxylate (**169**)**



The general procedure of amide *N*-protection (page 129) was followed using 1-(but-3-ynyl)piperazine-2,5-dione **177** (257 mg, 1.55 mmol), Et_3N (0.32 mL, 2.3 mmol, 1.5 equiv), $(Boc)_2O$ (501 mg, 2.3 mmol, 1.5 equiv) and 4-DMAP (52 mg, 0.46 mmol, 0.3 equiv) in DCM (9 mL). The mixture was stirred for 1 h at reflux. The crude material was purified by flash column chromatography on silica gel (eluent: Pet. ether/EtOAc, 3:1 to 1:2) to give **169** (360 mg, 1.35 mmol, 87%) as a white foam.

R_f: 0.6 (EtOAc/MeOH, 9:1); ν_{max} ($CHCl_3$)/ cm^{-1} 1677, 1523, 1487, 1209, 1153, 1123, 839, 808, 731; 1H NMR (300 MHz, $CDCl_3$) δ : 4.17 (s, 2H, H5), 4.06 (s, 2H, H8), 3.40 (t, J 6.6, 2H, H4), 2.34 (td, J 6.6, 2.6, 2H, H3), 1.95 (t, J 2.6, 1H, H1), 1.37 (s, 9H, H11) ppm; ^{13}C NMR (101 MHz, $CDCl_3$) δ : 164.5 (C7), 164.3 (C6), 149.6 (C9), 84.4 (C10), 80.8 (C2), 70.9 (C1), 52.8 (C5), 48.1 (C4), 44.9 (C8), 27.8 (3C11), 17.3 (C3); HRMS (ESI) calculated for $C_{13}H_{18}N_2NaO_4$ $[M+Na]^+$ 289.1164, found 289.1154.

diketopiperazines (170**) and (**178**)**

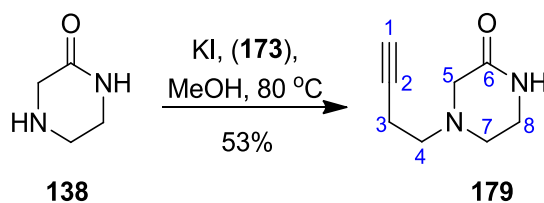


To a refluxing solution of **169** (70 mg, 0.26 mmol) in degassed toluene (30 mL) under inert atmosphere 0.11 M AIBN in toluene (54 mg, 0.34 mmol, 1.3 equiv) and 0.11 M PhSH in toluene (35 μ L, 0.34 mmol, 1.3 equiv) were added via syringe pump over 3 h. After completion of the reaction the mixture was allowed to cool to rt then concentrated and purified by flash column chromatography on silica gel (eluent: Pet. ether/EtOAc, 10:1 to 0:1) to give first **178** (45 mg, 0.12 mmol, 43%) as a colourless oil and then **170** (15 mg, 0.04 mmol, 27%) as a colourless oil. Compound **178** was obtained as 1.5:1.0 *Z/E** inseparable mixture of isomers.

178: *R*_f: 0.30 (Pet. ether/EtOAc, 1:2); ν_{max} (CHCl₃)/cm⁻¹: 2980, 2933, 1777, 1725, 1725, 1668, 1583, 1479, 1440, 1368, 1292, 1246, 1147, 970, 853, 742, 691; ¹H NMR (300 MHz, CDCl₃) δ : 7.34 – 7.30 (m, 10H, Ar(*E*), Ar(*Z*)), 6.33 (d, *J* 9.3, 1H, H11*), 6.25 (d, *J* 15.0, 1H, H11), 5.82 – 5.72 (m, 2H, H10*, H10), 4.32 (s, 2H, H4), 4.31 (s, 2H, H4*), 4.10 (s, 2H, H7*), 4.01 (s, 2H, H7), 3.54 (t, *J* 6.9, 2H, H8*), 3.47 (t, *J* 7.2, 2H, H8), 2.53 (q, *J* 6.9, 2H, H9*), 2.42 (q, *J* 7.2, 2H, H9), 1.53 (s, 9H, H1), 1.52 (s, 9H, H1*) ppm; ¹³C NMR (101 MHz, CDCl₃) δ 164.6 (CO, CO*), 164.4 (CO, CO*), 149.8 (NCO, NCO*), 135.4 (C12), 134.4 (C12*), 129.9 (11), 129.5 (11*), 129.2 (2C13, 2C13*), 129.2 (2C14, 2C14*), 127.7 (C10*), 127.0 (C10), 126.8 (C15), 126.0 (C15*), 85.0 (C2*), 84.9 (C2), 52.2 (C7), 52.2 (C7*), 48.4 (C4), 48.3 (C4*), 45.6 (C8*), 45.1 (C8), 30.9 (C9*), 28.0 (C(CH₃), C(CH₃)*), 27.3 (C9). HRMS (ESI) calculated for C₁₉H₂₄N₂NaO₄S [M+Na]⁺ 399.1354, found 399.1350.

170: R_f: 0.22 (Pet. ether/EtOAc, 1:2); ν_{\max} (CHCl₃)/cm⁻¹ 2979, 2928, 1776, 1726, 1675, 1480, 1440, 1368, 1295, 1149, 850, 744, 692; ¹H NMR (400 MHz, CDCl₃) δ 7.41 (d, *J* 8.0, 2H, H13), 7.30 (t, *J* 7.7, 2H, H14), 7.19 (t, *J* 7.3, 1H, H15), 4.64 (d, *J* 16.5, 1H, H4a), 4.06 (d, *J* 16.5, 1H, H4b), 4.00 (d, *J* 9.0, 1H, H7), 3.74 – 3.60 (m, 2H, 8a, 11a), 3.43 (dd, *J* 18.8, 10.3, 1H, H8b), 3.03 (dd, *J* 13.4, 8.4, 1H, H11b), 2.95 – 2.75 (m, 1H, H10), 2.32 – 2.26 (m, 1H, H9a), 1.82 (dt, *J* 20.3, 10.3, 1H, H9b), 1.55 (s, 9H, H1); ¹³C NMR (101 MHz, CDCl₃) δ 167.4 (C5), 163.3 (C6), 149.9 (C3), 135.7 (C12), 129.2 (2C13), 129.0 (2C14), 126.3 (C15), 84.9 (C2), 62.7 (C7), 49.7 (C4), 43.8 (C8), 41.7 (C10), 36.0 (C11), 28.8 (C9), 28.0 (3C1); HRMS (ESI) calculated for C₁₉H₂₄N₂NaO₄S [M+Na]⁺ 399.1354, found 399.1347.

4-(but-3-yn-1-yl)piperazin-2-one (**179**).

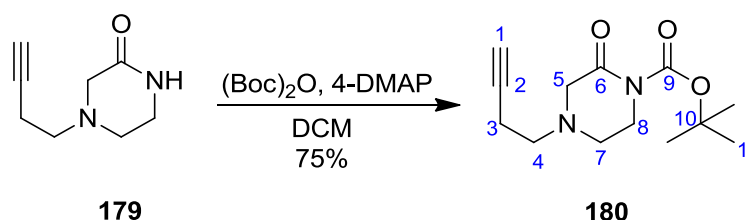


The general procedure of amide *N*-alkylation (page 129) was followed using 2-oxopiperazine **138** (50 mg, 0.5 mmol), but-3-ynyl 4-methylbenzenesulfonate **179** (112 mg, 0.5 mmol) and potassium iodide (6.4 mg, 0.04 mmol, 0.1 equiv) in MeOH (2 mL). The reaction mixture was stirred at 80 °C for 8 h and then the mixture was allowed to cool to rt, was concentrated under reduced pressure and purified by flash column chromatography on silica gel (EtOAc/MeOH, 1:0 to 8:2) to give **179** (41 mg, 53%) as a yellow solid.

R_f: 0.42 (EtOAc/MeOH, 8:2); mp: 100-102 °C; ν_{\max} (CHCl₃)/cm⁻¹ 3406, 3237, 2950, 2824, 1644, 1498, 1462, 1351, 1087, 1008; ¹H NMR (300 MHz, CDCl₃) δ 7.67 (s, 1H, NH), 3.32 (brs, 2H, H8), 3.2 (s, 2H, H5), 2.67 (t, *J* 5.4, 2H, H7), 2.62 (t, *J* 7.2, 2H, H4), 2.37 (td, *J* 7.2, 2.4, 2H, H3), 1.98 (t, *J*

2.4, 1H, H1) ppm; ^{13}C NMR (75 MHz, CDCl_3) δ 170.5 (C6), 82.0 (C2), 69.5 (C1), 56.5 (C4), 55.6 (C8), 48.5 (C5), 40.8 (C7), 16.9 (C3) ppm; HRMS (ESI) calculated for $\text{C}_8\text{H}_{12}\text{N}_2\text{NaO}$ $[\text{M}+\text{Na}]^+$ 175.0847, found 175.0842.

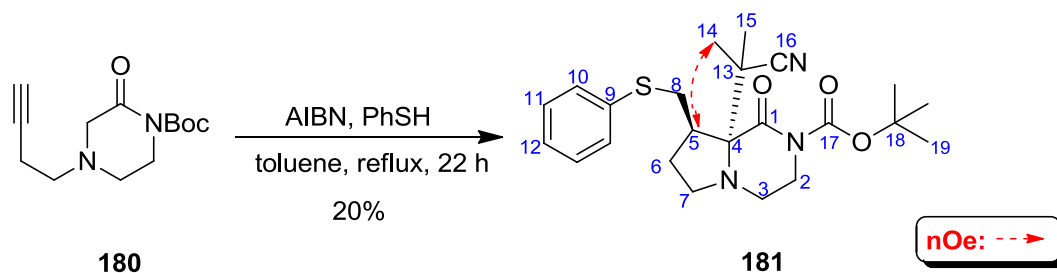
***tert*-butyl 4-(but-3-yn-1-yl)-2-oxopiperazine-1-carboxylate (**180**)**



The general procedure (page 129) was followed using **179** (41 mg, 0.27 mmol), $(\text{Boc})_2\text{O}$ (100 mg, 0.5 mmol, 1.8 equiv), 4-DMAP (30 mg, 0.27 mmol) in DCM (2 mL) and stirred for 5 h at rt. The crude material was purified by chromatography on silica gel (eluent: EtOAc) to give **180** (0.05 g, 0.19 mmol, 75%) as a white foam.

R_f: 0.73 (EtOAc/MeOH, 8:2); ν_{max} (CHCl_3)/ cm^{-1} 3265, 3004, 2970, 2947, 1737, 1455, 1367, 1288, 1229, 1146, 848, 778, 628; ^1H NMR (300 MHz, CDCl_3) δ 3.71 – 3.65 (m, 2H, H8), 3.27 (s, 2H, H5), 2.77 – 2.71 (m, 2H, H7), 2.60 (t, J 7.3, 2H, H4), 2.37 (td, J 7.3, 2.6, 2H, H3), 1.99 (t, J 2.6, 1H, H1), 1.45 (s, 9H, H11) ppm; ^{13}C NMR (75 MHz, CDCl_3) δ 167.0 (C6), 151.5 (C9), 83.2 (C10), 81.7 (C2), 69.5 (C1), 58.8 (C4), 55.2 (C8), 49.3 (C5), 45.4 (C7), 27.8 (3C11), 16.8 (C3) ppm; HRMS (ESI) calculated for $[\text{M}+\text{Na}]^+$ $\text{C}_{13}\text{H}_{20}\text{N}_2\text{O}_3\text{Na}$ 275.1372, found 275.1365.

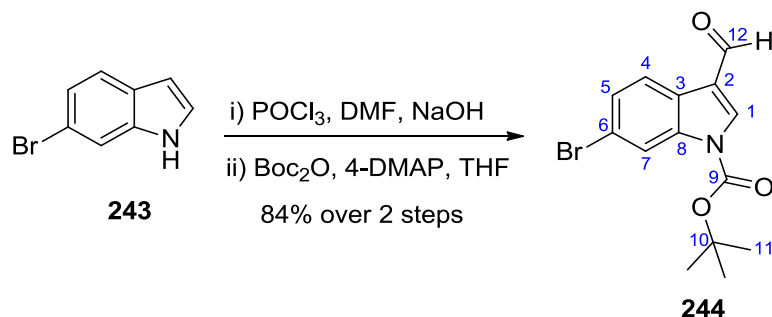
***tert*-butyl 8a-(2-cyanopropan-2-yl)-1-oxo-8-(phenylthiomethyl)-hexahydropyrrolo[1,2-*a*]pyrazine-2(1*H*)-carboxylate (**181**)**



To a refluxing solution of **180** (53 mg, 0.21 mmol) in degassed toluene (20 mL) and under an inert atmosphere solution of 0.42 M AIBN (68 mg, 0.42 mmol, 2.0 equiv) and PhSH 0.42 M (43 μ L, 0.42 mmol, 2.0 equiv) in degassed toluene were added via syringe pump over 16 h. The crude material was allowed to cool to rt and then it was concentrated and purified by HPLC to give **181** (18 mg, 20%) as a colourless oil.

R_f: 0.55 (Pet. ether/EtOAc, 1:1); ν_{max} (CHCl₃)/cm⁻¹ 2977, 2929, 2874, 2200, 2180, 1768, 1725, 1370, 1288, 1257, 1212, 1150, 747; ¹H-NMR (500 MHz, CDCl₃) δ : 7.37 (d, *J* 7.9, 2H, H10), 7.28 (t, *J* 7.7, 2H, H11), 7.19 (t, *J* 7.4, 1H, H12), 3.80 (dt, *J* 6.0, 3.5, 1H, H2a), 3.73 (td, *J* 11.5, 3.5, 1H, H2b), 3.50 (dd, *J* 12.6, 3.0, 1H, H8a), 3.30 (ddd, *J* 11.5, 8.5, 6.5, 1H, H7a), 3.18 (ddd, *J* 15.0, 11.5, 3.5, 1H, H3a), 3.09 – 3.01 (m, 2H, H3b, H7b), 2.82 – 2.76 (m, 1H, H5a), 2.64 (t, *J* 12.6, 1H, H8b), 2.31 (td, *J* 12.6, 6.5, 3.02, 1H, H6a), 1.82 – 1.74 (m, 1H, H6b), 1.51 (s, 9H, H19), 1.47 (s, 3H, H15), 1.46 (s, 3H, H14) ppm; ¹³C NMR (126 MHz, CDCl₃) δ : 171.0 (C1), 152.0 (C17), 135.4 (C9), 129.5 (2C10), 129.0 (2C11), 126.4 (C12), 125.0 (C16), 83.9 (C18), 78.1 (C4), 53.1 (C7), 49.1 (C3), 48.6 (C5), 44.2 (C2), 43.0 (C13), 36.2 (C8), 32.8 (C6), 28.0 (3C19), 24.3 (C15), 23.8 (C14); HRMS (ESI) calculated for C₂₃H₃₁N₃NaO₃S [M+Na]⁺ 452.1984 found 452.1982.

***tert*-butyl 6-bromo-3-formyl-1*H*-indole-1-carboxylate (**244**)**



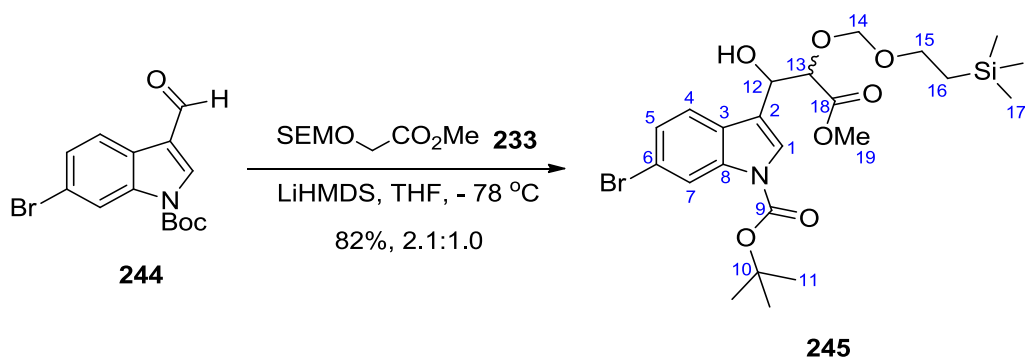
Formylation: POCl₃ (1.7 mL, 3.06 mmol, 1.1 equiv) was added to dry DMF (25 mL) dropwise at 0 °C. The solution was stirred for 20 min before a solution of 6-bromoindole **243** (2.88 g, 14.7 mmol) in dry DMF (20 mL) was added dropwise and the reaction mixture was allowed to warm to rt. After 1 h the mixture was cooled to 0 °C and a solution of sodium hydroxide 4.0 M was added until the pH \approx 7.8. The reaction mixture was allowed to warm to room temperature and stirred for another 1.5 h before water (100 mL) was added and the aqueous phase was extracted with EtOAc (3 \times 50 mL). The combined organic extracts were washed with brine (3 \times 50 mL), dried (MgSO₄) and concentrated under reduced pressure. The crude 6-bromo-1*H*-indole-3-carbaldehyde intermediate was used directly in the next step without additional purification. **Protection:** 6-bromo-1*H*-indole-3-carbaldehyde (2.58 g, 11.5 mmol) was dissolved in THF (60 mL) and Boc₂O (3.27 g, 15.0 mmol, 1.3 equiv) and 4-DMAP (281 mg 2.30 mmol, 0.2 equiv) were added at room temperature. The resulting mixture was stirred at room temperature for 1.5 h and the solvent was evaporated under reduced pressure. The residue was purified by flash column chromatography on silica gel (Pet. ether/EtOAc, 9:1) to give *N*-Boc formyl indole **244** (3.57 g, 84% over 2 steps) as a white solid.

R_f: 0.45 (Pet. ether/EtOAc, 2:1); mp: 144-145 °C FTIR (ATR) ν_{max} 1735, 1670, 1549, 1391, 1374, 1346, 1309, 1164, 1136, 1102, 841, 818, 802, 762; ¹H NMR (400 MHz, CDCl₃) ¹H NMR (300 MHz, CDCl₃) δ 10.01 (s, 1H, H12), 8.29 (d, *J* 1.5 Hz, 1H, H7), 8.13 (s, 1H, H1), 8.06 (d, *J* 8.4 Hz, 1H, H4), 7.42 (dd, *J* 8.4, 1.5 Hz, 1H, H5), 1.70 (s, 9H, H11). ¹³C NMR (101 MHz, CDCl₃) δ 185.2 (C12), 148.1

(C9), 136.3 (C8+C1), 127.6 (C5), 124.7 (C3), 123.0 (C4), 121.0 (C2), 119.6 (C6), 118.3 (C7), 85.1 (C10), 28.0 (3C11); HRMS (ESI) calculated for $C_{14}H_{14}NO_3NaBr$ $[M+Na]^+$ 346.0055, found 346.0052.

General procedure for aldol condensation

tert-butyl 6-bromo-3-(1-hydroxy-3-methoxy-3-oxo-2-((2-(trimethylsilyl)ethoxy)methoxy)propyl)-1*H*-indole-1-carboxylate (**245**)

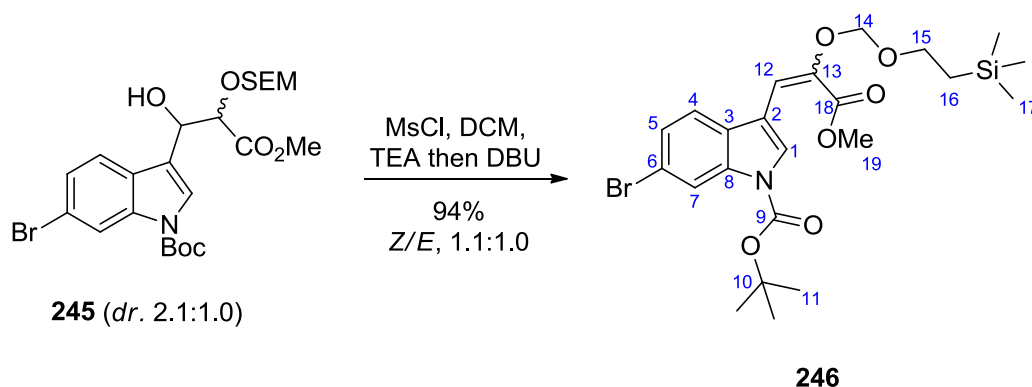


Methyl methoxy acetate **233** (4.36 mL, 19.8 mmol, 1.7 equiv) was dissolved in THF (70 mL) and to this was added LiHMDS (16.3 mL, 1.0 M in THF, 16.3 mmol, 1.4 equiv) at -78 °C and the reaction mixture was stirred for 30 min. To the mixture was then added a solution of formyl indole **244** (3.78 g, 11.7 mmol) in THF (40 mL). The solution was stirred at -78 °C for an additional 2 h and then quenched with a saturated NH_4Cl_{aq} solution (10 mL). After the mixture was warmed to room temperature it was concentrated under reduced pressure and EtOAc (50 mL) and water (50 mL) was added. The layers were separated and the aqueous phase was extracted with EtOAc (2 × 50 mL). The combined organic extracts were washed with brine (50 mL), dried over $MgSO_4$ and concentrated under reduced pressure. The residue was purified by flash column chromatography (Pet. ether/EtOAc, 8:1) to give aldol adduct **245** (5.20 g, 9.57 mmol, 82%) as a light yellow oil. The compound was obtained as a 2.1:1.0* mixture of isomers.

R_f: 0.31 (Pet. ether/EtOAc, 2:1); FTIR (ATR) V_{max} 3457, 2952, 2903, 1736, 1605, 1556, 1455, 1433, 1369, 1309, 1283, 1248, 1154, 1090, 1059, 1030, 859, 835, 767; ¹H NMR (400 MHz, CDCl₃) δ 8.28 (s, 1H, H7*), 8.25 (s, 1H, H7), 7.53 (s, 1H, H1), 7.51 (s, 1H, H1*), 7.46 (d, *J* 8.4, 1H, H4), 7.41 (d, *J* 8.4, 1H, H4*), 7.27 (dd, *J* 8.4, 1.8, 1H, H5*), 7.24 (dd, *J* 8.4, 1.8, 1H, H5), 5.19 (t, *J* 5.6, 1H, H12*), 5.15 (dd, *J* 5.6, 1H, H12), 4.66 (d, 7.1, 2H, H14*), 4.61 (d, *J* 4.0, 2H, H14), 4.43 (d, *J* 5.6, 1H, H13), 4.39 (d, *J* 4.7, 1H, H13*), 3.60 (s, 3H, H19), 3.57 (s, 3H, H19*), 3.42 – 3.28 (m, 2H, H15), 3.30 (ddd, *J* 11.8, 9.6, 5.4, 1H, H15a*), 3.16 (ddd, *J* 11.5, 9.6, 5.9, 1H, H15b*), 2.98 (d, *J* 5.6, 1H, OH), 2.94 (d, *J* 5.8, 1H, OH*), 1.57 (s, 9H, H11*), 1.56 (s, 9H, H11), 0.60 (ddd, *J* 13.6, 11.5, 5.4, 1H, H16a*), 0.75 – 0.56 (m, 2H, H16), 0.47 (ddd, *J* 13.6, 11.8, 5.9, 1H, H16b*), -0.17 (s, 9H, H17*), -0.15 (s, 9H, H17); ¹³C NMR (101 MHz, CDCl₃) δ 171.0 (C18), 170.8 (C18*), 149.2 (C9, C9*), 136.4 (C8*), 136.3 (C8), 127.8 (C3), 127.2 (C3*), 126.0 (C5, C5*), 124.6 (C1), 124.4 (C1*), 121.2 (C4), 120.8 (C4*), 119.3 (C2, C2*), 118.7 (C7*), 118.6 (C7, C6*), 118.4 (C6), 94.9 (C14), 94.8 (C14*), 84.6 (C10*), 84.5 (C10), 78.9 (C13), 78.7 (C13*), 69.0 (C12*), 68.3 (C12), 66.2 (C15, C15*), 52.3 (C19, C19*), 28.2 (C11), 28.1 (C11*), 17.9 (C16), 17.8 (C16*), -1.5 (C17), -1.4 (C17); HRMS (ESI) calculated for C₂₃H₃₄NO₇NaSiBr [M+Na]⁺ 566.1186, found 566.1190.

General procedure for β-elimination

***tert*-butyl 6-bromo-3-(3-methoxy-3-oxo-2-((2-(trimethylsilyl)ethoxy)methoxy)prop-1-en-1-yl)-1*H*-indole-1-carboxylate (246)**

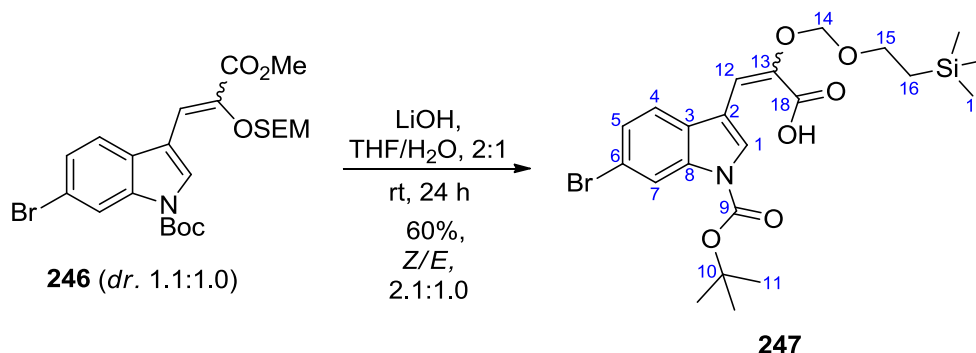


The mixture (*dr.* 2.1:1.0) of alcohols **245** (5.20 g, 9.57 mmol) was dissolved in dry DCM (100 mL) and MsCl (1.48 mL, 19.1 mmol, 2.0 equiv) was added followed by Et₃N (3.99 mL, 28.7 mmol, 3.0 equiv) at room temperature under inert atmosphere. After 4 h at room temperature the resulting mixture was quenched with a saturated NH₄Cl_{aq} solution (20 mL) and diluted with water (40 mL). The layers were separated and the aqueous phase was extracted with DCM (2 × 50 mL). The combined organic extracts were dried over MgSO₄, concentrated under reduced pressure and the residue was purified by flash column chromatography on silica gel (Pet. ether/EtOAc, 7:1) to give the desired enol ester **246** (4.79 g, 9.05 mmol, 94%) as a yellow oil. The compound was obtained as 1.1:1.0 *Z/E** inseparable mixture of stereoisomers.

R_f: 0.54 (Pet. ether/EtOAc, 2:1); FTIR (ATR) ν_{max} 2953, 1719, 1368, 1243, 1150, 1086, 857, 834, 755; ¹H NMR (400 MHz, CDCl₃) δ 8.26 (s, 2H, H7, H7*), 8.19 (s, 1H, H1*), 7.96 (s, 1H, H1), 7.47 (d, *J* 8.4, 1H, H4*), 7.31 (dd, *J* 8.4, 1.7, 1H, H5*), 7.27 – 7.26 (m, 2H, H4, H5), 7.09 (s, 1H, H12*), 6.60 (d, *J* 0.9, 1H, H12), 5.19 (s, 2H, H14*), 5.10 (s, 2H, H14), 3.76 (s, 3H, H19*), 3.75 – 3.69 (m, 2H, H15), 3.67 (s, 3H, H19), 3.61 – 3.48 (m, 2H, H15*), 1.59 (s, 9H, H11), 1.58 (s, 9H, H11*), 0.96 – 0.87 (m, 2H, H16), 0.80 – 0.70 (m, 2H, H16*), -0.05 (s, 9H, H7, H17), -0.23 (s, 9H, H17*); ¹³C NMR (75 MHz, CDCl₃) δ 164.5 (C18*), 164.3 (C18), 149.5 (C9), 149.4 (C9*), 144.6 (C13), 142.32 (C13*), 136.0 (C8), 135.9 (C8*), 129.6 (C3), 128.8 (C3*), 128.4 (C1*), 126.8 (C1), 126.6 (C5*), 126.3 (C5), 120.4 (C4*), 120.2 (C4), 119.0 (C6*), 118.9 (C7+C7*), 118.6 (C6), 114.6 (C12*), 113.8 (C2*), 113.6 (C12), 109.3 (C2), 95.6 (C14*), 95.0 (C14), 85.2 (C10*), 84.8 (C10), 68.0 (C15*), 67.2 (C15), 52.5 (C19*), 52.5 (C19), 28.5 (3C11, 3C11*), 18.5 (C16), 18.4 (C16*), -1.0 (3C17), -1.3 (3C17*); HRMS (ESI) calculated for C₂₃H₃₂NO₆BrSiNa [M+Na]⁺ 548.1080, found 548.1077.

General procedure for ester hydrolysis

3-(6-bromo-1-(*tert*-butoxycarbonyl)-1*H*-indol-3-yl)-2-((2-(trimethylsilyl)ethoxy)methoxy)acrylic acid (**247**)



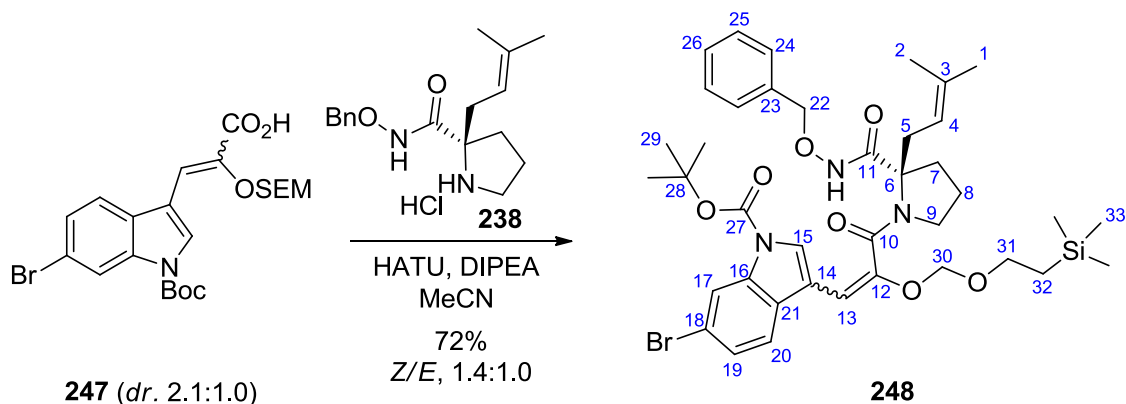
LiOH·H₂O (1.46 g, 35.0 mmol, 5.0 equiv) was added to a solution of the mixture (*dr.* 1.1:1.0) of enol ester **246** (3.70 g, 6.99 mmol) in THF/H₂O (126 mL, 2:1) at room temperature under inert atmosphere. The resulting mixture was stirred for 24 h before the volatile organics were removed under reduced pressure and the residue was diluted with water (40 mL). To the solution was added slowly 1.0 N aqueous potassium hydrogen sulfate solution to reach pH \approx 2. The resulting solution was extracted with EtOAc (3 x 30 mL). The combined organic extracts were washed with brine (20 mL), dried over MgSO₄ and concentrated under reduced pressure. The residue was purified by flash column chromatography on silica gel (Pet. ether/EtOAc, 2:1) to give α,β -unsaturated acid **247** (2.16 g, 4.19 mmol, 60%) as a yellow solid. The compound was obtained as an inseparable mixture (2.1:1.0 *Z**/*E*) of isomers.

R_f: 0.3 (Pet. ether/EtOAc, 2:1); mp: 104-105 °C; FTIR (ATR) ν_{max} 2950, 1737, 1686, 1374, 1250, 1153, 834; ¹H NMR (400 MHz, CDCl₃) δ 11.14 (s, 2H, CO₂H, CO₂H*), 8.75 – 8.44 (m, 4H, H1, H1*, H7, H7*), 7.76 (d, *J* 8.4, 1H, H4*), 7.62 – 7.55 (m, 3H, H4, H5, H5*), 7.57 (s, 1H, H12*), 7.11 (d, *J* 0.8, 1H, H12), 5.56 (s, 2H, H14*), 5.47 (s, 2H, H14), 4.19 – 4.06 (m, 2H, H15), 4.00 – 3.86 (m, 2H, H15*), 1.93 (s, 9H, H11*), 1.92 (s, 9H, H11), 1.35 – 1.19 (m, 2H, H16), 1.19 – 0.98 (m, 2H, H16*), 0.35 – 0.22 (m, 9H, H17), 0.16 – 0.04 (m, 9H, H17*); ¹³C NMR (101 MHz, CDCl₃) δ 168.8 (C18*),

167.3 (C18), 149.0 (C9), 148.9 (C9*), 142.4 (C13), 141.1 (C13*), 135.4 (C8+C8*), 129.2 (C3), 128.5 (C1*), 128.2 (C3*), 127.9 (C1), 126.3 (C5*), 126.0 (C5), 119.9 (C4*), 119.5 (C4), 118.6 (C6*), 118.4 (C7+C7*), 118.3 (C6), 116.6 (C12*), 113.3 (C2*), 112.8 (C12), 112.4 (C2), 95.3 (C14*), 95.0 (C14), 84.9 (C10*), 84.5 (C10), 67.8 (C15*), 66.9 (C15), 28.1 (3C11, 3C11*), 18.1 (C16), 17.9 (C16*), -1.4 (3C17), -1.7 (3C17*); HRMS (ESI) calculated for C₂₂H₂₉NO₆BrSi [M]⁺ 510.0948, found 510.0942.

General procedure for coupling reaction

tert-butyl (*R*)-3-(3-(2-((benzyloxy)carbamoyl)-2-(3-methylbut-2-en-1-yl)pyrrolidin-1-yl)-3-oxo-2-((2-(trimethylsilyl)ethoxy)methoxy)prop-1-en-1-yl)-6-bromo-1*H*-indole-1-carboxylate (**248**)



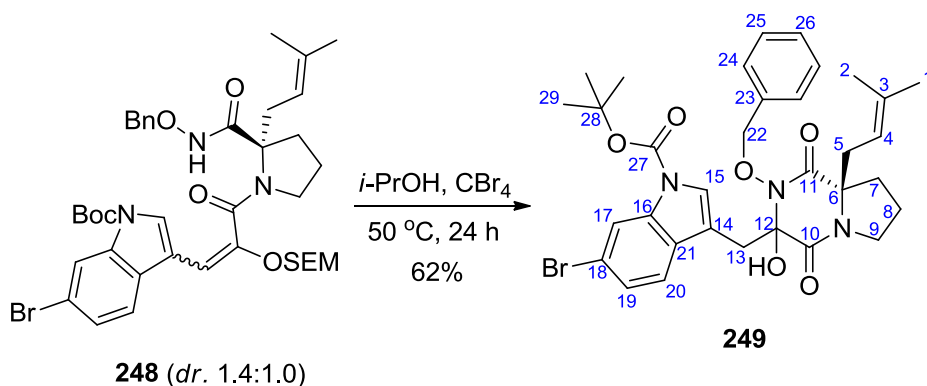
DIPEA (1.0 mL, 6.2 mmol, 1.5 equiv) and HATU (7.7 g, 4.6 mmol, 1.1 equiv) were added at rt to proline derivative **238**¹²⁸ (1.8 g, 6.2 mmol, 1.5 equiv) and to a mixture of (*dr*. 2.1:1.0) enol acid **247** (2.16 g, 4.19 mmol) in dry MeCN (100 mL). The resulting mixture was stirred for 16 h before the solvents were removed under reduced pressure. To the resulting crude oil was added EtOAc (40 mL) and the organic phase was washed successively with 1.0 N aqueous potassium hydrogen sulfate solution (15 mL), water (15 mL) and brine (15 mL). The organic layer was dried over MgSO₄ and concentrated under reduced pressure. The crude mixture was purified by flash column chromatography on silica gel (Pet. ether/EtOAc, 2:1) to afford first (*Z*)-**248** (1.38 g, 1.76 mmol, 42%) as a yellow oil and then (*E*)-**248** (980 mg, 1.26 mmol, 30%) as a yellow oil.

(*Z*)-**248** R_f: 0.64 (Pet. ether/EtOAc, 1:1); [α]_D²²: -52 (*c* 0.66, CHCl₃); FTIR (ATR) ν_{max} 2958, 1736, 1628, 1366, 1250, 1153, 1083, 1005, 836, 750, 697; ¹H NMR (400 MHz, CDCl₃) δ 10.30 (s, 1H, NH), 8.23 (s, 1H, H17), 7.95 (s, 1H, H15), 7.39 – 7.19 (m, 7H, H19, H20, H24, H25, H26), 5.78 (s, 1H, H13), 5.15 (d, *J* 6.7, 1H, H30a), 5.02 – 4.97 (m, 1H, H4), 4.89 (d, *J* 11.2, 1H, H22a), 4.79 (d, *J* 6.7, 1H, H30b), 4.78 (d, *J* 11.2, 1H, H22b), 3.72 – 3.54 (m, 2H, H9a, H31a), 3.54 – 3.37 (m, 2H, H9b, H31b), 3.04 (dd, *J* 14.7, 7.6, 1H, H5a), 2.71 (dd, *J* 14.7, 7.1, 1H, H5b), 2.52 – 2.48 (m, 1H, H7a), 2.07 – 1.99 (m, 1H, H7b), 1.69 (s, 3H, H1), 1.67 – 1.64 (m, 1H, H8a), 1.59 (s, 9H, H29), 1.58 – 1.56 (m, 1H, H8b), 1.55 (s, 3H, H2), 0.93 – 0.81 (m, 1H, H32a), 0.78 – 0.65 (m, 1H, H32b), -0.15 (s, 9H, H33); ¹³C-NMR (75 MHz, CDCl₃) δ 171.4 (C11), 164.4 (C10), 149.4 (C27), 146.0 (C12), 136.7 (C3), 135.8 (C23), 135.4 (C21), 129.3 (2C24, C16), 128.5 (C26), 128.4 (2C25), 126.0 (C15 + C19), 125.9 (C18), 119.5 (C20), 118.6 (C17), 117.5 (C4), 113.3 (C14), 102.4 (C13), 92.3 (C30), 84.6 (C28), 77.7 (C22), 70.6 (C6), 67.6 (C31), 52.1 (C9), 35.0 (C7), 31.6 (C5), 28.1 (3C29), 26.4 (C1), 23.1 (C8), 18.3 (C2), 17.9 (C32), -1.6 (3C33); HRMS (ESI) calculated for C₃₉H₅₂N₃O₇SiNaBr [M+Na]⁺ 804.2656, found 804.2667.

(*E*)-**248** R_f: 0.54 (Pet. ether/EtOAc, 1:1); [α]_D²²: -59 (*c* 0.62, CHCl₃); FTIR (ATR) ν_{max} 2958, 1736, 1628, 1366, 1250, 1153, 1083, 1005, 836, 750, 697; ¹H-NMR (400 MHz, CDCl₃) 10.45 (s, 1H, NH), 8.40 (br s, 1H, H17), 7.58 (s, 1H, H15), 7.41 – 7.31 (m, 7H, H19, H20, H24, H25, H26), 6.11 (s, 1H, H13), 5.17 (d, *J* 6.8, 1H, H30a), 5.10 (d, *J* 6.8, 1H, H30b), 4.92 (d, *J* 10.8, 1H, H22a), 4.83 (d, *J* 10.8, 1H, H22b), 4.66 (t, *J* 7.6, 1H, H4), 3.86 – 3.74 (m, 2H, H31), 3.66 – 3.60 (m, 1H, H9a), 3.18 – 3.07 (m, 2H, H9b, H5a), 2.57 – 2.49 (m, 2H, H5b, H7a), 1.65 – 1.59 (m, 3H, H7b, H8), 1.58 (s, 9H, H29), 1.55 (s, 3H, H1), 1.54 (s, 3H, H2), 1.02 – 0.98 (m, 2H, H32), 0.06 (s, 9H, H33); ¹³C NMR (75 MHz, CDCl₃) δ 170.4 (C11), 165.6 (C10), 150.0 (C27), 149.0 (C12), 136.0 (C21), 135.9 (C3), 135.6 (C23), 129.3 (C16), 128.5 (2C24), 128.4 (C26+2C25), 126.1 (C15), 123.9 (C19, C18), 119.9 (C20), 118.6 (C17), 117.7 (C4), 113.4 (C14), 96.5 (C13), 93.4 (C30), 84.4 (C28), 78.0 (C22), 70.8 (C6), 67.4 (C31), 50.5 (C9), 34.9 (C7), 32.5 (C5), 28.0 (3C29) 26.1 (C1), 23.0 (C8), 18.3 (C2), 18.2 (C32), -1.3 (3C33); HRMS (ESI) calculated for C₃₉H₅₂N₃O₇SiNaBr [M+Na]⁺ 804.2656, found 804.2661.

General procedure for DKP preparation

tert-butyl 3-(((8*R*)-2-(benzyloxy)-3-hydroxy-8a-(3-methylbut-2-en-1-yl)-1,4-dioxooctahydropyrrolo[1,2-*a*] pyrazin-3-yl)methyl)-6-bromo-1*H*-indole-1-carboxylate (**249**)



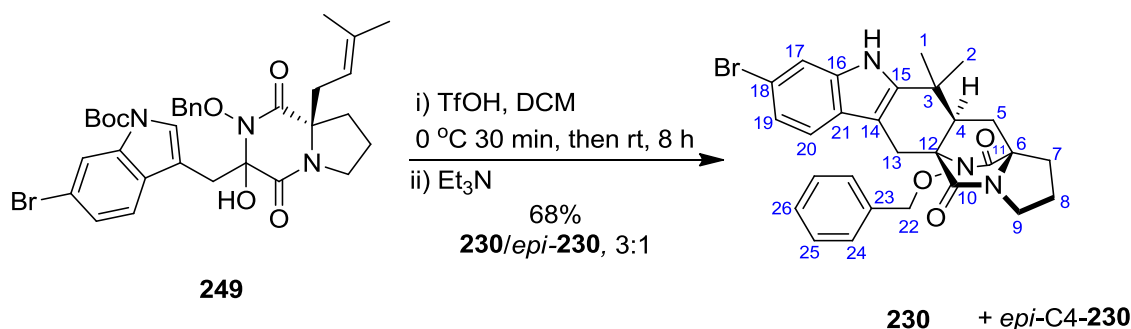
CBr₄ (199 mg, 0.6 mmol, 0.2 equiv) was added to a solution of the mixture (*dr.* 1.4:1.0) of SEM enol **248** (2.36 g, 3.02 mmol) in dry *i*-PrOH (100 mL) at room temperature. The mixture was heated to 50 °C and after 24 h allowed to cool to rt and the solvent was evaporated under reduced pressure. The resulting crude material was purified by flash column chromatography on silica gel (Pet. ether/EtOAc, 3:1) to afford a single diastereoisomer of **249** (1.24 g, 62%) as a yellow solid.

R_f: 0.43 (Pet. ether/EtOAc, 1:1); mp: 77-78 °C, [α]_D^{20.5}: +44 (*c* 2.55, CHCl₃); FTIR (ATR) ν_{max} 3325, 2980, 1736, 1642, 1365, 1252, 1153, 1084, 749, 697; ¹H NMR (400 MHz, CDCl₃) δ 8.31 (s, 1H, H17), 7.65 – 7.63 (m, 2H, H24), 7.45 – 7.41 (m, 4H, H26, H25, H20), 7.38 (s, 1H, H15), 7.29 (dd, *J* 8.5, 1.8, 1H, H19), 5.20 (d, *J* 9.1, 1H, H22a), 5.08 (d, *J* 9.1, 1H, H22b), 5.08 – 5.04 (m, 1H, H4), 4.15 (brs, 1H, OH), 3.68 (d, *J* 14.1, 1H, H13a), 3.45 (d, *J* 14.1, 1H, H13b), 3.23 (ddd, *J* 12.5, 9.7, 6.2, 1H, H9a), 3.18 (ddd, *J* 12.5, 10.1, 5.0, 1H, H9b), 2.44 (dd, *J* 14.3, 8.3, 1H, H5a), 2.22 (dd, *J* 14.3, 7.3, 1H, H5b), 1.84 – 1.76 (m, 1H, H7a), 1.74 (s, 3H, H1), 1.72 – 1.68 (m, 1H, H8a), 1.64 (s, 9H, H29), 1.56 (s, 3H, H2), 0.95 – 0.87 (m, 1H, H8b), 0.76 – 0.68 (m, 1H, H7b); ¹³C-NMR (75 MHz, CDCl₃) δ 165.3 (C11), 164.4 (C10), 149.1 (C27), 137.9 (C3), 135.7 (C21), 135.5 (C23), 129.5 (2C24), 128.8 (C26+C16), 128.5

(2C25), 127.2 (C15), 125.8 (C19), 121.1 (C20), 118.3 (C18), 118.0 (C17), 117.2 (C4), 112.8 (C14), 90.9 (C12), 84.3 (C28), 78.8 (C22), 67.7 (C6), 44.3 (C9), 36.4 (C5), 33.8 (C7), 33.5 (C13), 28.1 (3C29), 26.0 (C1), 19.1 (C8), 18.1 (C2); HRMS (ESI) calculated for $C_{33}H_{38}N_3O_6NaBr$ $[M+Na]^+$ 674.1842, found 674.1848.

General procedure for cationic cyclisation

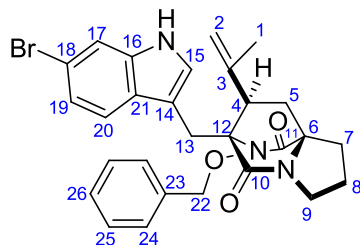
Bridged DKP (230)



TfOH (32 μ L, 0.36 mmol, 2.2 equiv) was added to solution of hydroxy-DKP **249** (107 mg, 0.16 mmol) in DCM (6.5 mL) at -50 °C under inert atmosphere. The resulting mixture was stirred for 8 h between -50 °C and -40 °C, then allowed to warm to rt and stirred for 16 h before triethylamine (112 μ L, 0.8 mmol, 5.0 equiv) was added. The resulting mixture was diluted with DCM (5 mL), and washed successively with H₂O (10 mL), saturated NH₄Cl_{aq} (10 mL), and brine (10 mL). The organic extracts were dried over MgSO₄ and concentrated under reduced pressure. The residue was purified by flash column chromatography on silica gel (Pet. ether/EtOAc, 1:1) to afford first compound **230** (45 mg, 0.08 mmol, 52%) as a yellow solid and *epi*-C4-**230** (14 mg, 0.03 mmol, 16%) as a yellow foam.

230: R_f: 0.23 (EtOAc/MeOH 4:1); mp: 202-204 °C; $[\alpha]_D^{20}$ -50 (*c* 0.7, CHCl₃); FTIR (ATR) ν_{\max} 3310, 2958, 1680, 1463, 1362, 1055; ¹H NMR (500 MHz, CDCl₃) δ 7.79 (s, 1H, NH), 7.53 – 7.46 (m, 2H, H25), 7.46 – 7.34 (m, 5H, H24, H26, H17, H20), 7.22 (d, *J* 8.3, 1H, H19), 5.10 (d, *J* 9.8, 1H, H22a), 4.99 (d, *J* 9.8, 1H, H22b), 3.59 (d, *J* 15.8, 1H, H13a), 3.45 (dt, *J* 11.5, 7.1, 1H, H9a), 3.42 (dt, *J* 11.5,

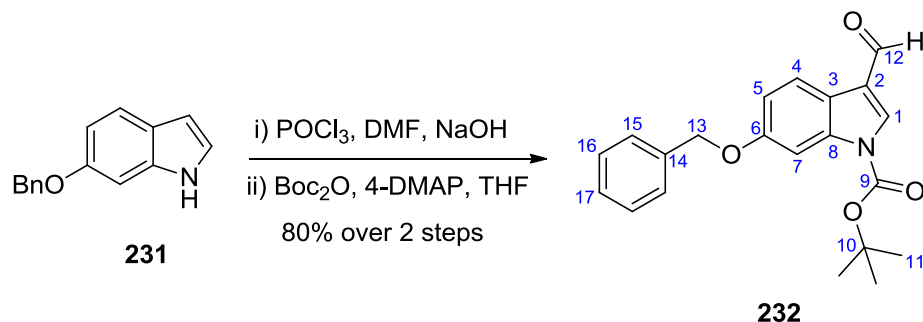
and triethylamine (112 μ L, 0.8 mmol, 5.0 equiv) was added. The resulting mixture was diluted with DCM (5 mL), and washed successively with H₂O (10 mL), saturated NH₄Cl_{aq} (10 mL), and brine (10 mL). The organic extracts were dried over MgSO₄ and concentrated under reduced pressure. The residue was purified by flash column chromatography on silica gel (Pet. ether/EtOAc, 1:1) to afford first compound **S3** (64 mg, 0.12 mmol, 74%) as a yellow foam.



S3

S3: R_f: 0.32 (EtOAc/MeOH 4:1); [α]_D²⁰ -34 (*c* 0.7, CHCl₃); FTIR (ATR) ν_{\max} 3320, 2955, 1670, 1443, 1378, 1089; ¹H NMR (300 MHz, CDCl₃) δ 8.41 (s, 1H, NH), 7.52 (d, *J* 1.6, 1H, Ar, CH), 7.41 (d, *J* 8.5, 1H, Ar, CH), 7.35 (d, *J* 2.3, 1H, Ar, CH), 7.30 – 7.08 (m, 4H, Ar, CH), 6.91 – 6.71 (m, 2H, Ar, CH), 4.82 (d, *J* 8.5, 1H, H22a), 4.77 (s, 1H, H2a), 4.63 (s, 1H, H2b), 3.85 (d, *J* 8.5, 1H, H22b), 3.65 (t, *J* 6.8, 2H, H9), 3.40 (s, 2H, H13), 3.07 (dd, *J* 10.2, 6.1, 1H, H4), 2.82 (dt, *J* 13.4, 6.8, 1H, H7a), 2.25 (dd, *J* 13.4, 10.2, 1H, H5a), 2.16 – 1.99 (m, 2H, H8), 1.92 (dd, *J* 13.4, 7.0, 1H, H7b), 1.81 (dd, *J* 13.4, 6.1, 1H, H5b), 1.55 (s, 3H, H1); ¹³C NMR (101 MHz, CDCl₃) δ 172.0 (C11), 167.2 (C10), 142.2 (C3), 136.2 (Ar, C), 134.0 (Ar, C), 129.8 (2Ar, CH), 128.8 (Ar, CH), 128.2 (2Ar, CH), 127.8 (C15), 125.0 (Ar, C), 122.6 (Ar, CH), 120.3 (Ar, CH), 116.1 (Ar, C), 115.3 (C2), 113.8 (Ar, CH), 110.6 (C14), 78.6 (C22), 74.2 (C12), 66.7 (C6), 50.2 (C4), 44.9 (C9), 37.7 (C5), 29.4 (C7), 24.2 (C8), 23.6 (C13), 19.3 (C1); HRMS (ESI) calculated for C₂₈H₂₈N₃O₃NaBr [M+Na]⁺ 556.1212, found 556.1227.

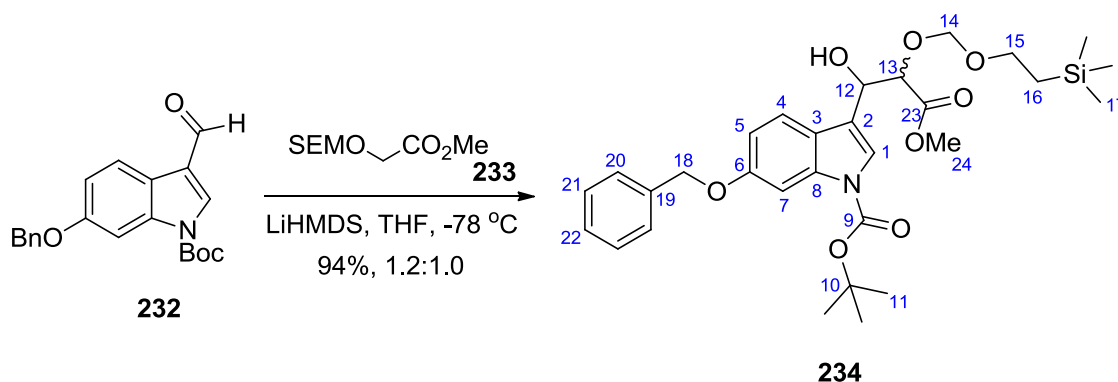
***tert*-butyl 6-(benzyloxy)-3-formyl-1*H*-indole-1-carboxylate (**232**)**¹²⁹



Formylation was achieved according to the general procedure (page 140) using 6-benzyloxyindole **231** (4.44 mg 19.9 mmol) in dry DMF (20 mL), POCl₃ (2.37 mL, 25.8 mmol, 1.3 equiv) in dry DMF (30 mL), NaOH until pH \approx 7.8. The resulting 6-(benzyloxy)-1*H*-indole-3-carbaldehyde which was used directly in the next step without additional purification. The general procedure for *N*-Boc protection was then followed dissolving the crude material in THF (80 mL), using Boc₂O (5.2 g, 23.9 mmol, 1.2 equiv) and 4-DMAP (486 mg, 3.98 mmol, 0.2 equiv). The residue was purified by flash column chromatography on silica gel (Pet. ether/EtOAc, 8:1) to give *N*-Boc formyl indole **232** (5.58 g, 80% over 2 steps) as a yellow solid.

R_f: 0.50 (Pet. ether/EtOAc, 1:1); mp: 115-116 °C; ¹H NMR (400 MHz, CDCl₃) δ 10.05 (s, 1H, H12), 8.17 (d, *J* 8.7, 1H, H4), 8.12 (s, 1H, H1), 7.83 (d, *J* 1.9, 1H, H7), 7.48 (d, *J* 7.2, 2H, H15), 7.41 (t, *J* 7.2, 2H, H16), 7.36 (d, *J* 7.2, 1H, H17), 7.09 (dd, *J* 8.7, 2.3, 1H, H5), 5.15 (s, 2H, H13), 1.71 (s, 9H, H11); ¹³C NMR (101 MHz, CDCl₃) δ 185.5 (C12), 157.8 (C6), 148.6 (C9), 136.9 (C8), 136.7 (C14), 135.4 (C1), 128.4 (2C16), 127.8 (C17), 127.4 (2C15), 122.4 (C4), 121.4 (C2), 119.7 (C3), 114.1 (C5), 100.3 (C7), 85.3 (C10), 70.1 (3C13), 27.9 (C11); HRMS (ESI) calculated for C₂₁H₂₁NO₄Na [M+Na]⁺ 374.1368, found 374.1374.

***tert*-butyl 6-(benzyloxy)-3-(1-hydroxy-3-methoxy-3-oxo-2-((2(trimethylsilyl)ethoxy)methoxy)propyl)-1*H*-indole-1-carboxylate (**234**)**

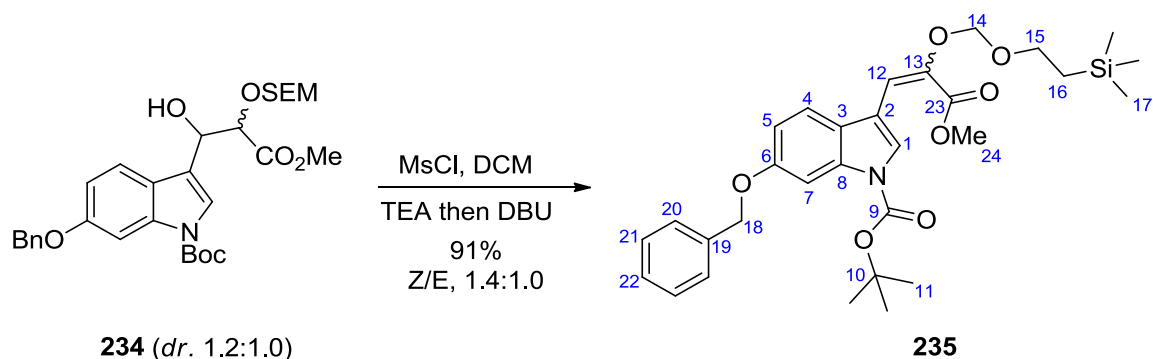


The general procedure (page 141) for aldol condensation was followed using formylindole **232** (920 mg, 2.62 mmol), ester **233** (1.15 g, 5.24 mmol, 2.0 equiv), LiHMDS (3.93 mL, 1.0 M in THF, 3.93 mmol, 1.5 equiv) and THF (15 mL + 10 mL). The crude material was purified by flash column chromatography (Pet. ether/EtOAc, 4:1) to give aldol adduct **234** (1.39 g, 2.43 mmol, 94%) as a yellow oil. The compound was obtained as an inseparable 1.2:1.0 mixture of isomers.

R_f: 0.38 (Pet. ether/EtOAc, 1:1); FTIR (ATR) ν_{max} 3463, 2952, 2894, 1731, 1617, 1570, 1485, 1440, 1370, 1319, 1249, 1206, 1156, 1015, 1092, 1024, 934, 857, 835, 767, 696; ¹H NMR (400 MHz, CDCl₃) δ 7.85 (s, 1H, H7*), 7.57 (d, *J* 8.7, 1H, H4*), 7.56 (s, 1H, H1*), 7.51 – 7.44 (m, 2H, H20*), 7.87 (s, 1H, H7), 7.59 – 7.49 (m, 2H, H4 + H1), 7.49 – 7.44 (m, 2H, H20), 7.43 – 7.36 (m, 4H, H21*, H21), 7.36 – 7.30 (m, 2H, H22*, H22), 6.97 (m, 2H, H5*, H5), 5.33 – 5.27 (m, 1H, H12), 5.26 – 5.22 (m, 1H, H12*), 5.12 (s, 4H, H18*, H18), 4.80 (d, *J* 7.1, 1H, H14a), 4.73 (d, *J* 7.1, 1H, H14b), 4.72 (d, *J* 2.9, 2H, H14*), 4.56 (d, *J* 5.6, 1H, H13*), 4.53 (d, *J* 4.7, 1H, H13), 3.71 (s, 3H, H24*), 3.68 (s, 3H, H24), 3.57 – 3.37 (m, 2H, H15*), 3.42 (ddd, *J* 11.8, 9.7, 5.4, 1H, H15a), 3.28 (ddd, *J* 11.8, 9.7, 5.9, 1H, H15b), 3.04 (d, *J* 5.6, 1H, OH*), 3.02 (d, *J* 5.8, 1H, OH), 1.66 (s, 9H, H11), 1.65 (s, 9H, H11*), 0.87 – 0.68 (m, 3H, H16*, H16a), 0.60 (ddd, *J* 13.6, 11.8, 5.9, 1H, H16b), -0.07 (s, 9H, H17), -0.04 (s, 9H, H17*); ¹³C NMR (101 MHz, CDCl₃) δ 171.2 (C23*), 171.0 (C23), 157.4 (C6, C9), 157.2 (C9*, C6*), 149.8 (C8), 149.7 (C8*), 137.3 (C19), 137.2 (C19*), 136.6 (2C21*), 128.7 (2C21), 128.6

(C22*), 128.1 (C22), 127.9 (2C20*), 127.8 (2C20), 122.9 (C1*, C3*), 122.8 (C1, C4*), 122.5 (C3), 120.4 (C2*), 120.2 (C4), 119.6 (C2), 119.4 (C5*), 113.0 (C5), 112.8 (C7*), 100.9 (C7), 100.7 (C14*), 94.9 (C14), 94.8 (C10*), 83.9 (C10), 83.7 (C13*), 78.9 (C18*), 78.8 (C13), 70.6 (C18), 70.4 (C12*), 69.4 (C12), 68.6 (C15*), 66.2 (C15), 52.4 (C24), 52.2 (C24*), 28.4 (C11), 28.2 (C11*), 17.9 (C16*, C16), -1.5 (C17*) -1.4 (C17); HRMS (ESI) calculated for C₃₀H₄₁NO₈NaSi [M+Na]⁺ 594.2499, found 594.2501.

tert-butyl 6-(benzyloxy)-3-(3-methoxy-3-oxo-2-((2-(trimethylsilyl)ethoxy)methoxy)prop-1-en-1-yl)-1H-indole-1-carboxylate (235**)**

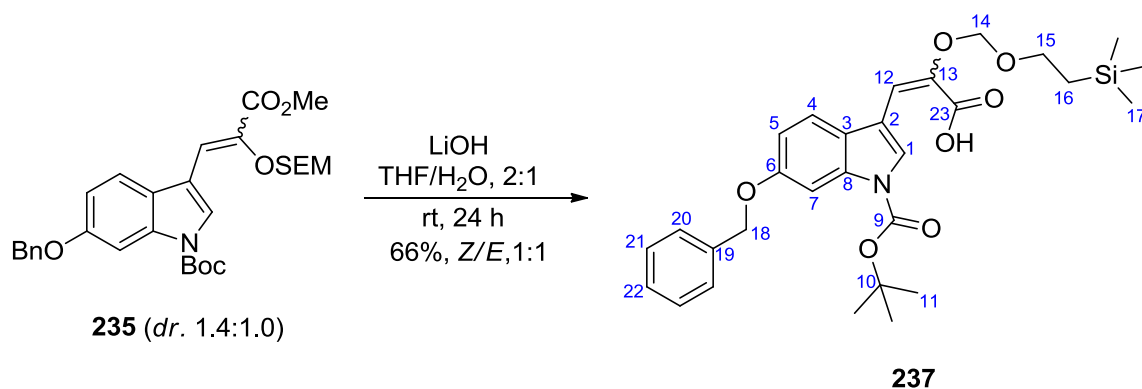


The general procedure for β -elimination (page 142) was followed using mixture (*dr.* 1.2:1.0) of hydroxyl ester **234** (1.34 g, 2.34 mmol), MsCl (0.36 mL, 4.68 mmol, 2.0 equiv), Et₃N (0.98 mL, 7.02 mmol, 3.0 equiv), DCM (24 mL) and DBU (1.75 mL, 11.7 mmol, 5.0 equiv). The residue was purified by flash column chromatography (Pet. ether/Et₂O, 9:1) to give **235** (1.19 g, 2.15 mmol, 91%) as a yellow oil. The compound was obtained as a *Z:E**=1.4:1.0 inseparable mixture of isomers.

R_f: 0.42 (Pet. ether/EtOAc, 4:1); FTIR (ATR) ν_{max} 2952, 1734, 1615, 1487, 1439, 1372, 1327, 1249, 1221, 155, 1089, 995, 857, 767, 696; ¹H NMR (400 MHz, CDCl₃) δ 8.12 (s, 1H, H1*), 7.89 (s, 1H, H1), 7.76 (s, 1H, H7), 7.75 (s, 1H, H7*), 7.51 (d, *J* 8.7, 1H, H4*), 7.38 (d, *J* 7.2, 4H, H20, H20*), 7.34 – 7.27 (m, 5H, H4, H21, H21*), 7.27 – 7.20 (m, 2H, H22, H22*), 7.14 (s, 1H, H12), 6.92 (dd, *J* 8.7, 2.3, 1H, H5*), 6.89 (dd, *J* 8.6, 2.3, 1H, H5), 6.65 (d, *J* 0.9, 1H, H12*), 5.18 (s, 2H, H14*), 5.09 (s, 2H,

H14), 5.05 (s, 4H, H18, H18*), 3.77 (s, 3H, H24*), 3.76 – 3.69 (m, 2H, H15), 3.68 (s, 3H, H24), 3.64 – 3.55 (m, 2H, H15*), 1.58 (s, 18H, H11, H11*), 0.97 – 0.88 (m, 2H, H16), 0.81 – 0.71 (m, 2H, H16*), -0.05 (s, 9H, H17), -0.22 (s, 9H, H17*); ^{13}C NMR (101 MHz, CDCl_3) δ 164.2 (C23*), 164.1 (C23), 157.3 (C6*), 157.1 (C6), 149.5 (C9), 149.4 (C9*), 143.7 (C13), 141.5 (C13*), 137.1 (C19), 137.0 (C19*), 135.8 (C8, C8*), 128.4 (2C21, 2C21*), 127.8 (C22, C22*), 127.5 (2C20, 2C20*), 126.7 (C1*), 124.9 (C1), 124.4 (C3), 123.5 (C3*), 119.4 (C4*), 119.0 (C4), 115.1 (C12*), 113.5 (C2*), 113.2 (C2), 113.0 (C5*), 112.7 (C5), 110.0 (C12), 100.6 (C7, C7*), 95.1 (C14*), 94.7 (C14), 84.0 (C10*), 83.7 (C10), 70.4 (C18+C18*), 67.5 (C15*), 66.6 (C15), 52.0 (C24, C24*), 28.1 (3C11, 3C11*), 18.0 (C16), 17.9 (C16*), -1.4 (3C17), -1.7 (3C17*); HRMS (ESI) calculated for $\text{C}_{30}\text{H}_{39}\text{NO}_7\text{SiNa}$ $[\text{M}+\text{Na}]^+$ 576.2394, found 576.2402.

3-(6-(benzyloxy)-1-(*tert*-butoxycarbonyl)-1*H*-indol-3-yl)-2-((2-(trimethylsilyl) ethoxy) methoxy) acrylic acid (237)

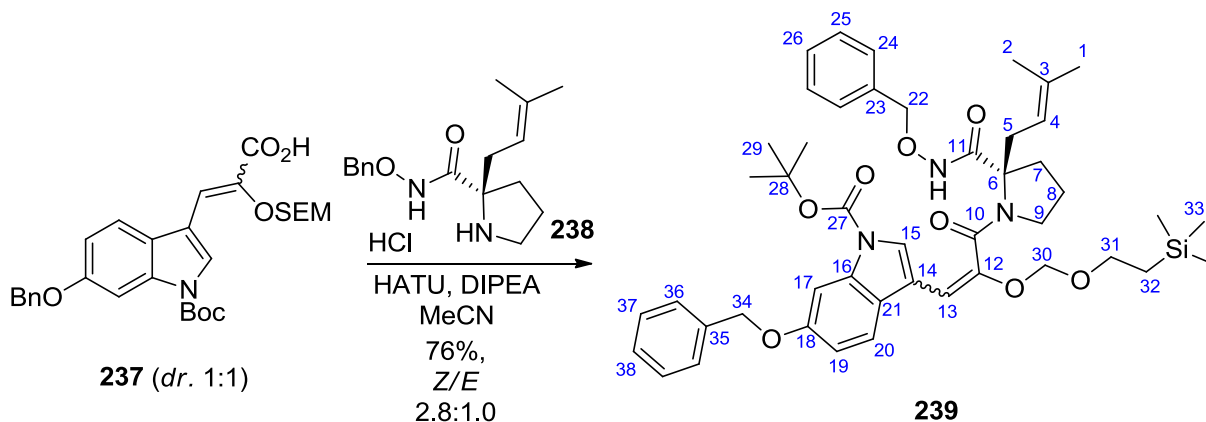


The general procedure for ester hydrolysis (page 144) was followed using mixture (*dr.* 1.4:1.0) of ester **235** (510 mg, 0.92 mmol), $\text{LiOH}\cdot\text{H}_2\text{O}$ (193 mg, 4.60 mmol, 5.0 equiv) and $\text{THF}/\text{H}_2\text{O}$ (20 mL, 2:1). The crude oil was purified by flash column chromatography (Pet. ether/ Et_2O , 4:1 to 3:2) to give enol

acid **237** (360 mg, 60%) as a light yellow solid. The compound was obtained as 1:1 *Z/E** inseparable mixture of isomers.

R_f: 0.18 (Pet. ether/EtOAc, 2:1); mp: 121-122 °C; FTIR (ATR) ν_{max} 2918, 2959, 1731, 1615, 1487, 1441, 1369, 1248, 1218, 1150, 1087, 1021, 934, 833, 806, 733, 694; ¹H NMR (400 MHz, CDCl₃) δ 8.35 (d, *J* 0.8, 1H, H1*), 8.30 (s, 1H, H1), 7.91 (s, 1H, H7*), 7.87 (s, 1H, H7), 7.67 – 7.60 (m, 1H, H4), 7.56 – 7.30 (m, 11H, H4, H21, H21*, H22, H22*, H20, H20*), 7.07 – 7.01 (m, 2H, H5*, H5), 6.98 (s, 2H, H12, H12*), 5.32 (s, 2H, H14), 5.25 (s, 2H, H14*), 5.17 (s, 2H, H18), 5.15 (s, 2H, H18*), 3.93 – 3.84 (m, 2H, H15*), 3.78 – 3.70 (m, 2H, H15), 1.70 (s, 9H, H11), 1.69 (s, 9H, H11*), 1.06 (m, 2H, H16), 0.95 – 0.88 (m, 2H, H16*), 0.07 (s, 9H, H17*), -0.09 (s, 9H, H17); ¹³C NMR (101 MHz, CDCl₃) δ 168.9 (C23*), 166.8 (C23), 157.4 (C6*), 157.2 (C6), 149.6 (C9), 149.5 (C9*), 141.9 (C13), 140.8 (C13*), 137.1 (C19), 137.0 (C19*), 135.9 (C8, C8*), 128.6 (2C21, 2C21*), 128.0 (C22, C22*), 127.6 (2C20, 2C20*), 127.5 (C1*), 126.9 (C1), 124.5 (C3), 123.4 (C3*), 119.5 (C4*), 118.9 (C4), 114.0 (C12*), 113.5 (C2*), 113.2 (C5*), 113.0 (C5), 112.4 (C2), 111.6 (C12), 100.7 (C7), 100.6 (C7*), 95.4 (C14), 95.3 (C14*), 84.3 (C10), 84.0 (C10*), 70.5 (C18, C18*), 67.8 (C15*), 67.0 (C15), 28.2 (3C11), 28.2 (3C11*), 18.2 (C16), 18.0 (C16*), -1.3 (3C17), -1.6 (3C17*); HRMS (ESI) calculated for C₂₉H₃₆NO₇Si [M]⁺ 538.2261, found 538.2267.

(*R*)-tert-butyl 6-(benzyloxy) -3-(3-(2-((benzyloxy)carbamoyl) -2-(3-methylbut-2-en-1-yl) pyrrolidin-1-yl)-3-oxo-2-((2-(trimethylsilyl)ethoxy)methoxy)prop-1-en-1-yl)-1*H*-indole-1 carboxylate (239**)**



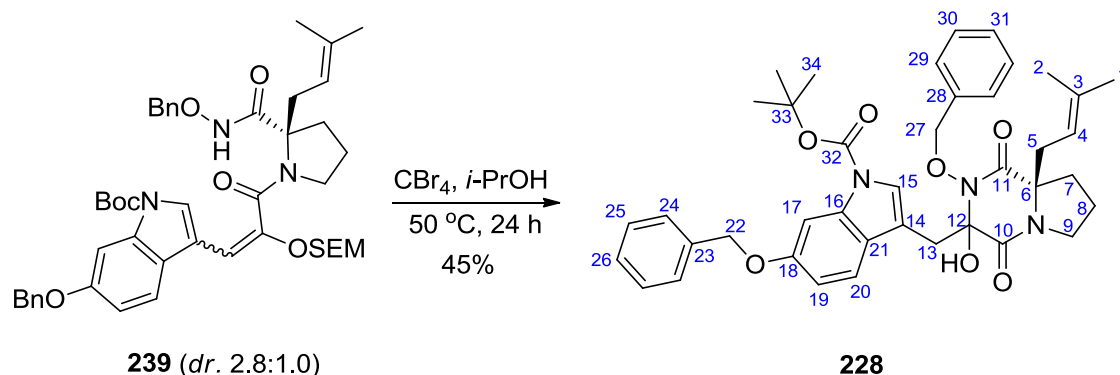
The general procedure for the coupling reaction (page 145) was followed using of proline derivative **238** (158 mg, 0.55 mmol), mixture (*dr.* 1:1) of acid **237** (300 mg, 0.55 mmol), HATU (229 mg, 0.60 mmol, 1.1 equiv), DIPEA (0.14 mL, 0.83 mmol, 1.5 equiv) and MeCN (15 mL). The crude material was purified by flash column chromatography (Pet. ether/EtOAc, 4:1) to give (*E*)-**239** (90 mg, 20%) as a light yellow oil followed by (*Z*)-**239** (250 mg, 56%) as a light yellow oil.

(*E*)-**239**: *R*_f 0.50 (Pet. ether/EtOAc, 1:1); [α]_D^{20.5}: -28 (*c* 0.58, CHCl₃); FTIR (ATR) ν_{max} 2954, 1730, 1621, 1485, 1442, 1250, 1212, 1153, 1086, 1024, 968, 856, 836, 751, 697, 665; ¹H NMR (400 MHz, CDCl₃) δ 10.54 (s, 1H, NH), 7.89 (s, 1H, H17), 7.50 (s, 1H, H15), 7.45 – 7.28 (m, 11H, H20, H24, H25, H26, H36, H37, H38), 7.00 (dd, *J* 8.6, 2.3, 1H, H19), 6.15 (s, 1H, H13), 5.18 (d, *J* 6.9, 1H, H30a), 5.14 (s, 2H, H34), 5.12 (d, *J* 6.9, 1H, H30b), 4.93 (d, *J* 10.9, 1H, H22a), 4.83 (d, *J* 10.9, 1H, H22b), 4.74 – 4.70 (m, 1H, H4), 3.89 – 3.72 (m, 2H, H31), 3.68 – 3.59 (m, 1H, H9a), 3.23 – 3.03 (m, 2H, H5a, H9b), 2.61 – 2.46 (m, 2H, H5b, H7a), 1.65 – 1.62 (m, 1H, H7b), 1.62 – 1.59 (m, 2H, H8), 1.58 (s, 9H, H29), 1.57 (s, 3H, H1), 1.55 (s, 3H, H2), 1.06 – 0.99 (m, 2H, H32), 0.10 – 0.06 (m, 9H, H33); ¹³C NMR (101 MHz, CDCl₃) δ 170.4 (C11), 165.7 (C10), 160.0 (C18), 149.5 (C12), 149.4(C27), 137.0(C35), 136.9 (C21) 136.5 (C3), 136.0 (C23), 135.6 (C16), 129.5 (2C24), 128.8

(2C36), 128.5 (C26), 128.4 (2C25), 128.0 (C38), 127.9 (2C37), 127.56 (C15), 119.2 (C20), 117.8 (C4), 113.5 (C14), 112.9 (C19), 100.6 (C17), 95.9 (C13) 93.3 (C30), 83.7 (C28), 77.9 (C22), 68.2 (C6+C34), 67.2 (C31), 50.5 (C9), 34.9 (C7), 32.4 (C5), 27.9 (3C29), 26.0 (C1), 22.9 (C8), 18.2 (C2), 18.1 (C32), -1.6 (3C33); HRMS (ESI) calculated for $C_{46}H_{59}N_3O_8SiNa$ $[M+Na]^+$ 832.3969, found 832.3951.

(*Z*)-**239**: R_f: 0.42 (Pet. ether/EtOAc, 1:1); $[\alpha]_D^{20.5}$: -44 (*c* 0.58, CHCl₃); FTIR (ATR) ν_{max} 2954, 1731, 1692, 1628, 1552, 1372, 1321, 1251, 1221, 1156, 1083, 1007, 856, 837, 749, 697; ¹H NMR (400 MHz, CDCl₃) δ 10.18 (s, 1H, NH), 8.00 (s, 1H, H15), 7.83 (s, 1H, H17), 7.54 – 7.28 (m, 11H, H20, H24, H25, H26, 36, H37, H38), 7.01 (dd, *J* 8.6, 2.3, 1H, H19), 5.92 (s, 1H, H13), 5.27 (d, *J* 6.7, 1H, H30a), 5.15 (s, 2H, H34), 5.10 (t, *J* 7.5, 1H, H4), 5.01 (d, *J* 11.2, 1H, H22a), 4.90 (d, *J* 6.7, 1H, H30b), 4.92 – 4.86 (d, *J* 11.2, 1H, H22b), 3.84 – 3.72 (m, 1H, H31a), 3.72 – 3.65 (m, 1H, H9a), 3.64 – 3.48 (m, 2H, H31b, H9b), 3.16 (dd, *J* 14.7, 7.6, 1H, H5a), 2.81 (dd, *J* 14.7, 7.2, 1H, H5b), 2.50 (dd, *J* 12.7, 5.7, 1H, H7a), 2.04 (td, *J* 12.7, 6.6, 1H, H7b), 1.81 (s, 3H, H1), 1.78 – 1.71 (m, 2H, H8), 1.68 (s, 9H, H29), 1.67 (s, 3H, H2), 1.04 – 0.93 (m, 1H, H32a), 0.87 – 0.77 (m, 1H, H32b), -0.04 (s, 9H, H33); ¹³C NMR (101 MHz, CDCl₃) δ 171.6 (C11), 164.8 (C10), 157.2 (C18), 149.8 (C27), 145.4 (C12), 137.1 (C35), 136.7 (C3), 135.8 (C23), 135.6 (C16), 129.3 (2C24), 128.6 (2C36), 128.5 (C26), 128.4 (2C25), 128.0 (C38), 127.6 (2C37), 124.6 (C15), 123.7 (C21), 118.9 (C20), 117.5 (C4), 113.4 (C14), 103.3 (C19), 112.8 (C13), 100.8 (C17), 92.2 (C30), 83.9 (C28), 77.8 (C22), 70.5 (C6+C34), 67.51 (C31), 52.2 (C9), 35.1 (C7), 31.5 (C5), 28.2 (3C29), 26.5 (C1), 23.2 (C8), 18.3 (C2), 17.9 (C32), -1.6 (3C33); HRMS (ESI) calculated for $C_{46}H_{59}N_3O_8SiNa$ $[M+Na]^+$ 832.3969, found 832.4003.

***tert*-butyl 6-(benzyloxy)-3-(((8a*R*)-2-(benzyloxy)-3-hydroxy-8a-(3-methylbut-2-en-1-yl)-1,4-dioxooctahydropyrrolo[1,2-*a*]pyrazin-3-yl)methyl)-1*H*-indole-1-carboxylate (**228**)**

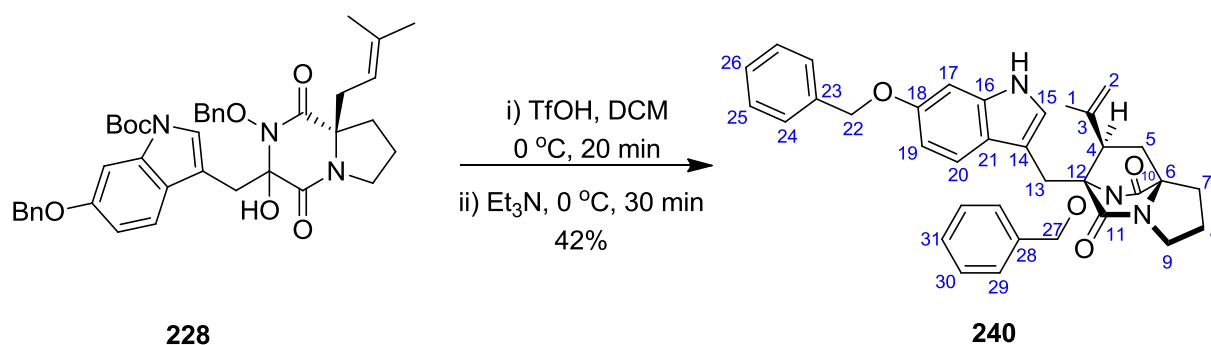


The general procedure for SEM cleavage and cyclization (page 147) was followed using mixture (*dr.* 2.8:1.0) of SEM ether **239** (340 mg, 0.42 mmol), CBr₄ (27 mg, 0.08 mmol, 0.2 equiv) and *i*-PrOH (15 mL). The residue was purified by flash column chromatography (Pet. ether/EtOAc, 4:1) to afford a single diastereoisomer of hydroxy-DKP **228** (130 mg, 45%) as a light yellow oil.

R_f: 0.51 (Pet. ether/EtOAc, 1:1); [α]_D²¹: +36 (*c* 0.9, CHCl₃); FTIR (ATR) ν_{max} 3420, 2900, 1805, 1662, 1324, 1249, 1233, 1189, 1112, 1089, 1055, 980, 749, 697 ; ¹H NMR (400 MHz, CDCl₃) δ 7.83 (s, 1H, H17), 7.69 (dd, *J* 7.7, 1.6, 2H, H20), 7.53 – 7.35 (m, 9H, H24, H25, H26, H29, H30, H31), 7.34 (s, 1H, H15), 6.93 (dd, *J* 8.7, 2.3, 1H, H19), 5.22 (d, *J* 9.1, 1H, H27a), 5.13 (s, 2H, H22), 5.12 (d, *J* 9.1, 1H, H27b), 5.11 – 5.07 (t, *J* 8.3, 1H, H4), 4.48 (s, 1H, OH), 3.71 (d, *J* 13.8, 1H, H13a), 3.48 (d, *J* 13.8, 1H, H13b), 3.35 (ddd, *J* 12.3, 9.8, 6.1, 1H, H9a), 3.16 (ddd, *J* 12.3, 10.2, 5.0, 1H, H9b), 2.47 (dd, *J* 14.2, 8.3, 1H, H5a), 2.22 (dd, *J* 14.2, 7.0, 1H, H5b), 1.84 – 1.79 (m, 1H, H7a), 1.77 (s, 3H, H1), 1.75 – 1.69 (m, 1H, H8a), 1.67 (s, 9H, H34), 1.59 (s, 3H, H2), 1.13 – 0.97 (m, 1H, H8b), 0.72 (dt, *J* 12.3, 10.2, 1H, H7b); ¹³C NMR (101 MHz, CDCl₃) δ 165.3 (C10), 164.6 (C11), 157.0 (C18), 149.6 (C32), 137.5 (C3), 137.1 (C23), 136.0 (C16), 135.6 (C28), 129.4 (2xAr, CH), 128.7 (Ar, CH), 128.5 (2xAr,

CH), 128.4 (2xAr, CH), 127.9 (Ar, CH), 127.6 (2xAr, CH), 125.6 (C15), 124.0 (C21), 120.4 (C20), 117.2 (C4), 112.8 (C14), 112.5 (C19), 100.2 (C17), 90.9 (C12), 83.6 (C33), 78.7 (C27), 70.4 (C22), 67.7 (C6), 44.2 (C9), 36.3 (C5), 33.8 (C7), 33.6 (C13), 28.2 (3C34), 26.0 (C1), 19.0 (C8), 18.1 (C2); HRMS (ESI) calculated for $C_{40}H_{45}N_3O_7Na$ $[M+Na]^+$ 702.3155, found 702.3168.

(6*R*,7*R*,8*aR*)-10-(benzyloxy)-6-((6-(benzyloxy)-1*H*-indol-3-yl)methyl)-7-(prop-1-en-2-yl)tetrahydro-1*H*-6,8*a*-(epiminomethano)indolizine-5,9(6*H*)-dione (240**)**

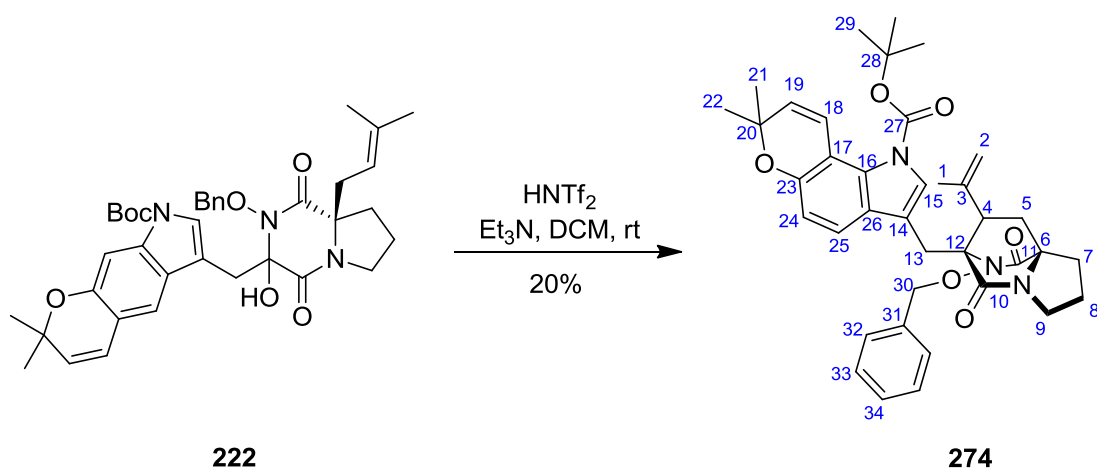


The general procedure for cationic cyclisation (page 148) was followed using hydroxy-DKP **228** (32 mg, 0.05 mmol) in dry DCM (2.0 mL). TfOH (10 μ L, 0.12 mmol, 2.5 equiv) was added at 0 °C and the reaction mixture was stirred for 20 min before Et₃N (65 μ L, 0.47 mmol, 5.0 equiv) was added. The residue was purified by flash column chromatography on silica gel (Pet. ether/EtOAc, 1:1) to afford **240** (11 mg, 42%) as a yellow oil.

R_f: 0.25 (Pet. ether/EtOAc, 1:2); $[\alpha]_D^{22}$: -28 (*c* 0.4, CHCl₃); FTIR (ATR) ν_{\max} 2955, 1678, 1627, 1453, 1366, 1262, 1164, 1014, 907, 747, 696, 667; ¹H NMR (400 MHz, CDCl₃) δ 7.99 (s, 1H, NH), 7.60 – 7.11 (m, 12H, Ar, CH), 7.00 – 6.78 (m, 2H, Ar, CH), 5.12 (s, 2H, H22), 4.80 (d, *J* 8.5, 1H, H27a), 4.78 (s, 1H, H2a), 4.67 (s, 1H, H2b), 3.91 (d, *J* 8.4, 1H, H27b), 3.65 (td, *J* 6.9, 2.6, 2H, H9), 3.41 (d, *J* 2.6, 2H, H13), 3.11 (dd, *J* 10.2, 6.1, 1H, H4), 2.82 (dt, *J* 13.5, 6.9, 1H, H7a), 2.25 (dd, *J* 13.3, 10.2, 1H, H5a), 2.16 – 2.03 (m, 2H, H8), 2.00 – 1.85 (m, 1H, H7b), 1.81 (dd, *J* 13.3, 6.1, 1H, H5b), 1.56 (s, 3H,

H1); ^{13}C NMR (101 MHz, CDCl_3) δ 172.1 (C10), 167.3 (C11), 155.6 (C18), 142.3 (C3), 137.6 (C23), 135.9 (C16), 134.2 (C28), 130.0 (2xAr, CH), 128.7 (Ar, CH), 128.6 (2xAr, CH), 128.2 (2xAr, CH), 127.8 (Ar, CH), 127.4 (2xAr, CH), 123.6 (C21), 123.2 (C15), 119.7 (C20), 116.0 (C2), 110.4 (C14), 110.0 (C19), 95.8 (C17), 78.7 (C27), 74.3 (C12), 70.7 (C22), 66.7 (C6), 50.2 (C4), 44.2 (C9), 37.8 (C5), 29.4 (C7), 24.2 (C8), 23.7 (C13), 19.4 (C1); HRMS (ESI) calculated for $\text{C}_{35}\text{H}_{35}\text{N}_3\text{O}_4\text{Na}$ $[\text{M}+\text{Na}]^+$ 584.2525, found 584.2520.

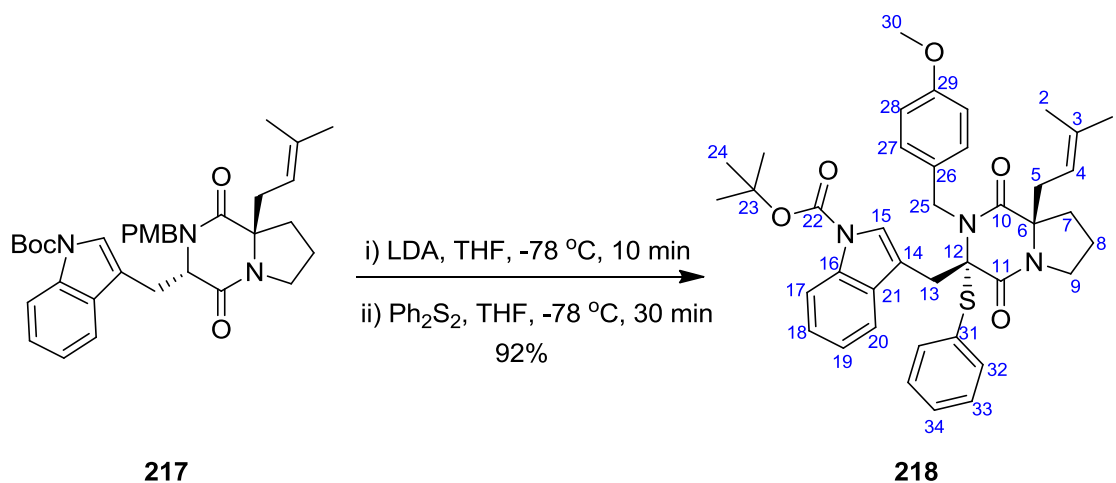
Bridged DKP (**274**)



HNTf₂ (26 μL of 0.5 M solution in DCM, 0.04 mmol) was added to a solution of **222** (22 mg, 0.04 mmol) in DCM (0.5 mL) at $-10\text{ }^\circ\text{C}$. The ice bath was removed and the mixture was stirred until no starting material was shown by TLC analysis. Then DCM (10 mL) was added and the crude mixture was washed with NaHCO_3 (7 mL) and brine (5 mL), dried over MgSO_4 before being concentrated under reduced pressure. The crude product was purified by flash column chromatography on silica gel (eluent: Pet. ether/EtOAc, 1:1) and semi prep-HPLC (H_2O :MeCN gradient 40.14 min) to give **274** (4 mg, 0.30 mmol, 20%) as a light yellow oil.

R_f: 0.34 (Pet. ether/EtOAc, 1:2); [α]_D²¹ - 14 (*c* 0.35, CHCl₃); FTIR (ATR) ν_{max} 2974, 2926, 2854, 1792, 1693, 1589, 1397, 1350, 1277, 1155, 1119, 980, 812, 754; ¹H NMR (300 MHz, CDCl₃) δ 7.56 (s, 1H, Ar, CH), 7.25 – 7.15 (m, 4H, Ar, CH), 7.04 (d, *J* 9.9 Hz, 1H, H19), 6.92 (d, *J* 6.6 Hz, 2H, Ar, CH), 6.78 (d, *J* 8.4 Hz, 1H, Ar, CH), 5.62 (d, *J* 9.9 Hz, 1H, H18), 4.91 (d, *J* 8.6 Hz, 1H, H30a), 4.78 (s, 1H, H2a), 4.68 (s, 1H, H2b), 4.14 (d, *J* 8.6 Hz, 1H, H30b), 3.70 – 3.60 (m, 2H, H9), 3.27 (s, 2H, H13), 3.11 (dd, *J* 10.2, 6.1 Hz, 1H, H4), 2.83 (dt, *J* 13.4, 6.9 Hz, 1H, H7a), 2.28 (dd, *J* 13.3, 10.2 Hz, 1H, H5a), 2.15 – 2.04 (m, 2H, H8), 1.92 (dd, *J* 13.4, 7.0 Hz, 1H, H7b), 1.81 (dd, *J* 13.3, 6.1 Hz, 1H, H5b), 1.57 (s, 9H, H29), 1.52 (s, 3H, CH₃), 1.50 (s, 3H, CH₃), 1.27 (s, 3H, CH₃); *Due to insufficient amount of material we were not able to run* ¹³C NMR to complete the assignment; HRMS (ESI) calculated for C₃₈H₄₃N₃O₆Na [M+Na]⁺ 660.3050, found 660.3052.

***tert*-butyl 3-(((3*S*,8*aR*)-2-(4-methoxybenzyl)-8*a*-(3-methylbut-2-en-1-yl)-1,4-dioxo-3-(phenylthio)octahydropyrrolo[1,2-*a*]pyrazin-3-yl)methyl)-1*H*-indole-1-carboxylate (**218**)**

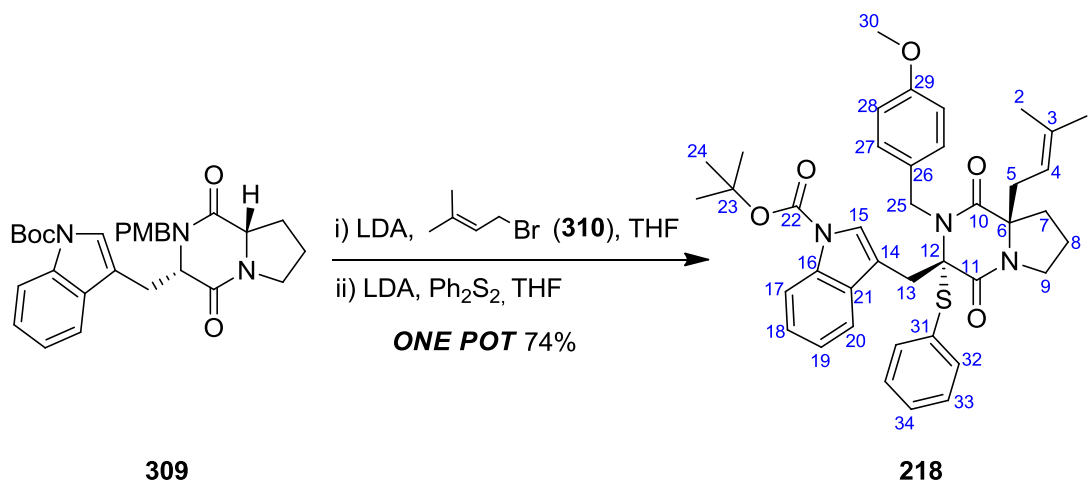


LDA (569 μ L of 0.8 M in Pet. Ether, 0.46 mmol, 1.3 equiv) was added to a solution of DKP **217** (200 mg, 0.35 mmol) in dry THF (10 mL) at -78 °C. After 10 min, a solution of Ph₂S₂ (152 mg, 0.70 mmol, 2.0 equiv) in THF (3 mL) was then added and the reaction mixture was stirred for an additional 30 min. The reaction was quenched at -78 °C by addition of 2 mL of water and was allowed to warm up

to rt. EtOAc (15 mL) was added and the organic phase was washed with saturated $\text{NH}_4\text{Cl}_{\text{aq}}$ (7 mL) and brine (7 mL) dried over MgSO_4 , and concentrated. The crude material was purified by flash column chromatography on silica gel (eluent: Pet. ether/EtOAc, 2:1) to give **218** (220 mg, 0.32 mmol, 92%) as a light yellow solid.

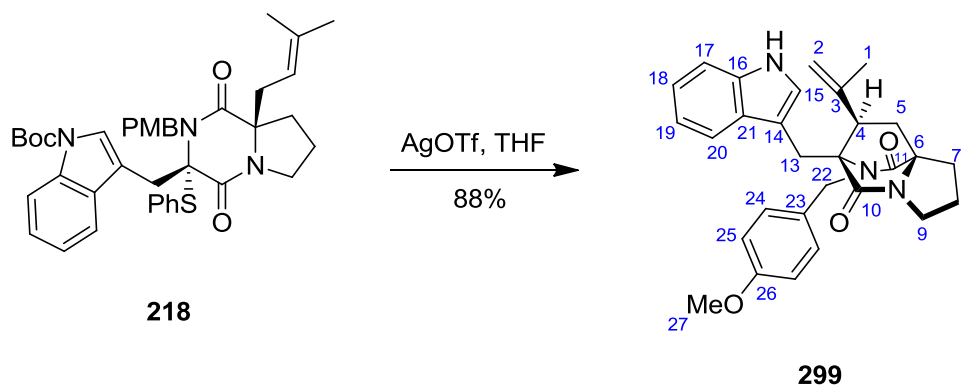
R_f: 0.58 (Pet. ether/EtOAc, 1:4); mp: 78-79 °C; $[\alpha]_D^{18.5}$ - 26 (*c* 0.70, CHCl_3); FTIR (ATR) ν_{max} 2979, 2934, 1733, 1658, 1611, 1513, 1453, 1368, 1307, 1271, 1250, 1156, 1109, 1080, 1035, 1017, 853, 813, 750; ^1H NMR (400 MHz, CDCl_3) δ 7.90 (d, *J* 8.1, 1H, H17), 7.48 (d, *J* 7.7, 1H, H20), 7.39 (d, *J* 6.7, 2H, H32), 7.28 (t, *J* 7.0, 1H, H34), 7.24 (d, *J* 7.4, 2H, H33), 7.20 (d, *J* 8.7, 2H, H27), 7.11 (t, *J* 7.5, 1H, H18), 7.04 (t, *J* 7.5, 1H, H19), 6.65 (d, *J* 8.7, 2H, H28), 6.53 (s, 1H, H15), 5.42 (d, *J* 15.2, 1H, H25a), 4.85 (d, *J* 15.2, 1H, H25b), 4.74 – 4.70 (m, 1H, H4), 3.83 (d, *J* 15.0, 1H, H13a), 3.66 (s, 3H, H30), 3.42 (ddd, *J* 12.6, 9.8, 6.9, 1H, H9a), 3.33 (d, *J* 15.0, 1H, H13b), 2.98 (ddd, *J* 12.6, 10.4, 4.2, 1H, H9b), 1.84 (dd, *J* 14.7, 8.2, 1H, H5a), 1.65 – 1.60 (m, 2H, H5b, H7), 1.43 (s, 12H, H24, H2), 1.40 – 1.31 (m, 1H, H8a), 1.29 – 1.14 (m, 1H, H8b), 1.12 (s, 3H, H1), 0.46 – 0.37 (m, 1H, H7b); ^{13}C NMR (101 MHz, CDCl_3) δ 170.0 (C10), 162.0 (C11), 158.8 (C29), 149.2 (C22), 137.4 (2C32), 134.9 (C3), 134.7 (C21), 130.6 (C16), 130.2 (C34), 130.1 (2C28), 129.7 (C31), 129.7 (C26), 129.1 (2C33), 125.6 (C15), 124.2 (C18), 122.5 (C19), 120.1 (C20), 118.0 (C4), 114.6 (C17), 114.0 (2C27), 113.8 (C14), 83.5 (C12), 83.3 (C23), 66.7 (C6), 55.1 (C30), 47.3 (C25), 44.8 (C9), 38.5 (C5), 32.0 (C7), 32.0 (C13), 28.0 (3C24), 25.8 (C2), 18.9 (C8), 17.5 (C1); HRMS (ESI) calculated for $\text{C}_{40}\text{H}_{45}\text{N}_3\text{O}_5\text{NaS}$ $[\text{M}+\text{Na}]^+$ 702.2978, found 702.2980.

tert-butyl 3-(((3*S*,8*aR*)-2-(4-methoxybenzyl)-8*a*-(3-methylbut-2-en-1-yl)-1,4-dioxo-3-(phenylthio)octahydropyrrolo[1,2-*a*]pyrazin-3-yl)methyl)-1*H*-indole-1-carboxylate (218**)**



LDA (0.27 mL of 0.8 M in Pet. ether, 0.22 mmol, 1.1 equiv) was added to a solution of DKP **309** (100 mg, 0.20 mmol) in dry THF (5 mL) at -78 °C and the mixture was stirred for 10 min. Prenyl bromide (23 μ L, 0.20 mmol, 1.0 equiv) was added and the reaction mixture was stirred for 30 min before LDA (0.35 μ L of 0.8 M in Pet. ether, 0.28 mmol, 1.4 equiv) was added at -78 °C. The mixture was stirred for additional 10 min and a solution of Ph₂S₂ (86 mg, 0.40 mmol, 2.0 equiv) in THF (3 mL) was then added. After 30 min the crude was quenched at -78 °C by addition of 1mL of water and was allowed to warm up to rt. EtOAc (15 mL) was added and the crude was washed with saturated NH₄Cl_{aq} (10 mL), brine (10 mL) dried over MgSO₄, and concentrated. The crude material was purified by flash column chromatography on silica gel (eluent: Pet. ether/EtOAc, 2:1) to give **218** (99 mg, 0.15 mmol, 74%) as a light yellow solid. *For full assignment of 218 see page 161*

Bridged DKP (**299**)

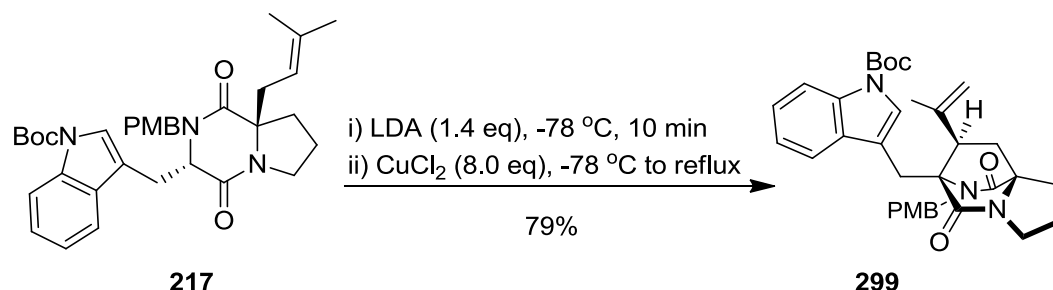


Silver triflate (190 mg, 0.51 mmol, 1.5 equiv) was added to a solution of **218** (230 mg, 0.34 mmol) in THF (10 mL) at -10 °C. After stirring the solution for 1 h, 1.0 M NaOH (5 mL) was added. The phases were separated and the aqueous phase was extracted with CH₂Cl₂ (10 mL). The combined organic extracts were washed with brine (5 mL), dried over MgSO₄ and the solvent was evaporated under reduced pressure. The crude product was purified by flash column chromatography on silica gel (eluent: Pet. ether/EtOAc, 1:1) to give **299** (170 mg, 0.30 mmol, 88%) as a light yellow foam.

R_f: 0.21 (Pet. ether/EtOAc, 1:1); [α]_D²¹ - 54 (*c* 1.2, CHCl₃); FTIR (ATR) ν_{max} 3318, 2926, 1677, 1612, 1512, 1440, 1394, 1247, 1177, 1100, 1030, 804; ¹H NMR (400 MHz, CDCl₃) δ 8.21 (s, 1H, NH), 7.60 (d, *J* 7.5, 1H, H17), 7.32 (d, *J* 7.4, 1H, H20), 7.22 – 7.14 (m, 2H, H18, H19), 7.09 (s, 1H, H15), 6.88 (d, *J* 8.7, 2H, H25), 6.72 (d, *J* 8.7, 2H, H24), 4.75 (s, 1H, H2a), 4.73 (d, *J* 15.3, 1H, H22a), 4.55 (s, 1H, H2b), 4.31 (d, *J* 15.3, 1H, H22b), 3.77 (s, 3H, H27), 3.70 – 3.57 (m, 2H, H9), 3.47 (d, *J* 17.4, 1H, H13a), 3.30 (d, *J* 17.4, 1H, H13b), 3.03 – 2.80 (m, 2H, H7a, H4), 2.22 (dd, *J* 13.4, 10.3, 1H, H5a), 2.15 – 2.00 (m, 2H, H8), 2.00 – 1.88 (m, 1H, H7b), 1.84 (dd, *J* 13.4, 5.4, 1H, H5b), 1.60 (s, 3H, H1); ¹³C NMR (101 MHz, CDCl₃) δ 173.9 (C11), 167.8 (C10), 158.7 (C26), 143.0 (C3), 135.8 (C16), 130.5 (C23), 128.6 (2C25), 128.1 (C21), 123.5 (C15), 122.1 (C18), 119.4 (C19), 118.4 (C17), 116.2 (C2), 113.7 (2C24), 111.1 (C20), 110.2 (C14), 69.6 (C12), 66.2 (C6), 55.3 (C27), 52.5 (C4), 45.8 (C22),

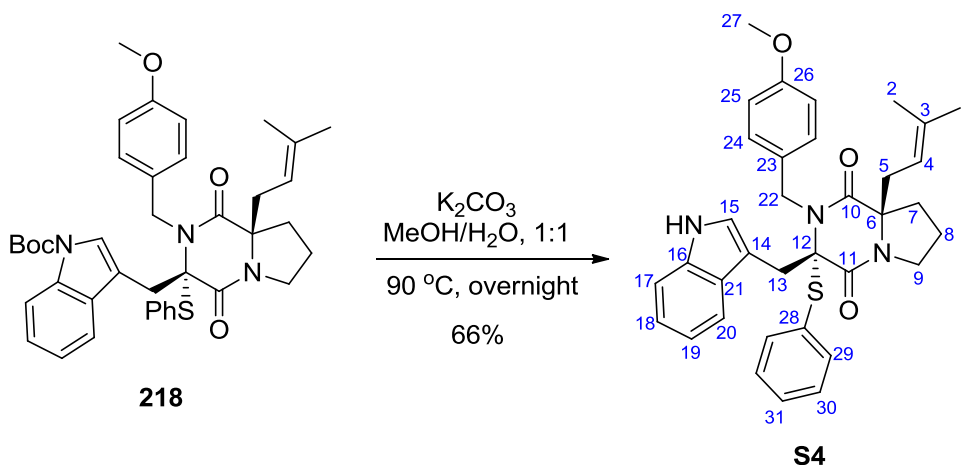
44.5 (C9), 36.6 (C5), 30.0 (C7), 25.3 (C13), 24.5 (C8), 19.1 (C1); HRMS (ESI) calculated for $C_{29}H_{31}N_3O_3Na$ $[M+Na]^+$ 492.2263, found 492.2260.

Bridged DKP (**299**) via Oxidative Radical Cyclisation



A condenser and an additional funnel containing CuCl_2 (245 mg, 1.82 mmol, 8.0 equiv) were connected to a three neck round bottom flask under argon atmosphere. Solution of DKP **217** (130 mg, 0.23 mmol) in dry THF (7 mL) was added to the flask and the solution was cooled to -78°C . LDA (0.40 mL of 0.8 M in Pet. ether, 0.32 mmol, 1.4 equiv) was then added and the mixture was stirred for 10 min. CuCl_2 was added portion-wise over 10 min and the solution immediately turned to dark blue-green. The cool bath was removed and the mixture was stirred for 15 min at rt and then gradually heated to reflux. After 1 h the oil bath was removed and the crude mixture was allowed to cool to rt. EtOAc (15 mL) was added and the crude was washed with 10 mL H_2O , saturated $\text{NH}_4\text{Cl}_{\text{aq}}$ (2×10 mL), brine (10 mL) dried over MgSO_4 , and concentrated. The crude product was purified by flash column chromatography on silica gel (eluent: Pet. ether/EtOAc, 1:1) to give **299** (170 mg, 0.30 mmol, 88%) as a light yellow foam. *For full assignment of 299 see page 164*

(3*S*,8*aR*)-3-((1*H*-indol-3-yl)methyl)-2-(4-methoxybenzyl)-8*a*-(3-methylbut-2-en-1-yl)-3-(phenylthio)hexahydropyrrolo[1,2-*a*]pyrazine-1,4-dione (S4)

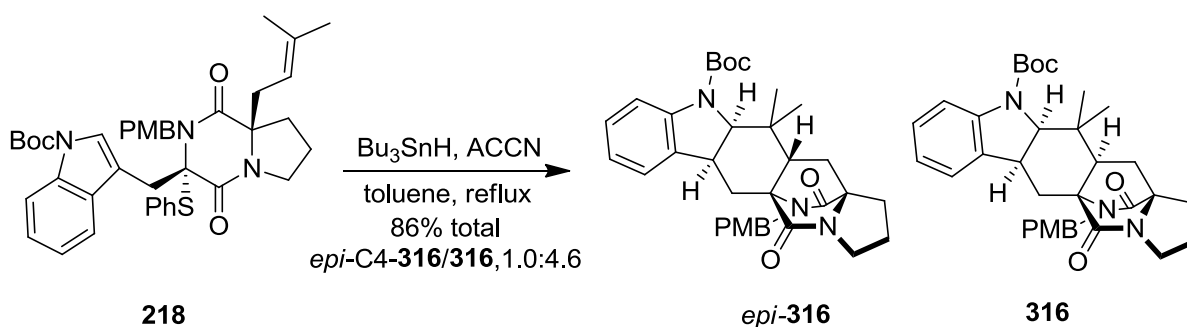


TFA (37 mg, 0.15 mmol, 1.5 equiv) was added to a solution of **218** (50 mg, 0.10 mmol) in DCM (2 mL) at rt. The crude material was stirred overnight before being washed with NaHCO₃ (5 mL) and brine (5 mL) and the organic extracts were dried over MgSO₄ and the solvent was evaporated under reduced pressure. The crude product was purified by flash column chromatography on silica gel (eluent: Pet. ether/EtOAc, 1:1) to give **S4** (25 mg, 0.04 mmol, 66%) as a light yellow foam.

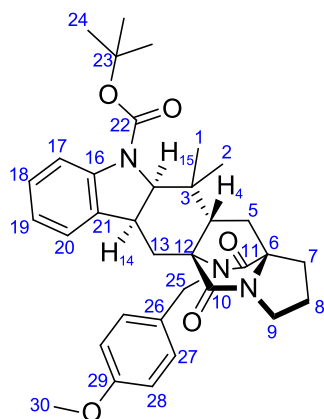
R_f: 0.19 (Pet. ether/EtOAc, 1:1); [α]_D²¹ - 61 (*c* 0.55, CHCl₃); FTIR (ATR) ν_{max} 3313, 2964, 1772, 1651, 1512, 1439, 1246, 1177, 1034, 809, 742, 693; ¹H NMR (300 MHz, CDCl₃) δ 7.88 (s, 1H, NH), 7.79 (d, *J* 6.8, 1H, H17), 7.55 – 7.42 (m, 4H, H29, H25), 7.39 – 7.29 (m, 3H, H31, H30), 7.17 (d, *J* 6.6, 1H, H20), 7.11 – 6.99 (m, 2H, H18, H19), 6.86 (d, *J* 8.7, 2H, H24), 5.61 (s, 1H, H15), 5.57 (d, *J* 15.1, 1H, H22a), 5.05 (d, *J* 15.1, 1H, H22b), 4.62 – 4.35 (m, 1H, H4), 4.01 (d, *J* 14.7, 1H, H13a), 3.82 (s, 3H, H27), 3.44 (d, *J* 14.7, 1H, H13b), 3.44 – 3.35 (m, 1H, H9a), 2.96 (ddd, *J* 12.6, 10.3, 4.2, 1H, H9b), 1.78 – 1.62 (m, 1H, H7a), 1.49 (s, 3H, H1), 1.46 – 1.38 (m, 1H, H5a), 1.38 – 1.32 (m, 1H, H8a), 1.30 – 1.25 (m, 1H, H5b), 1.25 – 1.20 (m, 1H, H8b), 1.13 (s, 3H, H2), 0.65 (dt, *J* 12.8, 10.4, 1H, H7b); ¹³C NMR (101 MHz, CDCl₃) δ 170.5 (C10), 162.3 (C11), 159.1 (C26), 137.2 (2C29), 135.5 (C16),

134.6 (C3), 131.2 (C28), 131.1 (2C25), 130.2 (C23), 130.0 (C31), 129.0 (2C30), 127.7 (C21), 125.0 (C15), 122.0 (C19), 120.6 (C17), 119.6 (C18), 118.1 (C4), 114.0 (2C24), 110.5 (C20), 108.8 (C14), 84.8 (C12), 66.5 (C6), 55.4 (C27), 47.5 (C22), 45.0 (C9), 38.4 (C5), 32.8 (C7), 32.2 (C13), 25.8 (C1), 18.9 (C8), 17.5 (C2); HRMS (ESI) calculated for $C_{35}H_{37}N_3O_3NaS$ $[M+Na]^+$ 602.2453, found 602.2432.

Indolines (**316**) and (*epi*-**316**)

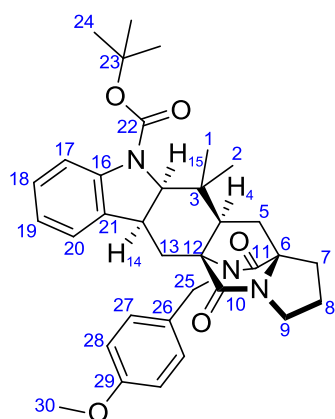


In a two neck flask connected with a condenser **218** (60 mg, 0.09 mmol) was dissolved in degassed toluene (3 mL) under an inert atmosphere. The mixture was warmed to reflux and solutions of 0.009 M ACCN in degassed toluene (6.0 mg, 0.026 mmol, 0.3 equiv) and 0.044 M Bu_3SnH in degassed toluene (35 μL , 0.132 mmol, 1.5 equiv) were added via a syringe pump over 8 h. After completion of the addition the mixture was allow to cooled to rt and the solvents was evaporated under reduced pressure. The crude material was purified by flash column chromatography on silica gel (eluent: Pet. ether/EtOAc, 1:1) to give *epi*-C4-**316** (7 mg, 0.01 mmol, 15%) and **316** (35 mg, 0.06 mmol, 71%).



epi-C4-316

epi-C4-316: Rf: 0.27 (Pet. ether/EtOAc, 1:1); $[\alpha]_D^{20.5} +100$ (*c* 0.32, CHCl₃); FTIR (ATR) ν_{\max} 2924, 1683, 1612, 1513, 1481, 1384, 1367, 1276, 1249, 1172, 11440, 1035, 752, 667; ¹H NMR (400 MHz, CDCl₃) δ 7.39 (d, *J* 7.7, 1H, H17), 7.32 (d, *J* 7.5, 1H, H20), 7.01 (t, *J* 7.7, 1H, H18), 6.91 (d, *J* 8.6, 2H, H27), 6.84 (td, *J* 7.5, 0.9, 1H, H19), 6.74 (d, *J* 8.6, 2H, H28), 5.11 (d, *J* 15.9, 1H, H25a), 4.32 (d, *J* 9.2, 1H, H15), 4.11 (d, *J* 15.9, 1H, H25b), 3.78 (t, *J* 8.0 1H, H14), 3.70 (s, 3H, H30), 3.40 – 3.26 (m, 1H, H9a), 3.21 – 3.03 (m, 2H, H13a+9b), 2.71 (dt, *J* 12.6, 6.1, 1H, H7a), 2.30 (dd, *J* 15.5, 6.0, 1H, H13b), 1.91 – 1.78 (m, 2H, H8), 1.77 – 1.69 (m, 1H, H4), 1.68 – 1.56 (m, 2H, H5a, H7b), 1.55 – 1.49 (m, 1H, H5b), 1.46 (s, 9H, H24), 0.84 (s, 3H, H1), 0.81 (s, 3H, H2); ¹³C NMR (101 MHz, CDCl₃) δ 173.9 (C11), 169.8 (10), 159.0 (C29), 153.2 (C22) 142.7 (C16), 133.6 (C21), 129.3 (C26), 128.6 (C27), 127.2 (C18), 125.6 (C20), 123.0 (C19), 115.4 (C17), 114.2 (C28), 81.2 (C23), 66.2 (C15), 65.6 (C6), 63.2 (C12), 55.3 (C30), 44.9 (C25), 44.4 (C9), 42.5 (C4), 38.0 (C3), 36.6 (C14), 30.8 (C5), 30.2 (C7), 28.5 (C24), 24.6 (C8), 23.5 (C2), 23.3 (C1), 19.4 (C13); HRMS (ESI) calculated for C₃₄H₄₁N₃O₅Na [M+Na]⁺ 594.2944, found 594.2936.

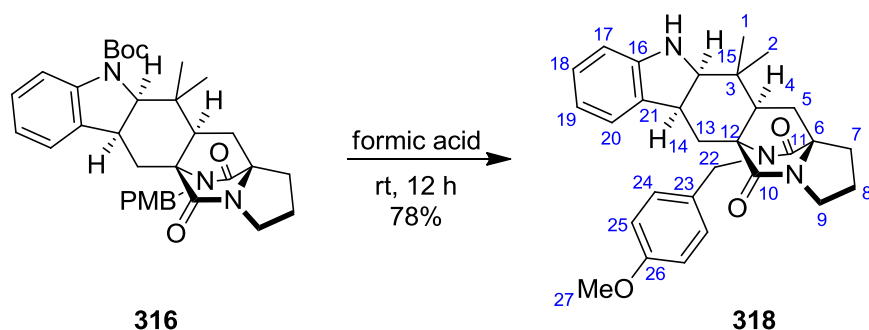


316

316: Rf: 0.20 (Pet. ether/EtOAc, 1:1); $[\alpha]_D^{20.5} +11$ (*c* 1.25, CHCl₃); FTIR (ATR) ν_{\max} 2972, 1680, 1611, 1512, 1478, 1460, 1383, 1351, 1278, 1247, 1172, 1145, 1107, 1054, 1034, 999, 813, 665; ¹H NMR (400 MHz, CDCl₃) δ 7.35 (d, *J* 7.4, 1H, H20), 7.30 (d, *J* 7.7, 1H, H17), 7.04 (d, *J* 8.6, 2H, H27), 7.01 (d, *J* 7.7, 1H, H18), 6.95 (d, *J* 7.4, 3.8, 1H, H19), 6.79 (d, *J* 8.6, 2H, H28), 4.85 (d, *J* 16.0, 1H, H25a), 4.24 (d, *J* 16.0, 1H, H25b), 4.06 (d, *J* 8.2, 1H, H15), 3.73 (s, 3H, H30), 3.63 (t, *J* 8.5, 1H, H14), 3.41 (ddd, *J* 11.8, 6.7, 5.4, 1H, H9a), 3.19 – 3.07 (m, 2H, H9b, H13a), 2.84 – 2.68 (m, 1H, H7a), 2.19 (dd, *J* 14.3,

9.4, 1H, H13b), 2.05 (dd, J 13.2, 10.6, 1H, H5a), 1.89 (dd, J 10.6, 5.4, 1H, H4), 1.87 – 1.82 (m, 2H, H8), 1.76 – 1.62 (m, 2H, H7b, H5b), 1.44 (s, 9H, H24), 0.83 (s, 3H, H2), 0.23 (s, 3H, H1); ^{13}C NMR (101 MHz, CDCl_3) δ 173.3 (C11), 168.8 (C10), 159.0 (C29), 153.3 (C22), 142.6 (C16), 134.6 (C21), 130.5 (C26), 128.0 (C27), 127.0 (C18), 123.8 (C20), 123.0 (C19), 116.0 (C17), 114.4 (C28), 81.2 (C23), 67.79 (C15), 66.2 (C6), 63.5 (C12), 55.3 (C30), 49.0 (C4), 44.4 (C25), 44.3 (C9), 39.5 (C3), 38.5 (C14), 31.8 (C5), 30.3 (C7), 28.6 (C2), 28.4 (C24), 24.5 (C8), 22.3 (C13), 15.7 (C1); HRMS (ESI) calculated for $\text{C}_{34}\text{H}_{41}\text{N}_3\text{O}_5\text{Na}$ $[\text{M}+\text{Na}]^+$ 594.2944, found 594.2950.

Deprotection of Indolines (**318**)

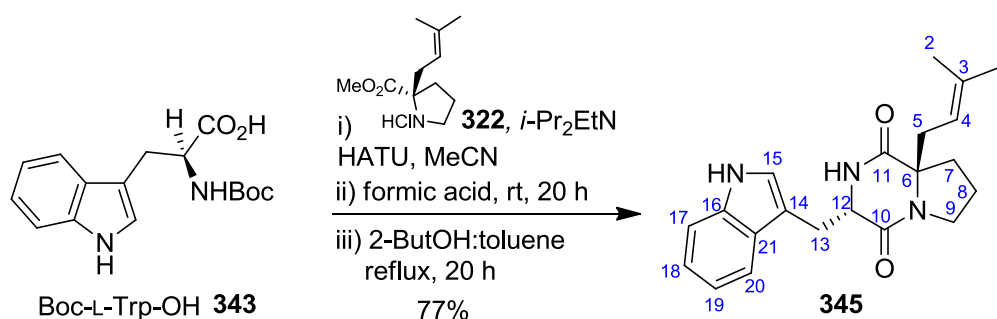


Indoline **316** (29 mg, 0.05 mmol) was diluted in 10 mL formic acid and stirred overnight at rt. Formic acid was then evaporated under reduced pressure and the crude material was purified by flash column chromatography on silica gel (eluent: Pet. ether/EtOAc, 1:2) to give from **318** (19 mg, 0.04 mmol, 78%).

R_f: 0.10 (Pet Ether/EtOAc, 1:1); mp: 233-235 °C; $[\alpha]_D^{20}$ +11 (c 1.8, CHCl_3); FTI (ATR) ν_{max} ^1H NMR (400 MHz, CDCl_3) δ 7.19 (d, J = 8.6 Hz, 2H, H24), 7.01 (td, J = 7.7, 1.0 Hz, 1H, H18), 6.96 (d, J = 7.2 Hz, 1H, H20), 6.90 (d, J = 8.6 Hz, 2H, H25), 6.69 (t, J = 7.2 Hz, 1H, H19), 6.57 (d, J = 7.7 Hz, 1H, H17), 4.89 (d, J = 15.9 Hz, 1H, H22a), 4.56 (d, J = 15.9 Hz, 1H, H22b), 3.79 (s, 3H, H27), 3.66 – 3.58 (m, 2H, H15, H9a), 3.47 (dt, J = 11.4, 7.5 Hz, 1H, H9b), 3.00 – 2.89 (m, 1H, H7a), 2.83 – 2.77 (m, 2H, H13a, H14), 2.23 – 2.12 (m, 2H, H13b, H5a), 2.08 – 1.97 (m, 3H, H8, H4), 1.94 – 1.84 (m,

¹H, H7b), 1.71 (dd, *J* = 12.8, 8.0 Hz, 1H, H5b), 0.94 (s, 3H, H2), 0.77 (s, 3H, H1); *NH* not observed ; ¹³C NMR (101 MHz, CDCl₃) δ 173.1 (C11), 168.7 (C10), 159.0 (C26), 150.4 (C16), 131.0 (C21), 130.3 (C23), 128.3 (2C24), 127.9 (C18), 124.3 (C20), 118.6 (C19), 114.4 (2C25), 109.1 (C17), 68.1 (C15), 66.2 (C6), 64.9 (C12), 55.3 (C27), 51.3 (C4), 44.5 (C22, C9), 38.5 (C14), 35.6 (C3), 32.6 (C5), 30.4 (C7), 29.9 (C2), 25.9 (C13), 24.5 (C8), 17.5 (C1); HRMS (ESI) calculated for C₂₉H₃₃N₃O₃Na [M+Na]⁺ 494.2420, found 494.2402.

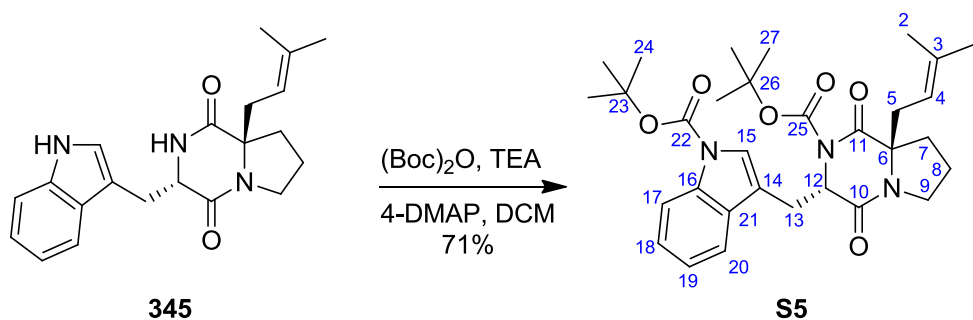
(3*S*,8*aR*)-3-((1*H*-indol-3-yl)methyl)-8*a*-(3-methylbut-2-en-1-yl)hexahydropyrrolo[1,2-*a*]pyrazine-1,4-dione (345)



A solution of Boc-L-Trp-OH **343** (3.9 g, 13.0 mmol) and proline **322** (3.0 g, 13.0 mmol) in MeCN (200 mL), was cooled to 0 °C and HATU (5.4 g, 14.3 mmol, 1.1 equiv), DIPEA (5.1 mL, 28.6 mmol, 2.2 equiv) were added. After 16 h the mixture was concentrated under reduced pressure and the resulting crude oil was dissolved in EtOAc (50 mL) and washed successively with a 1.0 N aqueous potassium hydrogensulfate solution (15 mL), water (15 mL) and brine (15 mL). The organic layer was dried over MgSO₄ and the solvent was evaporated under reduced pressure. The crude material was dissolved in formic acid (100 mL) stirred for 20 h at rt and then the acid was evaporated under reduced pressure. To the residual oil, 2-butanol (150 mL) and toluene (50 mL) were added and the mixture was heated at reflux for 20 h. The solvent evaporated under reduced pressure and the crude product was purified by flash column chromatography on silica gel (EtOAc/MeOH, 9:1) to give **345** (3.5 g, 77%) as a white solid.

R_f: 0.37 (EtOAc/MeOH, 9:1); mp: 182-183 °C; [α]_D²⁰ -81 (*c* 1.8, CHCl₃); FTI (ATR) ν_{max} 3277, 2977, 2925, 1642, 1424, 1299, 1214, 1102, 1010, 741, 665; ¹H NMR (400 MHz, CDCl₃) δ 8.59 (s, 1H, CONH), 7.57 (d, *J* 7.8, 1H, H20), 7.39 (d, *J* 7.8, 1H, H17), 7.23 (t, *J* 7.4, 1H, H18), 7.13 (t, *J* 7.8, 1H, H19), 7.05 (s, 1H, H15), 5.76 (s, 1H, NH), 5.10 – 5.06 (m, 1H, H4), 4.40 (dd, *J* 11.2, 3.1, 1H, H12), 3.85 – 3.81 (m, 1H, H9a), 3.81 – 3.73 (m, 1H, H13a), 3.63 – 3.51 (m, 1H, H9b), 2.86 (dd, *J* 14.8, 11.2, 1H, H13b), 2.45 (qd, *J* 14.2, 8.3, 2H, H5), 2.13 – 2.08 (m, 2H, H7), 2.06 – 1.93 (m, 2H, H8), 1.69 (s, 3H, H1), 1.57 (s, 3H, H2); ¹³C NMR (101 MHz, CDCl₃) δ 171.6 (C11), 165.5 (C10), 137.8 (C16), 136.8 (C21), 126.6 (C3), 123.6 (C15), 122.7 (C18), 119.9 (C19), 118.6 (C20), 117.2 (C4), 111.7 (C17), 109.9 (C14), 68.6 (C6), 54.5 (C12), 45.1 (C9), 36.1 (C5), 34.6 (C7), 28.2 (C13), 26.0 (C1), 20.5 (C8), 17.8 (C2); HRMS (ESI) calculated for C₂₁H₂₅N₃O₂Na [M+Na]⁺ 374.1844, found 374.1849.

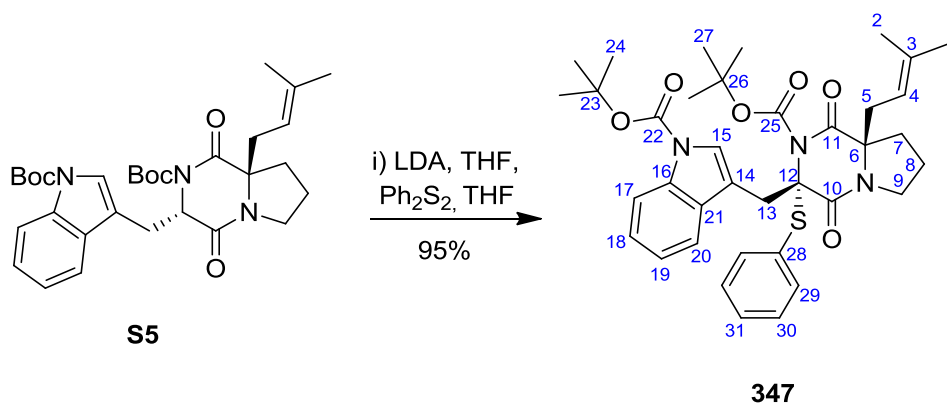
(8a*R*)-tert-butyl 3-((1-(tert-butoxycarbonyl)-1*H*-indol-3-yl)methyl)-8a-(3-methylbut-2-en-1-yl)-1,4-dioxohexahydropyrrolo [1,2-*a*]pyrazine-2(1*H*)-carboxylate (S5)



(Boc)₂O (5.7 g, 26.5 mmol, 3.0 equiv), 4-DMAP (336 mg, 2.65 mmol, 0.3 equiv) and TEA (3.0 mL, 22.1 mmol, 2.5 equiv) was added to a solution of **345** (3.1 g, 8.83 mmol) in DCM (70 mL) was added at rt. After 16 h stirring the crude mixture was washed with NH₄Cl_{aq}, brine and the solvents was evaporated under reduced pressure. The crude material was purified by flash column chromatography on silica gel (eluent: Pet. ether/EtOAc, 1:2) to give **S5** (3.4 g, 71%) as a white solid

R_f: 0.71 (Pet. ether/EtOAc, 2:1); mp: 107-108 °C; [α]_D²³ 120 (*c* 1.0, CHCl₃); FTI (ATR) ν_{\max} 2979, 1732, 1659, 1455, 1368, 1256, 1155, 1082, 748; ¹H NMR (400 MHz, CDCl₃) δ 8.09 (d, *J* 8.2, 1H, H17), 7.49 (d, *J* 7.8, 1H, H20), 7.33 – 7.25 (td, *J* 7.7, 1.0, 1H, H18), 7.26 (s, 1H, H15), 7.23 – 7.15 (td, *J* 7.7, 1.0, 1H, H19), 4.96 – 4.91 (m, 1H, H4), 4.84 (dd, *J* 4.8, 2.4, 1H, H12), 3.63 (ddd, *J* 12.4, 9.8, 6.0, 1H, H9a), 3.56 (dd, *J* 14.5, 2.4, 1H, H13a), 3.47 (dd, *J* 14.5, 4.8, 1H, H13b), 3.28 – 3.16 (m, 1H, H9b), 2.29 (dd, *J* 14.2, 8.5, 1H, H5a), 2.18 (dd, *J* 14.2, 7.2, 1H, H5b), 1.66 (s, 3H, H2), 1.65 (s, 9H, C(CH₃)₃), 1.63 – 1.61 (m, 1H, H8a), 1.61 – 1.59 (m, *J* 4.5, 2.8, 1H, H7a), 1.57 (s, 9H, C(CH₃)₃), 1.52 (s, 3H, H1), 1.27 – 1.15 (m, 1H, H8b), 0.66 – 0.51 (m, 1H, H7b); ¹³C NMR (101 MHz, CDCl₃) δ 169.0 (C11), 164.0 (C10), 151.0 (CO₂C(CH₃)₃), 149.4 (CO₂C(CH₃)₃), 137.4 (C3), 135.2 (C16), 130.4 (C21), 126.0 (C15), 124.7 (C18), 122.5 (C19), 119.8 (C20), 116.5 (C4), 115.0 (C17), 114.1 (C14), 83.7 (CO₂C(CH₃)₃), 83.6 (CO₂C(CH₃)₃), 69.2 (C6), 60.2 (C12), 44.20 (C9), 37.6 (C5), 33.6 (C13), 29.2 (C7), 28.2 (CO₂C(CH₃)₃), 28.1 (CO₂C(CH₃)₃), 26.1 (C1), 19.2 (C8), 17.9 (C2); HRMS (ESI) calculated for C₃₁H₄₁N₃O₆Na [M+Na]⁺ 574.2893, found 574.2886.

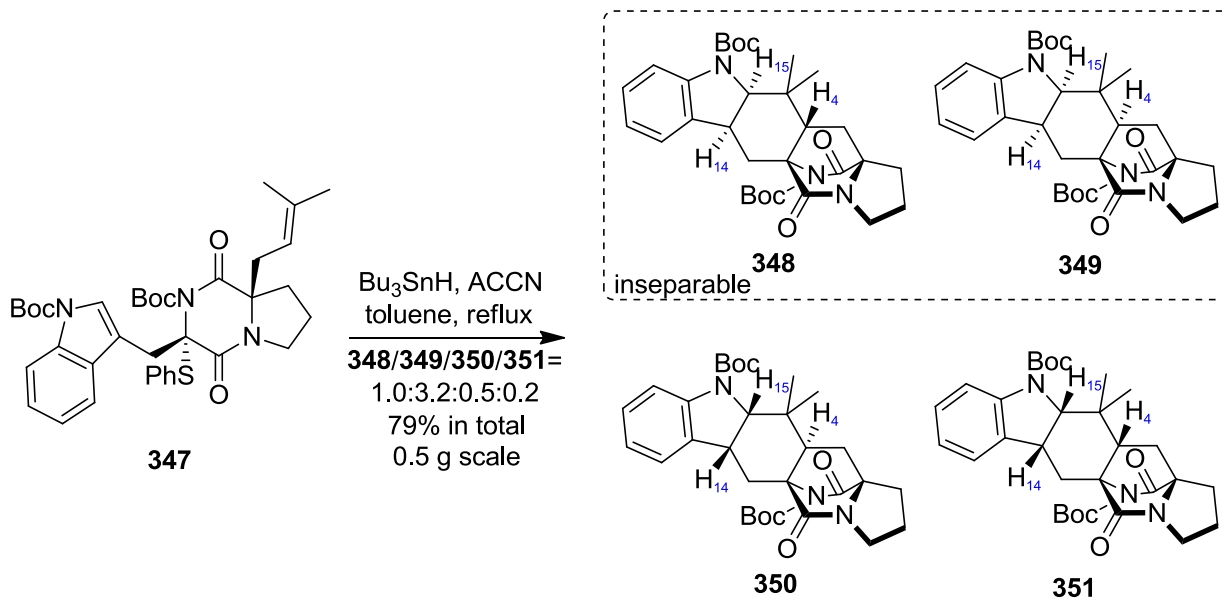
(8a*R*)-tert-butyl 3-((1-(tert-butoxycarbonyl)-1*H*-indol-3-yl)methyl)-8a- (3-methylbut-2-en-1-yl) - 1,4-dioxo-3-(phenylthio)hexahydropyrrolo[1,2-*a*]pyrazine-2(1*H*)-carboxylate (347**)**



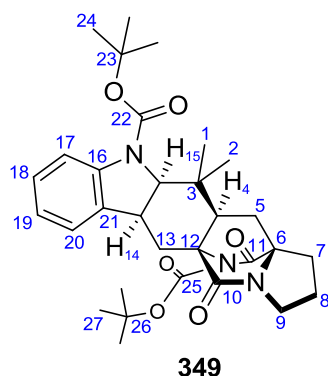
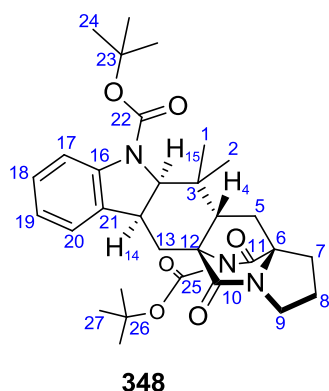
The general procedure (page 161) was followed using **S5** (200 mg, 0.36 mmol) in THF (20 mL), 0.8 M LDA (0.64 mL, 0.51 mmol, 1.4 equiv), Ph₂S₂ (158 mg, 0.73 mmol, 2.0 equiv) in THF (7 mL). The crude material was purified by flash column chromatography on silica gel (eluent: Pet. ether/EtOAc, 1:1) to give **347** (227 mg, 0.34 mmol, 95%) as white solid.

R_f: 0.71 (Pet. ether/EtOAc, 1:2); mp: 102-103 °C; [α]_D²³ 118 (*c* 1.1, CHCl₃); FTI (ATR) ν_{\max} 2978, 1733, 1659, 1453, 1364, 1252, 1148, 1080, 851, 749, 694; ¹H NMR (400 MHz, CDCl₃) δ 8.06 (d, *J* 7.9, 1H, H17), 7.75 (d, *J* 7.4, 1H, H20), 7.64 (d, *J* 7.0, 2H, H29), 7.60 (s, 1H, H15), 7.41 – 7.33 (m, 1H, H31), 7.31 (d, *J* 7.6, 2H, H30), 7.28 – 7.22 (td, *J* 7.7, 1.0, 1H, H18), 7.20 (td, *J* 7.7, 1.0, 1H, H19), 4.53 – 4.49 (m, 1H, H4), 4.10 (d, *J* 14.4, 1H, H13a), 3.91 (d, *J* 14.4, 1H, H13b), 3.37 – 3.23 (m, 1H, H9a), 3.15 – 2.99 (m, 1H, H9b), 1.71 – 1.67 (m, 1H, H7a), 1.64 (s, 9H, OCCH₃), 1.63 (s, 9H, OCCH₃), 1.45 (s, 3H, H1), 1.41 – 1.29 (m, 3H, H8, H5a), 1.06 (s, 3H, H2), 0.91 (dd, *J* 14.8, 7.2, 1H, H5b), 0.86 -0.77 (m, 1H, H7b); ¹³C NMR (101 MHz, CDCl₃) δ 169.2 (C10), 162.1 (C11), 151.7 (CO₂C(CH₃)₃), 149.5 (CO₂C(CH₃)₃), 138.1 (2C29), 135.25 (C16), 134.9 (C3), 130.3 (C28), 130.1 (C31), 130.0 (C21), 128.7 (2C30), 126.5 (C15), 124.6 (C18), 122.7 (C19), 120.7 (C17), 116.9 (C4), 115.0 (C20), 114.5 (C14), 84.7 (CO₂C(CH₃)₃), 83.7 (CO₂C(CH₃)₃), 80.0 (C12), 67.5 (C6), 45.0 (C9), 36.6 (C5), 32.2 (C13), 31.0 (C7), 28.2 (CO₂C(CH₃)₃), 28.0 (CO₂C(CH₃)₃), 25.8 (C1), 18.8 (C8), 17.3 (C2); HRMS (ESI) calculated for C₃₇H₄₅N₃O₆NaS [M+Na]⁺ 682.2927, found 682.2939.

Indolines (348), (349), (350) and (351)

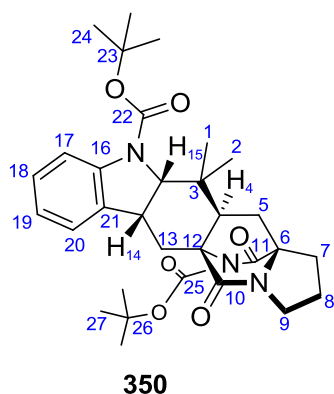


The general procedure for radical cyclisation (page 167) was followed using SPh-DKP **347** (500 mg, 0.76 mmol) in degassed toluene (25 mL), 0.02 M ACCN (93 mg, 0.38 mmol, 0.5 equiv) and 0.06 M Bu_3SnH (326 μL , 1.21 mmol, 1.6 equiv) which were added via of a syringe pump over 8 h. After completion of the addition the mixture was allow to cooled to rt and the solvents was evaporated under reduced pressure. The crude material was purified by flash column chromatography on silica gel (eluent: Pet. ether/EtOAc, 1:1) to give as yellow light yellow foam, **348** and **349** as an inseparable mixture (275 mg, 67%), **350** (38 mg, 9%) and **351** (13 mg, 3%) in 79% total yield and ratio $\text{348/349/350/351} = 1.0:3.2:0.5:0.2$;



Mixture 348*:349: R_f: 0.54 (Pet. ether/EtOAc, 1:2); FTI (ATR) ν_{\max} 2978, 1724, 1690, 1480, 1459, 1383, 1270, 1250, 1146, 750; ^1H NMR (400 MHz, CDCl_3) δ 7.54 (d, J 7.4 Hz, 1H, H20*), 7.47 (d, J 7.5 Hz, 2H, H20), 7.17 – 6.97 (m, 6H, Ar, CH), 4.49 (d,

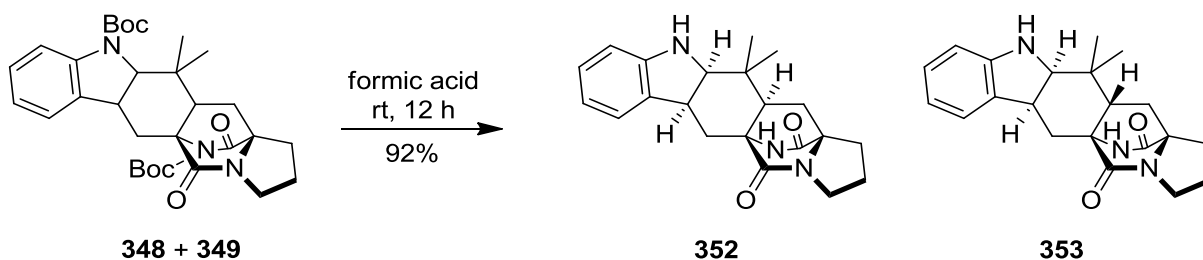
J 9.2 Hz, 1H, H15*), 4.41 (d, J 8.5 Hz, 1H, H15), 3.93 (t, J 7.8 Hz, 2H, H14, H14*), 3.64 – 3.53 (m, 2H, H13a, H9a), 3.53 – 3.43 (m, 2H, H9a*, H13a*), 3.33 – 3.17 (m, 2H, H9b, H9b*), 2.82 – 2.74 (m, 1H, H7a), 2.74 – 2.67 (m, 1H, H7a*), 2.37 (dd, J 10.2, 6.4 Hz, 1H, H4), 2.22 – 2.14 (m, 4H, H5a, H5a*, H13b, H13b*), 1.98 – 1.84 (m, 5H, H8, H8*, H4*), 1.82 – 1.71 (m, 4H, H5b, H5b*, H7b, H7b*), 1.57 (s, 18H, $(\text{CH}_3)_3$, $(\text{CH}_3)_3^*$), 1.56 (s, 9H, $(\text{CH}_3)_3$), 1.55 (s, 9H, $(\text{CH}_3)_3^*$), 1.12 (s, 3H, CH_3^*), 0.99 (s, 3H, CH_3), 0.96 (s, 3H, CH_3^*), 0.37 (s, 3H, CH_3); ^{13}C NMR (101 MHz, CDCl_3) δ 171.0 (C11, C11*), 167.2 (C10, C10*), 153.4 ($\text{COC}(\text{CH}_3)_3$, $\text{COC}(\text{CH}_3)_3^*$), 150.8 ($\text{COC}(\text{CH}_3)_3$, $\text{COC}(\text{CH}_3)_3^*$), 142.7 (C16, C16*), 135.1 (C21, C21*), 127.3 (C18*), 127.1 (C18), 125.4 (C20*), 123.7 (C20), 123.3 (C19), 123.1 (C19*), 16.1 (C17), 115.5 (C17*), 81.2 ($^*\text{C}(\text{CH}_3)_3$), 81.2 ($\text{C}(\text{CH}_3)_3$), 81.2 ($\text{C}(\text{CH}_3)_3$, $^*\text{C}(\text{CH}_3)_3$), 68.0 (C15*), 66.3 (C6), 66.0 (C15*), 65.7 (C6*), 64.1 (C12, C12*), 48.4 (C4), 44.5 (C9), 44.4 (C9*), 41.9 (C4*), 39.4 (C3), 38.2 (C14), 38.0 (C14*), 36.9 (C3*), 31.89 (C5, C5), 30.1 (C7), 30.0 (C7*), 28.5 ($\text{C}(\text{CH}_3)_3$, $(\text{CH}_3)_3^*$, CH_3 , CH_3^*), 28.0 ($\text{C}(\text{CH}_3)_3$), 27.9 ($(\text{CH}_3)_3$), 24.4 (C8*), 24.2 (C8), 23.8 (C13), 21.8 (C13*), 15.6 (CH_3 , CH_3); HRMS (ESI) calculated for $\text{C}_{31}\text{H}_{41}\text{N}_3\text{O}_6\text{Na}$ $[\text{M}+\text{Na}]^+$ 574.2893, found 574.2887.



350: R_f: 0.32 (Pet. ether/EtOAc, 1:2); [α]_D²³ -80.4 (*c* 1.7, CHCl₃); FTI (ATR) ν_{max} 2978, 1724, 1690, 1479, 1458, 1367, 1250, 1146, 848, 750; ¹H NMR (400 MHz, CDCl₃) δ 7.52 (d, *J* 8.0 Hz, 1H, H17), 7.17 (t, *J* 7.7 Hz, 1H, H18), 7.07 (d, *J* 7.3 Hz, 1H, H20), 6.97 (t, *J* 7.4 Hz, 1H, H19), 4.43 (d, *J* 9.3 Hz, 1H, H15), 4.05 – 3.95 (m, 1H, H14), 3.68 (ddd, *J* 11.6, 7.7, 4.0 Hz, 1H, H9a), 3.49 – 3.40 (m, 1H, H9b), 3.36 – 3.21 (m, 2H, H13), 2.77 – 2.68 (m, 1H, H7a), 2.23 (t, *J* 9.3 Hz, 1H, H4), 2.01 – 1.92 (m, 2H, H8a, H5a), 1.93 – 1.83 (m, 1H, H8b), 1.77 – 1.68 (m, 1H, H7b), 1.60 (s, 9H, C(CH₃)₃), 1.56 (s, 9H, C(CH₃)₃), 1.53 – 1.48 (m, 1H, H5b), 0.94 (s, 3H, CH₃), 0.91 (s, 3H, CH₃); ¹³C NMR (101 MHz, CDCl₃) δ 171.0 (C11), 168.0 (C10), 153.4 (COC(CH₃)₃), 150.4 (COC(CH₃)₃), 143.0 (C16), 135.4 (C21), 127.6 (C18), 123.2 (C20), 122.7 (C19), 116.2 (C17), 84.8 (C(CH₃)₃), 81.3 (C(CH₃)₃), 66.2 (C6), 66.1 (C15), 64.6 (C12), 46.7 (C4), 44.6 (C9), 38.0 (C14), 37.6 (C3), 32.9 (C5), 30.4 (C7), 28.4 (C(CH₃)₃), 28.0 (C(CH₃)₃), 24.2 (C8), 24.0 (CH₃), 23.0 (CH₃), 19.8 (C13); HRMS (ESI) calculated for C₃₁H₄₁N₃O₆Na [M+Na]⁺ 574.2893, found 574.2894.

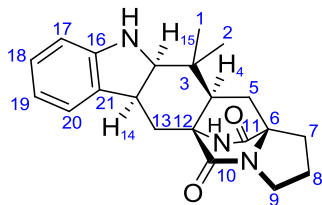
Deprotection of indolines

Indolines **352** and **353**



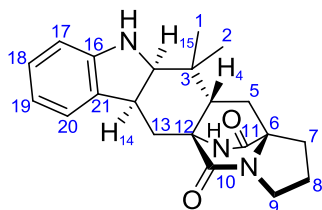
Indoline derivatives **348** and **349** (528 mg, 0.96 mmol) were diluted in 25 mL formic acid and stirred overnight at rt. Formic acid was then evaporated under reduced pressure and the crude material was

purified by flash column chromatography on silica gel (eluent: Pet. ether/EtOAc, 1:3) to give **352** (180 mg, 0.51 mmol, 52%), **353** (130 mg, 0.37 mmol, 38%) as white solids.



352

352: R_f: 0.18 (Pet. ether/EtOAc, 1:2); mp: 246-247 °C; [α]_D²³ -69 (*c* 1.0, CHCl₃); FTI (ATR) ν_{max} 2958, 1676, 1606, 1461, 1395, 1257, 1070, 1022, 746, 665; ¹H NMR (400 MHz, CDCl₃) δ 7.22 (d, *J* 7.2 Hz, 1H, H20), 7.02 (t, *J* 7.6 Hz, 1H, H18), 6.87 (s, 1H, NH), 6.76 (t, *J* 7.2 Hz, 1H, H19), 6.61 (d, *J* 7.6 Hz, 1H, H17), 3.70 – 3.65 (m, 1H, H15), 3.64 – 3.49 (m, 2H, H14, H9a), 3.41 – 3.30 (m, 1H, H9b), 3.12 (dd, *J* 15.1, 7.8 Hz, 1H, H13a), 2.76 (brs, 1H, H7a), 2.16 – 2.04 (m, 1H, H5a), 2.06 – 1.90 (m, 3H, H8, H4), 1.86 – 1.73 (m, 2H, H7b, 13b), 1.73 – 1.62 (m, 1H, H5b), 0.94 (s, 3H, H1), 0.63 (s, 3H, H2); *NH not observed*; ¹³C NMR (101 MHz, CDCl₃) δ 169.0 (C11, C10), 150.2 (C16), 130.9 (C21), 127.7 (C20), 124.1 (C18), 118.9 (C19), 108.9 (C17), 68.7 (C15), 60.1 (C6), 51.0 (C4), 44.2 (C9), 38.5 (C14), 36.5 (C3), 32.2 (C5), 29.5 (C7), 28.9 (C2), 27.3 (C13), 24.6 (C8), 16.6 (C1); HRMS (ESI) calculated for C₂₁H₂₅N₃O₂Na [M+Na]⁺ 374.1844, found 374.1836.

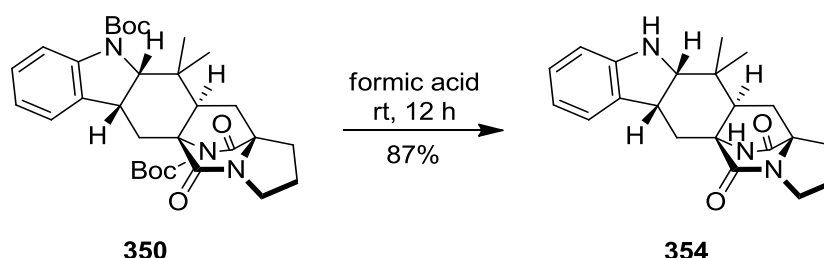


353

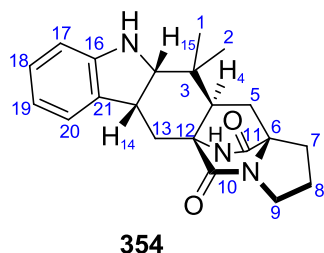
353: R_f: 0.18 (Pet. ether/EtOAc, 1:2); mp: 260-261 °C; [α]_D²¹ -70 (*c* 0.3, CHCl₃); FTI (ATR) ν_{max} 2918, 2849, 1682, 1611, 1482, 1464, 1408, 1321, 1294, 1251, 1122, 1028, 940, 919, 744, 665, 589; ¹H NMR (300 MHz, CDCl₃) δ 7.15 (d, *J* 7.2 Hz, 1H, H20), 7.06 (td, *J* 7.7, 1.2 Hz, 1H, H18), 6.82 (s, 1H, NH), 6.77 (td, *J* 7.2, 0.9 Hz, 1H, H19), 6.70 (d, *J* 7.7 Hz, 1H, H17), 3.80 (brs, 1H, NH) 3.47 (d, *J* 6.9 Hz, 1H, H15), 3.45 (dd, *J* 6.2, 2.0 Hz, 2H, H9), 3.19 (dt, *J* 12.1, 6.1 Hz, 1H, H14), 2.78 (dt, *J* 13.1, 6.5 Hz, 1H, H7a), 2.30 (dd, *J* 10.2, 4.7 Hz, 1H, H4), 2.11 – 2.01 (m, 2H, H7b, H5a), 2.01 – 1.89 (m, 2H, H13), 1.89 – 1.80 (m, 3H, H5b, H8), 1.04 (s, 3H, H2), 1.03 (s, 3H, H1); ¹³C NMR (101

MHz, CDCl₃) δ 173.5 (C11), 169.5 (C10), 149.6 (C16), 134.8 (C21), 127.7 (C18), 123.7 (C20), 119.6 (C19), 110.7 (C17), 70.8 (C15), 66.8 (C6), 60.8 (C12), 53.5 (C3), 44.1 (C9), 40.4 (C4), 35.2 (C14), 32.7 (C5), 29.4 (C7), 29.2 (C8), 27.2 (C2), 24.5 (C13), 22.8 (C1). HRMS (ESI) calculated for C₂₁H₂₅N₃O₂Na [M+Na]⁺ 374.1844, found 374.1848.

Indoline (354)

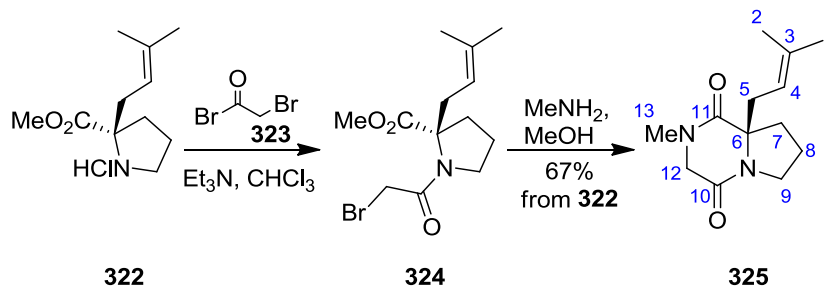


Indoline derivatives **350** (88 mg, 0.16 mmol) was diluted in 15 mL formic acid and stirred overnight at rt. Formic acid was then evaporated under reduced pressure and the crude material was purified by flash column chromatography on silica gel (eluent: EtOAc) to give **354** (50 mg, 0.14 mmol, 87%) as white solid.



R_f: 0.22 (EtOAc); mp: 210-211 °C; [α]_D²³ -17 (*c* 1.0, CHCl₃); FTI (ATR) ν_{max} 2925, 1673, 1610, 1463, 1401, 1368, 1330, 1124, 1017, 746, 665; ¹H NMR (400 MHz, CDCl₃) δ 7.20 (d, *J* 7.5 Hz, 1H, H20), 7.06 (td, *J* 7.7, 1.2 Hz, 1H, H18), 6.77 (td, *J* 7.5, 0.8 Hz, 1H, H19), 6.72 (d, *J* 7.7 Hz, 1H, H17), 6.30 (s, 1H, NH), 3.84 (s, 1H, NH), 3.60 – 3.52 (m, 2H, H14, H9a), 3.44 – 3.32 (m, 2H, H15, H9b), 2.74 (ddd, *J* 12.7, 6.9, 5.4 Hz, 1H, H7a), 2.47 (dd, *J* 10.4, 5.8 Hz, 1H, H4), 2.38 (dd, *J* 13.0, 6.4 Hz, 1H, H13a), 2.12 (dd, *J* 13.3, 10.4 Hz, 1H, H5a), 2.07 – 1.90 (m, 2H, H8), 1.84 – 1.72 (m, 2H, H5b, H7b), 1.22 – 1.13 (m, 1H, H13b), 1.04 (s, 3H, H1), 0.90 (s, 3H, H2); ¹³C NMR (101 MHz, CDCl₃) δ 173.5 (C11), 169.7 (C10), 149.2 (C16), 135.1 (C21), 127.6 (C20), 123.8 (C18), 119.7 (C19), 110.6 (C17), 70.8 (C15), 67.3 (C6), 59.7 (C12), 45.4 (C4), 43.8 (C9), 36.7 (C14), 35.4 (C3), 31.7 (C7,C5), 29.4 (C13), 26.6(C1), 24.6(C8), 20.2 (C2); HRMS (ESI) calculated for C₂₁H₂₅N₃O₂Na [M+Na]⁺ 374.1844, found 374.1851.

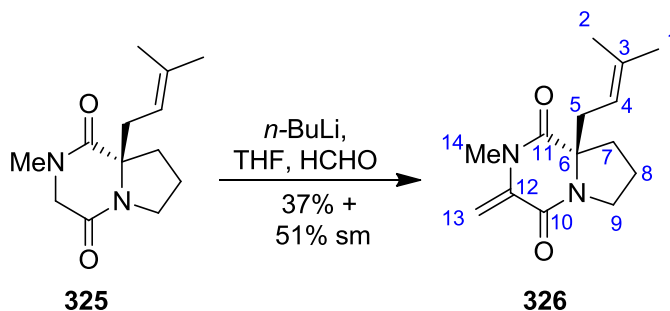
(*R*)-2-methyl-8a-(3-methylbut-2-en-1-yl)hexahydropyrrolo[1,2-*a*]pyrazine-1,4-dione (325)



Proline derivative **322**^{59b} (1.3 g, 5.7 mmol) was dissolved in CHCl_3 (40 mL) and to this was added triethylamine (1.9 mL, 13.7 mmol, 2.4 equiv) at $-10\text{ }^\circ\text{C}$. The reaction mixture was treated with bromoacetyl bromide **323** (1.26 mL, 13. mmol, 2.4 equiv) in chloroform (40 mL). After stirring for 4 hours the reaction was quenched with water (40 mL) and the layers separated. The organic phase was washed with saturated sodium hydrogen carbonate solution (30 mL), brine (30 mL) and the combined organic layers were dried over MgSO_4 and concentrated under reduced pressure. R_f 0.16 (3:1 Pet. ether/EtOAc). The crude material **324** (2.18 g, 5.7 mmol, 1.0 eq) was dissolved in MeOH (20mL) and treated with methylamine solution (28.59 mL of 2 M in methanol, 57.2 mmol, 10.0 equiv) at $0\text{ }^\circ\text{C}$. After 3 hours the reaction mixture was allowed to warm to room temperature and the reaction mixture concentrated under reduced pressure. The crude product was purified by flash column chromatography on silica gel (EtOAc/MeOH, 9:1) to give **325** (0.9 g, 3.8 mmol, 67%) as a white solid.

R_f : 0.12 (EtOAc); mp: $99\text{--}103\text{ }^\circ\text{C}$; $[\alpha]_D^{21}$ -60 (c 0.9, CHCl_3); FTI (ATR) ν_{max} 2953, 2880, 2840, 1660, 1598, 1402, 1385, 1078; ^1H NMR (400 MHz, CDCl_3) δ 5.08 – 5.03 (m, 1H, H4), 4.04 (d, J 17.0, 1H, H12a), 3.79 (dt, J 12.3, 8.4, 1H, H9a), 3.71 (d, J 17.0, 1H, H12b), 3.55 – 3.42 (m, 1H, H9b), 2.94 (s, 3H, H13), 2.51 (dd, J 14.1, 7.8, 1H, H5a), 2.37 (dd, J 14.1, 8.2, 1H, H5b), 2.18 – 2.11 (m, 2H, H7), 2.04 – 1.92 (m, 2H, H8), 1.70 (m, 3H, H2), 1.58 (s, 3H, H1); ^{13}C NMR (101 MHz, CDCl_3) δ 169.5 (C11), 162.7 (C10), 137.8 (C3), 117.2 (C4), 68.2 (C6), 53.6 (C12), 45.0 (C9), 36.7 (C7), 35.2 (C5), 33.5 (C13), 26.1 (C2), 20.5 (C8), 17.8 (C1); HRMS (ESI) calculated for $\text{C}_{13}\text{H}_{20}\text{N}_2\text{O}_2\text{Na}$ $[\text{M}+\text{Na}]^+$ 259.1422, found 259.1419.

**(*R*)-2methyl-8a-(3-methylbut-2-en-1yl)-3- methylenehexahydropyrrolo[1,2-a] pyrazine-1,4,-
dione (**326**)**



DKP **325** (0.9 mg, 3.80 mmol) was dissolved in THF (25 mL) and to this was added *n*-BuLi (7.12 mL of 1.6 M in hexane, 11.4 mmol, 3.0 equiv) at -78 °C. After 10 min formaldehyde (400 mg, 13.3 mmol, 3.5 equiv) in 5 mL THF was added and the reaction mixture was stirred for 20 min in the same temperature. The reaction mixture was allowed to warm to rt and then was warmed to reflux and stirred for 2 hours. The reaction mixture was quenched with a saturated NH₄Cl_{aq} solution (10 mL) before allowed to cool to rt. EtOAc (50 mL) were added and the crude material was washed with brine (50 mL), dried over MgSO₄ and concentrated under reduced pressure. The residue was purified by flash column chromatography (Pet. ether/EtOAc, 9:1) to give **326** (348 mg, 1.41 mmol, 37%) as a white foam.

R_f 0.5 (EtOAc/MeOH, 9:1); [α]_D²¹ -83 (*c* 0.8, CHCl₃); FTI (ATR) ν_{max} 2957, 1680, 1551, 1430, 1405, 1322, 1048; ¹H NMR (400 MHz, CDCl₃) δ 5.67 (s, 1H, H13a), 4.96 – 4.82 (m, 1H, H4), 4.78 (s, 1H, H13b), 3.83 (dt, *J* 12.5, 8.5 Hz, 1H, H9a), 3.66 – 3.52 (m, 1H, H9b), 3.16 (s, 3H, H14), 2.48 (dd, *J* 13.9, 7.8 Hz, 1H, H5a), 2.38 (dd, *J* 14.0, 8.3 Hz, 1H, H5b), 2.29 – 2.15 (m, 2H, H7), 2.04 - 1.99 (dd, *J* = 10.6, 6.4 Hz, 2H, H8), 1.60 (s, 3H, H2), 1.52 (s, 3H, H1); ¹³C NMR (101 MHz, CDCl₃) δ 168.4 (C11), 157.8 (C10), 139.6 (C12), 138.2 (C3), 116.9 (C4), 100.7 (C13), 68.3 (C6), 45.1 (C9), 37.7 (C5), 34.8 (C7), 29.8 (C14), 26.1 (C2), 20.2 (C8), 17.7 (C1); HRMS (ESI) calculated for C₁₄H₂₀N₂O₂Na [M+Na]⁺ 271.1422, found 271.1413.

Crystallographic information

Sulfide 218

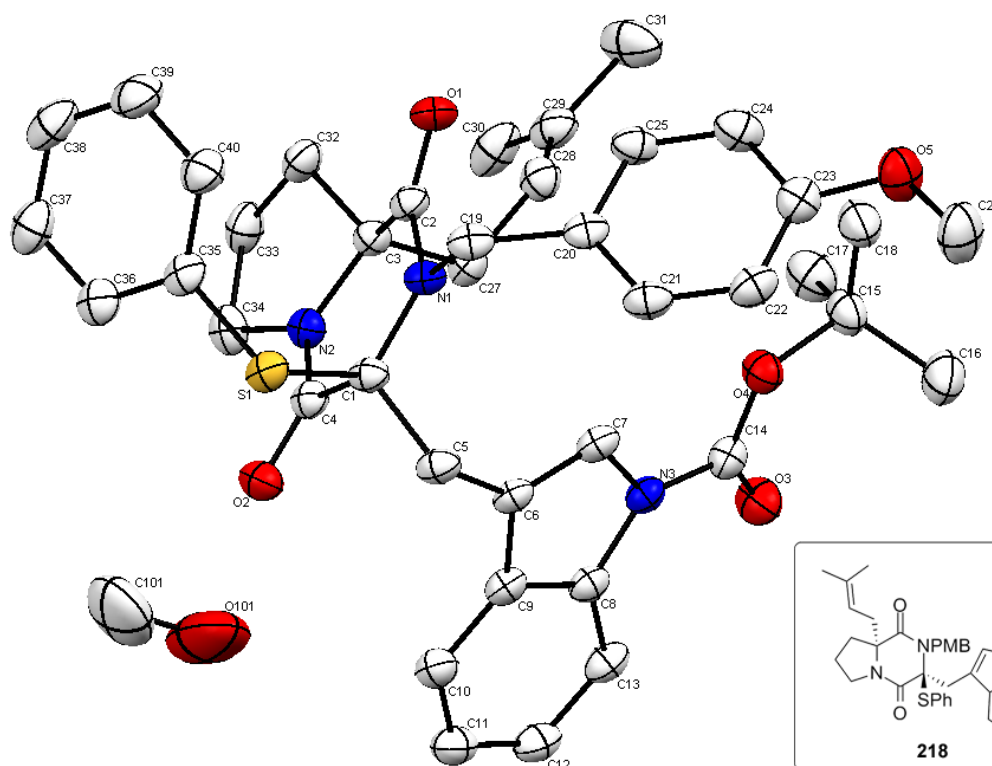


Table 1. Crystal data and structure refinement for **218**.

Identification code	218	
Empirical formula	C ₄₀ H ₄₅ N ₃ O ₅ S, CH ₃ OH	
Formula weight	711.89	
Temperature	120(2) K	
Wavelength	1.54178 Å	
Crystal system	Orthorhombic	
Space group	P 2 ₁ 2 ₁ 2 ₁	
Unit cell dimensions	a = 10.6567(3) Å	α = 90°.
	b = 13.9156(4) Å	β = 90°.

	$c = 24.7451(6) \text{ \AA}$	$\gamma = 90^\circ$.
Volume	$3669.56(17) \text{ \AA}^3$	
Z	4	
Density (calculated)	1.289 Mg/m^3	
Absorption coefficient	1.202 mm^{-1}	
F(000)	1520	
Crystal size	$0.34 \times 0.34 \times 0.24 \text{ mm}^3$	
Theta range for data collection	$6.34 \text{ to } 68.22^\circ$	
Index ranges	$-11 \leq h \leq 12, -16 \leq k \leq 16, -29 \leq l \leq 29$	
Reflections collected	28682	
Independent reflections	6618 [$R(\text{int}) = 0.0212$]	
Completeness to theta = 68.22°	98.9%	
Absorption correction	Semi-empirical from equivalents	
Max. and min. transmission	0.7612 and 0.6853	
Refinement method	Full-matrix least-squares on F^2	
Data / restraints / parameters	6618 / 0 / 467	
Goodness-of-fit on F^2	1.044	
Final R indices [$I > 2\sigma(I)$]	$R1 = 0.0332, wR2 = 0.0923$	
R indices (all data)	$R1 = 0.0336, wR2 = 0.0927$	
Absolute structure parameter	0.020(13)	
Largest diff. peak and hole	$0.730 \text{ and } -0.547 \text{ e.\AA}^{-3}$	

Notes:

The absolute structure has been determined from the diffraction data. The chirality at C(1) is S and at C(3) is R. The structure contains one molecule of methanol per diketopiperazine molecule which forms a hydrogen bond with O(2). The hydrogen atoms were fixed as riding models.

Table 2. Atomic coordinates ($\times 10^4$) and equivalent isotropic displacement parameters ($\text{\AA}^2 \times 10^3$)

for **218**. $U(\text{eq})$ is defined as one third of the trace of the orthogonalized U^{ij} tensor.

	x	y	z	$U(\text{eq})$
C(1)	8984(2)	6705(1)	1990(1)	25(1)
C(2)	9335(2)	7096(1)	1018(1)	25(1)
C(3)	8006(2)	6817(1)	886(1)	25(1)
C(4)	7575(2)	6645(1)	1865(1)	26(1)
C(5)	9389(2)	5836(1)	2334(1)	28(1)
C(6)	9101(2)	4885(1)	2076(1)	24(1)
C(7)	9685(2)	4486(1)	1648(1)	26(1)
C(8)	8145(2)	3444(1)	1887(1)	26(1)
C(9)	8113(2)	4234(1)	2238(1)	27(1)
C(10)	7233(2)	4257(1)	2654(1)	31(1)
C(11)	6428(2)	3484(1)	2708(1)	35(1)
C(12)	6477(2)	2704(1)	2359(1)	34(1)
C(13)	7341(2)	2664(1)	1945(1)	31(1)
C(14)	9372(2)	3047(1)	1065(1)	29(1)
C(15)	10778(2)	2982(1)	285(1)	36(1)
C(16)	11175(2)	1947(2)	374(1)	47(1)
C(17)	9752(2)	3064(2)	-132(1)	46(1)
C(18)	11874(2)	3617(2)	145(1)	42(1)
C(19)	11132(2)	7047(1)	1616(1)	28(1)
C(20)	12044(2)	6319(1)	1398(1)	27(1)
C(21)	12684(2)	5699(1)	1742(1)	32(1)
C(22)	13607(2)	5082(1)	1553(1)	36(1)
C(23)	13927(2)	5091(1)	1013(1)	33(1)
C(24)	13285(2)	5693(2)	660(1)	35(1)
C(25)	12368(2)	6295(1)	852(1)	32(1)
C(26)	15693(2)	4075(2)	1144(1)	52(1)
C(27)	8012(2)	5783(1)	635(1)	27(1)
C(28)	8741(2)	5684(1)	124(1)	32(1)
C(29)	8274(2)	5563(1)	-369(1)	38(1)
C(30)	6908(2)	5529(2)	-503(1)	45(1)
C(31)	9130(3)	5460(2)	-848(1)	58(1)

C(32)	7328(2)	7529(1)	522(1)	32(1)
C(33)	5944(2)	7301(1)	628(1)	36(1)
C(34)	5900(2)	7048(1)	1228(1)	34(1)
C(35)	8478(2)	8688(1)	2041(1)	30(1)
C(36)	7219(2)	8933(1)	2101(1)	34(1)
C(37)	6715(2)	9671(1)	1794(1)	42(1)
C(38)	7456(2)	10152(1)	1424(1)	46(1)
C(39)	8708(3)	9917(2)	1367(1)	48(1)
C(40)	9222(2)	9190(1)	1679(1)	39(1)
N(1)	9784(1)	6837(1)	1516(1)	24(1)
N(2)	7206(1)	6804(1)	1362(1)	26(1)
N(3)	9111(1)	3609(1)	1516(1)	26(1)
O(1)	9999(1)	7457(1)	674(1)	31(1)
O(2)	6818(1)	6518(1)	2234(1)	33(1)
O(3)	8766(1)	2346(1)	948(1)	39(1)
O(4)	10342(1)	3409(1)	803(1)	33(1)
O(5)	14869(1)	4564(1)	785(1)	44(1)
S(1)	9124(1)	7764(1)	2449(1)	29(1)
C(101)	6668(4)	7337(3)	3472(1)	94(1)
O(101)	6911(4)	6478(2)	3336(1)	122(1)

Indoline 318

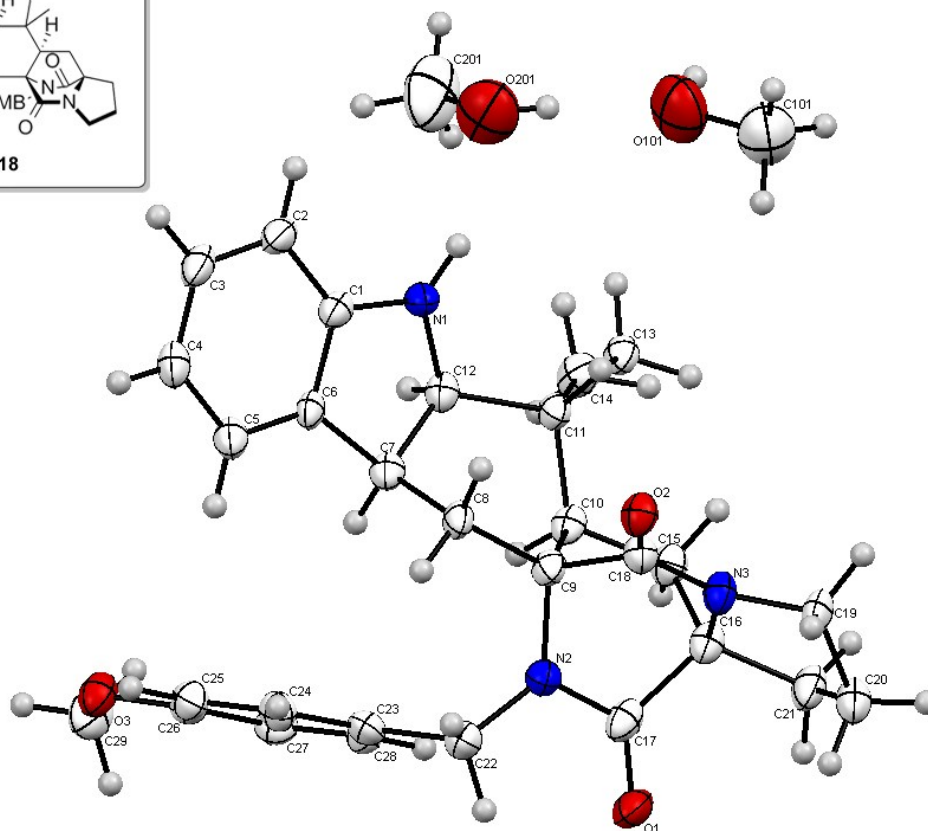
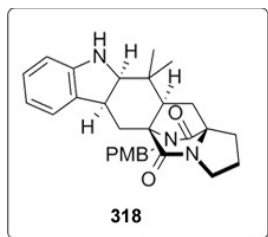


Table 1. Crystal data and structure refinement for **318**

Identification code	318	
Empirical formula	$C_{29}H_{33}N_3O_3, 2(CH_3OH)$	
Formula weight	535.67	
Temperature	120(2) K	
Wavelength	0.71073 Å	
Crystal system	Monoclinic	
Space group	$P 2_1$	
Unit cell dimensions	$a = 9.7410(9)$ Å	$\alpha = 90^\circ$.
	$b = 13.9612(9)$ Å	$\beta = 95.382(4)^\circ$.
	$c = 10.2677(10)$ Å	$\gamma = 90^\circ$.

Volume	1390.2(2) Å ³
Z	2
Density (calculated)	1.280 Mg/m ³
Absorption coefficient	0.087 mm ⁻¹
F(000)	576
Crystal size	0.56 x 0.38 x 0.03 mm ³
Theta range for data collection	3.03 to 27.48°.
Index ranges	-12<= <i>h</i> <=12, -17<= <i>k</i> <=18, -13<= <i>l</i> <=13
Reflections collected	17079
Independent reflections	3316 [R(int) = 0.0789]
Completeness to theta = 27.48°	99.6%
Absorption correction	Semi-empirical from equivalents
Max. and min. transmission	0.9974 and 0.9530
Refinement method	Full-matrix least-squares on F ²
Data / restraints / parameters	3316 / 1 / 360
Goodness-of-fit on F²	1.020
Final R indices [I>2σ(I)]	R1 = 0.0625, wR2 = 0.1361
R indices (all data)	R1 = 0.0919, wR2 = 0.1499
Absolute structure parameter	?
Extinction coefficient	0.039(5)
Largest diff. peak and hole	0.366 and -0.340 e.Å ⁻³

Notes:

It has not been possible to determine the absolute structure from the diffraction data as there are no heavy atoms present. The absolute structure has been determined from the synthetic scheme. The relative chirality of the chiral centres has been determined. The structure contains two methanol

groups per molecule. The hydrogen atoms have been fixed as riding models.

Table 2. Atomic coordinates ($\times 10^4$) and equivalent isotropic displacement parameters ($\text{\AA}^2 \times 10^3$)

for **318**. $U(\text{eq})$ is defined as one third of the trace of the orthogonalized U^{ij} tensor.

	x	y	z	$U(\text{eq})$
C(1)	5135(4)	7175(3)	2548(4)	26(1)
C(2)	5321(4)	8085(3)	3114(4)	31(1)
C(3)	4286(5)	8759(3)	2849(4)	33(1)
C(4)	3088(5)	8551(3)	2064(4)	32(1)
C(5)	2905(5)	7642(3)	1495(4)	31(1)
C(6)	3930(4)	6968(3)	1731(3)	24(1)
C(7)	3997(4)	5929(3)	1314(4)	26(1)
C(8)	3028(4)	5316(3)	2079(4)	26(1)
C(9)	3214(4)	4238(3)	1908(4)	26(1)
C(10)	4664(4)	4002(3)	1428(4)	26(1)
C(11)	5835(4)	4610(3)	2137(4)	25(1)
C(12)	5539(4)	5672(3)	1707(4)	27(1)
C(13)	5961(4)	4487(3)	3623(4)	30(1)
C(14)	7222(4)	4314(3)	1635(5)	35(1)
C(15)	4874(4)	2905(3)	1464(4)	30(1)
C(16)	3528(4)	2424(3)	1773(4)	27(1)
C(17)	2351(4)	2803(3)	796(4)	31(1)
C(18)	3006(4)	3711(3)	3208(4)	27(1)
C(19)	2893(5)	1999(3)	3976(4)	31(1)
C(20)	2597(5)	1164(3)	3041(4)	33(1)
C(21)	3531(5)	1335(3)	1943(5)	36(1)
C(22)	989(4)	4238(3)	264(4)	32(1)
C(23)	1336(4)	4953(3)	-774(4)	28(1)
C(24)	816(4)	5881(3)	-803(4)	29(1)
C(25)	1135(4)	6527(3)	-1752(4)	30(1)
C(26)	1971(4)	6256(3)	-2710(4)	29(1)
C(27)	2490(4)	5325(3)	-2717(4)	30(1)

C(28)	2172(4)	4682(3)	-1747(4)	29(1)
C(29)	2931(5)	6668(3)	-4699(4)	42(1)
N(1)	5970(3)	6380(2)	2714(3)	28(1)
N(2)	2190(3)	3763(2)	934(3)	28(1)
N(3)	3214(4)	2776(2)	3075(3)	29(1)
O(1)	1656(3)	2292(2)	9(3)	39(1)
O(2)	2677(3)	4098(2)	4217(3)	30(1)
O(3)	2239(3)	6952(2)	-3597(3)	36(1)
C(101)	9570(7)	4016(5)	5336(7)	69(2)
O(101)	10060(5)	4715(4)	4470(5)	80(1)
C(201)	9634(9)	6791(5)	2831(6)	85(2)
O(201)	8930(4)	6433(4)	3721(5)	77(1)

Indoline 352

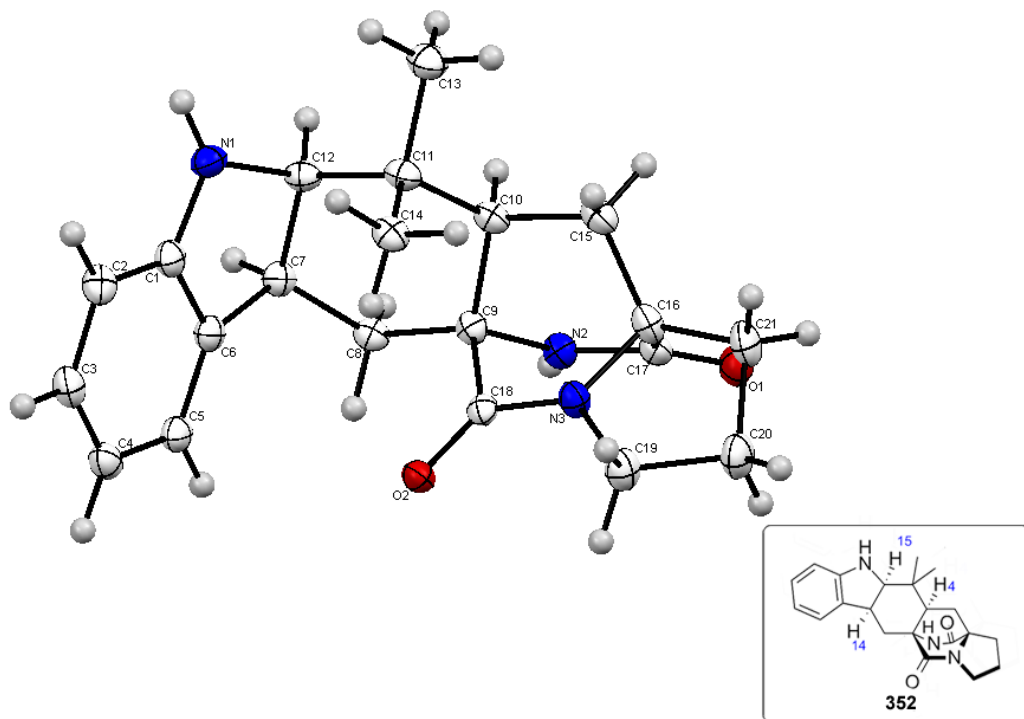


Table 1. Crystal data and structure refinement for **352**

Identification code	352	
Empirical formula	$C_{21}H_{25}N_3O_2$	
Formula weight	351.44	
Temperature	120(2) K	
Wavelength	1.54178 Å	
Crystal system	Orthorhombic	
Space group	P 2 ₁ 2 ₁ 2 ₁	
Unit cell dimensions	$a = 11.25880(10)$ Å	$\alpha = 90^\circ$.
	$b = 11.7630(2)$ Å	$\beta = 90^\circ$.
	$c = 12.8358(2)$ Å	$\gamma = 90^\circ$.
Volume	$1699.94(4)$ Å ³	

Z	4
Density (calculated)	1.373 Mg/m ³
Absorption coefficient	0.713 mm ⁻¹
F(000)	752
Crystal size	0.20 x 0.16 x 0.10 mm ³
Theta range for data collection	6.44 to 66.57°.
Index ranges	-13 ≤ h ≤ 13, -13 ≤ k ≤ 14, -14 ≤ l ≤ 15
Reflections collected	10076
Independent reflections	2910 [R(int) = 0.0278]
Completeness to theta = 66.57°	99.4%
Absorption correction	Semi-empirical from equivalents
Max. and min. transmission	0.9321 and 0.8705
Refinement method	Full-matrix least-squares on F ²
Data / restraints / parameters	2910 / 0 / 237
Goodness-of-fit on F²	1.068
Final R indices [I > 2σ(I)]	R1 = 0.0329, wR2 = 0.0849
R indices (all data)	R1 = 0.0344, wR2 = 0.0861
Absolute structure parameter	-0.1(2)
Largest diff. peak and hole	0.362 and -0.318 e.Å ⁻³

Notes:

It has not been possible to determine the absolute structure from the diffraction data due to the lack of heavier atoms, but the relative stereochemistry of the chiral centres has been confirmed. Thus it has been confirmed that the chirality of C(7) is opposite to that of C(9), C(10), C(12) and C(16). The structure has been shown with C(7) as *S* and C(9), C(10), C(12) and C(16) as *R* as this is the absolute structure as determined from the synthesis. The hydrogen atoms have been fixed as riding models.

Table 2. Atomic coordinates ($\times 10^4$) and equivalent isotropic displacement parameters ($\text{\AA}^2 \times 10^3$)

for **352**. $U(\text{eq})$ is defined as one third of the trace of the orthogonalized U^{ij} tensor.

	x	y	z	$U(\text{eq})$
C(1)	6316(2)	6332(2)	11490(1)	22(1)
C(2)	5272(2)	5835(2)	11847(1)	23(1)
C(3)	4515(2)	5335(2)	11128(1)	24(1)
C(4)	4770(2)	5360(1)	10070(1)	24(1)
C(5)	5817(2)	5864(1)	9718(1)	22(1)
C(6)	6594(2)	6336(1)	10428(1)	20(1)
C(7)	7739(2)	6996(1)	10299(1)	20(1)
C(8)	8603(2)	6717(1)	9409(1)	20(1)
C(9)	9528(1)	5811(1)	9648(1)	19(1)
C(10)	10077(2)	5960(2)	10752(1)	20(1)
C(11)	9153(2)	5982(2)	11648(1)	21(1)
C(12)	8266(2)	6969(1)	11419(1)	20(1)
C(13)	9809(2)	6281(2)	12662(1)	27(1)
C(14)	8521(2)	4834(2)	11791(1)	22(1)
C(15)	11081(2)	5066(2)	10885(1)	25(1)
C(16)	11168(2)	4338(2)	9893(1)	23(1)
C(17)	11439(1)	5160(1)	8989(1)	21(1)
C(18)	9085(1)	4580(1)	9478(1)	17(1)
C(19)	10007(2)	2633(2)	9461(2)	26(1)
C(20)	11324(2)	2418(2)	9243(2)	30(1)
C(21)	11961(2)	3294(2)	9925(2)	28(1)
N(1)	7180(1)	6909(1)	12066(1)	23(1)
N(2)	10536(1)	5913(1)	8904(1)	20(1)
N(3)	9975(1)	3853(1)	9674(1)	21(1)
O(1)	12337(1)	5141(1)	8453(1)	27(1)
O(2)	8089(1)	4312(1)	9169(1)	21(1)

Indoline 353

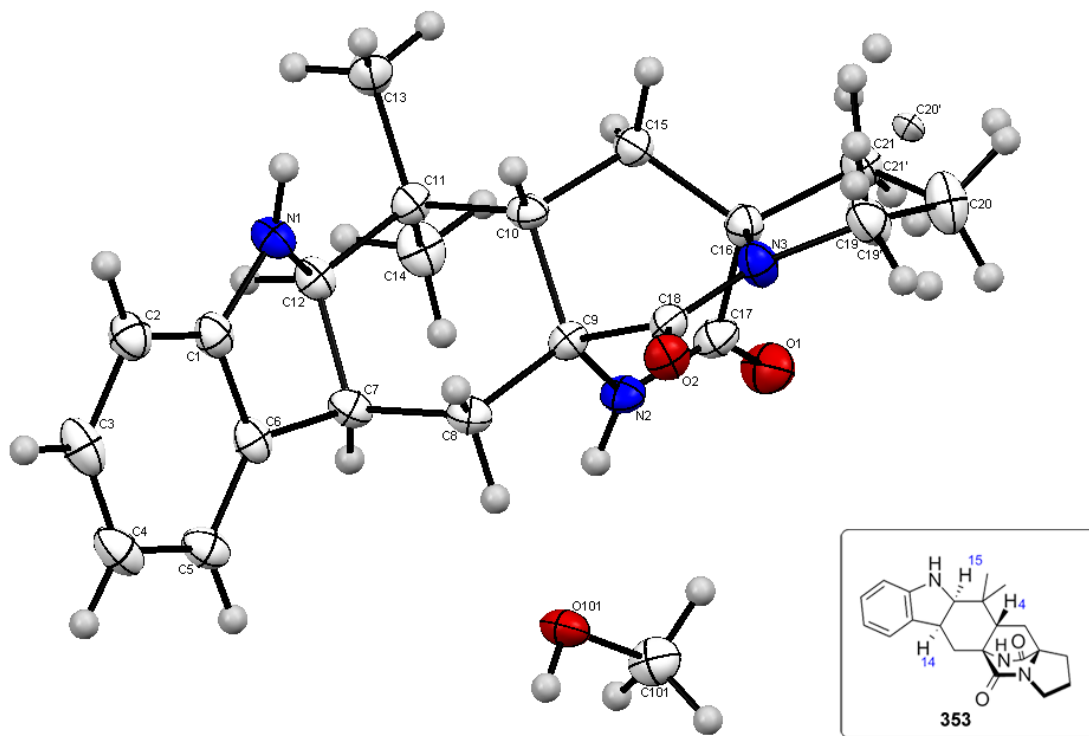


Table 1. Crystal data and structure refinement for **353**

Identification code	353	
Empirical formula	$C_{21}H_{25}N_3O_2$, CH_4O	
Formula weight	383.48	
Temperature	100(2) K	
Wavelength	0.71073 Å	
Crystal system	Orthorhombic	
Space group	$P 2_1 2_1 2_1$	
Unit cell dimensions	$a = 8.0470(17)$ Å	$\alpha = 90^\circ$.
	$b = 10.678(3)$ Å	$\beta = 90^\circ$.
	$c = 22.331(5)$ Å	$\gamma = 90^\circ$.
Volume	$1918.8(8)$ Å ³	
Z	4	

Density (calculated)	1.328 Mg/m ³
Absorption coefficient	0.089 mm ⁻¹
F(000)	824
Crystal size	0.12 x 0.10 x 0.01 mm ³
Theta range for data collection	3.12 to 27.47°.
Index ranges	-10 ≤ h ≤ 9, -13 ≤ k ≤ 13, -29 ≤ l ≤ 25
Reflections collected	14736
Independent reflections	2518 [R(int) = 0.0754]
Completeness to theta = 27.47°	99.8%
Absorption correction	Semi-empirical from equivalents
Max. and min. transmission	0.9991 and 0.9894
Refinement method	Full-matrix least-squares on F ²
Data / restraints / parameters	2518 / 4 / 267
Goodness-of-fit on F²	1.131
Final R indices [I > 2σ(I)]	R1 = 0.0628, wR2 = 0.1274
R indices (all data)	R1 = 0.0727, wR2 = 0.1319
Absolute structure parameter	?
Largest diff. peak and hole	0.314 and -0.337 e.Å ⁻³

Notes:

The structure contains one molecule of methanol per bridge diketopiperazine. It has not been possible to determine the absolute structure from the diffraction data due to the lack of heavier atoms, but the relative stereochemistry of the chiral centres has been confirmed. Thus it has been confirmed that the chirality of C(7) and C(10) is opposite to that of C(9) and C(12). The structure has been shown with C(7) and C(10) as *S* and C(9), C(12) and C(16) as *R* as the chirality of C(16) has been determined from the synthesis. The atom C(20)/C(20') is disordered over two positions at a refined occupancy

ratio of 0.74 (1):0.26 (1). The hydrogen atoms have been fixed as riding models.

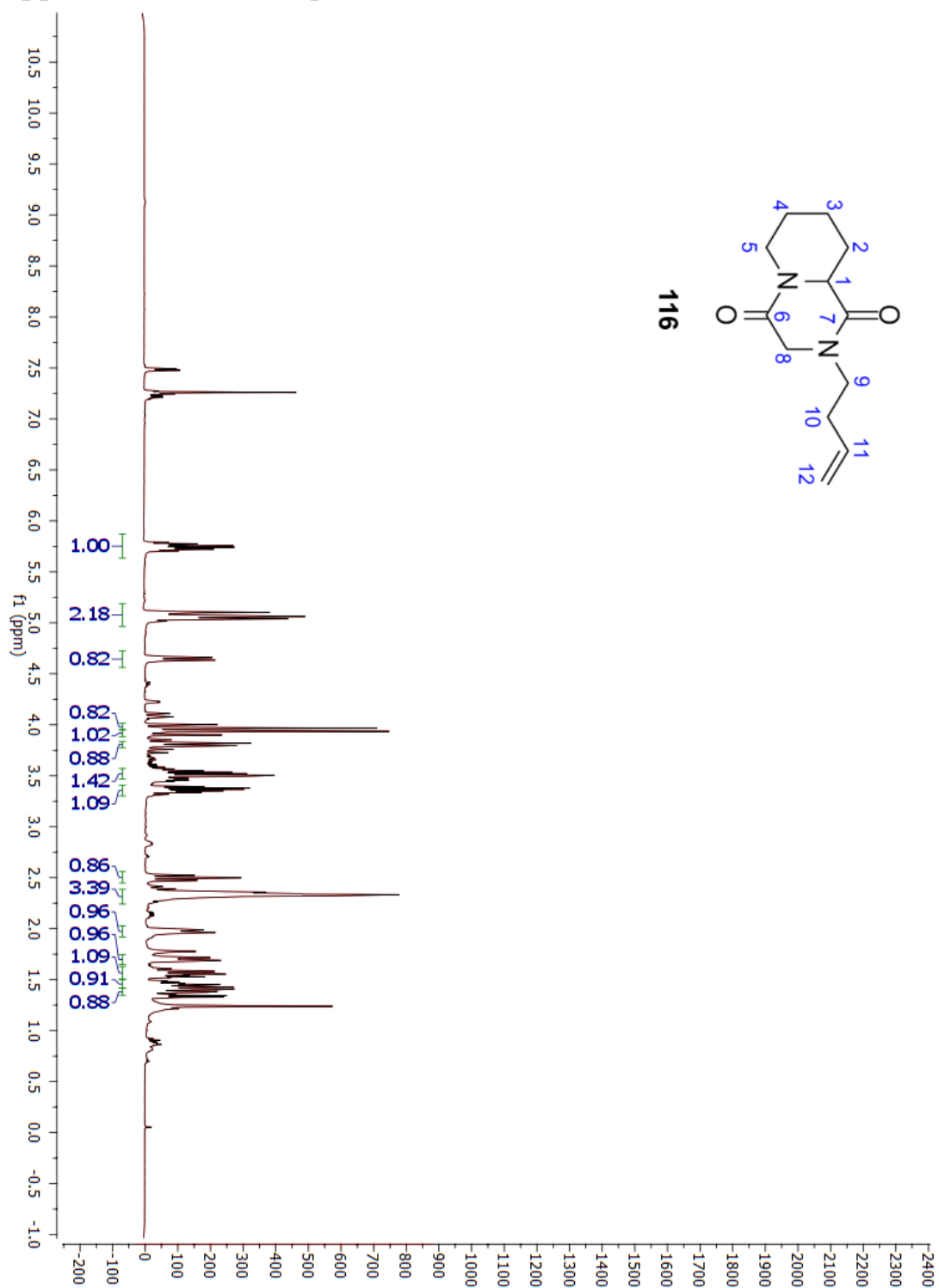
Table 2. Atomic coordinates ($\times 10^4$) and equivalent isotropic displacement parameters ($\text{\AA}^2 \times 10^3$)

for **353**. U(eq) is defined as one third of the trace of the orthogonalized U^{ij} tensor.

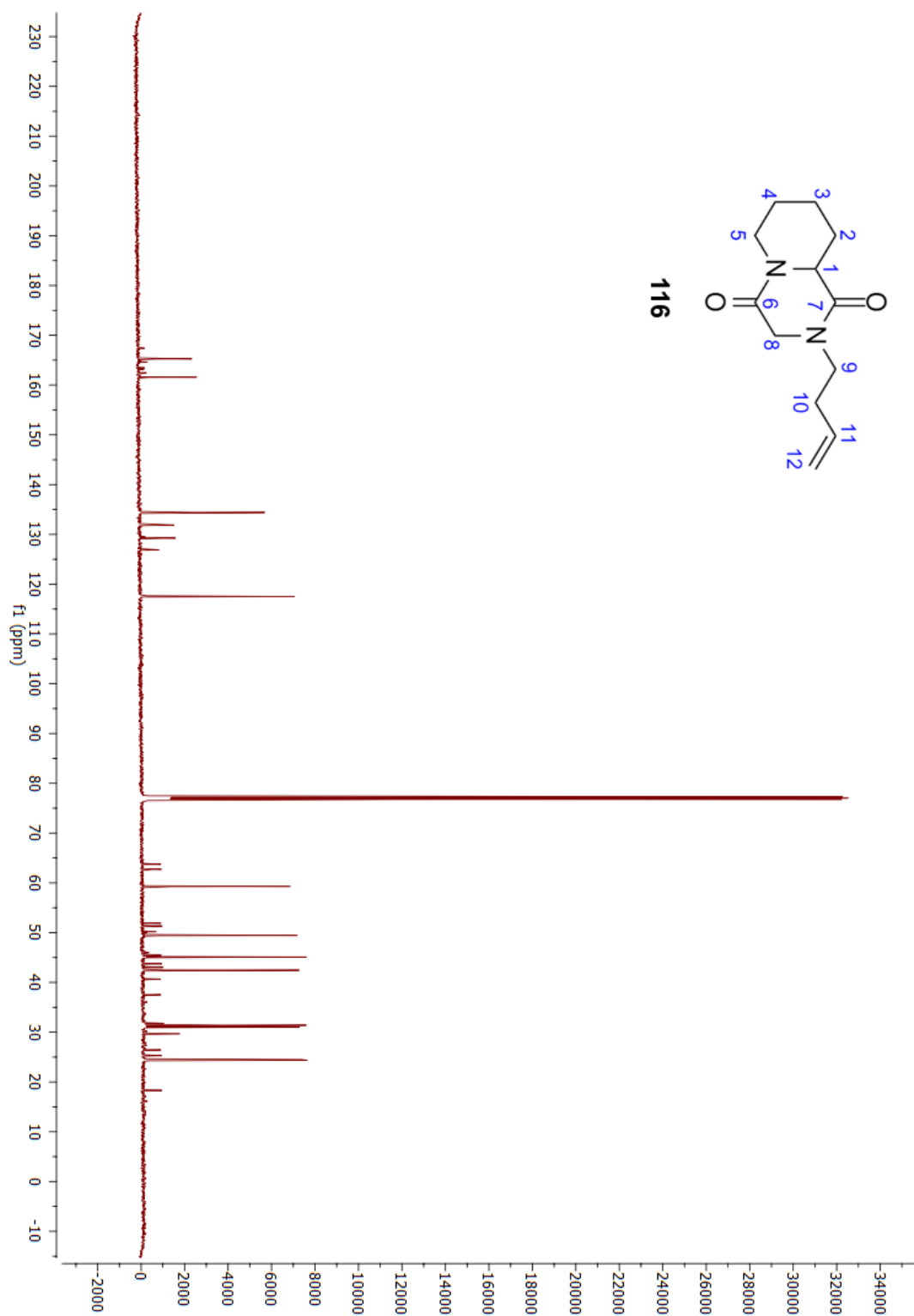
	x	y	z	U(eq)
C(1)	5305(4)	7426(3)	6455(2)	24(1)
C(2)	5609(5)	7887(3)	5884(1)	28(1)
C(3)	4697(5)	7362(3)	5411(2)	33(1)
C(4)	3518(5)	6441(3)	5506(2)	32(1)
C(5)	3192(5)	6021(3)	6086(2)	26(1)
C(6)	4092(4)	6506(3)	6557(1)	23(1)
C(7)	3980(4)	6300(3)	7227(1)	22(1)
C(8)	2667(4)	7200(3)	7479(1)	24(1)
C(9)	2851(4)	7529(3)	8134(1)	20(1)
C(10)	4683(4)	7875(3)	8305(1)	20(1)
C(11)	6009(4)	6955(3)	8075(1)	21(1)
C(12)	5762(4)	6697(3)	7409(1)	22(1)
C(13)	7746(4)	7531(3)	8176(2)	28(1)
C(14)	5968(5)	5666(3)	8386(2)	29(1)
C(15)	4742(4)	8111(3)	8988(1)	23(1)
C(16)	2979(4)	8070(3)	9245(1)	23(1)
C(17)	2307(4)	6751(3)	9131(2)	25(1)
C(18)	1845(4)	8718(3)	8293(1)	22(1)
C(19)	1283(5)	9973(3)	9230(2)	33(1)
C(20)	1268(9)	9465(6)	9850(2)	35(2)
C(21)	2773(5)	8559(3)	9880(1)	29(1)
C(19')	1283(5)	9973(3)	9230(2)	33(1)
C(20')	2321(18)	9893(9)	9806(4)	18(4)
C(21')	2773(5)	8559(3)	9880(1)	29(1)
N(1)	6052(4)	7766(2)	6997(1)	23(1)
N(2)	2264(3)	6532(3)	8535(1)	23(1)
N(3)	1945(4)	8930(3)	8878(1)	26(1)

O(1)	1926(3)	5998(2)	9523(1)	36(1)
O(2)	1077(3)	9382(2)	7930(1)	26(1)
C(101)	-101(5)	3629(4)	8662(2)	31(1)
O(101)	643(3)	4222(2)	8150(1)	28(1)

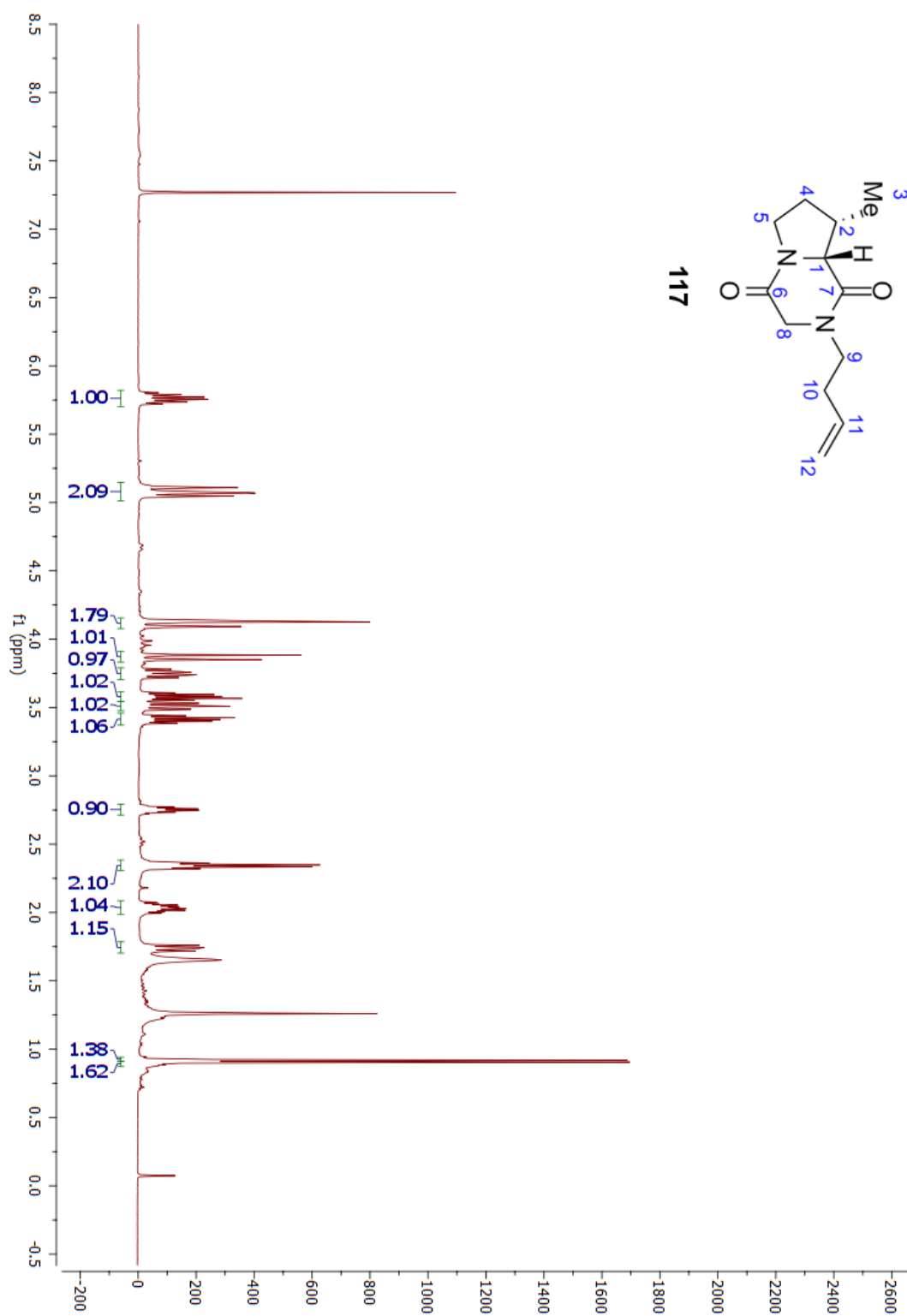
Appendix 1. ^1H -NMR spectrum of **(116)** (500 MHz, CDCl_3)



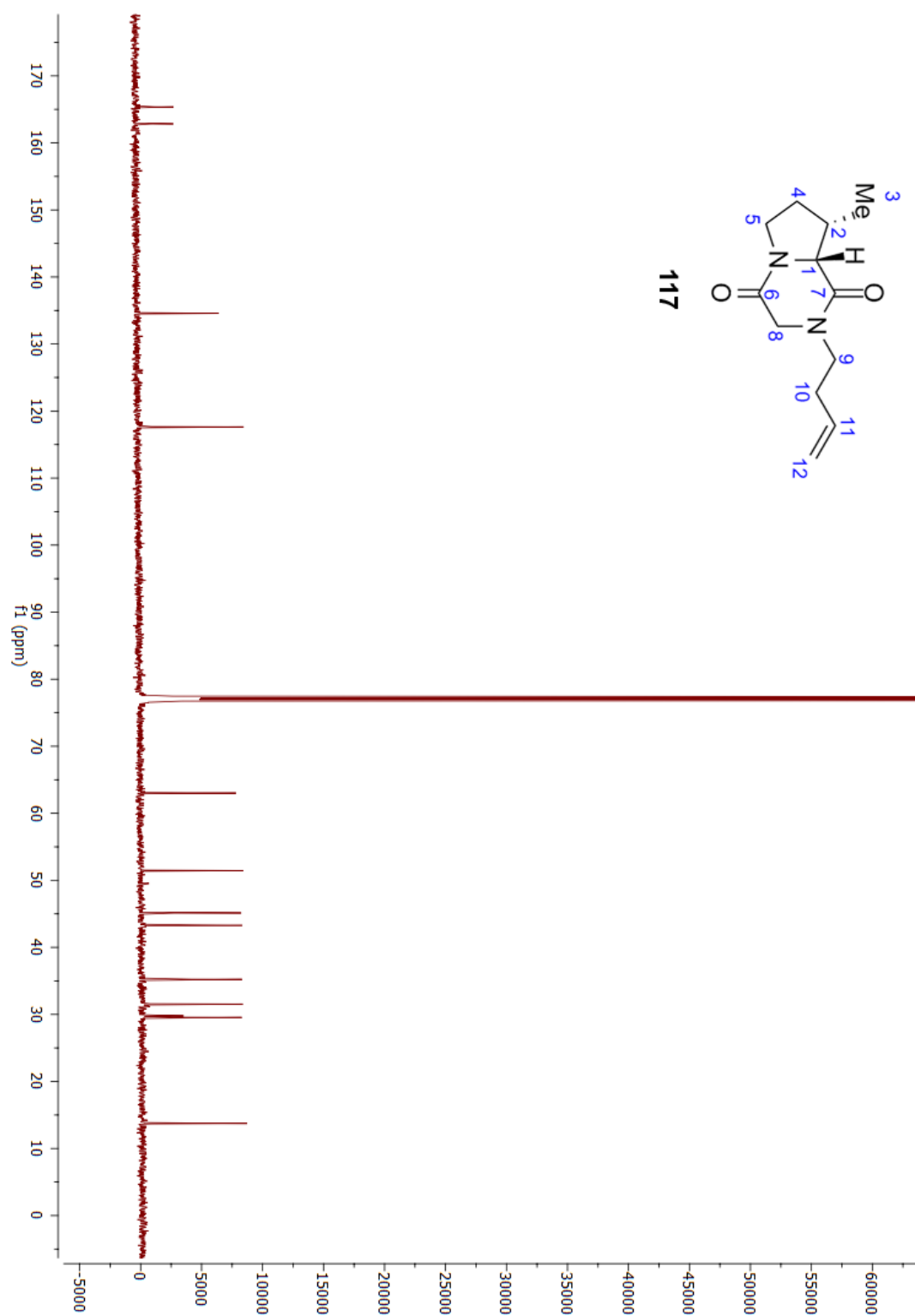
Appendix 2. ^{13}C -NMR spectrum of (**116**) (126 MHz, CDCl_3)



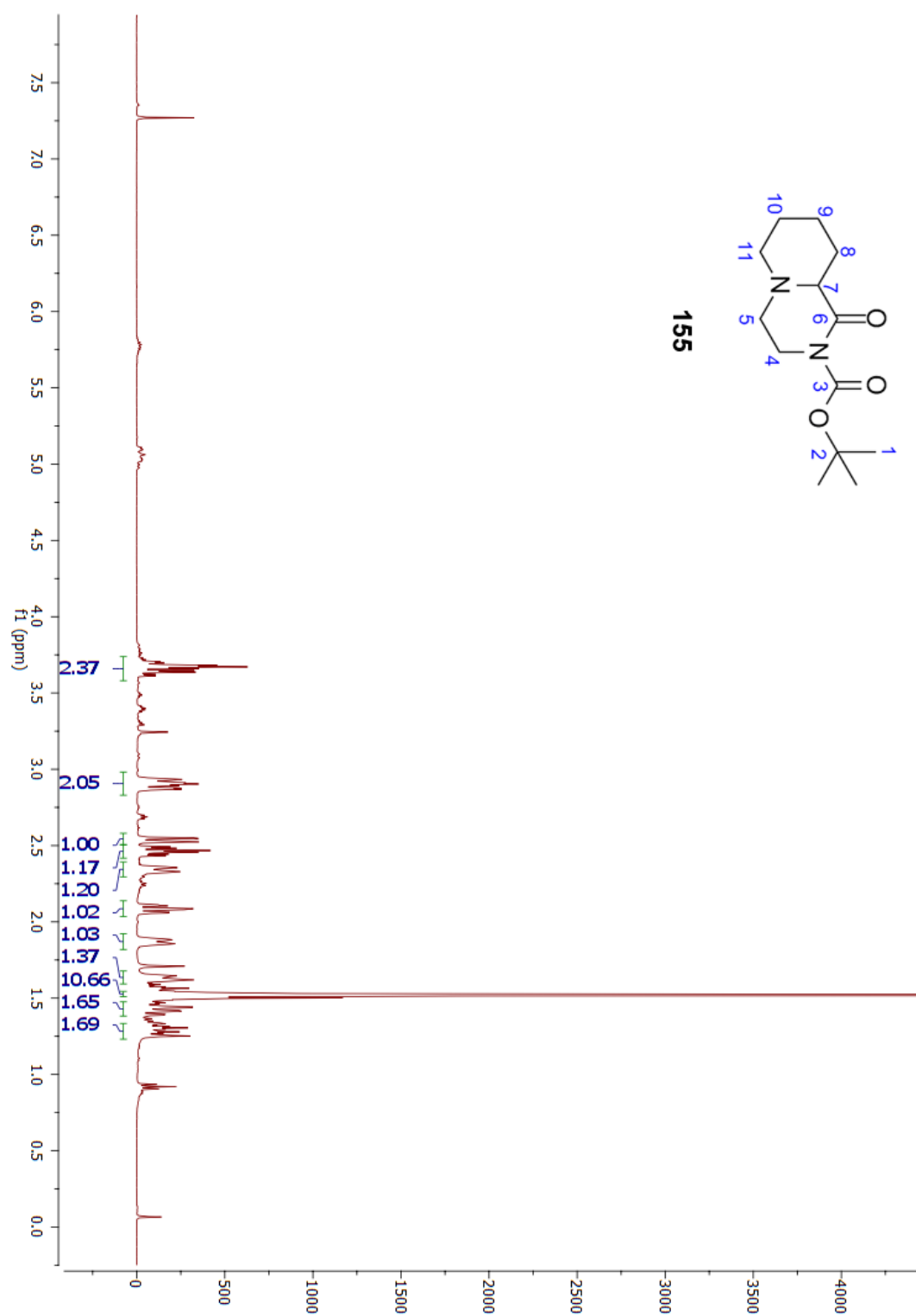
Appendix 3. ^1H -NMR spectrum of (**117**) (500 MHz, CDCl_3)



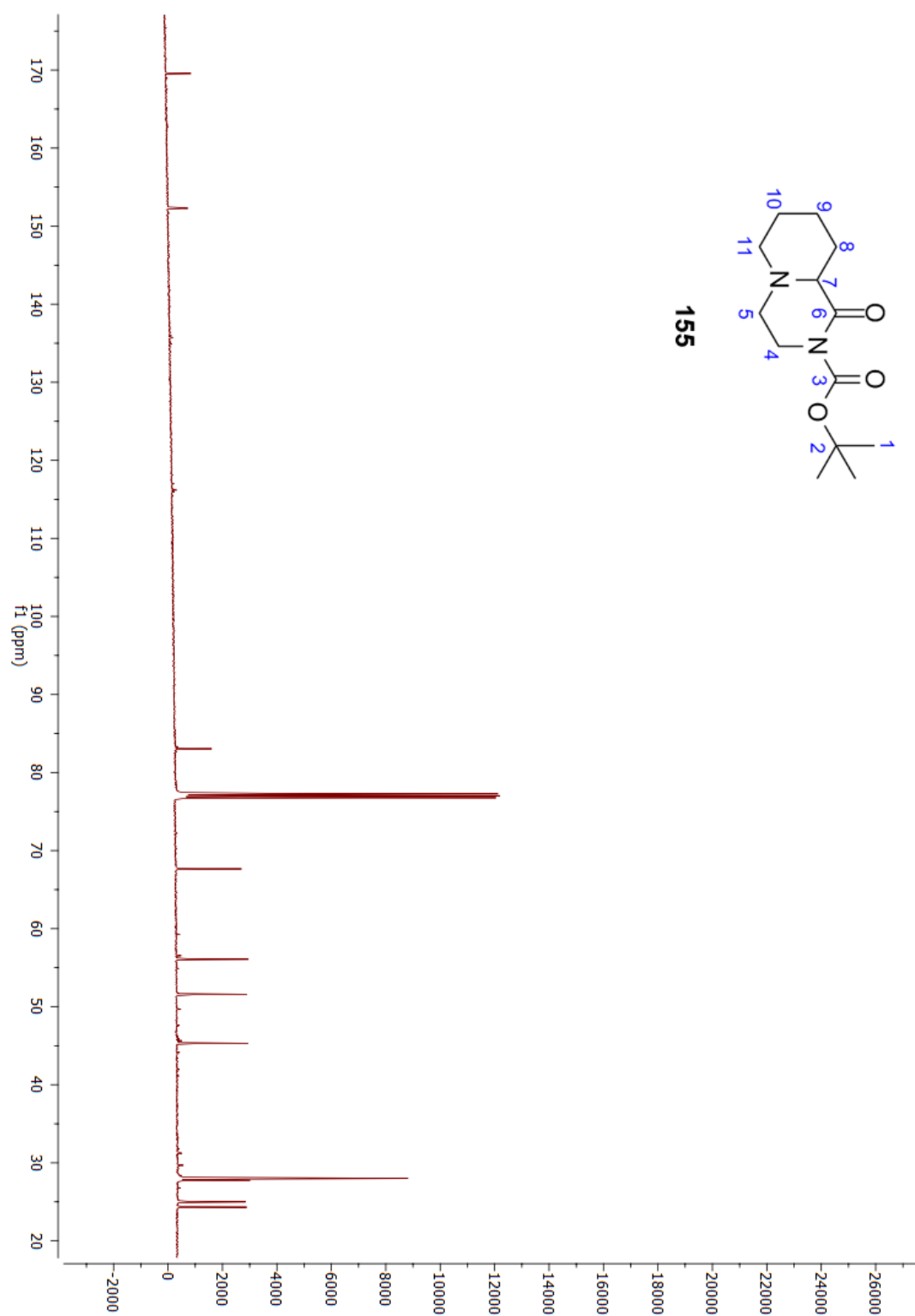
Appendix 4. ^{13}C -NMR spectrum of (**117**) (126 MHz, CDCl_3)



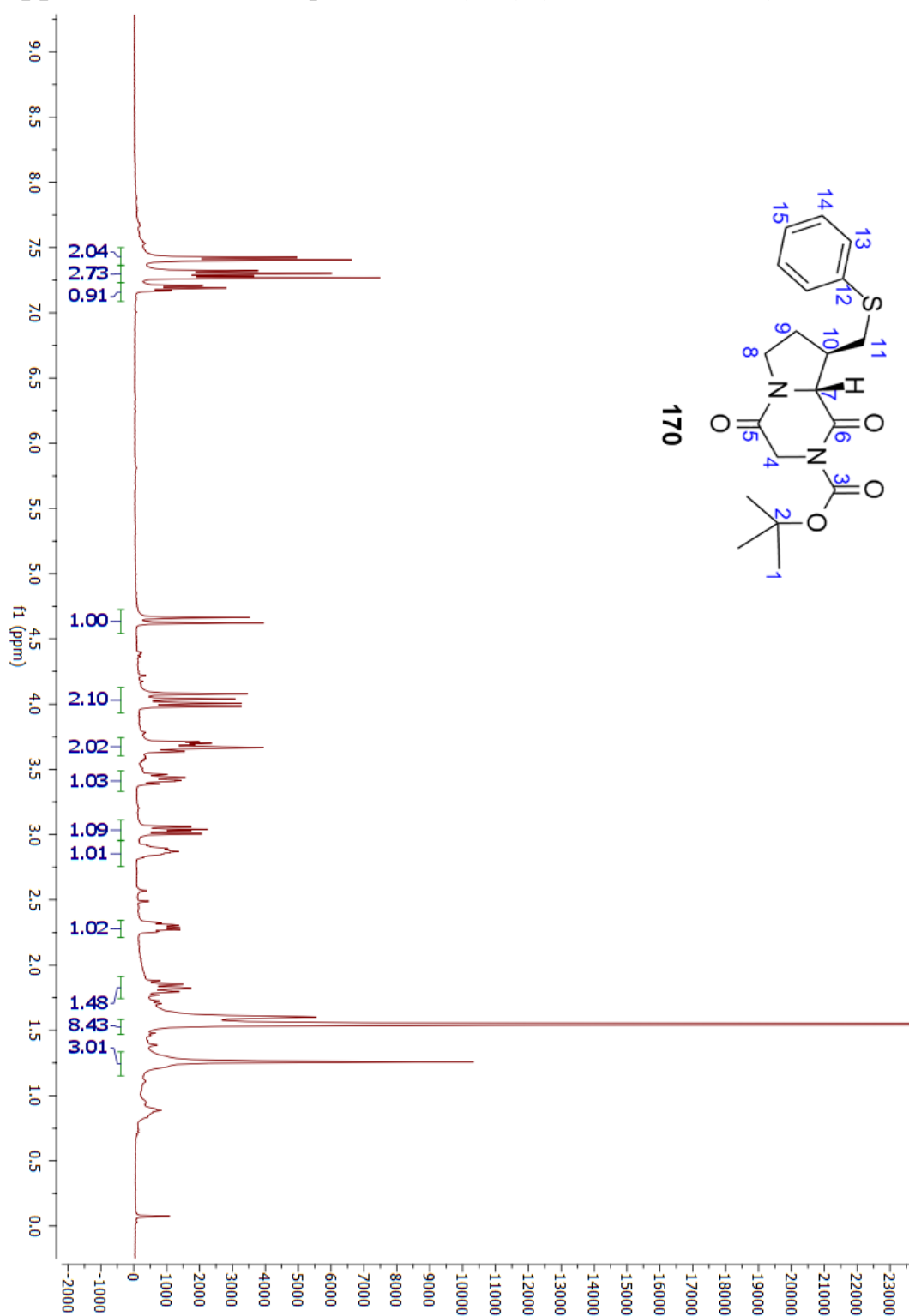
Appendix 5. ^1H -NMR spectrum of (**155**) (500 MHz, CDCl_3)



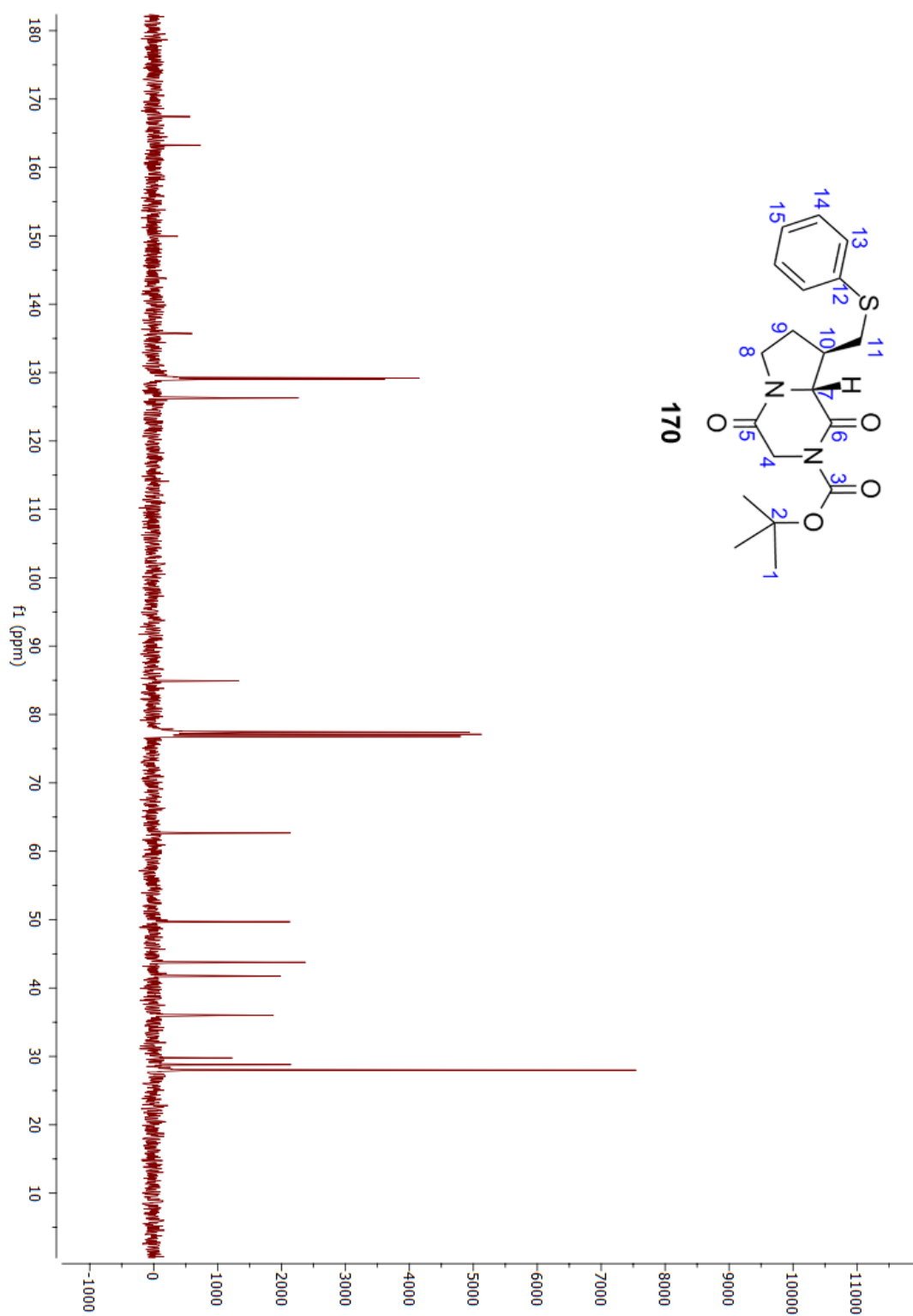
Appendix 6. ^{13}C -NMR spectrum of (**155**) (126 MHz, CDCl_3)



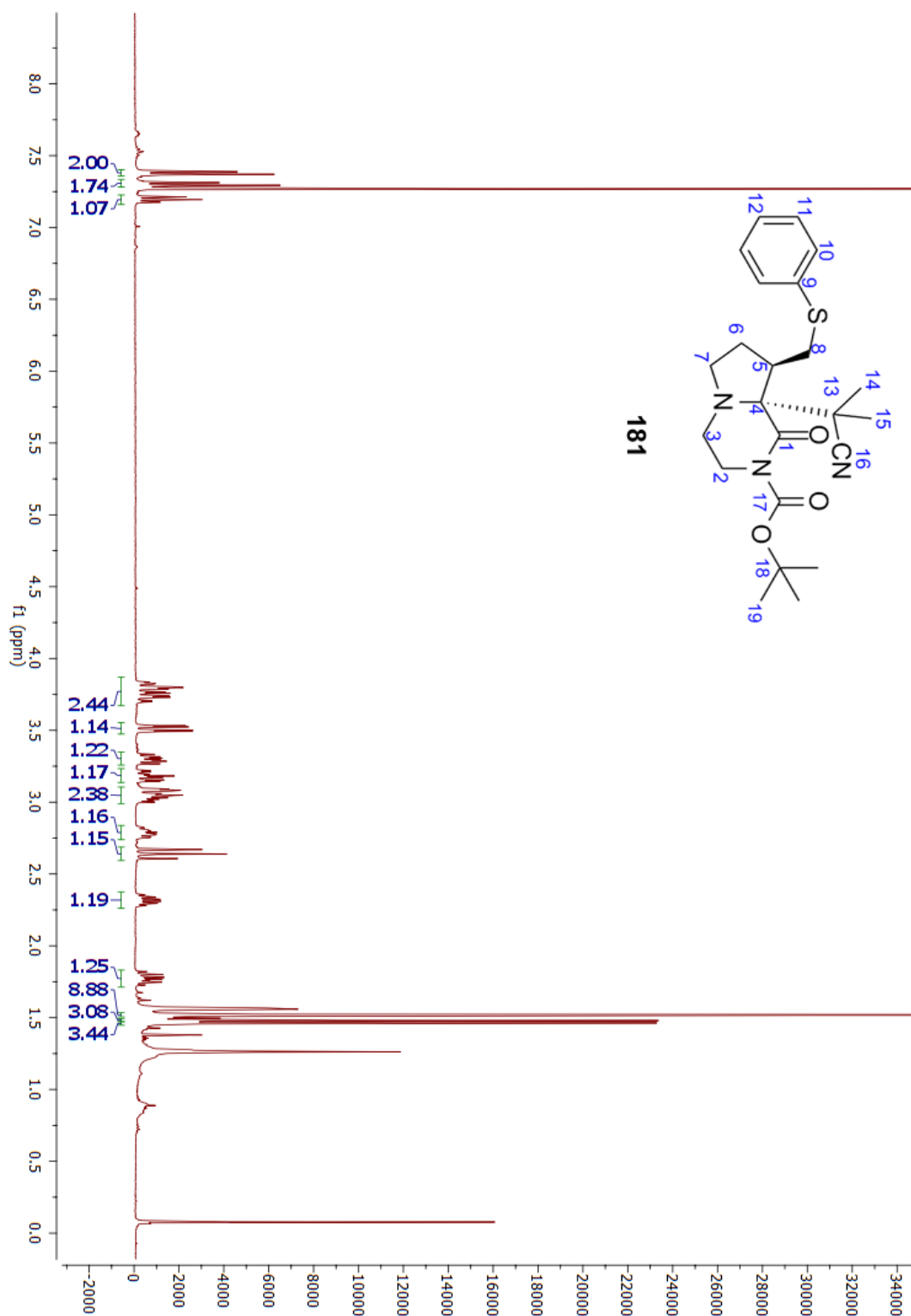
Appendix 7. ^1H -NMR spectrum of (**170**) (400 MHz, CDCl_3)



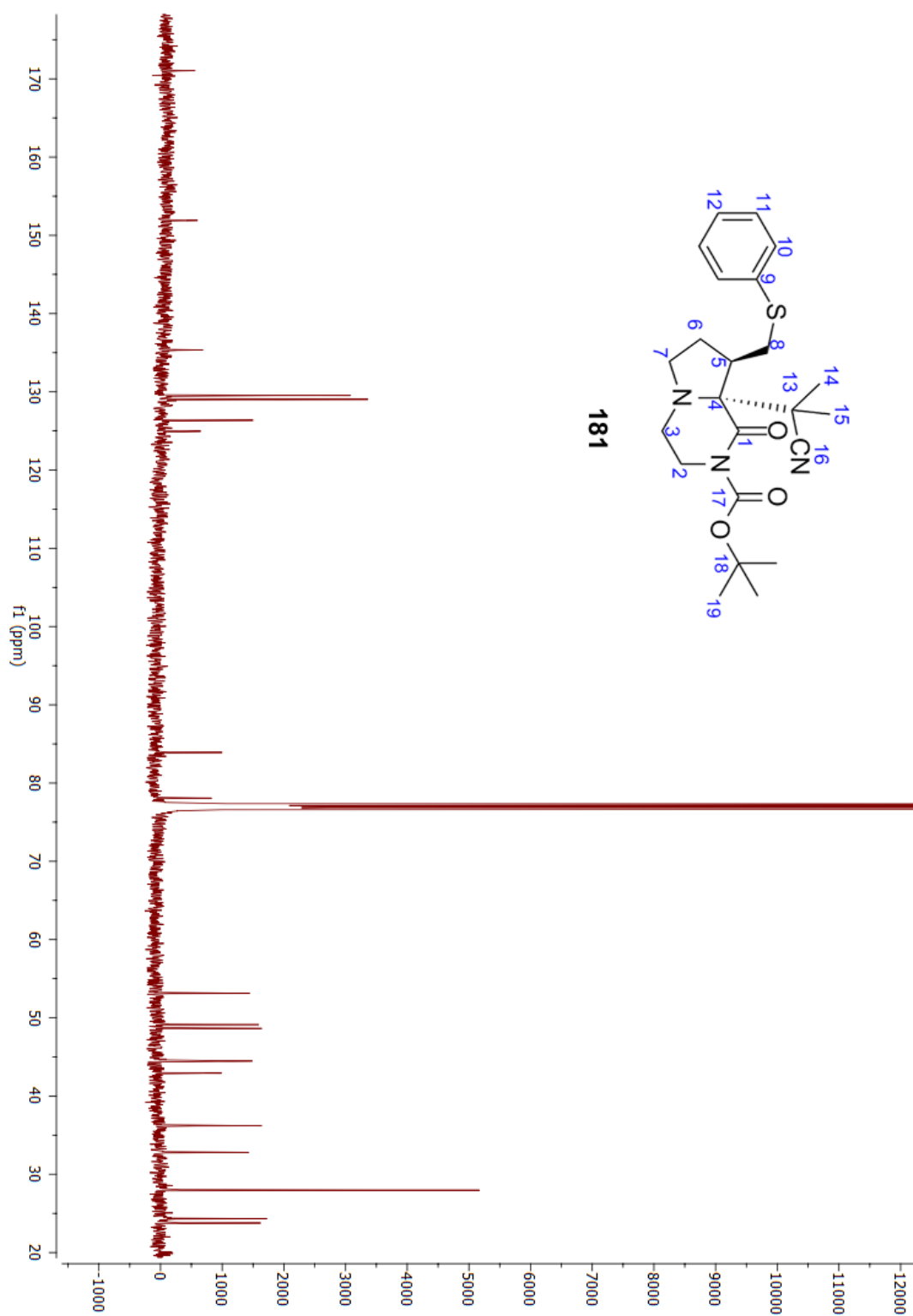
Appendix 8. ^{13}C -NMR spectrum of (**170**) (101 MHz, CDCl_3)



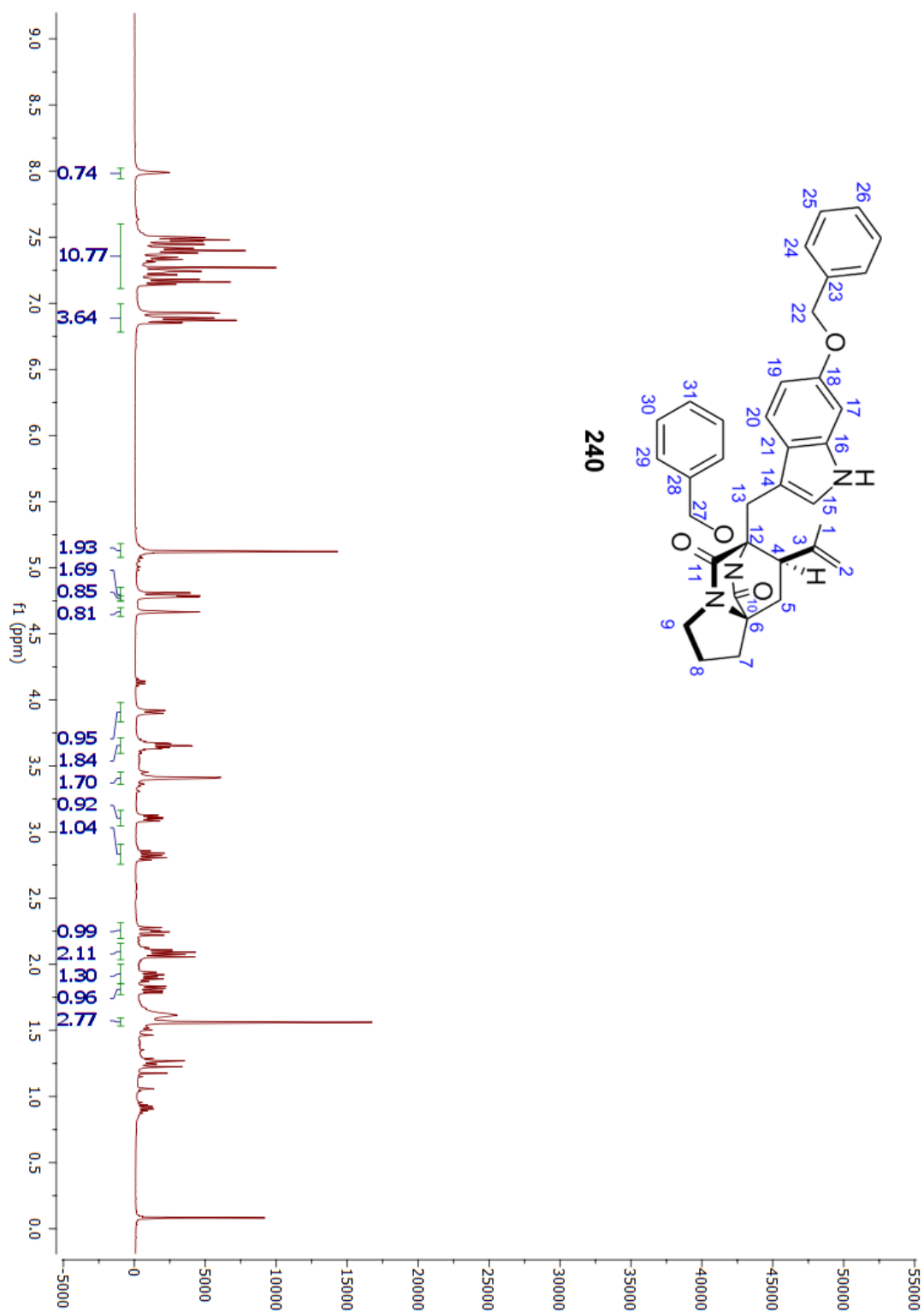
Appendix 9. ^1H -NMR spectrum of (**181**) (500 MHz, CDCl_3)



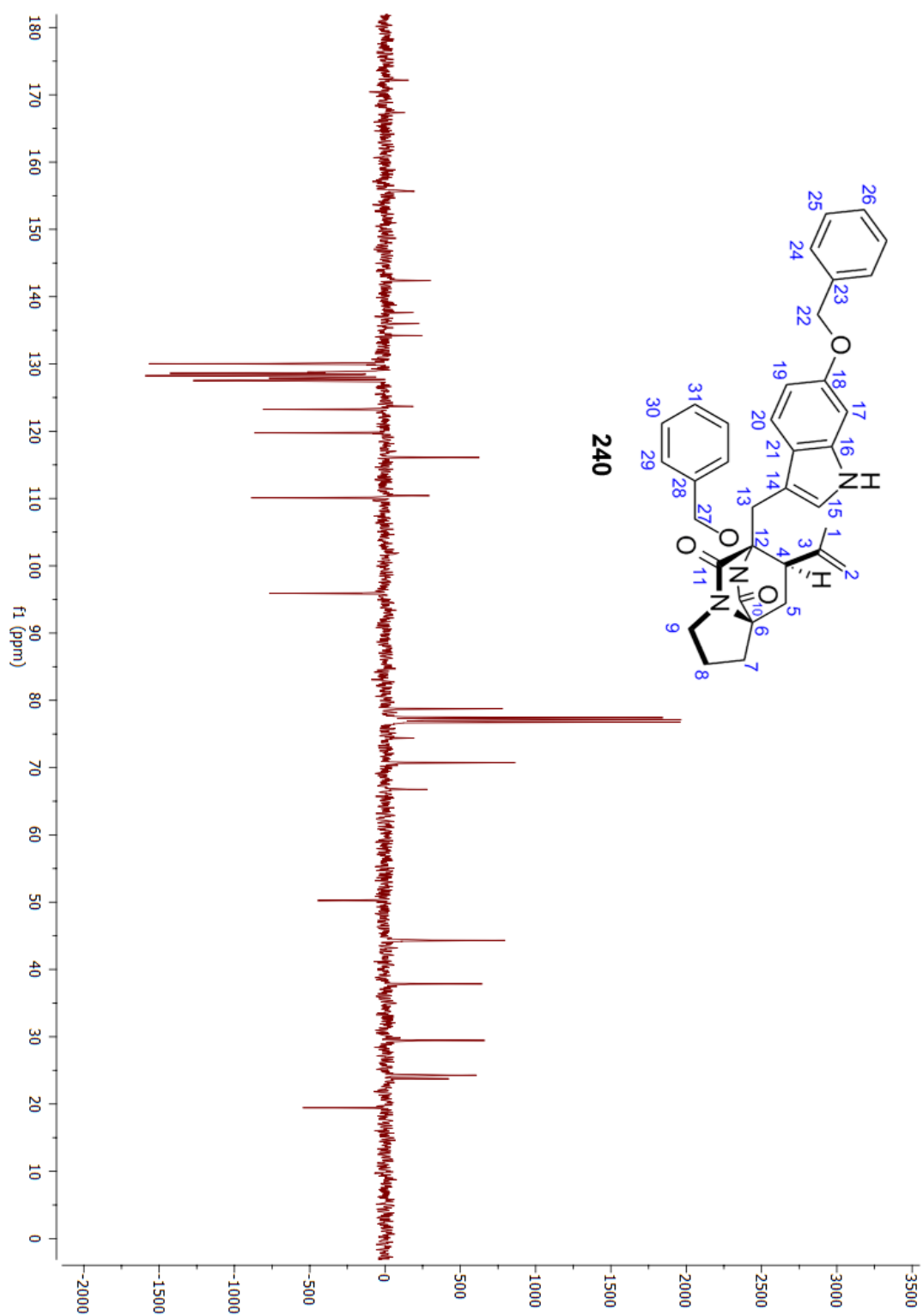
Appendix 10. ^{13}C -NMR spectrum of (**181**) (126 MHz, CDCl_3)



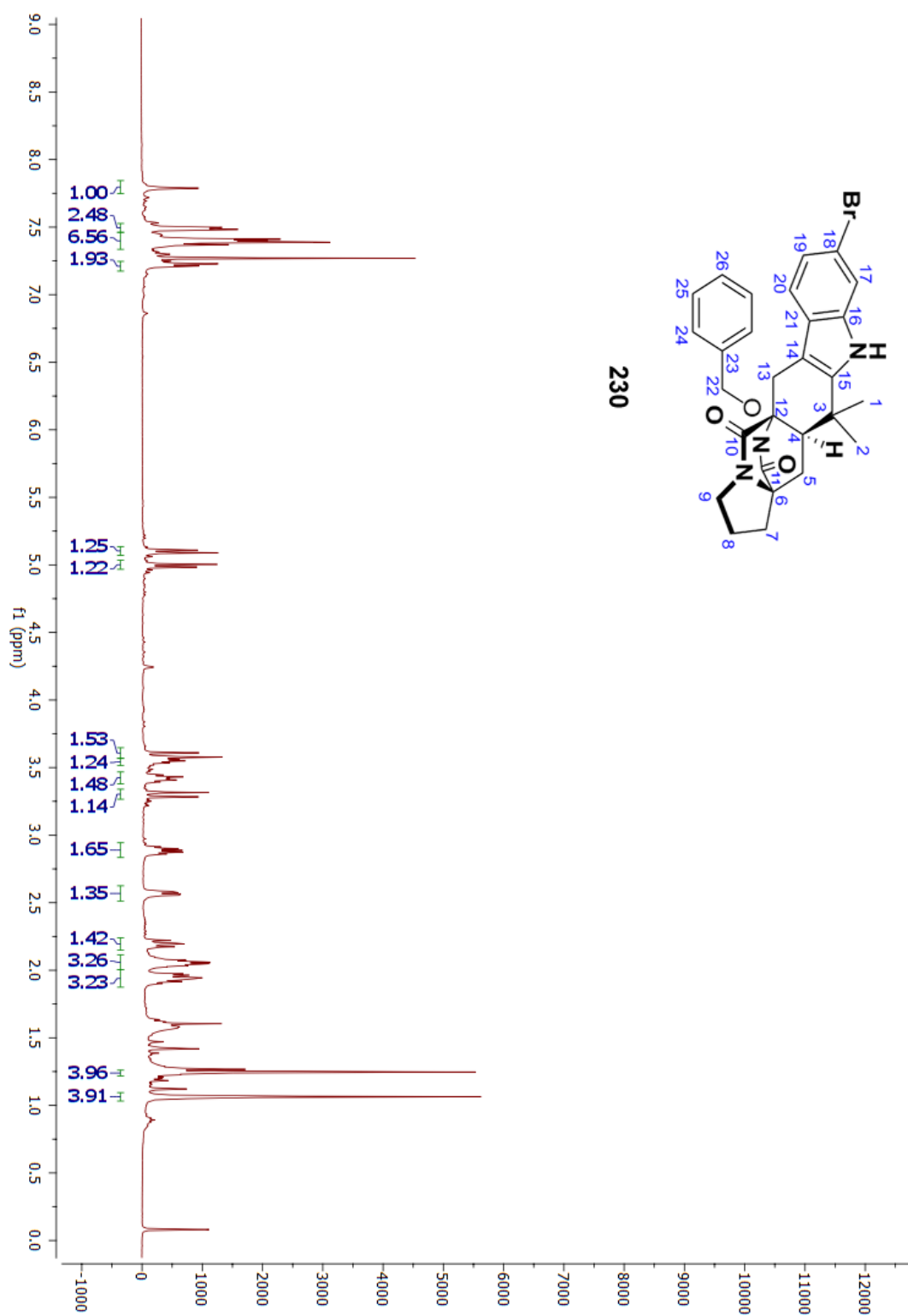
Appendix 11. ^1H -NMR spectrum of (**240**) (400 MHz, CDCl_3)



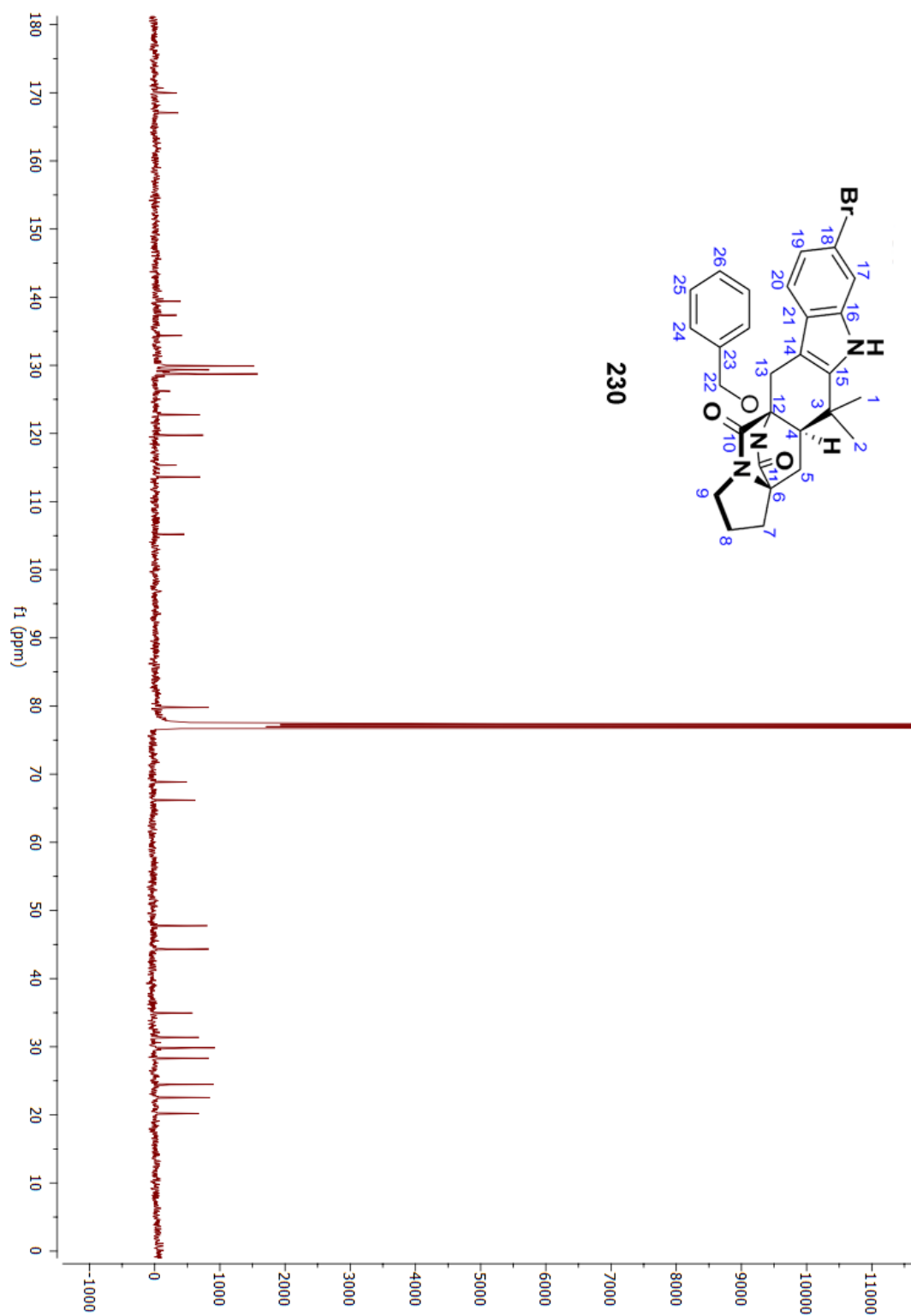
Appendix 12. ^{13}C -NMR spectrum of (**240**) (101 MHz, CDCl_3)



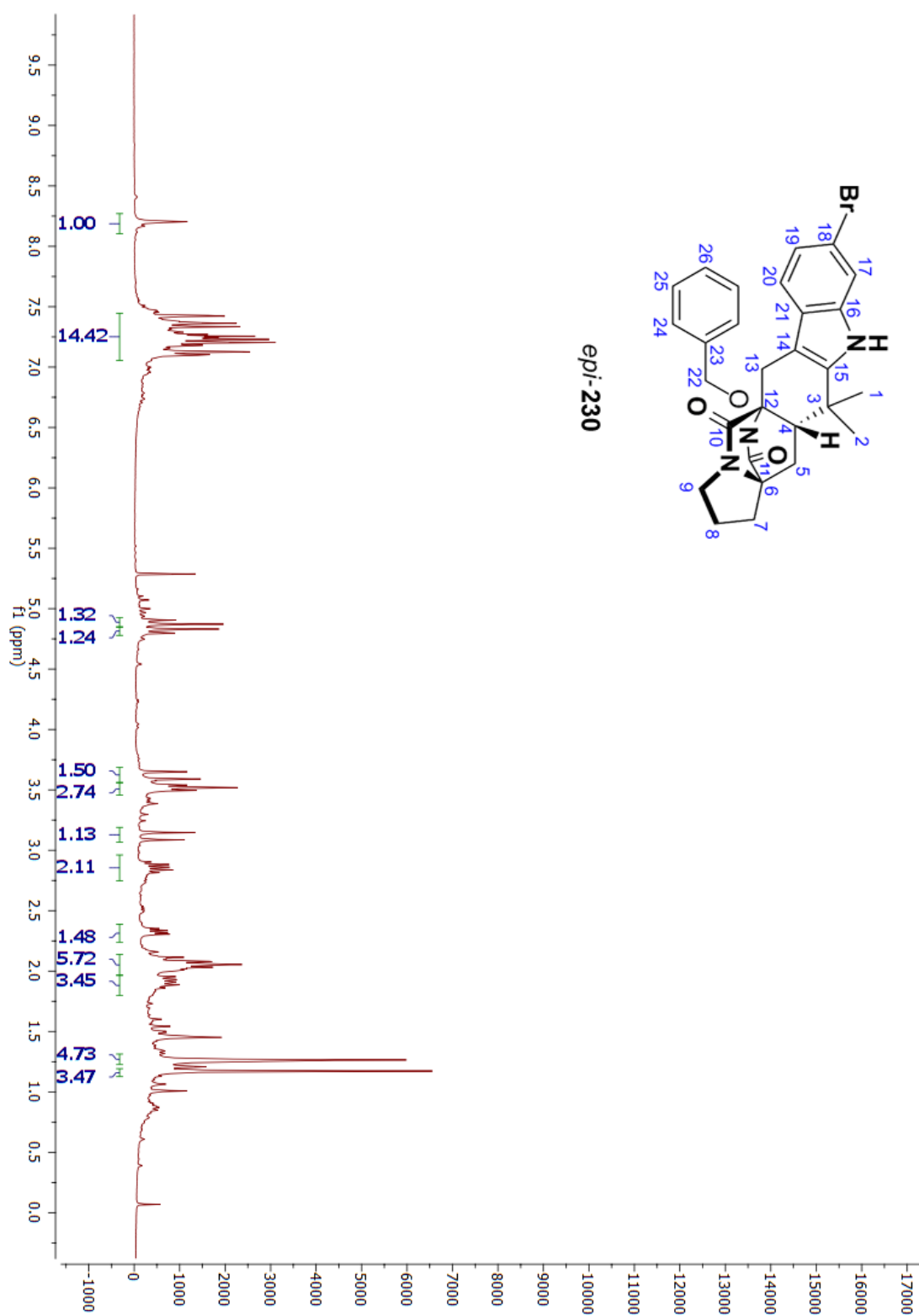
Appendix 13. ^1H -NMR spectrum of (**230**) (500 MHz, CDCl_3)



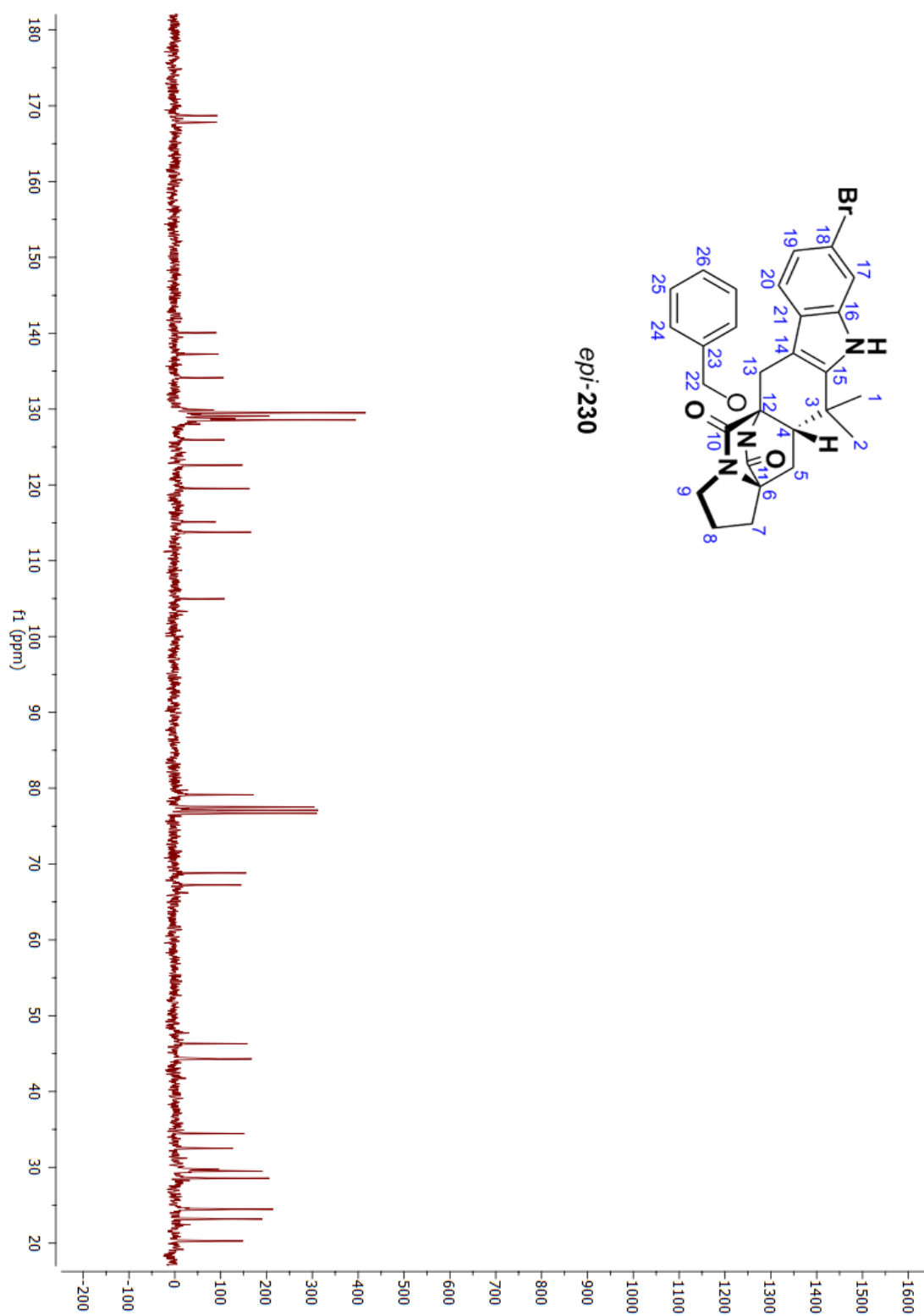
Appendix 14. ^{13}C -NMR spectrum of (**230**) (126 MHz, CDCl_3)



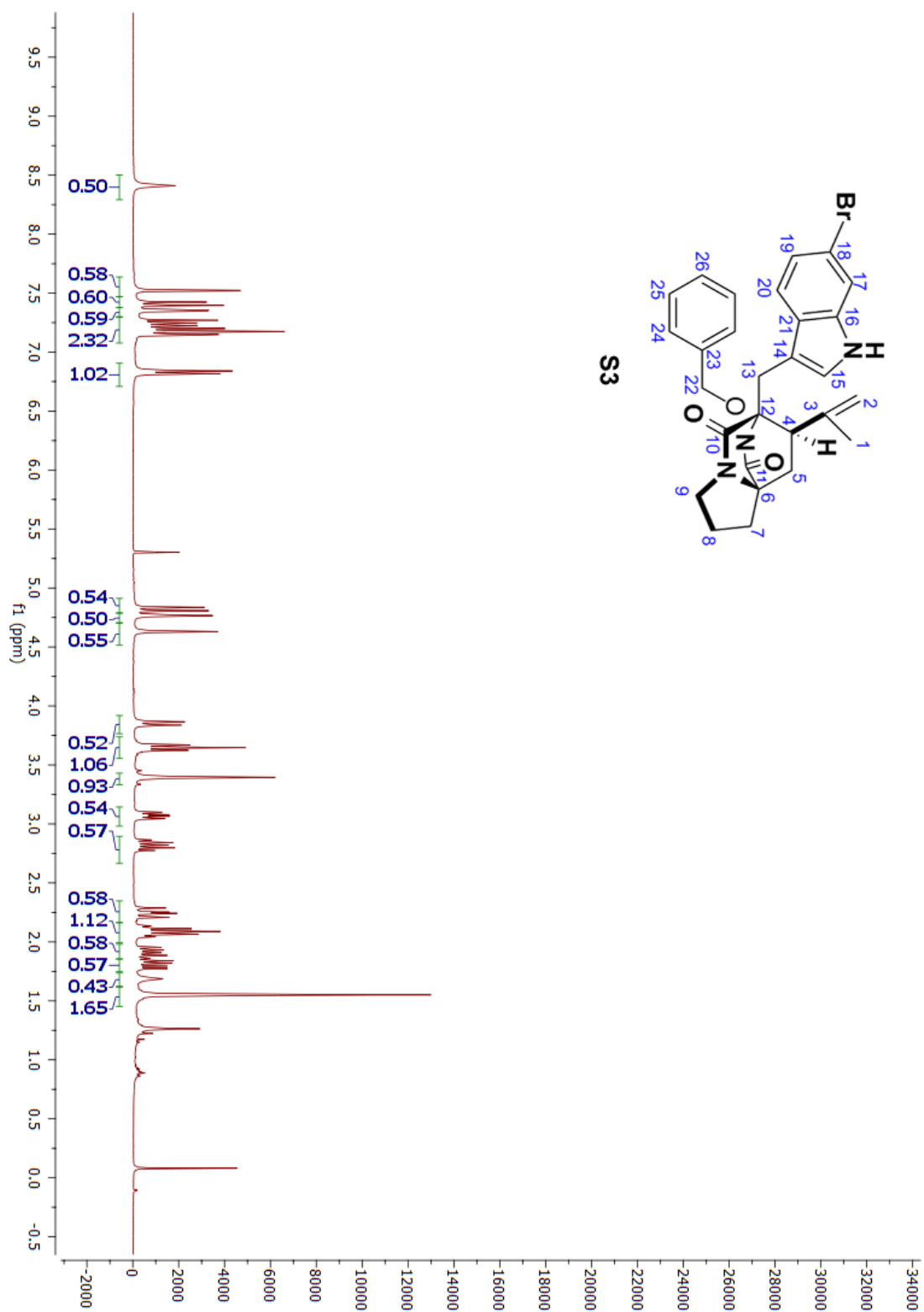
Appendix 15. ^1H -NMR spectrum of (*epi*-**230**) (300 MHz, CDCl_3)



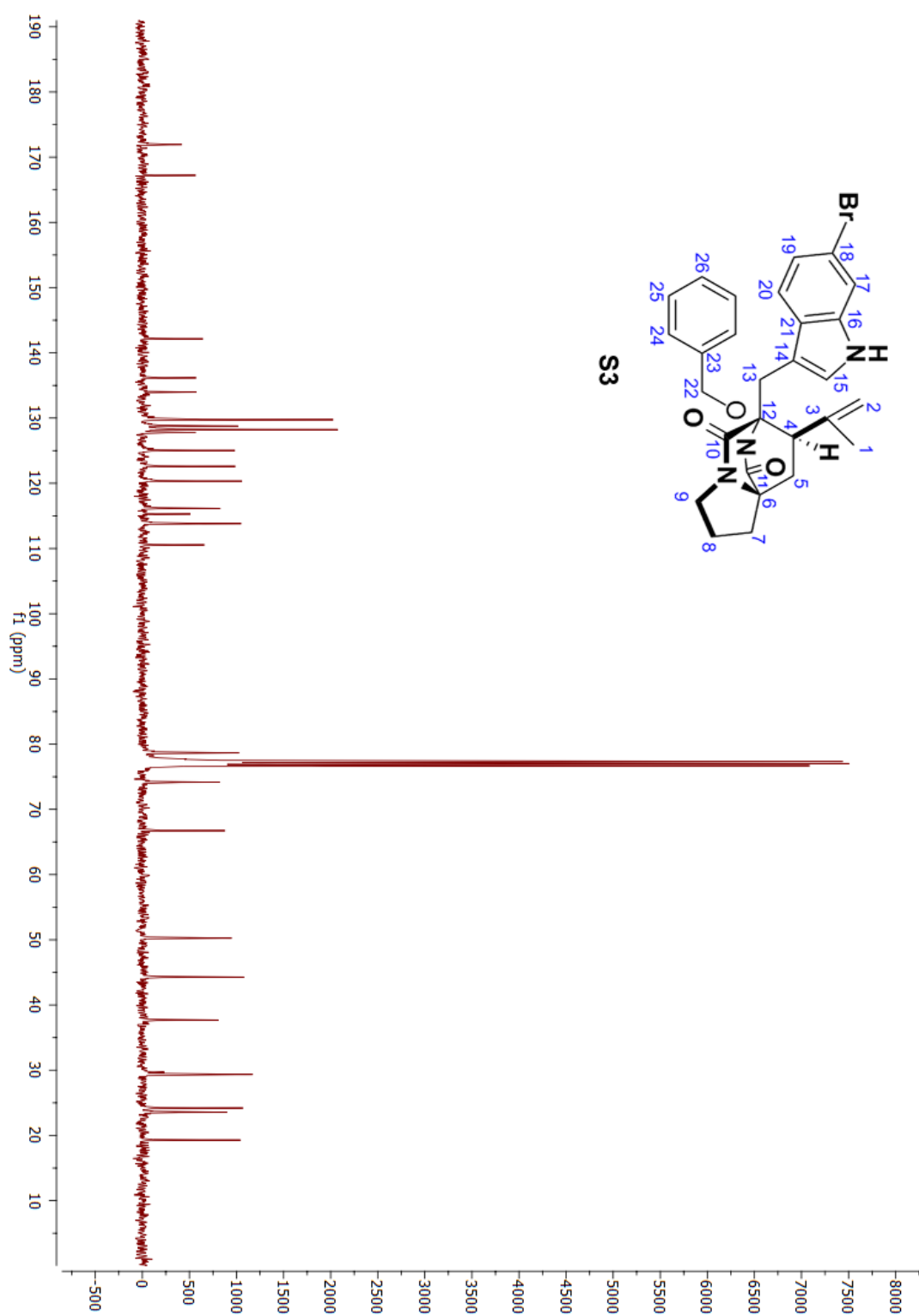
Appendix 16. ^{13}C -NMR spectrum of (*epi*-**230**) (75 MHz, CDCl_3)



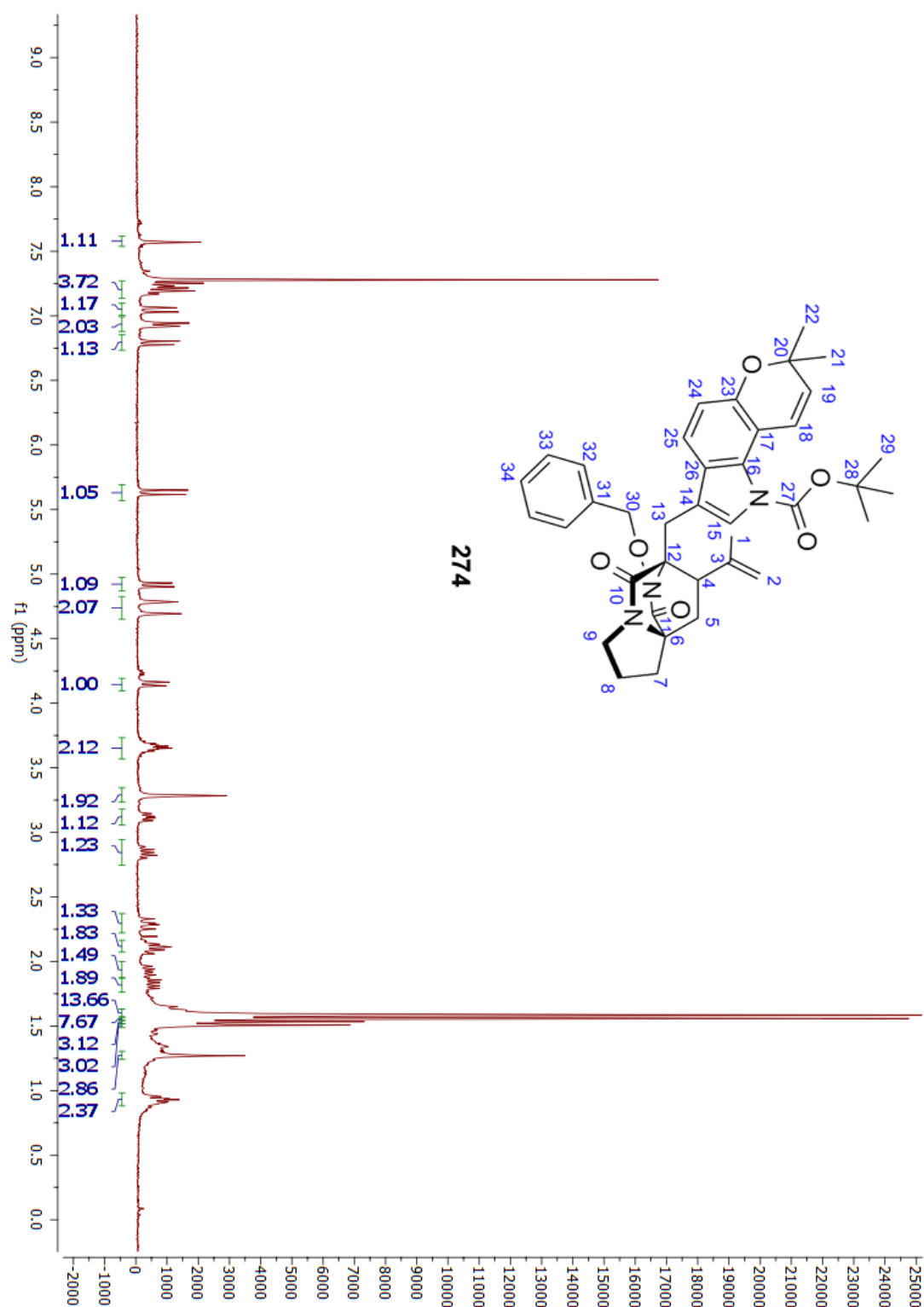
Appendix 17. ^1H -NMR spectrum of (**S3**) (300 MHz, CDCl_3)



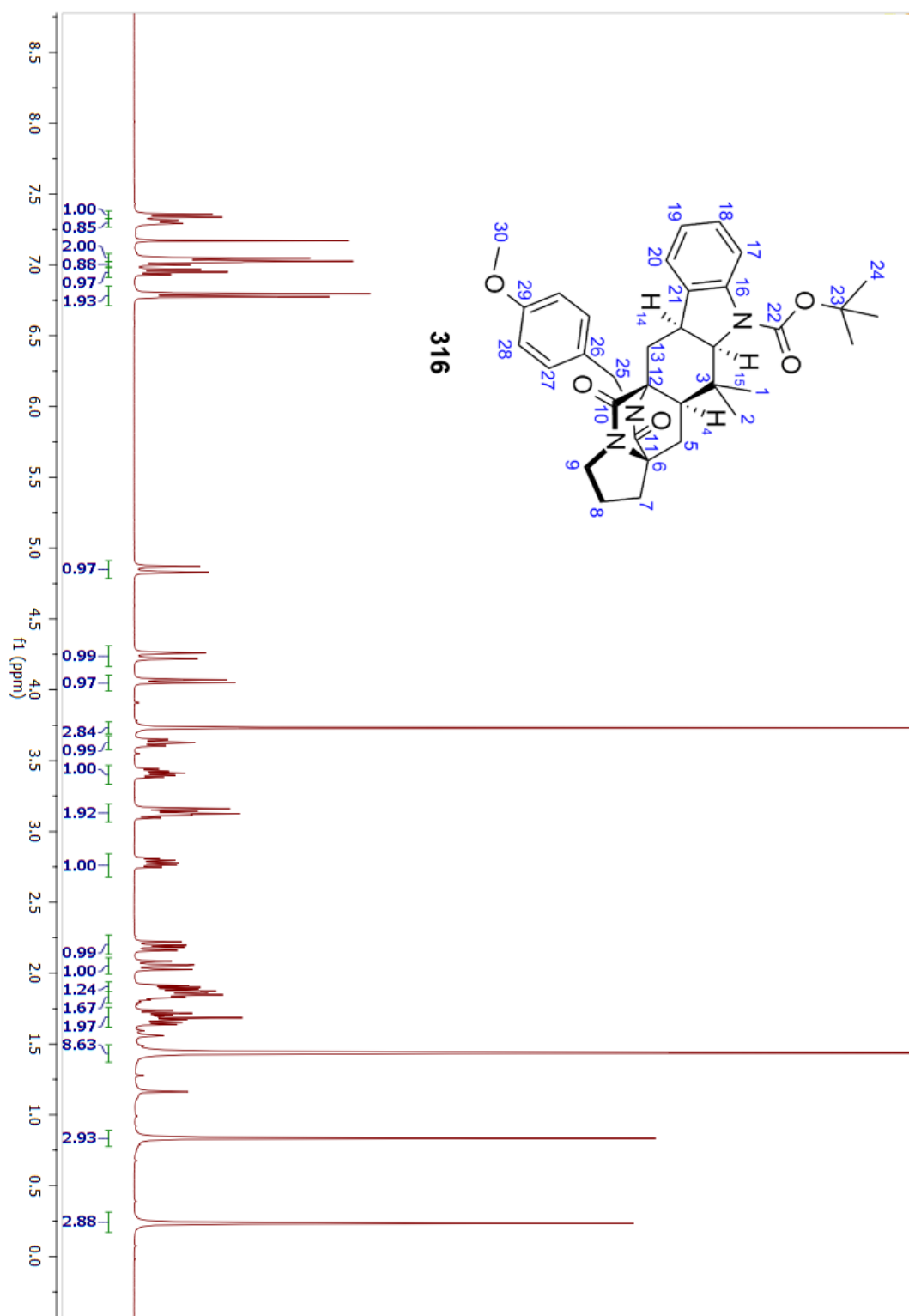
Appendix 18. ^{13}C -NMR spectrum of (**S3**) (101 MHz, CDCl_3)



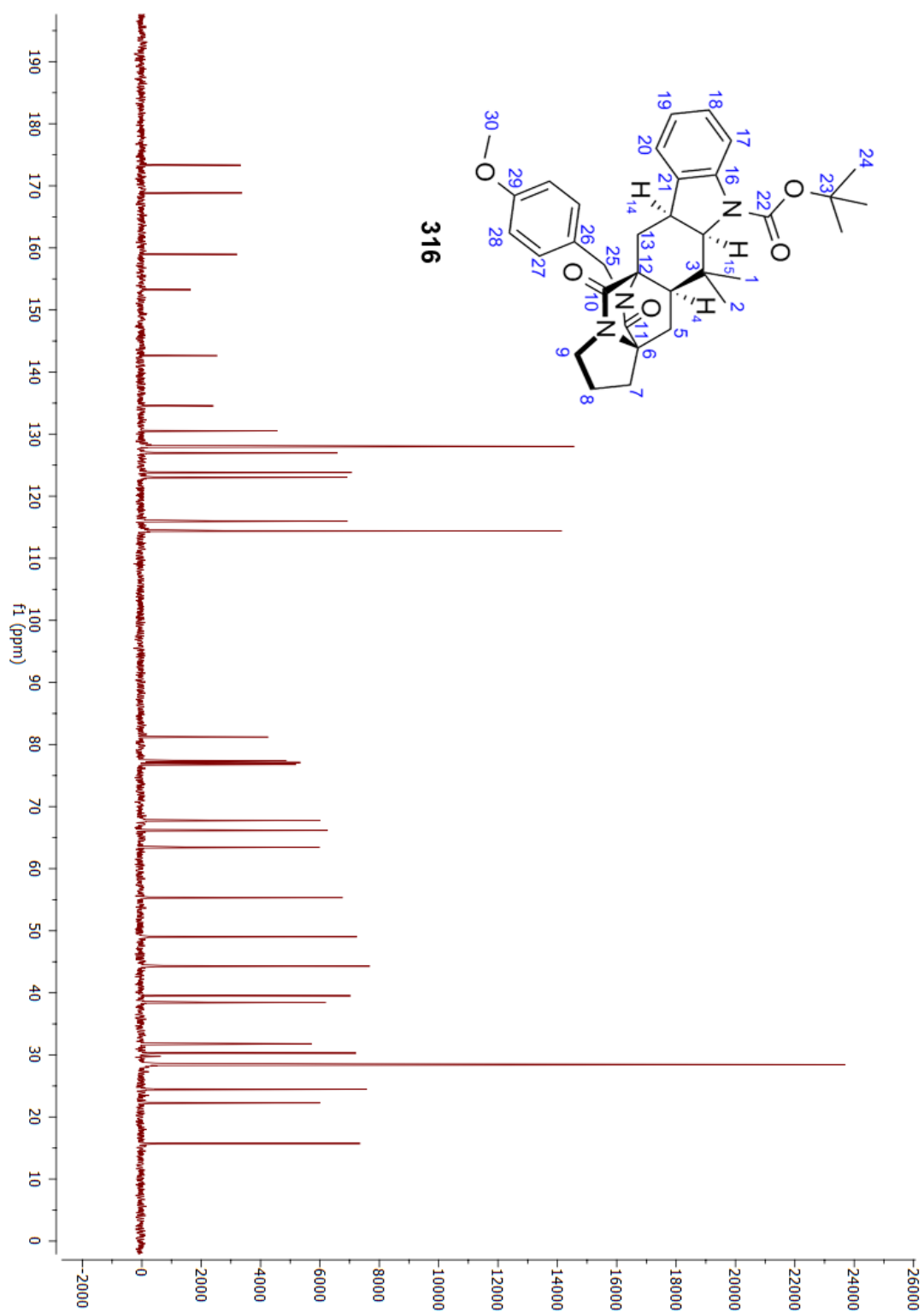
Appendix 19. ^1H -NMR spectrum of (**274**) (300 MHz, CDCl_3)



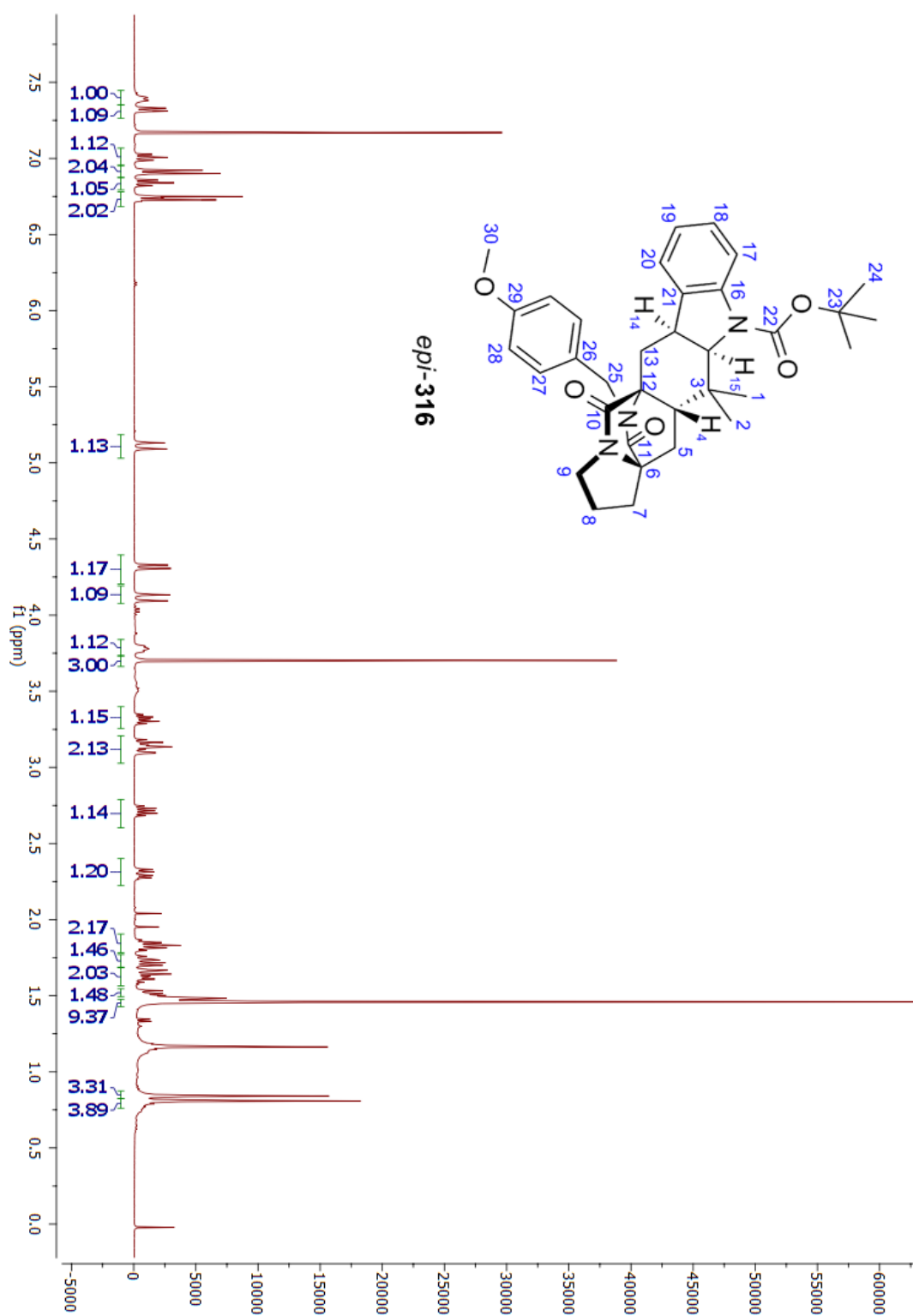
Appendix 20. ^1H -NMR spectrum of **(316)** (400 MHz, CDCl_3)



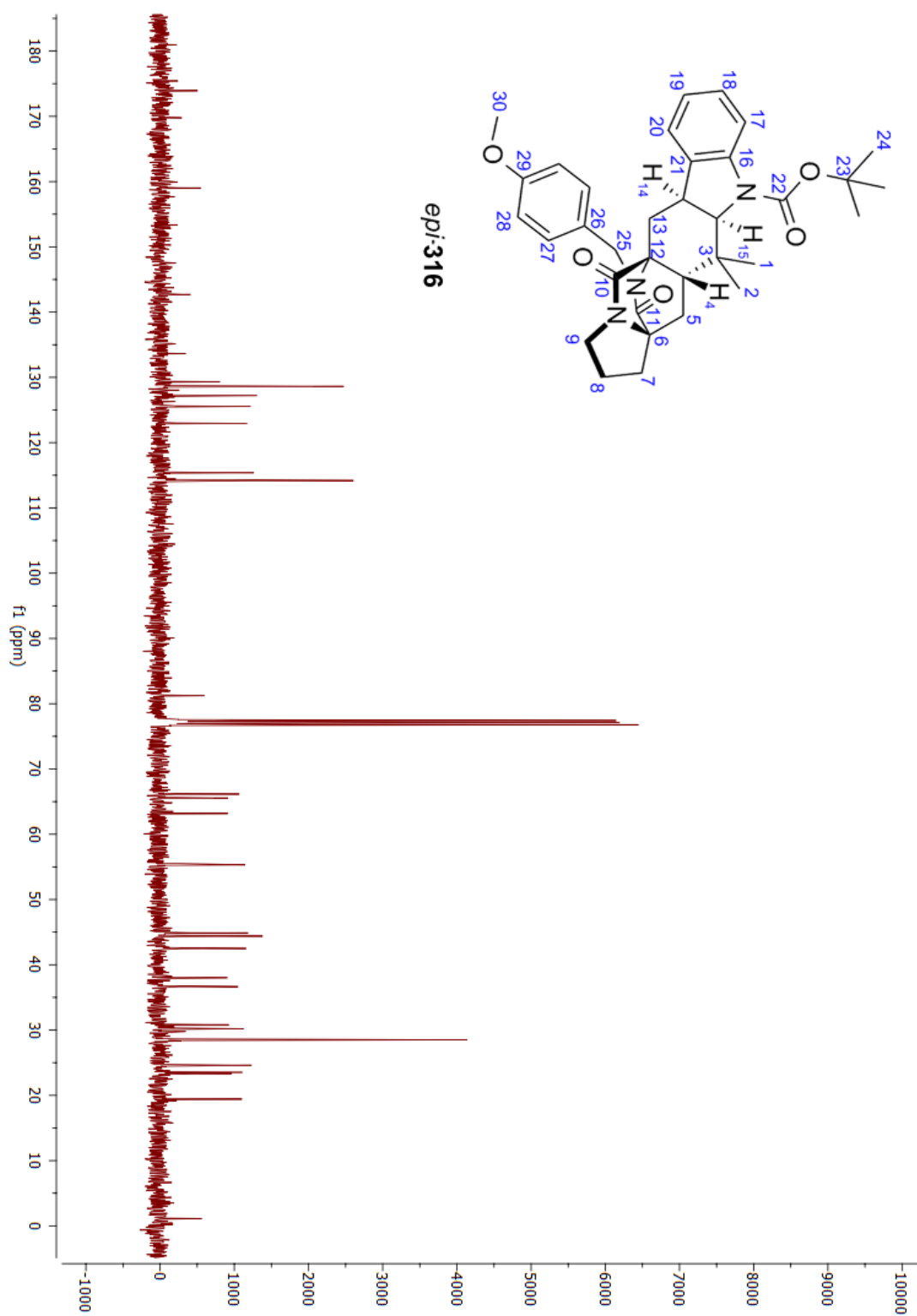
Appendix 21. ^{13}C -NMR spectrum of (**316**) (101 MHz, CDCl_3)



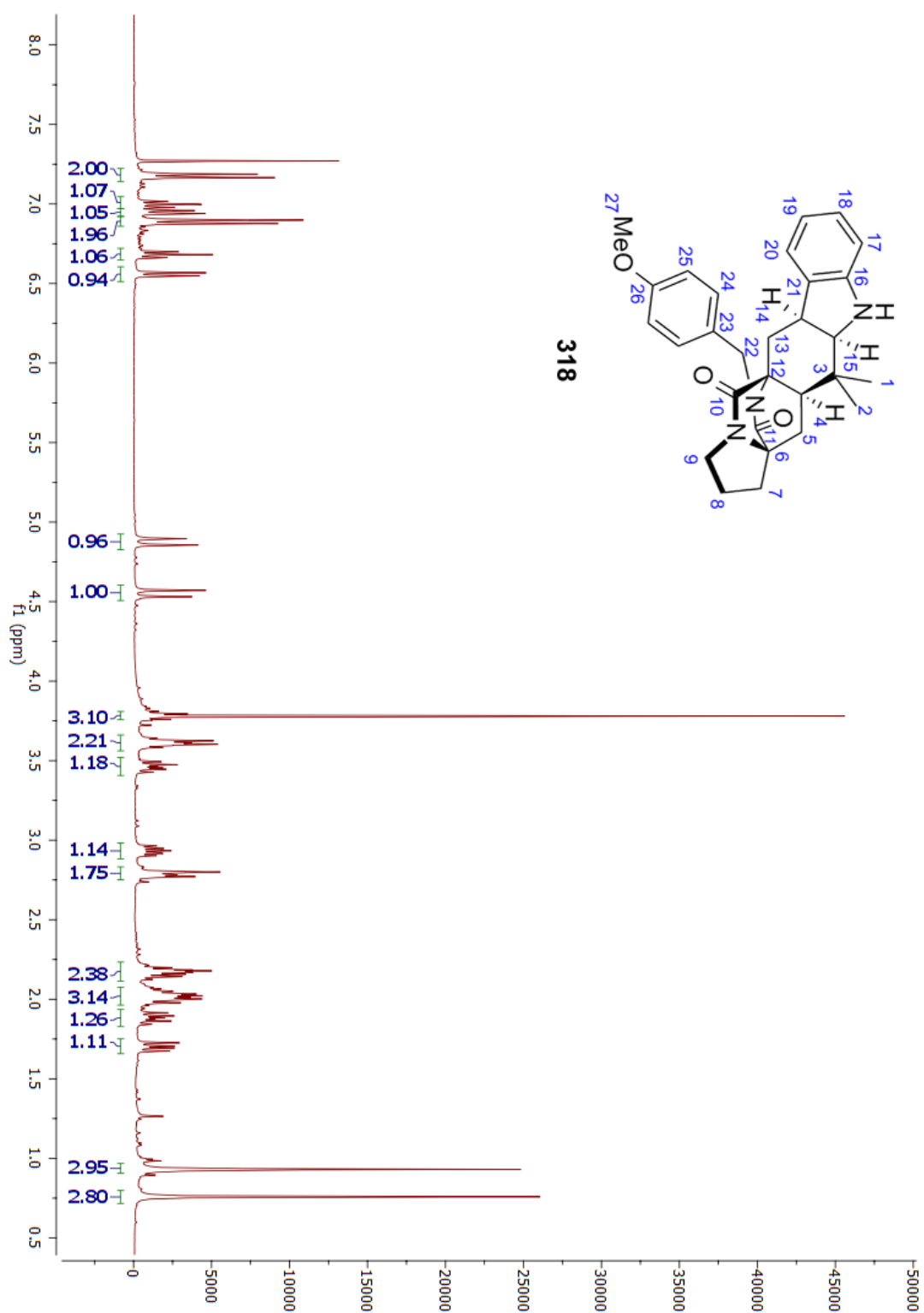
Appendix 22. ¹H-NMR spectrum of (*epi*-**316**) (400 MHz, CDCl₃)



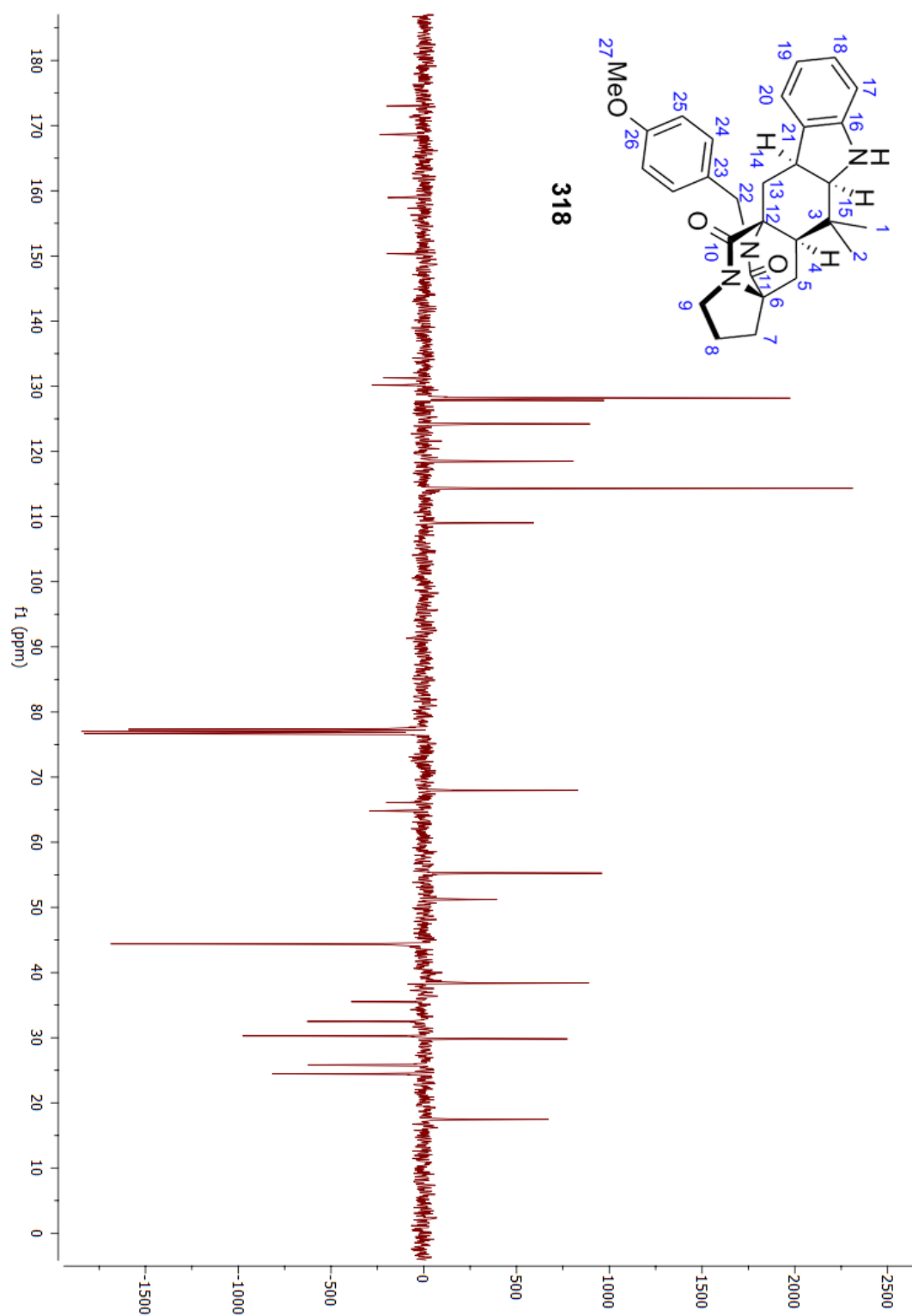
Appendix 23. ^{13}C -NMR spectrum of (*epi*-**316**) (101 MHz, CDCl_3)



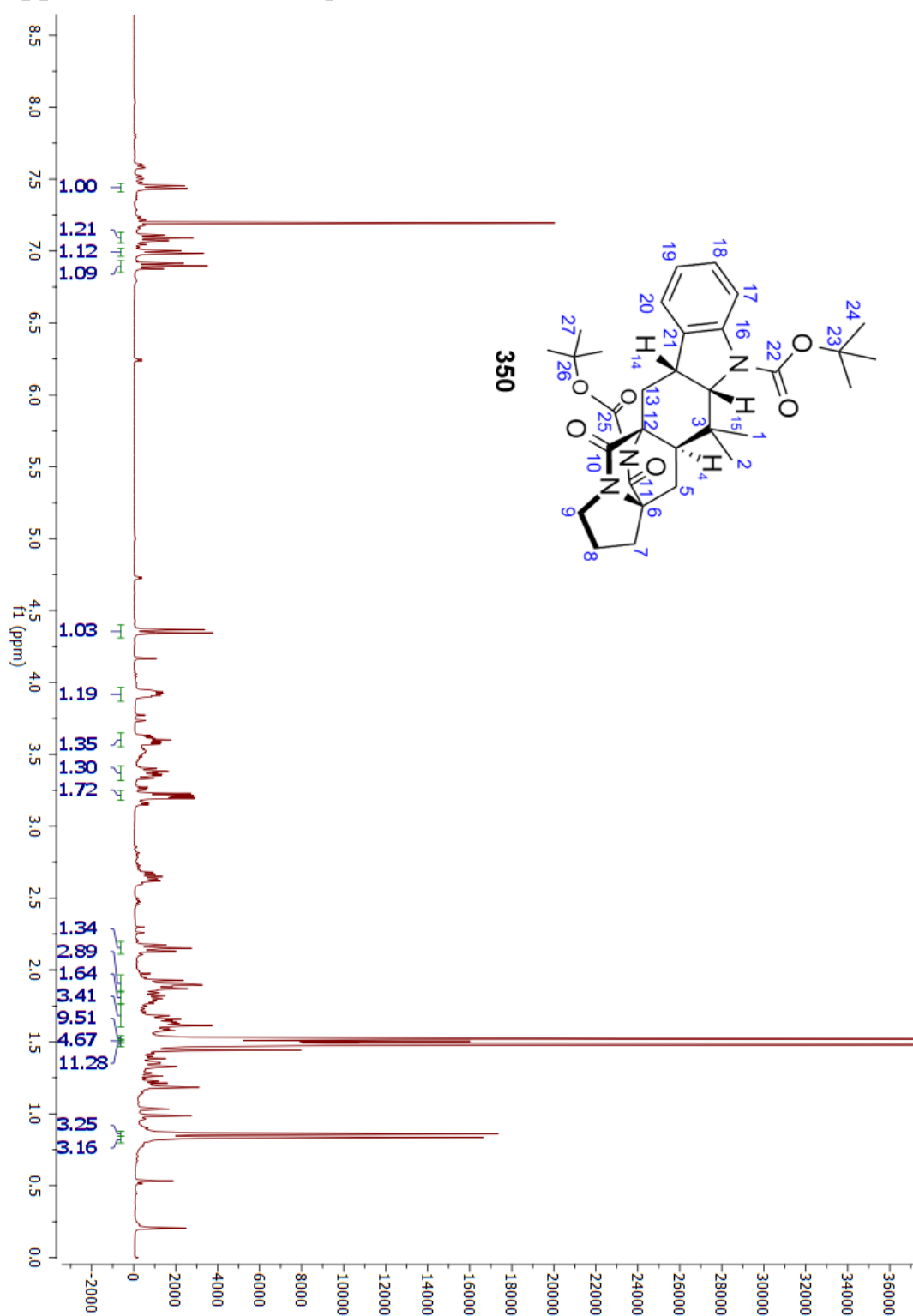
Appendix 24. ^1H -NMR spectrum of **(318)** (400 MHz, CDCl_3)



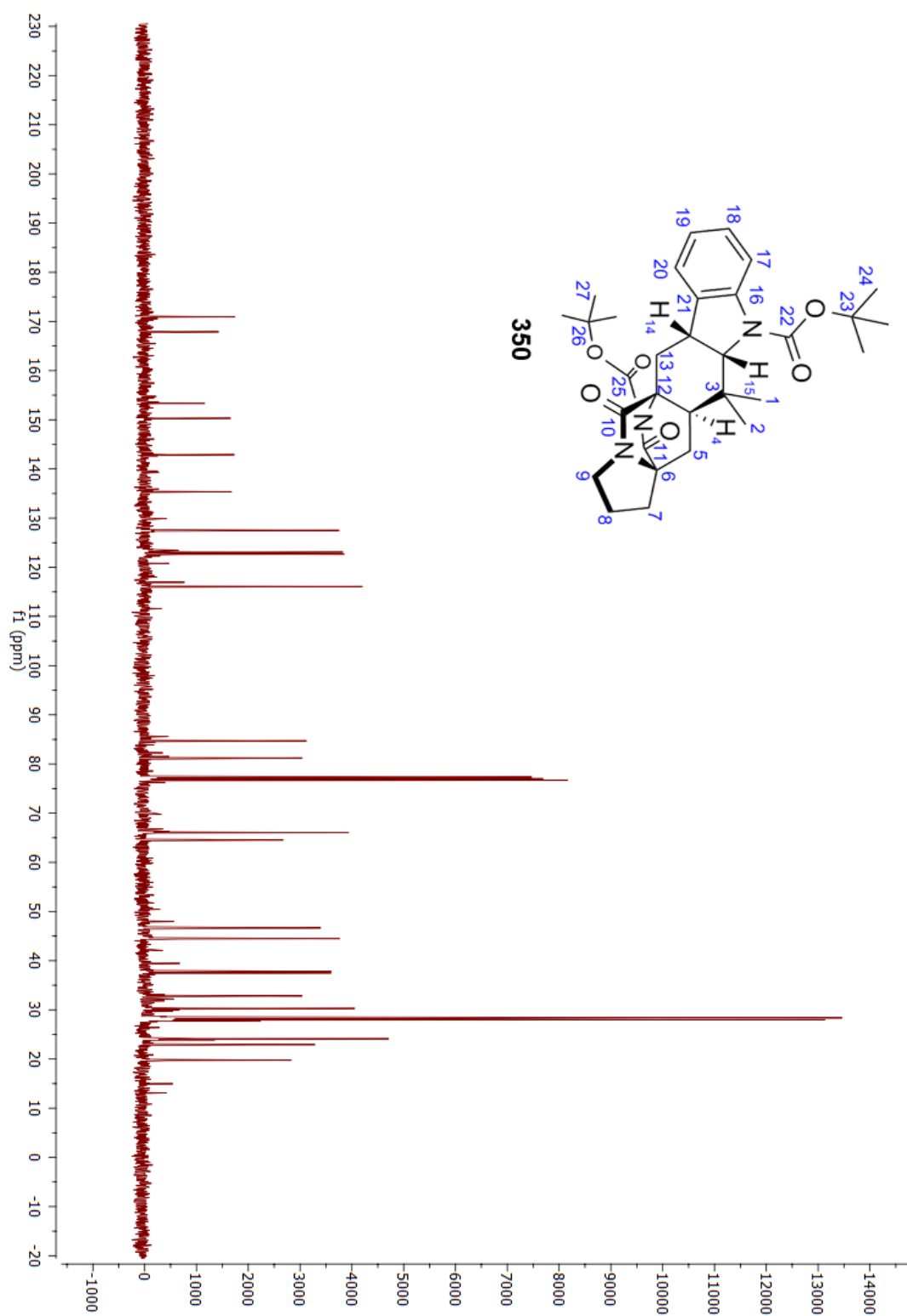
Appendix 25. ^{13}C -NMR spectrum of (**318**) (101 MHz, CDCl_3)



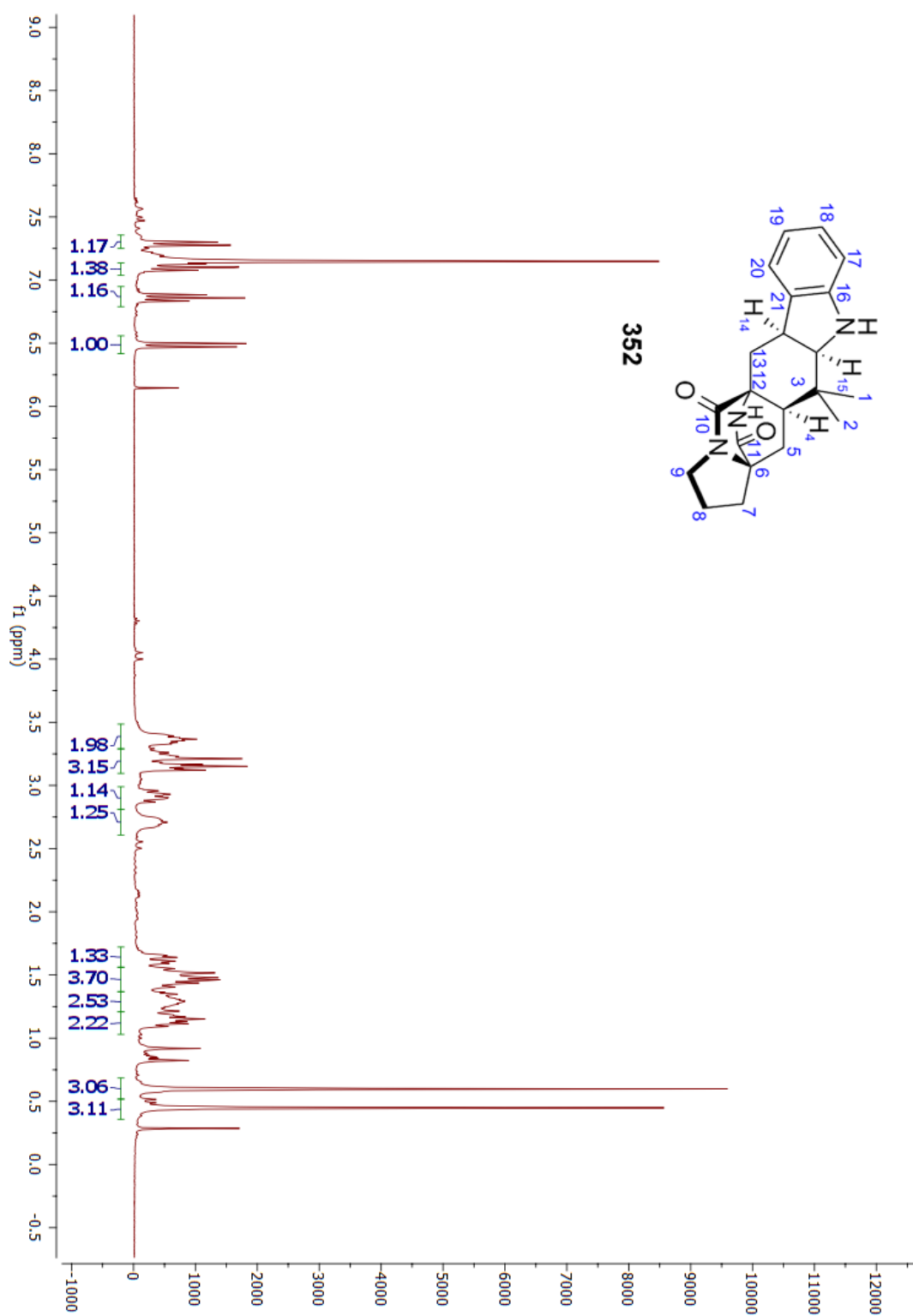
Appendix 26. ^1H -NMR spectrum of (**350**) (400 MHz, CDCl_3)



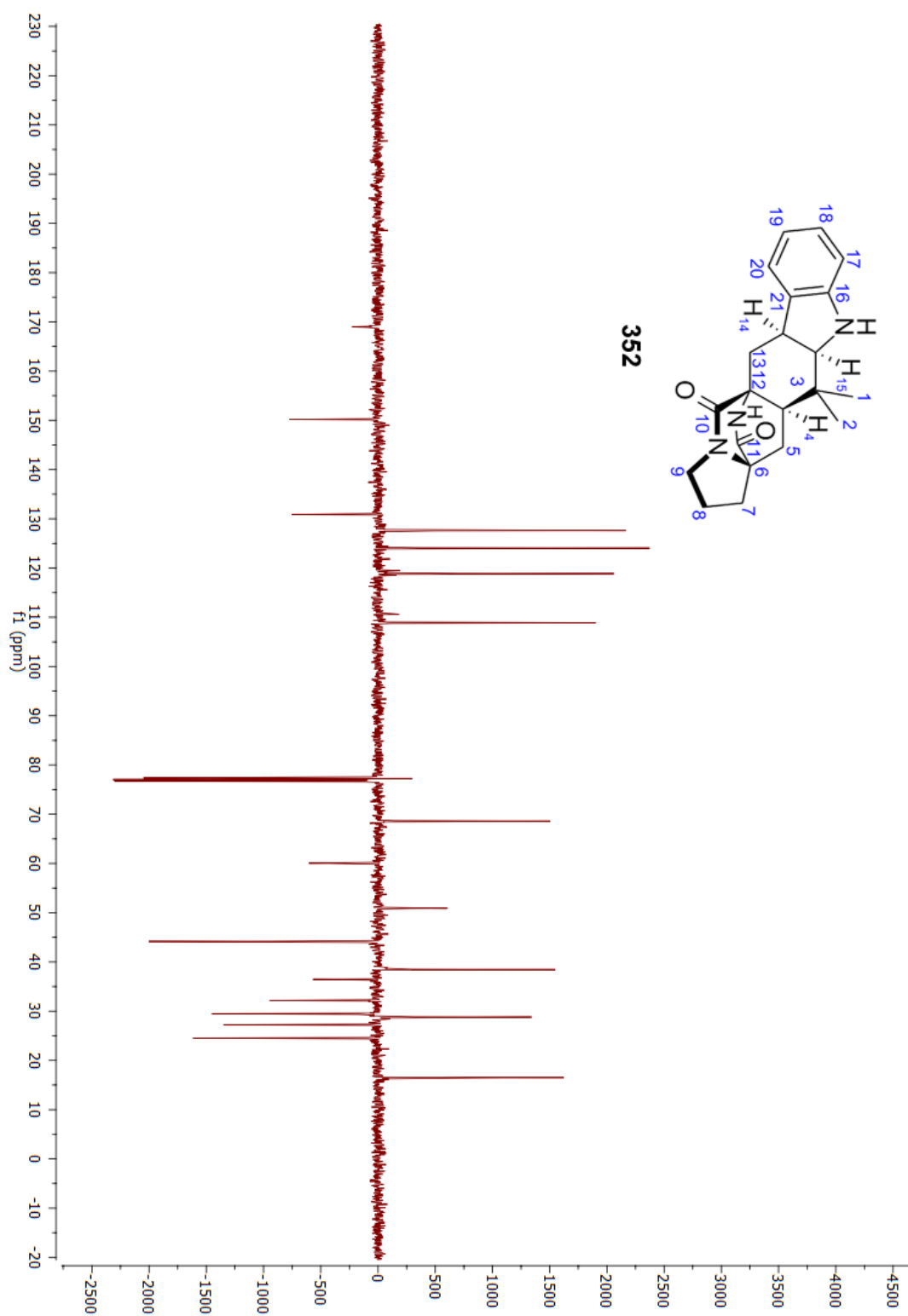
Appendix 27. ^{13}C -NMR spectrum of (**350**) (101 MHz, CDCl_3)



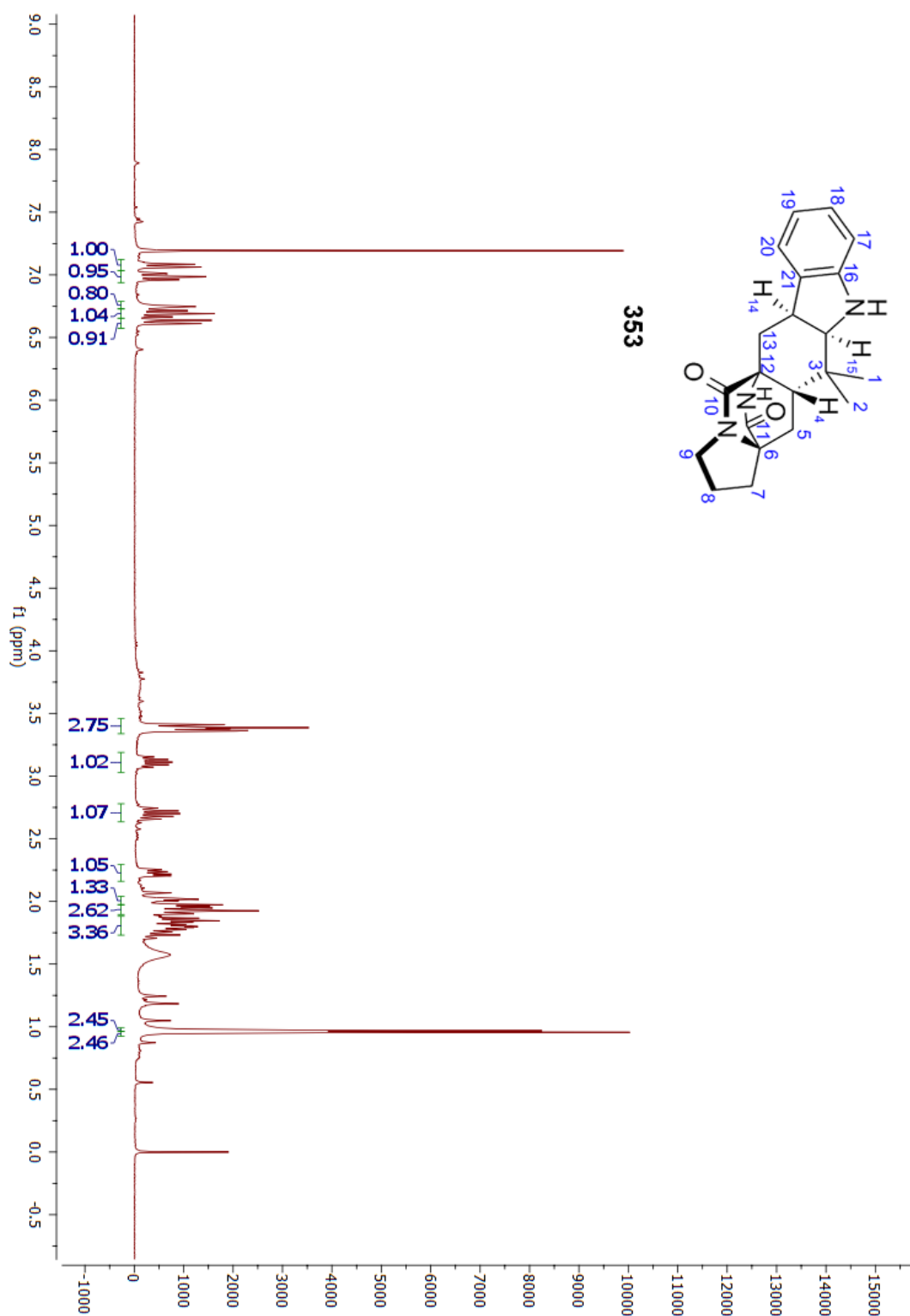
Appendix 28. ^1H -NMR spectrum of **(352)** (400 MHz, CDCl_3)



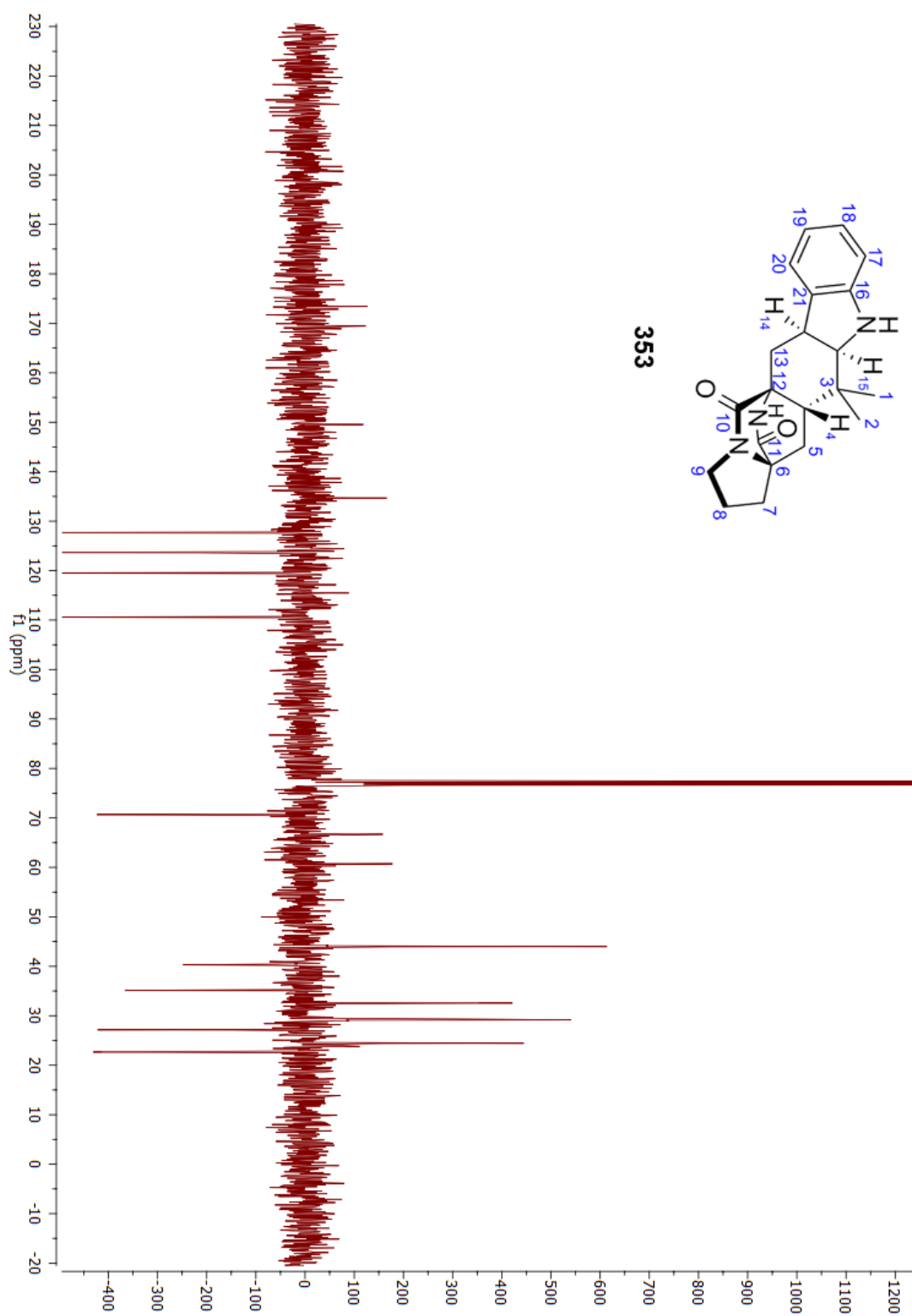
Appendix 29. ^{13}C -NMR spectrum of (**352**) (101 MHz, CDCl_3)



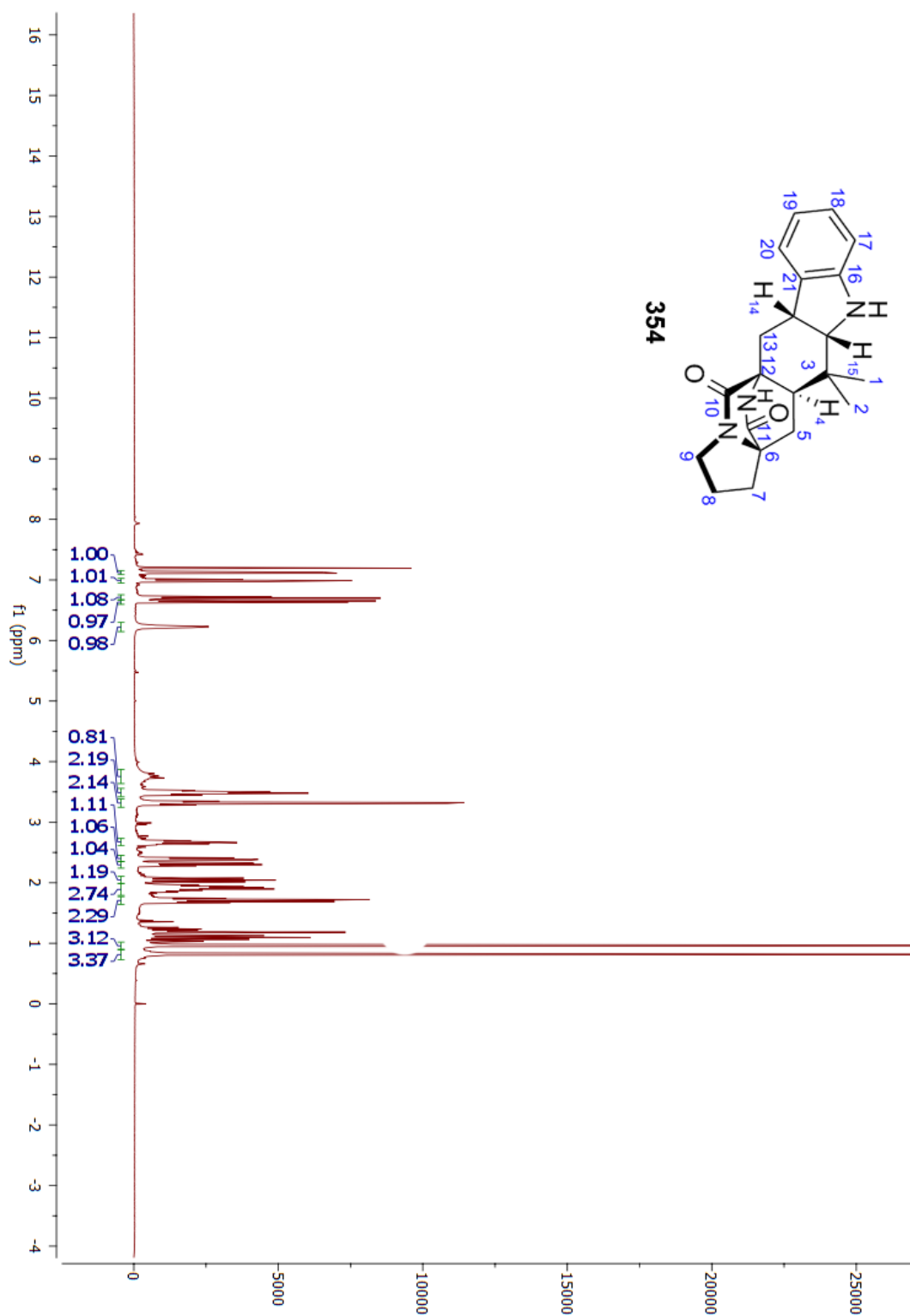
Appendix 30. ^1H -NMR spectrum of (**353**) (300 MHz, CDCl_3)



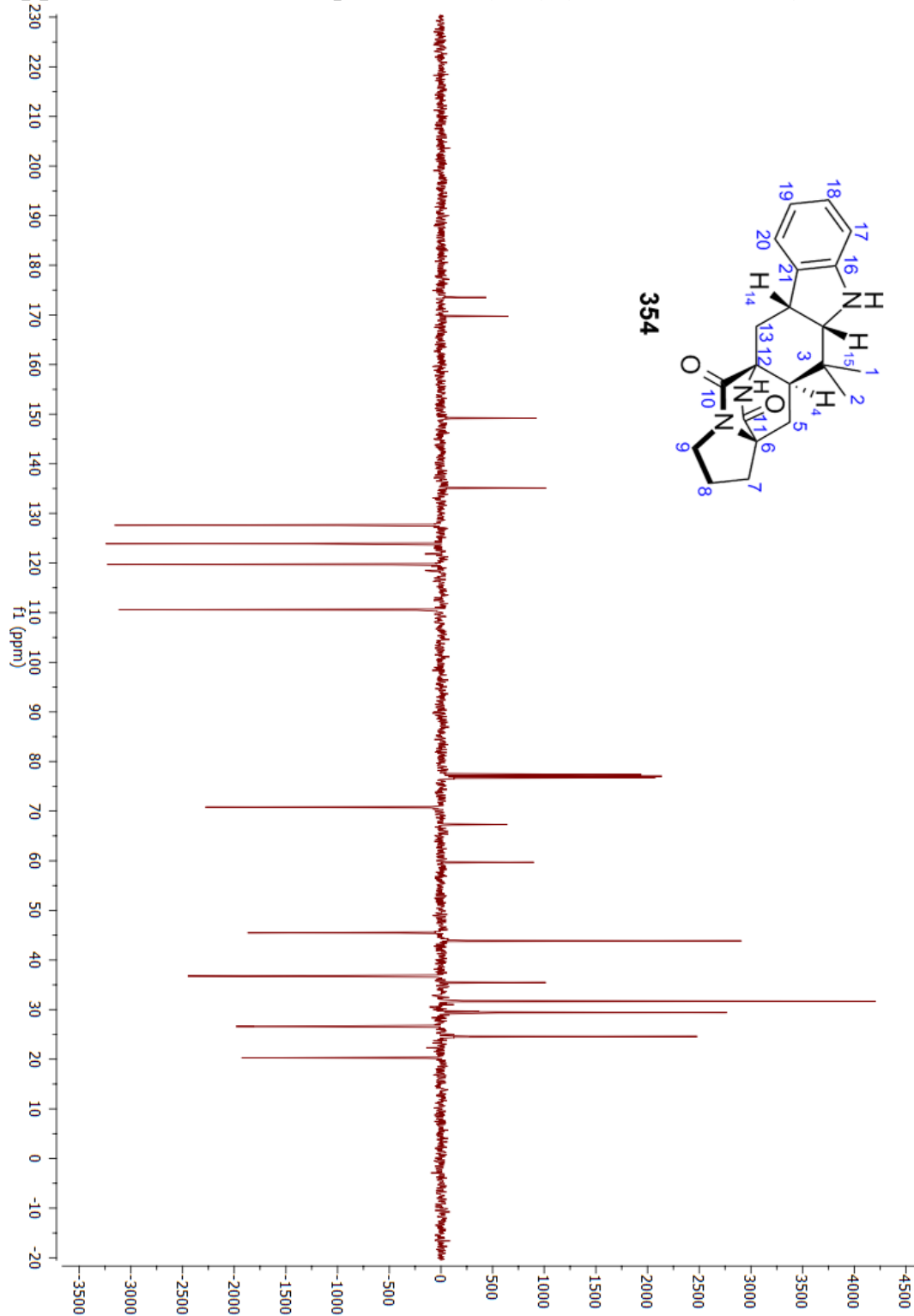
Appendix 31. ^{13}C -NMR spectrum of (**353**) (101 MHz, CDCl_3)



Appendix 32. ^1H -NMR spectrum of (**354**) (400 MHz, CDCl_3)



Appendix 33. ^{13}C -NMR spectrum of (**354**) (101 MHz, CDCl_3)



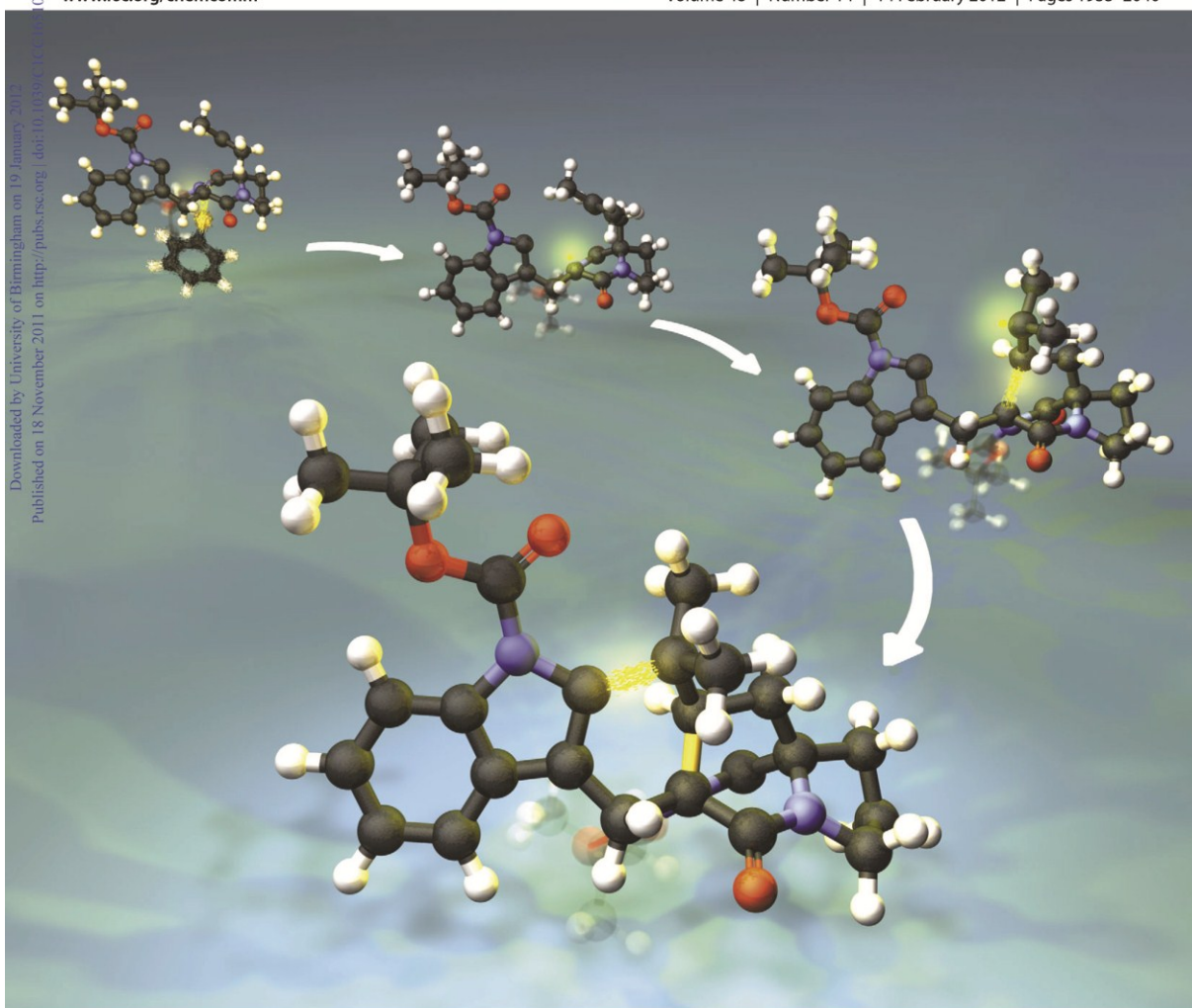
ChemComm

Chemical Communications

www.rsc.org/chemcomm

Volume 48 | Number 14 | 14 February 2012 | Pages 1933–2040

Downloaded by University of Birmingham on 19 January 2012
Published on 18 November 2011 on <http://pubs.rsc.org> | doi:10.1039/C1CC12008K



ISSN 1359-7345

RSC Publishing

COMMUNICATION

Nigel Simpkins *et al.*

Rapid access to polycyclic indolines related to the stephacidin alkaloids using a radical cascade



1359-7345(2012)48:14;1-D

Rapid access to polycyclic indolines related to the stephacidin alkaloids using a radical cascade†

Nigel Simpkins,* Ilias Pavlakos and Louise Male

Received 19th October 2011, Accepted 17th November 2011

DOI: 10.1039/c1cc16510k

A new and very rapid access to indoline intermediates useful for the synthesis of alkaloids related to the stephacidins has been established using a radical cascade process initiated from a sulphur-substituted diketopiperazine.

Stephacidins A (**1**) and B (**2**), first described in 2002 by Qian-Cutrone and co-workers, were isolated from the mitosporic fungus *Aspergillus ochraceus* WC76466.¹ These cytotoxic alkaloids were clearly related to members of the prenylated indole family, particularly avrainvillamide (**3**), which had been previously isolated by two other research groups (Fig. 1).^{2,3}

These compounds quickly became the focus of attention for a number of research groups, due to their intriguing structures and *in vitro* activity against several tumour cell lines.⁴ Most notably stephacidin B showed very low μM IC₅₀ values against testosterone-dependent LNCaP (prostate) cells, and appeared to exert this effect through a novel mode of action.

Subsequently, Myers and co-workers demonstrated the interconversion of alkaloids **2** and **3** in cell culture medium, and established that **2** exerts its antiproliferative activity through dissociation into the electrophilic monomer **3**—subsequently shown to bind the nuclear chaperone nucleophosmin.⁵ Syntheses of one or more members of this group were also demonstrated by the research groups of Myers, Baran and Williams.⁶

The seminal work of Baran established the pivotal role of indoline intermediates in achieving the ascent in oxidation state from stephacidin to avrainvillamide (and thus to stephacidin B), and this approach was also used to access biologically active model compounds, *e.g.*, the preparation of avrainvillamide model **6** from **4** via indoline **5** Scheme 1.⁷

Notwithstanding the brevity and elegance of such contributions, we became interested in new and very short enantiospecific routes that would provide direct access to indolines like **5**. We have recently described a cationic cascade approach to members of this family of alkaloids, which culminated in the synthesis of the calmodulin inhibitor malbrancheamide B.⁸ Herein we describe a strategically related approach, using a radical cascade,

which conveniently enables direct access to the indoline intermediate **5** shown in Scheme 1.⁹

Our analysis of the key radical cascade is shown in Scheme 2. The desired indoline (**5**, $R = R_1 = \text{H}$) would arise from a precursor diketopiperazine (DKP) **7** in which an appropriate substituent X would serve to deliver an initial carbon-centred radical. Tandem 6-*exo-trig* and 6-*endo-trig* cyclisations would then furnish **5**.

The strategy raises issues of regiocontrol and stereocontrol (specifically at C-6), as well as requiring proper choice of the radical initiating group X, and possible nitrogen protecting groups R and R_1 .¹⁰

The first iteration of the above concept utilised our previously described regio- and stereo-controlled substitution of mixed proline DKPs via enolate intermediates, Scheme 3.¹¹

DKP **8** was easily assembled in five steps, starting from tryptophan, using standard techniques. Conversion into fully substituted DKP **9a** (a particular variant of **7**) was then possible *in one pot* by sequential prenylation and sulfenylation. As noted for a related example,¹¹ the initial alkylation proceeds with complete retention of configuration at the proline residue, and the sulfenylation occurs with clean inversion of configuration (although the latter outcome is of no consequence here).

The doubly Boc-protected DKP **9b** was also readily available via protection and high-yielding sulfenylation of prenylated DKP **10**. In this case we chose to assemble the latter compound from a preformed prenylated proline residue and a protected tryptophan unit, as in our earlier malbrancheamide work.⁸

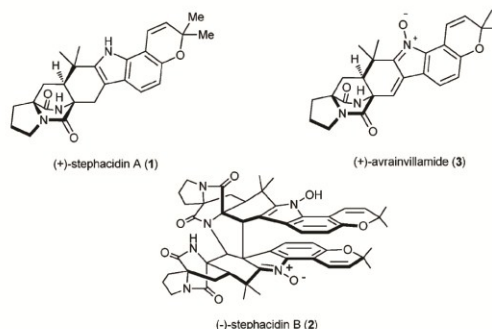
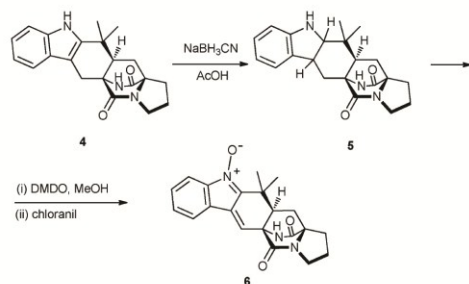


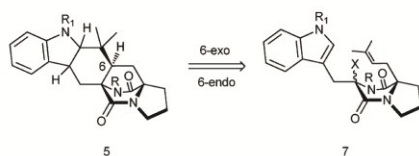
Fig. 1 The stephacidins and avrainvillamide.

School of Chemistry, University of Birmingham, Edgbaston, Birmingham, B15 2TT, UK. E-mail: n.simpkins@bham.ac.uk

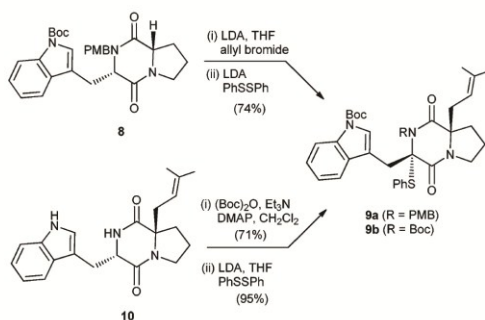
† Electronic supplementary information (ESI) available: Experimental procedures, compound characterisation data, and copies of NMR spectra. CCDC 848586. For ESI and crystallographic data in CIF or other electronic format see DOI: 10.1039/c1cc16510k



Scheme 1 Baran's access to avrainvillamide model 6 (L-series).



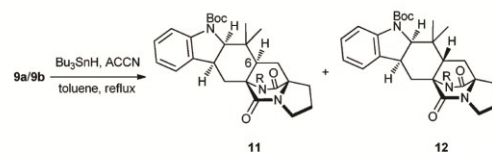
Scheme 2 Analysis of the planned radical cascade.



Scheme 3 Preparation of sulphenylated DKPs.

To our satisfaction, treatment of sulphenyl DKP **9a** with Bu₃SnH and ACCN [1, 10-azobis (cyclohexanecarbonitrile)] in toluene at reflux provided indolines **11** and **12** in 86% combined yield, and in a 4.6:1 ratio favouring the C-6 diastereoisomer required for natural product synthesis, Scheme 4.¹²

The structural assignments shown, including stereochemistry, were supported by detailed NMR analysis, including nOe experiments.¹³ Subsequent comparison with structures determined



Scheme 4 Cascade cyclisation to give fused indolines (*R* = PMB or Boc).

by X-ray crystallography further secured the identities of these compounds (*vide infra*).

The stereochemical outcome at C-6 seen in Scheme 4 follows our predictions, based on previous work on analogous cationic cyclisations, in which minimisation of interactions between the DKP nitrogen protection and the *gem*-dimethyl of the prenyl appendage seems to be important.^{8,11}

Unfortunately, removal of the PMB protection from indoline **11** proved equally problematic as for the indoles in this series.¹⁴ To address this issue we carried out the double radical cyclisation with the all Boc-protected system **9b**. This reaction provided the all Boc-protected analogues of **11** and **12**, along with lesser amounts of other indoline isomers in 79% combined yield (see ESI for details†). Again, isomers with the correct C-6 stereochemistry for stephacidin synthesis predominated in an overall 3:1 ratio. Subsequent treatment of an inseparable mixture of the two major indolines (**11** and **12**, *R* = Boc) with formic acid enabled isolation of the major product **5** as a crystalline solid. Subsequent X-ray structure determination then confirmed our stereochemical assignments for this series of compounds (Fig. 2).^{15,16}

The all *syn* arrangement of hydrogen atoms at the newly formed asymmetric centres imbues the molecule with a distinctive bent shape. This arrangement arises from a transition state in which the benzenoid part of the reacting indole is orientated away from the Boc protection residing on the DKP.

We have described a novel radical cascade entry to the prenylated indole family of alkaloids, which provides indoline products that are key stepping stones to avrainvillamide, stephacidin B, and their bioactive analogues. The synthetic sequences from commercial materials to the indolines **11/12** are only 7 steps long. Further streamlining, involving optimisation of stereocontrol and protecting group issues, and application to more highly substituted targets, is underway.

We acknowledge the University of Birmingham for support of IP. The NMR instruments used in this research were obtained through Birmingham Science City: Innovative Uses

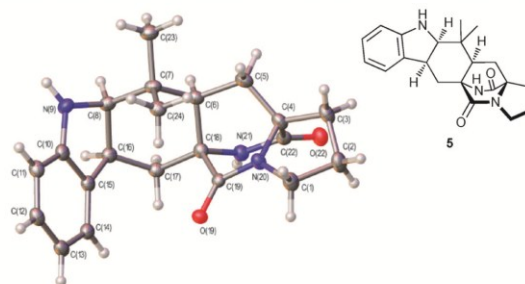


Fig. 2 The structure of indoline **5** with non-H atoms drawn at 50% probability level and H-atoms shown as small spheres of arbitrary radii.

for Advanced Materials in the Modern World (West Midlands Centre for Advanced Materials Project 2), with support from Advantage West Midlands (AWM) and part funded by the European Regional Development Fund (ERDF).

We would also like to thank Professor Phil Baran of The Scripps Research Institute for kindly providing NMR spectra of their indoline intermediate.

Notes and references

- 1 J. Qian-Cutrone, S. Huang, Y.-Z. Shu, D. Vyas, C. Fairchild, A. Menendez, K. Krampitz, R. Dalterio, S. E. Klotz and Q. Gao, *J. Am. Chem. Soc.*, 2002, **124**, 14556–14557.
- 2 W. Fenical, P. Jensen, X. C. Chang, *US Patent*, 6,066,635, 2000.
- 3 Y. Sugie, H. Hirai, T. Inagaki, M. Ishiguro, Y.-J. Kim, Y. Kojima, T. Sakakibara, S. Sakemi, A. Sugiura, Y. Suzuki, L. Brennan, J. Duignan, L. Huang, J. Sutcliffe and N. Kojima, *J. Antibiot.*, 2001, **54**, 911–916.
- 4 (a) K. A. Miller and R. M. Williams, *Chem. Soc. Rev.*, 2009, **38**, 3160–3174; (b) C. F. Nising, *Chem. Soc. Rev.*, 2010, **39**, 591–599.
- 5 J. E. Wulff, R. Siegrist and A. G. Myers, *J. Am. Chem. Soc.*, 2007, **129**, 14444–14451, and references therein.
- 6 (a) S. B. Herzon and A. G. Myers, *J. Am. Chem. Soc.*, 2005, **127**, 5342–5344; (b) P. S. Baran, B. D. Hafenstein, N. B. Ambhaikar, C. A. Guerrero and J. D. Gallagher, *J. Am. Chem. Soc.*, 2006, **128**, 8678–8693; (c) G. D. Artman III, A. W. Grubbs and R. M. Williams, *J. Am. Chem. Soc.*, 2007, **129**, 6336–6342. See also ref. 4.
- 7 (a) The initially described method used $\text{Na}_2\text{WO}_4\text{--H}_2\text{O}_2$ for indoline oxidation, see P. S. Baran, C. A. Guerrero, B. D. Hafenstein and N. B. Ambhaikar, *Angew. Chem., Int. Ed.*, 2005, **44**, 3892–3895; (b) an improved method using DMDO was subsequently described, see B. D. Hafenstein, M. Escribano, E. Petricci and P. S. Baran, *Bioorg. Med. Chem. Lett.*, 2009, **19**, 3808–3810.
- 8 (a) F. Frebault, N. S. Simpkins and A. Fenwick, *J. Am. Chem. Soc.*, 2009, **131**, 4214–4215; (b) F. C. Frebault and N. S. Simpkins, *Tetrahedron*, 2010, **66**, 6585–6596.
- 9 Key aspects of the new approach compared to the previous cationic method are that DKP assembly is streamlined, and the key radical cascade is effected under neutral conditions—which is critical for formation of the acid sensitive stephacidin systems.
- 10 (a) Both 5-*exo* and 6-*endo* modes of cyclisation have been observed in reactions of 3-substituted indoles, see S. R. Flanagan, D. C. Harrowven and M. Bradley, *Tetrahedron Lett.*, 2003, **44**, 1795–1798; (b) See also, C. V. Stevens, E. V. Meenen, Y. Eeckhout, B. Vanderhoydonck and W. Hooghe, *Chem. Commun.*, 2005, 4827–4829.
- 11 M. Pichowicz, N. S. Simpkins, A. J. Blake and C. Wilson, *Tetrahedron*, 2008, **64**, 3713–3735. For reasons that are not clear, we were previously unable to effect the synthesis of **9a** using this method.
- 12 In a two neck flask fitted with a condenser, **9a** (60 mg, 0.09 mmol) was dissolved in degassed toluene (3 mL) under an inert atmosphere. The mixture was warmed to reflux and solutions of 0.009 M ACCN in degassed toluene (6.0 mg, 0.026 mmol, 0.3 equiv) and 0.044 M Bu_3SnH in degassed toluene (35 μL , 0.132 mmol, 1.5 equiv) were added via a syringe pump over 8 h. After completion of the addition the mixture was allowed to cool to r.t. and the solvent was evaporated under reduced pressure. The crude material was purified by flash column chromatography on silica gel (eluent: pet. ether/EtOAc, 1:1) to give **11** (35 mg, 0.061 mmol, 71%) and **12** (7 mg, 0.014 mmol, 15%).
- 13 For indoline **11**, the assigned stereochemistry at C-6 was supported by nOe correlations with between H-6 and protons on the PMB group and also to H-8 (alpha to the indolic nitrogen). These correlations were not observed in indoline **12**.
- 14 R. M. Williams, T. Glinka, E. Kwast, H. Coffman and J. K. Stille, *J. Am. Chem. Soc.*, 1990, **112**, 808–821.
- 15 $\text{C}_{21}\text{H}_{25}\text{N}_3\text{O}_2$, $M = 351.44$, Orthorhombic, $a = 11.2588(1)$, $b = 11.7630(2)$, $c = 12.8358(2)$ Å, $U = 1699.94(4)$ Å³, $T = 120(2)$ K, space group $P2_1 2_1 2_1$, $Z = 4$, 10076 reflections measured, 2910 unique ($R_{\text{int}} = 0.0278$) which were used in all calculations. The final $R1$ was 0.0329 ($I > 2\sigma(I)$) and $wR(F_2)$ was 0.0861 (all data). CCDC 848586.
- 16 Interestingly, the major indoline diastereomer from our radical reactions does not correspond to that obtained by Baran and co-workers using Gribble reduction of the corresponding indole, see ESI for further detail.

List of references

- (1) (a) Dinsmore, C. J.; Beshore, D. C. *Tetrahedron* **2002**, *58*, 3297; (b) Martins, M. B.; Carvalho, I. *Tetrahedron* **2007**, *63*, 9923.
- (2) (a) Wang, S.; Golec, J.; Miller, W.; Milutinovic, S.; Folkes, A.; Williams, S.; Brooks, T.; Hardman, K.; Charlton, P.; Wren, S.; Spencer, J. *Bioorg. Med. Chem. Lett.* **2002**, *12*, 2367; (b) Folkes, A.; Roe, M. B.; Sohal, S.; Golec, J.; Faint, R.; Brooks, T.; Charlton, P. *Bioorg. Med. Chem. Lett.* **2001**, *11*, 2589; (c) Brooks, T. D.; Wang, S. W.; Bruenner, N.; Charlton, P. A. *Anti-Cancer Drugs* **2004**, *15*, 37; (d) Einholm, A. P.; Pedersen, K. E.; Wind, T.; Kulig, P.; Overgaard, M. T.; Jensen, J. K.; Bodker, J. S.; Christensen, A.; Charlton, P.; Andreasen, P. A. *Biochem. J.* **2003**, *373*, 723.
- (3) (a) McClelland, K.; Milne, P. J.; Lucieto, F. R.; Frost, C.; Brauns, S. C.; Van De Venter, M.; Du Plessis, J.; Dyason, K. *J. Pharm. Pharmacol.* **2004**, *56*, 1143; (b) Cheng, Y.; Manwell, J. In *U.S. Pat. Appl. Publ.* **2005**, US20050096323A1, 23.
- (4) (a) Kanzaki, H.; Imura, D.; Nitoda, T.; Kawazu, K. *J. Biosci. Bioeng.* **2000**, *90*, 86; (b) Nicholson, B.; Lloyd, G. K.; Miller, B. R.; Palladino, M. A.; Kiso, Y.; Hayashi, Y.; Neuteboom, S. T. C. *Anticancer Drugs* **2006**, *17*, 25; (c) Kanoh, K.; Kohno, S.; Katada, J.; Takahashi, J.; Uno, I. *J. Antibiot.* **1999**, *52*, 134.
- (5) Sinha, S.; Srivastava, R.; De, C. E.; Singh, R. K. *Nucleos. Nucleot. Nucl.* **2004**, *23*, 1815.
- (6) (a) Houston, D. R.; Synstad, B.; Eijssink, V. G. H.; Stark, M. J. R.; Eggleston, I. M.; van Aalten, D. M. F. *J. Med. Chem.* **2004**, *47*, 5713; (b) Asano, N. *Glycobiology* **2003**, *13*, 93R; (c) Byun, H.-G.; Zhang, H.; Mochizuki, M.; Adachi, K.; Shizuri, Y.; Lee, W.-J.; Kim, S.-K. *J. Antibiot.* **2003**, *56*, 102.
- (7) (a) Fdhila, F.; Vazquez, V.; Sanchez, J. L.; Riguera, R. *J. Nat. Prod.* **2003**, *66*, 1299; (b) Kanokmedhakul, S.; Kanokmedhakul, K.; Phonkerd, N.; Soyong, K.; Kongsaree,

- P.; Suksamrarn, A. *Planta Med.* **2002**, *68*, 834; (c) Sugie, Y.; Hirai, H.; Inagaki, T.; Ishiguro, M.; Kim, Y. J.; Kojima, Y.; Sakakibara, T.; Sakemi, S.; Sugiura, A.; Suzuki, Y.; Brennan, L.; Duignan, J.; Huang, L. H.; Sutcliffe, J.; Kojima, N. *J. Antibiot.* **2001**, *54*, 911;
- (d) Abraham, W.-R. *Drug Des. Rev.* **2005**, *2*, 13; (e) De, K. T. R.; Iglewski, B. H. *Infect. Immun.* **2000**, *68*, 4839; (f) Kozlovsky, A. G.; Zhelifonova, V. P.; Adanin, V. M.; Antipova, T. V.; Ozerskaya, S. M.; Ivanushkina, N. E.; Grafe, U. *Appl. Biochem. Microbiol.* **2003**, *39*, 393.
- (8) (a) Kwon, O. S.; Park, S. H.; Yun, B.-S.; Pyun, Y. R.; Kim, C.-J. *J. Antibiot.* **2000**, *53*, 954; (b) Song, M. K.; Hwang, I. K.; Rosenthal, M. J.; Harris, D. M.; Yamaguchi, D. T.; Yip, I.; Go, V. L. W. *Exp. Biol. Med. (Maywood, NJ, U. S.)* **2003**, *228*, 1338; (c) Hwang, I. K.; Go, V. L. W.; Harris, D. M.; Yip, I.; Kang, K. W.; Song, M. K. *Diabetes Obes. Metab.* **2003**, *5*, 317.
- (9) Kilian, G.; Jamie, H.; Brauns, S. C. A.; Dyason, K.; Milne, P. J. *Pharmazie* **2005**, *60*, 305.
- (10) Imamura, M.; Prasad, C. *Peptides* **2003**, *24*, 445.
- (11) Lopez-Rodriguez, M. L.; Morcillo, M. J.; Fernandez, E.; Porras, E.; Orensanz, L.; Beneytez, M. E.; Manzanares, J.; Fuentes, J. A. *J. Med. Chem.* **2001**, *44*, 186.
- (12) (a) Wyatt, P. G.; Allen, M. J.; Borthwick, A. D.; Davies, D. E.; Exall, A. M.; Hatley, R. J. D.; Irving, W. R.; Livermore, D. G.; Miller, N. D.; Nerozzi, F.; Sollis, S. L.; Szardenings, A. K. *Bioorg. Med. Chem. Lett.* **2005**, *15*, 2579; (b) Brooks, D. P.; Glaxo Group Limited, UK . **2005**, WO2005000311A1, 99.
- (13) Witiak, D. T.; Wei, Y. *Prog. Drug Res.* **1990**, *35*, 249.
- (14) Huang, R.; Zhou, X.; Xu, T.; Yang, X.; Liu, Y. *Chem. Biodiversity* **2010**, *7*, 2809.
- (15) (a) Miller, K. A.; Tsukamoto, S.; Williams, R. M. *Nat. Chem.* **2009**, *1*, 63; (b) Miller, K. A.; Figueroa, M.; Valente, M. W. N.; Greshock, T. J.; Mata, R.; Williams, R. M.

Bioorg. Med. Chem. Lett. **2008**, *18*, 6479; (c) Williams, R. M. *Chem. Pharm. Bull.* **2002**, *50*, 711.

(16) Birch, A. J.; Wright, J. J. *J. Chem. Soc., Chem. Commun.* **1969**, *13*, 644.

(17) Coetzer, J. *Acta Crystallogr.* **1974**, *B30*, 2254.

(18) Paterson, R. R. M.; Simmonds, M. J. S.; Kemmelmeier, C.; Blaney, W. M. *Mycol. Res.* **1990**, *94*, 538.

(19) (a) Birch, A. J.; Wright, J. J. *Tetrahedron* **1970**, *26*, 2329; (b) Birch, A. J.; Russell, R. A. *Tetrahedron* **1972**, *28*, 2999.

(20) Yamazaki, M.; Okuyama, E.; Kobayashi, M.; Inoue, H. *Tetrahedron Lett.* **1981**, *22*, 135.

(21) (a) Ondeyka, J. G.; Goegelman, R. T.; Schaeffer, J. M.; Kelemen, L.; Zitano, L. *J. Antibiot.* **1990**, *43*, 1375; (b) Liesch, J. M.; Wichmann, C. F. *J. Antibiot.* **1990**, *43*, 1380; (c) Blanchflower, S. E.; Banks, R. M.; Everett, J. R.; Manger, B. R.; Reading, C. *J. Antibiot.* **1991**, *44*, 492.

(22) Blanchflower, S. E.; Banks, R. M.; Everett, J. R.; Reading, C. *J. Antibiot.* **1993**, *46*, 1355.

(23) Banks, R. M.; Blanchflower, S. E.; Everett, J. R.; Manger, B. R.; Reading, C. *J. Antibiot.* **1997**, *50*, 840.

(24) Whyte, A. C.; Gloer, J. B.; Wicklow, D. T.; Dowd, P. F. *J. Nat. Prod.* **1996**, *59*, 1093.

(25) (a) Polonsky, J.; Merrien, M. A.; Prangé, T.; Pascard, C. *J. Chem. Soc., Chem. Commun.* **1980**, *12*, 601; (b) Prangé, T.; Billion, M. A.; Vuilhorgne, M.; Pascard, C.; Polonsky, J.; Moreau, S. *Tetrahedron Lett.* **1981**, *22*, 1977.

(26) Qian-Cutrone, J.; Haung, S.; Shu, Y. Z.; Vyas, D.; Fairchild, C.; Menendez, A.; Krampitz, K.; Dalterio, R.; Klohr, S. E.; Gao, Q. *J. Am. Chem. Soc.* **2002**, *124*, 14556.

(27) Tsukamoto, S.; Kato, H.; Samizo, M.; Nojiri, Y.; Onuki, H.; Hirota, H.; Ohta, T. *J. Nat. Prod.* **2008**, *71*, 2064.

- (28) Hayashi, H.; Nishimoto, Y.; Nozaki, H. *Tetrahedron Lett.* **1997**, *38*, 5655.
- (29) Hayashi, H.; Nishimoto, Y.; Akiyama, K.; Nozaki, H. *Biosci. Biotech. Bioch.* **2000**, *64*, 111.
- (30) Fenical, W.; Jensen, P. R.; Cheng, X. C.; *U.S. Patent*: **2000**, 6,066,635
- (31) Qian-Cutrone, J.; Krampitz, K. D.; Shu, Y. Z.; Chang, L. P. *U.S. Patent* **2001**, 6, 291.
- (32) Greshock, T. J.; Grubbs, A. W.; Jiao, P.; Wicklow, D. T.; Gloer, J. B.; Williams, R. M. *Angew. Chem., Int. Ed.* **2008**, *47*, 3573.
- (33) Fuchser, J. *Ph.D. Dissertation, University of Gottingen* **1995**.
- (34) (a) Martínez-Luis, S.; Rodríguez, R.; Acevedo, L.; González, M. C.; Lira-Rocha, A.; Mata, R. *Tetrahedron* **2006**, *62*, 1817; (b) Figueroa, M.; del Carmen González, M.; Mata, R. *Nat. Prod. Res.* **2008**, *22*, 709.
- (35) (a) Porter, A. E. A.; Sammes, P. G. *J. Chem. Soc.* **1970**, 1103; (b) Baldas, J.; Birch, A. J.; Russell, R. A. *J. Chem. Soc., Perkin Trans. 1* **1974**, 50.
- (36) Steyn, P. S. *Tetrahedron* **1973**, *29*, 107.
- (37) Williams, R. M.; Kwast, E.; Coffman, H.; Glinka, T. *J. Am. Chem. Soc.* **1989**, *111*, 3064.
- (38) Sanz-Cervera, J. F.; Glinka, T.; Williams, R. M. *Tetrahedron* **1993**, *49*, 8471.
- (39) Ding, Y.; Wet, J. R. d.; Cavalcoli, J.; Li, S.; Greshock, T. J.; Miller, K. A.; Finefield, J. M.; Sunderhaus, J. D.; McAfoos, T. J.; Tsukamoto, S.; Williams, R. M.; Sherman, D. H. *J. Am. Chem. Soc.* **2010**, *132*, 12733.
- (40) Kato, H.; Yoshida, T.; Tokue, T.; Nojiri, Y.; Hirota, H.; Ohta, T.; Williams, R. M.; Tsukamoto, S. *Angew. Chem., Int. Ed.* **2007**, *46*, 2254.
- (41) Tsukamoto, S.; Kawabata, T.; Kato, H.; Greshock, T. J.; Hirota, H.; Ohta, T.; Williams, R. M. *Org. Lett.* **2009**, *11*, 1297.
- (42) Finefield, J. M.; Kato, H.; Greshock, T. J.; Sherman, D. H.; Tsukamoto, S.; Williams, R. M. *Org. Lett.* **2011**, *13*, 3802.

- (43) Finefield, J. M.; Greshock, T. J.; Sherman, D. H.; Tsukamoto, S.; Williams, R. M. *Tetrahedron Lett.* **2011**, 52, 1987.
- (44) Tsukamoto, S.; Kato, H.; Greshock, T. J.; Hirota, H.; Ohta, T.; Williams, R. M. *J. Am. Chem. Soc.* **2009**, 131, 3834.
- (45) (a) Nussbaum, F. *Angew. Chem., Int. Ed.* **2003**, 42, 3068; (b) Myers, A. G.; Herzon, S. B. *J. Am. Chem. Soc.* **2003**, 125, 12080.
- (46) Herzon, S. B.; Myers, A. G. *J. Am. Chem. Soc.* **2005**, 127, 5342.
- (47) Baran, P. S.; Guerrero, C. A.; Hafensteiner, B. D.; Ambhaikar, N. B. *Angew. Chem., Int. Ed.* **2005**, 44, 3892.
- (48) (a) Somei, M. *Heterocycles* **1999**, 50, 1157; (b) Masanori, S. In *Adv. Heterocycl. Chem.*; Academic Press: **2002**; Vol. 82, p 101.
- (49) Wulff, J. E.; Herzon, S. B.; Siegrist, R.; Myers, A. G. *J. Am. Chem. Soc.* **2007**, 129, 4898.
- (50) Myers, A. G.; Wulff, J. E.; Siegrist, R.; Nising, C. F.; Chan, K. P.; President and Fellows of Harvard College, USA . **2009**, WO2009020768A1, p 227.
- (51) Grisendi, S.; Mecucci, C.; Falini, B.; Pandolfi, P. P. *Nat. Rev. Cancer.* **2006**, 6, 493.
- (52) (a) Trost, B. M. *Pure Appl. Chem.* **1988**, 60, 1615; (b) Stambuli, J. P.; Silverman, S. M.; Schwörer, U. *J. Am. Chem. Soc.* **2006**, 128, 13328.
- (53) Trost, B. M.; Cramer, N.; Bernsmann, H. *J. Am. Chem. Soc.* **2007**, 129, 3086.
- (54) (a) Gassman, P. G.; van Bergen, T. J. *J. Am. Chem. Soc.* **1974**, 96, 5508; (b) Gassman, P. G.; Gruetzmacher, G.; van Bergen, T. J. *J. Am. Chem. Soc.* **1974**, 96, 5512.
- (55) Trost, B. M.; Mignani, S. M.; Nanninga, T. N. *J. Am. Chem. Soc.* **1986**, 108, 6051.
- (56) Greshock, T. J.; Grubbs, A. W.; Williams, R. M. *Tetrahedron* **2007**, 63, 6124.
- (57) Sanz-Cervera, J. F.; Williams, R. M. *J. Am. Chem. Soc.* **2002**, 124, 2556.

- (58) (a) Stocking, E. M.; Sanz-Cervera, J. F.; Unkefer, C. J.; Williams, R. M. *Tetrahedron* **2001**, 57, 5303; (b) Titouani, S. L.; Lavergne, J. P.; Vaillefont, P.; Jaquier, R. *Tetrahedron* **1980**, 36, 2961.
- (59) (a) Frebault, F. C.; Simpkins, N. S. *Tetrahedron* **2010**, 66, 6585; (b) Frebault, F. C.; Simpkins, N. S.; Fenwick, A. J. *Am. Chem. Soc.* **2009**, 131, 4214.
- (60) Baldwin, J. E. *J. Chem. Soc., Chem. Commun.* **1976**, 734.
- (61) (a) Fleming, I. *Frontier Orbitals and Organic Chemical Reactions*; John Wiley and Sons Ltd., **1976**; (b) Fukui, K. *Acc. Chem. Res.* **1971**, 4, 57; (c) Kirby, A. J.; Editor *Stereoelectronic Effects*; Oxford Univ Press, **1996**; (d) Fossey, J.; Lefort, D.; Sorba, J. *Free Radicals in Organic Chemistry*; Wiley, **1995**.
- (62) (a) Beckwith, A. L. J.; Schiesser, C. H. *Tetrahedron* **1985**, 41, 3925; (b) Beckwith, A. L. J.; Lawrence, T. J. *Chem. Soc., Perkin Trans. 2* **1979**, 1535; (c) Beckwith, A. L. J.; Phillipou, G.; Serelis, A. K. *Tetrahedron Lett.* **1981**, 22, 2811; (d) Athelstan L.J, B. *Tetrahedron* **1981**, 37, 3073.
- (63) (a) Bürgi, H. B.; Dunitz, J. D.; Shefter, E. *J. Am. Chem Soc.* **1973**, 95, 5065; (b) Bürgi, H. B.; Dunitz, J. D. *Acc. Chem. Res.* **1983**, 16, 153; (c) Bürgi, H. B.; Dunitz, J. D.; Lehn, J. M.; Wipff, G. *Tetrahedron* **1974**, 30, 1563; (d) Arnaud, R.; Douady, J.; Subra, R. *Nouv. J. Chim.* **1981**, 5, 181; (e) Nagase, S.; Kern, C. W. *J. Am. Chem Soc.* **1980**, 102, 4513; (f) Houk, K. N.; Paddon-Row, M. N.; Spellmeyer, D. C.; Rondan, N. G.; Nagase, S. *J. Org. Chem* **1986**, 51, 2874.
- (64) (a) Rajanbabu, T. V. *Acc. Chem. Res.* **1991**, 24, 139; (b) Kirschning, A. *Angew. Chem., Int. Ed.* **2010**, 49, 2971.
- (65) Giese, B. *Radicals in Organic Synthesis: Formation of Carbon-Carbon Bonds*; Pergamon Press, **1986**.
- (66) Houk, K. N. *J. Am. Chem Soc.* **1973**, 95, 4092.
- (67) (a) Julia, M.; Maumy, M. *Bull. Soc. Chim. Fr.* **1969**, 2427; (b) Julia, M.; Maumy, M.; Mion, L. *Bull. Soc. Chim. Fr.* **1967**, 2641.

- (68) Julia, M.; Mansour, B.; Mansuy, D. *Tetrahedron Lett.* **1976**, 17, 3443.
- (69) (a) Beckwith, A. L. J.; Blair, I. A.; Phillipou, G. *Tetrahedron Lett.* **1974**, 15, 2251; (b) Beckwith, A.; Gream, G.; Struble, D. *Aust. J. Chem.* **1972**, 25, 1081; (c) Julia, M.; Descoins, C.; Baillarge, M.; Jacquet, B.; Uguen, D.; Groeger, F. A. *Tetrahedron* **1975**, 31, 1737.
- (70) Park, S. U.; Chung, S. K.; Newcomb, M. *J. Am. Chem. Soc.* **1986**, 108, 240.
- (71) (a) Wilt, J. W. *J. Am. Chem. Soc.* **1981**, 103, 5251; (b) Chatgililoglu, C.; Woynar, H.; Ingold, K. U.; Davies, A. G. *J. Chem. Soc. Perkin Trans 2* **1983**; (c) Wilt, J. W. *Tetrahedron* **1985**, 41, 3979.
- (72) (a) Bachi, M. D.; Frolow, F.; Hoornaert, C. *J. Org. Chem.* **1983**, 48, 1841; (b) Burnett, D. A.; Choi, J. K.; Hart, D. J.; Tsai, Y. M. *J. Am. Chem. Soc.* **1984**, 106, 8201.
- (73) (a) Curran, D. P.; Shen, W. *J. Am. Chem. Soc.* **1993**, 115, 6051; (b) Curran, D. P.; Kim, D.; Ziegler, C. *Tetrahedron Lett.* **1991**, 47, 6189; (c) Curran, D. P.; Kim, D.; Liu, H. T.; Shen, W. *J. Am. Chem. Soc.* **1988**, 110, 5900.
- (74) Lathbury, D. C.; Parsons, P. J.; Pinto, I. *J. Chem. Soc., Chem. Commun.* **1988**, 81.
- (75) (a) Heiba, E. A. I.; Dessau, R. M. *J. Am. Chem. Soc.* **1967**, 89, 3772; (b) Broka, C. A.; Reichert, D. E. C. *Tetrahedron Lett.* **1987**, 28, 1503; (c) Miyata, O.; Naito, T. *Acad. Sci. Paris, Chem.* **2001**, 4, 401; (d) Kyoko, N.; Koichiro, O.; Kiitiro, U. *Bull. Chem. Soc. Jpn.* **1987**, 60, 3465; (e) Bosch, E.; Bachi, M. D. *J. Org. Chem.* **1993**, 58, 5581; (f) Alcaide, B.; Rodriguez-Campos, I. M.; Rodriguez-Lopez, J.; Rodriguez-Vicente, A. *J. Org. Chem.* **1999**, 64, 5377; (g) Wille, U.; Jargstorff, C. *Eur. J. Org. Chem.* **2003**, 16, 3173; (h) Wille, U. *Tetrahedron Lett.* **2002**, 43, 1239; (i) Wille, U. *J. Am. Chem. Soc.* **2002**, 124, 14; (j) Wille, U.; Lietzau, L. *Tetrahedron* **1999**, 55, 10119; (k) Wille, U.; Plath, C. *Liebigs Ann.* **1997**, 111; (l) Renaud, P.; Beaufils, F.; Feray, L.; Schenk, K. *Angew. Chem., Int. Ed.* **2003**, 42, 4230; (m) Beaufils, F.; Dénès, F.; Renaud, P. *Org. Lett.* **2004**, 6, 2563; (n) Dénès, F.; Beaufils, F.; Renaud, P. *Org. Lett.* **2007**, 9, 4375; (o)

Beaufils, F.; Dénès, F.; Becattini, B.; Renaud, P.; Schenk, K. *Adv. Synth. Catal.* **2005**, 347, 1587.

(76) Escoubet, S.; Gastaldi, S.; Vanthuyne, N.; Gil, G.; Siri, D.; Bertrand, M. P. *J. Org. Chem.* **2006**, 71, 7288.

(77) Baran, P. S.; Guerrero, C. A.; Ambhaikar, N. B.; Hafensteiner, B. D. *Angew. Chem., Int. Ed.* **2005**, 44, 606.

(78) (a) Greshock, T. J.; Grubbs, A. W.; Tsukamoto, S.; Williams, R. M. *Angew. Chem., Int. Ed.* **2007**, 46, 2262; (b) Artman, G. D.; Grubbs, A. W.; Williams, R. M. *J. Am. Chem. Soc.* **2007**, 129, 6336; (c) Greshock, T. J.; Williams, R. M. *Org. Lett.* **2007**, 9, 4255.

(79) Baran, P. S.; Hafensteiner, B. D.; Ambhaikar, N. B.; Guerrero, C. A.; Gallagher, J. D. *J. Am. Chem. Soc.* **2006**, 128, 8678.

(80) Williams, R. M.; Glinka, T.; Kwast, E.; Coffman, H.; Stille, J. K. *J. Am. Chem. Soc.* **1990**, 112, 808.

(81) Hafensteiner, B. D.; Escribano, M.; Petricci, E.; Baran, P. S. *Bioorg. Med. Chem. Lett.* **2009**, 19, 3808.

(82) Williams, R. M.; Sanz-Cervera, J. F.; Sancenón, F.; Marco, J. A.; Halligan, K. *J. Am. Chem. Soc.* **1998**, 120, 1090.

(83) Williams, R. M.; Glinka, T.; Kwast, E. *J. Am. Chem. Soc.* **1988**, 110, 5927.

(84) (a) Pichowicz, M.; Simpkins, N. S.; Blake, A. J.; Wilson, C. *Tetrahedron Lett.* **2006**, 47, 8413; (b) Pichowicz, M.; Simpkins, N. S.; Blake, A. J.; Wilson, C. *Tetrahedron* **2008**, 64, 3713.

(85) Hara, T.; Durell, S. R.; Myers, M. C.; Appella, D. H. *J. Am. Chem. Soc.* **2006**, 128, 1995.

(86) Ellis, D. A.; Wolkenberg, S. E.; Boger, D. L. *J. Am. Chem. Soc.* **2001**, 123, 9299.

(87) Escolano, C. *Angew. Chem., Int. Ed.* **2005**, 44, 7670.

- (88) Fagan, P. J.; Hauptman, E.; Shapiro, R.; Casalnuovo, A. *J. Am. Chem. Soc.* **2000**, *122*, 5043.
- (89) (a) Tlili, A.; Xia, N.; Monnier, F.; Taillefer, M. *Angew. Chem., Int. Ed.* **2009**, *48*, 8725; (b) Zhao, D.; Wu, N.; Zhang, S.; Xi, P.; Su, X.; Lan, J.; You, J. *Angew. Chem., Int. Ed.* **2009**, *48*, 8729; (c) Altman, R. A.; Shafir, A.; Choi, A.; Lichtor, P. A.; Buchwald, S. L. *J. Org. Chem.* **2008**, *73*, 284.
- (90) (a) Torraca, K. E.; Huang, X.; Parrish, C. A.; Buchwald, S. L. *J. Am. Chem. Soc.* **2001**, *123*, 10770; (b) Vorogushin, A. V.; Huang, X.; Buchwald, S. L. *J. Am. Chem. Soc.* **2005**, *127*, 8146.
- (91) Aranyos, A.; Old, D. W.; Kiyomori, A.; Wolfe, J. P.; Sadighi, J. P.; Buchwald, S. L. *J. Am. Chem. Soc.* **1999**, *121*, 4369.
- (92) (a) Othman, R. B.; Bousquet, T.; Othman, M.; Dalla, V. *Org. Lett.* **2005**, *7*, 5335; (b) Zhang, L.; Kozmin, S. A. *J. Am. Chem. Soc.* **2004**, *126*, 10204; (c) Tranchant, M. J.; Moine, C.; Othman, R. B.; Bousquet, T.; Othman, M.; Dalla, V. *Tetrahedron Lett.* **2006**, *47*, 4477.
- (93) Othman, R. B.; Affani, R.; Tranchant, M. J.; Antoniotti, S.; Dalla, V.; Duñach, E. *Angew. Chem., Int. Ed.* **2010**, *49*, 776.
- (94) Concellon, J. M.; Rodriguez-Solla, H.; Bardales, E.; Huerta, M. *Eur. J. Org. Chem.* **2003**, 1775.
- (95) Fabre, J. L.; Farge, D.; James, C.; Lavé, D. *Tetrahedron Lett.* **1985**, *26*, 5447.
- (96) Stocking, E. M.; Sanz-Cervera, J. F.; Williams, R. M. *J. Am. Chem. Soc.* **2000**, *122*, 1675.
- (97) Miller, K. A.; Welch, T. R.; Greshock, T. J.; Ding, Y.; Sherman, D. H.; Williams, R. M. *J. Org. Chem.* **2008**, *73*, 3116.
- (98) Domingo, L. R.; Zaragoza, R. J.; Williams, R. M. *J. Org. Chem.* **2003**, *68*, 2895.
- (99) Jin, S.; Wessig, P.; Liebscher, J. *J. Org. Chem.* **2001**, *66*, 3984.

- (100) Adams, L. A.; Valente, M. W. N.; Williams, R. M. *Tetrahedron* **2006**, 62, 5195.
- (101) Williams, R. M.; Maruyama, L. K. *J. Org. Chem.* **1987**, 52, 4044.
- (102) Williams, R. M.; Cao, J.; Tsujishima, H.; Cox, R. J. *J. Am. Chem. Soc.* **2003**, 125, 12172.
- (103) Cushing, T. D.; Sanz-Cervera, J. F.; Williams, R. M. *J. Am. Chem. Soc.* **1993**, 115, 9323.
- (104) Davies, S. G.; Christopher Garner, A.; Ouzman, J. V. A.; Roberts, P. M.; Smith, A. D.; Snow, E. J.; Thomson, J. E.; Tamayo, J. A.; Vickers, R. J. *Org. Biomol. Chem.* **2007**, 5, 2138.
- (105) (a) Davies, S. G.; Rodriguez-Solla, H.; Tamayo, J. A.; Garner, A. C.; Smith, A. D. *Chem. Commun.* **2004**, 2502; (b) Bull, S. D.; Davies, S. G.; Garner, A. C.; Parkes, A. L.; Roberts, P. M.; Sellers, T. G. R.; Smith, A. D.; Tamayo, J. A.; Thomson, J. E.; Vickers, R. J. *New J. Chem.* **2007**, 31, 486; (c) Bull, S. D.; Davies, S. G.; Epstein, S. W.; Garner, A. C.; Mujtaba, N.; Roberts, P. M.; Savory, E. D.; Smith, A. D.; Tamayo, J. A.; Watkin, D. J. *Tetrahedron* **2006**, 62, 7911; (d) Bull, S. D.; Davies, S. G.; O'Shea, M. D. *J. Chem. Soc., Perkin Trans. 1* **1998**, 3657.
- (106) (a) Groaning, M. D.; Meyers, A. I. *Tetrahedron* **2000**, 56, 9843; (b) Seebach, D.; Maetzke, T.; Petter, W.; Kloetzer, B.; Plattner, D. A. *J. Am. Chem. Soc.* **1991**, 113, 1781.
- (107) Seebach, D.; Boes, M.; Naef, R.; Schweizer, W. B. *J. Am. Chem. Soc.* **1983**, 105, 5390.
- (108) (a) Benson, O.; Demirdji, S. H.; Haltiwanger, R. C.; Koch, T. H. *J. Am. Chem. Soc.* **1991**, 113, 8879; (b) Bordwell, F. G.; Lynch, T. Y. *J. Am. Chem. Soc.* **1989**, 111, 7558; (c) Pasto, D. J. *J. Am. Chem. Soc.* **1988**, 110, 8164; (d) Viehe, H. G.; Janousek, Z.; Merenyi, R.; Stella, L. *Acc. Chem. Res.* **1985**, 18, 148; (e) Benson, S. W.; Egger, K. W.; Golden, D. M. *J. Am. Chem. Soc.* **1965**, 87, 468.
- (109) Blanksby, S. J.; Ellison, G. B. *Acc. Chem. Res.* **2003**, 36, 255.

(110) (a) Harrowven, D. C.; Stenning, K. J.; Whiting, S.; Thompson, T.; Walton, R. *Org. Biomol. Chem.* **2011**, 9; (b) Flanagan, S. R.; Harrowven, D. C.; Bradley, M. *Tet. Lett.* **2003**, 44, 1795; (c) Li, H.; Boonnak, N.; Padwa, A. *J. Org. Chem.* **2011**, 76, 9488; (d) Paleo, E.; Osornio, Y. M.; Miranda, L. D. *Org. Biomol. Chem.* **2011**, 9; (e) Tucker, J. W.; Narayanam, J. M. R.; Krabbe, S. W.; Stephenson, C. R. J. *Org. Lett.* **2009**, 12, 368; (f) Gribble, G. W.; Fraser, H. L.; Badenock, J. C. *Chem. Commun.* **2001**; (g) Bennasar, M. L.; Roca, T.; Grier, R.; Bosch, J. *J. Org. Chem.* **2001**, 66, 7547; (h) Miranda, L. D.; Cruz-Almanza, R.; Pavón, M.; Romero, Y.; Muchowski, J. M. *Tet. Lett.* **2000**, 41, 10181; (i) Tsuge, O.; Hatta, T.; Tsuchiyama, H. *Chem. Lett.* **1998**, 27, 155; (j) Zhang, W.; Pugh, G. *Tet. Lett.* **1999**, 40, 7591; (k) Ziegler, F. E.; Belema, M. *J. Org. Chem.* **1997**, 62, 1083; (l) J. Moody, C.; L. Norton, C. *J. Chem. Soc. Perkin Trans 1* **1997**; (m) Caddick, S.; Aboutayab, K.; Jenkins, K.; West, R. I. *J. Chem. Soc. Perkin Trans 1* **1996**; (n) Yang, C. C.; Chang, H. T.; Fang, J. M. *J. Org. Chem.* **1993**, 58, 3100; (o) Byers, J. H.; Kosterlitz, J. A.; Steinberg, P. L. *C.R. Acad. Sci., Ser. IIc: Chem.* **2001**, 4, 471.

(111) Chern, C.-Y.; Huang, Y.-P.; Kan, W. M. *Tetrahedron Lett.* **2003**, 44, 1039.

(112) Ueki, T.; Kinoshita, T. *Org. Biomol. Chem.* **2005**, 3, 295.

(113) Meng, W.-H.; Wu, T.-J.; Zhang, H.-K.; Huang, P.-Q. *Tetrahedron: Asymmetry* **2004**, 15, 3899.

(114) (a) Braslau, R.; Burrill, L. C.; Siano, M.; Naik, N.; Howden, R. K.; Mahal, L. K. *Macromolecules* **1997**, 30, 6445; (b) Langer, T.; Illich, M.; Helmchen, G. *Synlett* **1996**, 1137; (c) Porter, N. A.; Su, Q.; Harp, J. J.; Rosenstein, I. J.; McPhail, A. T. *Tetrahedron Lett.* **1993**, 34, 4457; (d) Porter, N. A.; Rosenstein, I. J. *Tetrahedron Lett.* **1993**, 34, 7865; (e) Rathke, M. W.; Lindert, A. *J. Am. Chem. Soc.* **1971**, 93, 4605; (f) Cohen, T.; McNamara, K.; Kuzemko, M. A.; Ramig, K.; Landi, J. J.; Jr, n. *Tetrahedron* **1993**, 49, 7931; (g) Chung, S. K.; Dunn, L. B. *J. Org. Chem.* **1983**, 48, 1125; (h) Frazier, R. H.;

Harlow, R. L. *J. Org. Chem.* **1980**, *45*, 5408; (i) Alvarez-Ibarra, C.; Csáký, A. G.; Colmenero, B.; Quiroga, M. L. *J. Org. Chem.* **1997**, *62*, 2478.

(115) Kaiser, E. M. *J. Am. Chem. Soc.* **1967**, *89*, 3659.

(116) (a) Schmittel, M.; Burghart, A.; Werner, H.; Laubender, M.; Söllner, R. *J. Org. Chem.* **1999**, *64*, 3077; (b) Ryter, K.; Livinghouse, T. *J. Am. Chem. Soc.* **1998**, *120*, 2658; (c) Hirao, T.; Fujii, T.; Ohshiro, Y. *Tetrahedron* **1994**, *50*, 10207; (d) Paolobelli, A. B.; Latini, D.; Ruzziconi, R. *Tetrahedron Lett.* **1993**, *34*, 721; (e) Fujii, T.; Hirao, T.; Ohshiro, Y. *Tetrahedron Lett.* **1992**, *33*, 5823; (f) Baciocchi, E.; Casu, A.; Ruzziconi, R. *Tetrahedron Lett.* **1989**, *30*, 3707; (g) Ito, Y.; Konoike, T.; Saegusa, T. *J. Am. Chem. Soc.* **1975**, *97*, 649.

(117) (a) Kise, N.; Kumada, K.; Terao, Y.; Ueda, N. *Tetrahedron* **1998**, *54*, 2697;

(b) Inaba, S.-i.; Ojima, I. *Tetrahedron Lett.* **1977**, *18*, 2009.

(118) Kohno, Y.; Narasaka, K. *Bull. Chem. Soc. Jpn.* **1995**, *68*, 322.

(119) P. W. R. Harris; M. A. Brimble; V. J. Muir; M. Y. H. Lai; N. S. Trotter; Callis, D. *J. Tetrahedron* **2005**, *61*, 10018.

(120) (a) For examples of this type of reaction using ammonia and other amines, s. T. B., C. Hounsou and B. P. Deprez *Bioorg. Med. Chem. Lett.* **2007**, *17*, 789; (b) G. N. Maw; C. M. N. Allerton; E. Gbekor; Million, W. A. *Bioorg. Med. Chem. Lett.* **2003**, *13*, 1425.

(121) Artman, G. D.; Grubbs, A. W.; Williams, R. M. *J. Am. Chem. Soc.* **2007**, *129*, 6336.

(122) Nelson, L. A. K.; Shaw, A. C.; Abrams, S. R. *Tetrahedron* **1991**, *47*, 3259.

(123) Gribble, G. W.; Lord, P. D.; Skotnicki, K.; Dietz, S. E.; Eaton, J. T.; Johnson, J. *J. Am. Chem. Soc.* **1974**, *96*, 7812.

(124) Cushing, T. D.; Sanz-Cervera, J. F.; Williams, R. M. *J. Am. Chem. Soc.* **1996**, *118*, 557.

(125) (a) Snider, B. B. *Tetrahedron* **2009**, *65*, 10738; (b) Snider, B. B.; Armanetti, L.; Baggio, R. *Tetrahedron Lett.* **1993**, *34*, 1701; (c) Kates, S. A.;

Dombroski, M. A.; Snider, B. B. *J. Org. Chem.* **1990**, *55*, 2427; (d) Snider, B. B.; Buckman, B. O. *Tetrahedron* **1989**, *45*, 6969; (e) Snider, B. B.; Mohan, R.; Kates, S. A. *Tetrahedron Lett.* **1987**, *28*, 841.

(126) For expected titration results see: <http://istcgroup.com/pdf/Pure%20>.

(127) (a) Jana, G. K.; Sinha, S. *Tetrahedron Lett.* **2010**, *51*, 1994; (b) Coogan, M. P.; Stanton, L. S.; Walther, T. *J. Organomet. Chem.* **2003**, *677*, 125.

(128) Frebault, F.; Simpkins, N. S.; Fenwick, A. *J. Am. Chem. Soc.* **2009**, *131*, 4214.

(129) Montagne, C.; Fournet, G.; Joseph, B. *Synthesis* **2005**, 136.